

Distribution Agreement

In presenting this thesis or dissertation as a partial fulfillment of the requirements for an advanced degree from Emory University, I hereby grant to Emory University and its agents the non-exclusive license to archive, make accessible, and display my thesis or dissertation in whole or in part in all forms of media, now or hereafter known, including display on the world wide web. I understand that I may select some access restrictions as part of the online submission of this thesis or dissertation. I retain all ownership rights to the copyright of the thesis or dissertation. I also retain the right to use in future works (such as articles or books) all or part of this thesis or dissertation.

Signature:

Arielle Nicole Valdez-Sinon

Date

Regulation of protein synthesis and stress granule dynamics in neural cells by Cdh1-APC

By

Arielle Nicole Valdez-Sinon
Doctor of Philosophy

Graduate Division of Biological and Biomedical Science
Neuroscience

Gary J. Bassell, Ph.D.
Advisor

Victor Faundez, M.D., Ph.D.
Committee Member

Yue Feng, M.D., Ph.D.
Committee Member

Chad McKinley Hales, M.D., Ph.D.
Committee Member

Nicholas T. Seyfried, Ph.D.
Committee Member

Accepted:

Lisa A. Tedesco, Ph.D.
Dean of the James T. Laney School of Graduate Studies

Date

Regulation of protein synthesis and stress granule dynamics in neural cells by Cdh1-APC

By

Arielle Nicole Valdez-Sinon
B.A., Boston University, 2013

Advisor: Gary J. Bassell, PhD

An abstract of
A dissertation submitted to the Faculty of the
James T. Laney School of Graduate Studies of Emory University
in partial fulfillment of the requirements for the degree of
Doctor of Philosophy
in Graduate Division of Biological and Biomedical Sciences
Neuroscience
2020

Abstract

Regulation of protein synthesis and stress granule dynamics in neural cells by Cdh1-APC

By Arielle Nicole Valdez-Sinon

Maintaining a homeostatic balance between protein degradation and protein synthesis at synapses is necessary for learning and memory. Perturbation of protein homeostasis can compromise synaptic function, and several neurodevelopmental brain disorders are characterized by dysregulated protein homeostasis, including Angelman Syndrome, Fragile X Syndrome, and Autism Spectrum Disorders. Ubiquitination is a post-translational modification that is a primary mechanism of targeting proteins for degradation. While the E3 Ubiquitin Ligase Anaphase Promoting Complex and its regulatory subunit Cdh1 (Cdh1-APC) has been previously shown to regulate learning and memory, the underlying molecular mechanisms are unclear. In this study, we have identified a novel role of Cdh1-APC as a regulator of protein synthesis in neurons. Inhibition of Cdh1-APC activity leads to a decrease in protein synthesis in postmitotic cortical neurons. Proteomic profiling revealed that Cdh1-APC interacts with known regulators of translation, including mRNA binding proteins, initiation factors, ribosomal proteins, and stress granule proteins. Inhibition and knockdown of Cdh1-APC activity caused an increase in stress granule formation, suggesting a novel mechanism by which Cdh1-APC may regulate the dynamic balance between translational repression within stress granules and protein synthesis. Furthermore, the interaction between Cdh1-APC and the Fragile X Mental Retardation Protein (FMRP), an RNA binding protein necessary for proper neurodevelopment, was shown to regulate stress granule formation and downstream changes in protein synthesis. We propose a model in which Cdh1-APC targets key stress granule proteins, such as FMRP, and inhibits the formation of stress granules, leading to increases in protein synthesis. As Cdh1-APC has been primarily studied in the context of mitotic cells and progressing cell cycle, these findings from neurons demonstrate a novel role for Cdh1-APC independent of its well-characterized targeting of mitotic proteins for degradation. Elucidation of an interdependent role for Cdh1-APC in regulation of stress granules and protein synthesis in cortical neurons has implications for how Cdh1-APC can regulate protein synthesis-dependent synaptic plasticity underlying learning and memory.

Regulation of protein synthesis and stress granule dynamics in neural cells by Cdh1-APC

By

Arielle Nicole Valdez-Sinon
B.A., Boston University, 2013

Advisor: Gary J. Bassell, Ph.D.

A dissertation submitted to the Faculty of the
James T. Laney School of Graduate Studies of Emory University
in partial fulfillment of the requirements for the degree of
Doctor of Philosophy
in Graduate Division of Biological and Biomedical Sciences
Neuroscience
2020

Acknowledgements

This work is dedicated to all the individuals who have supported and motivated me throughout this journey.

I would first like to thank my advisor Dr. Gary Bassell for his mentorship and guidance throughout my PhD. I am thankful for his constant support and ability to tailor his mentorship based upon my personal goals and needs. I thank him for his continued commitment to seeking out opportunities for my career development; it was incredible to have a mentor that was such an advocate for young females in science.

Thank you to Dr. Victor Faundez for his continued scientific and spiritual guidance beginning as far back as my time in medical school. Thank you for always giving me confidence in my place as a scientist and always pushing me to think critically.

I would like to thank my committee members Dr. Yue Feng, Dr. Chad Hales, and Dr. Nick Seyfried for their expert guidance throughout my dissertation research.

Additionally, I would like to thank members of the Bassell lab for all of the mentorship, guidance, and assistance during my time in the lab. I specifically would like to thank Dr. Kristen Thomas for mentoring me when I first started in the lab; there is no doubt that her mentorship was formative in my early training. Thank you to previous lab members Dr. Katie Williams, Dr. Paul Donlin-Asp, and Dr. Marius Ifrim for their guidance during their time in the lab. Thank you to Dr. Nisha Raj, Pernille Bülow, Megan Merritt-Garza, Dr. Anwasha Banerjee, and Dr. Zachary McEachin for their scientific advice, and of course, friendship. Thank you to Dr. Liang Shi for his expertise and contributions to this work. I would also like to specifically thank Austin Lai for his time and commitment to this work. My dissertation project was able to move forward to exciting new directions because of his hard work, and I am forever grateful for that.

Thank you to Nusaiba Baker, Dr. Amanda Mener, and Dr. LeslieAnn Kao for their amazing friendship and support.

Thank you to my family-especially my mother, father, and brother for celebrating when times were good and reassuring me when times were hard.

Finally, thank you to my husband, Chris Sinon. Thank you for being my primary source of encouragement, love, and inspiration the last 4.5 years.

Table of Contents

Chapter 1 : General Introduction	1
1.1. Protein Synthesis.....	3
1.1.1. Local Protein Synthesis in Neurons	4
1.1.2. Stress Granules.....	6
1.2. Ubiquitination	8
1.2.1. Addition of Ubiquitin onto Substrates	9
1.2.2. Ubiquitination is Dysregulated in Neurodevelopmental Disorders	11
1.3. Fragile X Syndrome.....	13
1.3.1. Dysregulation of Dendritic Spines in Fragile X Syndrome	14
1.3.2. Aberrant mGluR-LTD in Fragile X Syndrome.....	15
1.3.3. Dysregulated Protein Synthesis in Fragile X Syndrome.....	16
1.4. FMRP Functions as a Translational Repressor.....	17
1.4.1. FMRP Directly Binds RNA	18
1.4.2. FMRP Interacts with the RNA-Induced Silencing Complex.....	20
1.4.3. FMRP Binds Polyribosomes.....	20
1.4.4. Regulation of FMRP and <i>FMRI</i> mRNA by Association with other RNA-binding Proteins	22
1.5. Reversal of FMRP-mediated Repression.....	23
1.5.1. FMRP Modification as a Molecular Switch	24
1.5.2. Ubiquitination of FMRP	26
1.6. The Anaphase Promoting Complex (APC).....	27
1.6.1. Role of APC in Mitotic Cells.....	29
1.6.2. Role of APC in Postmitotic Neurons	31
1.7. Critical Questions in the Field	35
1.8. Dissertation Hypothesis and Objectives	35
1.9. Figures.....	37
Chapter 2 : Materials & Methods	42
Cell Culture.....	43
Pharmacology	44
Plasmids	44
Antibodies	45
FMRP Immunoprecipitation	46
FLAG Immunoprecipitation	47
Puromycylation.....	48
FMRP Expression.....	48
Western Blotting	48
Silver Staining.....	49
Proteomics Analysis.....	49
Bioinformatic Analysis	50
Ubiquitin Immunoprecipitation	50
Immunofluorescence.....	51
Quantification of Stress Granules	51
Statistical analysis.....	52

Chapter 3 : Cdh1-APC Regulates FMRP-Mediated Protein Synthesis.....	53
3.1. Introduction.....	54
3.2. Results.....	55
3.2.1. Cdh1-APC Ubiquitinates FMRP Downstream of mGluR5 Signaling in Cortical Neurons.....	55
3.2.2. Cdh1-APC Reverses FMRP-mediated Repression of Protein Synthesis.....	56
3.2.3. Cdh1-APC Interaction with FMRP Affects FMRP Expression	57
3.2.4. Cdh1-APC Interaction with FMRP Regulates Protein Synthesis	58
3.3. Discussion	59
3.4. Figures.....	63
3.5. Supplemental Figures.....	70
Chapter 4 : Cdh1-APC Associates with Translational Machinery and is a Novel Regulator of Protein Synthesis.....	71
4.1. Introduction.....	72
4.2. Results.....	73
4.2.1. Cdh1-APC Regulates Protein Synthesis Independent of Cell Cycle	73
4.2.2. Cdh1-APC interactome is enriched with regulators of protein synthesis	73
4.3. Discussion	75
4.4. Figures.....	79
4.5. Tables.....	83
4.6. Supplemental Figures.....	104
Chapter 5 : Cdh1-APC Regulates Stress Granule Dynamics	105
5.1. Introduction.....	106
5.2. Results.....	107
5.2.1. Cdh1-APC Interacts with Stress Granule Proteins	107
5.2.2. Cdh1-APC Antagonizes Stress Granule Assembly	107
5.2.3. Stress granule formation reduces protein synthesis	109
5.2.4. Cdh1-APC regulates stress granules in a FMRP-dependent mechanism	109
5.3. Discussion	111
5.4. Figures.....	114
5.5. Tables	120
5.6. Supplemental Figures.....	139
Chapter 6 : General Discussion	144
6.1. Summary	145
6.2. Cdh1-APC activity across the lifespan	145
6.2.1. Cdh1-APC and neurodevelopment	146
6.2.2. Cdh1-APC and neurodegeneration	147
6.2.3. Relationship between neurodevelopment and neurodegeneration.....	148
6.3. Insight into mRNP granules.....	149
6.4. Targeting of E3 ligases as potential therapeutic options	150
6.5. Future Directions	152
6.5.1. Consequences of Cdh1-APC interaction with FMRP and other proteins.....	152
6.5.2. Determine if Cdh1 localization affects protein synthesis	155

6.5.3 Identify if Cdh1-APC solely regulates protein synthesis via FMRP	157
6.5.4. Elucidate if Cdh1 regulates spine density downstream of FMRP	158
6.6. Concluding Remarks.....	159
6.7. Figures.....	161
References	165

Figures & Tables

Figure 1-1: The Ubiquitination Pathway	37
Figure 1-2: mGluR stimulation promotes the ubiquitination of FMRP.....	39
Figure 1-3: FMRP and Cdh1-APC interact in <i>vitro</i>	40
Figure 1-4: Proposed model and hypothesis for dissertation.....	41
Figure 3-1: Cdh1-APC regulates FMRP ubiquitination in neurons downstream of mGluR signaling.....	63
Figure 3-2: Cdh1 reverses FMRP-mediated repression of translation.....	65
Figure 3-3: Cdh1-APC interaction affects FMRP expression	67
Figure 3-4: Cdh1-APC interaction with FMRP regulates protein synthesis.....	69
Supplemental Figure 3-1: Validation of Cdh1 Knockdown	70
Figure 4-1: Cdh1-APC regulates protein synthesis independent of cell cycle	79
Figure 4-2: Cdh1 interactome is enriched with translational regulators.....	80
Figure 4-3: Cdh1-APC's interactome is enriched with noncanonical binding partners linked to translation.....	81
Table 4-1: Cdh1 interactome	92
Table 4-2: Biological Processes Gene Ontology analysis	103
Supplemental Figure 4-1: Cdh1-APC does not affect protein synthesis in fibroblasts	104
Figure 5-1: Confirmed stress granule interactors of Cdh1.....	114
Figure 5-2: Cdh1-APC regulates stress granule formation in neurons	115
Figure 5-3: Knockdown of Cdh1 increases stress granule formation.....	116
Figure 5-4: Cdh1-APC interaction with FMRP regulates stress granule formation.....	117
Figure 5-5: Cdh1-APC regulates stress granule dynamics via a FMRP-dependent mechanism	118
Table 5-1: Table of stress granule proteins in Cdh1 interactome	121
Table 5-2: FMRP interactome	138
Supplemental Figure 5-1: Neuronal morphology during Sodium Arsenite treatment.....	139
Supplemental Figure 5-2: proTAME treatment increases stress granule formation.....	140
Supplemental Figure 5-3: Stress granule formation decreases protein synthesis	141
Supplemental Figure 5-4: Cdh1 does not colocalize with stress granules.....	142
Supplemental Figure 5-5: Overlap between Cdh1 and FMRP interactome	143
Figure 6-1: Stress granule dynamics across the lifespan	161
Figure 6-2: Cdh1-APC regulates protein synthesis via stress granules	162
Figure 6-3: Cdh1-APC has a dual role in protein homeostasis.....	163

Chapter 1 :

General Introduction

Portions of this chapter were adapted from the following publication:

Banerjee A, Ifrim MF, **Valdez AN**, Raj N, Bassell GJ. (2018) Aberrant RNA Translation in Fragile X Syndrome: From FMRP Mechanisms to Emerging Therapeutic Strategies. *Brain Res.* 1693(Pt A): 24-36. PMID: 29653083

The intricate connections between neurons and the synaptic networks that arise from these connections are critical for higher brain functions. The structure and functioning of a synapse changes as the connection between two neurons is altered such as during development, learning, and memory. Synaptic strength can be altered through the insertion or removal of receptors needed to propagate the electrochemical signal to the postsynaptic neuron, or the physical structure of the synapse can be affected through cytoskeleton remodeling of the postsynaptic site. This ability of the synapse to change and lead to altered neuronal connectivity is critical for learning and memory. During molecular forms of learning and memory, postsynaptic activation of receptors, typically N-methyl-D-aspartate receptors (NMDAR) or metabotropic glutamate receptors (mGluR), leads to the downstream synthesis and activation of effector molecules that eventually trigger the insertion or removal of postsynaptic receptors (Bear and Malenka, 1994). For example, Long Term Potentiation (LTP) leads to an increase in synaptic strength following the insertion of α -amino-3-hydroxy-5-methyl-4-isoxazolepropionic acid receptors (AMPA)(Bear and Malenka, 1994). Inversely, Long Term Depression (LTD) leads to a decrease in synaptic strength following the removal of AMPAR (Bear and Malenka, 1994). The balance of synthesis and degradation of proteins necessary for these receptor alterations is critical for learning and memory (Abraham and Williams, 2008; Bradshaw et al., 2003; Fonseca et al., 2006; Kauderer and Kandel, 2000; Santini et al., 2014). Dysregulated protein homeostasis can lead to improper forms of learning and memory and has been observed in several neurodevelopmental disorders, such as Angelman Syndrome (Greer et al., 2010; Kishino et al., 1997; Lee et al., 2014), Autism Spectrum Disorder (Tastet et al., 2015; Tsai et al., 2012; Yi et al., 2015), and Fragile X Syndrome (Gross and Bassell, 2012; Gross et al., 2010; Sharma et al., 2010). Thus, it is crucial that neurons tightly regulate protein turnover via both the synthesis and degradation of proteins.

1.1. Protein Synthesis

The synthesis of proteins is a multi-stepped process that can be regulated at various phases. The process begins with the unwinding of the DNA double helix by DNA helicases, which allows for one of the strands to act as a template for transcription, the synthesis of RNA. In eukaryotes, multiple RNA polymerases are recruited to carry out transcription (Alberts et al., 2019). Different classes of RNA require distinct RNA polymerases; RNA polymerase I is utilized for most rRNA genes, RNA polymerase II is utilized for protein-coding genes and miRNA genes, and RNA polymerase III is utilized for tRNA genes and 5S rRNA genes (Alberts et al., 2019). Following transcription, mRNA is capped at the 5' end and polyadenylation occurs in the nucleus; the 3' poly(A) tail of mRNA is critical for mRNA stability (Guhaniyogi and Brewer, 2001). Additionally, RNA splicing can occur in the nucleus by the spliceosome, which increases the diversity of protein product isoforms that are produced from one single gene (Lee and Rio, 2015). Mature RNA is then exported from the nucleus into the cytoplasm via nuclear export receptors (Kohler and Hurt, 2007). Once the RNA transcript has reached the cytoplasm, it is used to direct polypeptide polymerization to form a protein in the process known as translation.

In a translationally repressive state, eIF4E-binding proteins (eIF4-BP) bind to eIF4E. Following activation of the mammalian target of rapamycin (mTOR) pathway, eIF4-BP is phosphorylated and dissociates from eIF4E. eIF4E can then bind eIF4G to signal ribosome recruitment to the 5' end of the mRNA (Gingras et al., 2001). The 40S small ribosomal subunit, eIF1, eIF1A, eIF3, eIF5, and eIF2-GTP with Met-tRNA_i form the 43S pre-initiation complex (43S PIC) (Hinnebusch, 2014). The 43S pre-initiation complex is loaded onto the 5' end of the mRNA and scans for the AUG codon, known as the start codon (Hinnebusch, 2014). Once the AUG

sequence is recognized by the 43S PIC, the components of the complex disassemble, and the 60S large ribosomal subunit is recruited to the small ribosomal subunit to form the full 80S ribosome (Hinnebusch, 2014). The small ribosome subunit matches the mRNA codons to appropriate tRNAs carrying the amino acids (Alberts et al., 2019). Meanwhile, the large subunit catalyzes the peptide bonds between amino acids to form the elongating polypeptide chain. During elongation, the next charged tRNA is recruited to the A site of the ribosome. rRNA catalyzes peptide formation and the ribosome advances 3 nucleotides in the 3' direction of the mRNA (Alberts et al., 2019). The P site of the ribosome accommodates the growing polypeptide chain and the E site of the ribosome holds empty tRNA prior to it being released (Alberts et al., 2019). Once the ribosome reaches a stop codon (UGA, UAA, UAG), release factors cause the ribosome to catalyze the addition of a water molecule instead of an amino acid, and the completed polypeptide is released from the ribosome (Jackson et al., 2012). The protein can then be subjected to post-translational modifications, such as phosphorylation, acetylation, glycosylation, and ubiquitination (which will be discussed below in section 1.2). Post-translational modifications confer a diversity of functions and roles on proteins; proteins may only be present in certain cellular compartments, during specific phases of the cell cycle, or may only interact with other molecules dependent on its modifications (Walsh, 2006). Thus, the genetic code dictating a protein's amino acids is not the only critical determinant of a protein's function.

1.1.1. Local Protein Synthesis in Neurons

Neurons are a highly specialized cell type that require spatial regulation of gene expression to maintain polarity (Martin and Ephrussi, 2009). This is primarily accomplished through the efficient trafficking of mRNA from the nucleus directly to the sites where protein synthesis will occur as opposed to all proteins being synthesized in the soma (Sossin and DesGroseillers, 2006).

Typically, a form of neuronal stimulation recruits the mRNA to be trafficked to the site of synthesis. For example, stimulation of neurons with neurotrophin-3 leads to the localization of β -*Actin* mRNA and β -Actin protein to the neuronal growth cones (Bassell et al., 1998; Zhang et al., 1999). The localized synthesis of β -Actin at the growth cone is necessary for important developmental events, such as growth cone guidance in response to brain derived neurotrophic factor (BDNF) and netrin-1 (Welshhans and Bassell, 2011; Yao et al., 2006).

In order for mRNAs to be successfully trafficked to different locations within the cell, the mRNA must be bound to an RNA binding protein that may then interact with a motor protein (such as a member of the kinesin or dynein family) that will travel the cytoskeleton to bring the mRNA cargo to its destination. For example, zipcode binding protein 1 (ZBP1) binds to β -*Actin* mRNA via a 3' regulatory motif on the mRNA and controls its transport to dendrites (Kislauskis et al., 1994; Ross et al., 1997). Disruption of the interaction between ZBP1 and KIF11 (a kinesin-family motor protein) leads to de-localization of β -*Actin* mRNA and has severe impacts on cellular motility (Song et al., 2015). Aside from trafficking the mRNA to its final destination, RNA binding proteins may also act as translational repressors. As an RNA binding protein prevents the translation of mRNA during its trafficking, the RNA binding protein adds a level of regulation to the specificity of where the protein is synthesized (Brinegar and Cooper, 2016). Post-translational modifications of RNA binding proteins may act as molecular switches to allow for the release of mRNA and subsequent increase in the local translation of mRNA. For example, phosphorylation of ZBP1 halts its ability to repress β -*Actin* translation (Huttelmaier et al., 2005). As will be discussed further in-depth below, the dephosphorylation of another RNA binding protein known as the Fragile X Mental Retardation Protein (FMRP) regulates its ability to repress local translation of *PSD-95* mRNA (Ifrim et al., 2015; Muddashetty et al., 2011). The trafficking of RNA to

different subcellular compartments and its repression during that process are vital to the local synthesis of proteins in neurons.

1.1.2. Stress Granules

As will be further explored in Chapter 5, a way in which cells are further able to exert spatiotemporal control over protein synthesis is via the formation of stress granules (Buchan and Parker, 2009). Stress granules are membrane-less organelles that sequester pools of mRNA and prevent their translation (Buchan and Parker, 2009). Thus, stress granule formation is a way for cells to stall protein synthesis. Aside from containing mRNAs stalled in the process of initiation, stress granules contain translation initiation factors (eIF4E, eIF4G, eIF4A, eIF4B, eIF3, eIF2) and specific stress granule messenger ribonucleoproteins (mRNPs) (Buchan and Parker, 2009). Examples of stress granule-specific proteins are: FXR1, FXR2, FMRP, FUS, G3BP1, G3BP2, and TIA (Jain et al., 2016; Markmiller et al., 2018). About 50% of the stress granule proteome have RNA binding activity (Jain et al., 2016). The stoichiometry of stress granules is dependent on the type of stress the cell is experiencing (Buchan and Parker, 2009; Protter and Parker, 2016). For example, G3BP1 and Caprin are required for stress granule formation during oxidative stress (Solomon et al., 2007), but not during osmotic stress (Kedersha et al., 2016). Sequestration of mRNAs, mRNPs, and initiation factors may lead to a decrease in the concentration of these molecules in the cytosol, which may then affect downstream biochemical reactions (Buchan and Parker, 2009).

Stress granule assembly can be regulated by the modification (i.e. phosphorylation, acetylation, methylation) of stress granule mRNPs, protein-protein interaction of the mRNPs, and the microtubule network (Buchan and Parker, 2009). The formation of stress granules leads to the

sequestration of mRNAs and initiation factors (Buchan and Parker, 2009). Stress granules have a biphasic structure with a stable core and a shell that are assembled in a step-wise manner (Wheeler et al., 2016). The formation of the core is an early step in stress granule assembly (Wheeler et al., 2016). Untranslated mRNPs are then nucleated to form the core; individual cores then dock with one another to form the outer shell (Wheeler et al., 2016).

Following stress, RNA-binding proteins, such as Staufen (Thomas et al., 2009) and Grb7 (Tsai et al., 2008), disrupt interactions amongst stress granule components. Similar to how stress granule assembly is a multi-step process, stress granule disassembly occurs in an organized manner. First, larger, mature stress granules are broken up into smaller foci. Then, the outer shell of the granule is disassembled, which releases the previously sequestered mRNAs into the cytosol for translation (Wheeler et al., 2016). The remaining small foci containing the stress granule core are then cleared via autophagy.

The mechanisms underlying stress granule formation and disassembly are of particular interest for understanding the pathophysiology of neurodegenerative disease. Pervasive stress granule formation is an observed phenotype for some neurodegenerative diseases, such as amyotrophic lateral sclerosis (ALS) (Li et al., 2013; Monahan et al., 2016). A current objective of the neurodegenerative field is to manipulate stress granule formation to develop novel therapeutic options (Wolozin and Ivanov, 2019). It is currently unknown whether stress granule dynamics may be perturbed in neurodevelopmental diseases.

It is important to note that there is a shared biology between stress granules and other RNP granules, such as neuronal granules (Protter and Parker, 2016). For example, Caprin is a well described stress granule protein (Jain et al., 2016) that is also found to regulate mRNA localization and translation in neuronal dendrites (Nakayama et al., 2017; Shiina et al., 2005). Insight into how

these proteins are regulated and contribute to local protein synthesis in the context of stress granules may help to further the understanding of how they function in the context of other mRNP granules. Stress granule formation and disassembly and the proteins that modify these processes serve as a mechanism by which translation can be spatiotemporally regulated. The balance between stress granule formation and protein synthesis is a central focus of Chapter 5.

1.2. Ubiquitination

Aside from control over the synthesis of proteins, cells are able to regulate protein homeostasis through the degradation of proteins. A classic mechanism by which specific proteins are targeted and degraded is known as ubiquitination (Hegde, 2004). The ubiquitin-proteasome system (UPS) is required for both LTP (Karpova et al., 2006) and LTD (Hou et al., 2006).

Ubiquitination consists of a posttranslational modification where a small 76 amino acid protein known as ubiquitin is attached to lysine residues on a target substrate via an isopeptide bond (Hegde, 2004). Attachment of one single ubiquitin onto a substrate is known as monoubiquitination and typically signals a conformational change for the substrate (Hegde, 2004). Multiple single ubiquitins may also be attached on multiple lysines on a substrate (multiple monoubiquitination) and can signal endocytosis of the substrate (Hegde, 2004). Monoubiquitination can also regulate a substrate's interaction with other proteins. For example, monoubiquitination of SMAD4, a transcription factor, prevents its ability to bind its signaling partner SMAD2 (Dupont et al., 2009). Ubiquitin itself has six lysine residues (K6, K11, K27, K29, K48, K63), allowing for it to be ubiquitinated and eventually form a polyubiquitin chain (Swatek and Komander, 2016). The number of ubiquitins and the specific polyubiquitination branching patterns determine the ultimate fate of the substrate. Classically, polyubiquitination of a substrate

where the 11th (K11) or 48th lysine (K48) of ubiquitin is ubiquitinated leads to the recognition of the substrate by the 26S proteasome and the substrate's degradation (Swatek and Komander, 2016). Polyubiquitination occurring on the 63rd lysine (K63) of ubiquitin leads to other downstream signaling, such as DNA repair (Liu et al., 2018), endocytosis (Lauwers et al., 2009), or NF- κ B activation (Deng et al., 2000). The downstream consequences of other types of polyubiquitin chains are still not fully understood.

1.2.1. Addition of Ubiquitin onto Substrates

The attachment of ubiquitin onto lysine residues is accomplished by the coordinated activity of three classes of enzymes: ubiquitin-activating enzymes (E1 enzymes), ubiquitin-conjugating enzymes (E2 enzymes), and ubiquitin-ligase enzymes (E3 enzymes) (**Figure 1-1**) (Hegde, 2004). E1 enzymes catalyze the activation of ubiquitin with ATP (Hegde, 2004). During this reaction, the ubiquitin is covalently attached to a catalytic cysteine on the E1 enzyme (Hegde, 2004). The ubiquitin is then transferred to a cysteine on an E2 enzyme (Hegde, 2004). The E2-ubiquitin complex can then bind to an E3 enzyme (Hegde, 2004). While still attached to the E2-ubiquitin complex, the E3 enzyme will bind to a specific substrate, typically through a conserved recognition motif (Hegde, 2004). The E3 enzyme will catalyze the transfer of the ubiquitin from the cysteine on the E2 onto a lysine on the target substrate via an isopeptide bond (Hegde, 2004). There are many combinations of coordinated activity between E1s/E2s/E3s: humans have about 10 genes encoding E1 enzymes, 100 genes encoding E2 enzymes, and about 1000 genes encoding for E3 enzymes (Hicke et al., 2005). To further emphasize the diversity of E3 ubiquitin ligases, it is of note that 5% of the human genome encodes for E3 enzymes (George et al., 2018).

With the large diversity of E3 ubiquitin ligases, these enzymes can be categorized into three classes: HECT domain E3s, RING finger E3s, and RBR E3s (Morreale and Walden, 2016).

HECT (homologous to E6AP carboxyl terminus) domain E3 ligases contain a conserved domain at the C-terminus of the protein with a bi-lobar architecture (Morreale and Walden, 2016). The N-terminal lobe of the HECT domain recruits the E2-ubiquitin complex while the C-terminal lobe of the HECT domain contains the catalytic cysteine that allows for the ubiquitin transfer onto the substrate (Morreale and Walden, 2016). The N-terminus of HECT domain E3s determines substrate specificity. The E3 ubiquitin ligase E6-AP, which ubiquitinates tumor suppressor protein p53, is a prototypical HECT domain E3 ligase (Hegde, 2004; Huibregtse et al., 1993). The RING finger E3 ligases are the largest group of E3 ligases with each enzyme containing the critical RING (really interesting new gene) domain (Morreale and Walden, 2016). The RING domain is made up of seven cysteine residues and one histidine residue arranged as a folded domain that can then bind two zinc ions (Hegde, 2004). RING E3 ligases can function as monomers, homodimers, or heterodimers. Mdm2, which also ubiquitinates tumor suppressor p53, is a well-studied RING E3 ligase (Hegde, 2004). Interestingly, the form of p53 that is a substrate for E6-AP has an asparagine at position 268 while the form of p53 that is a substrate for Mdm2 has an aspartate at position 268 (Hengstermann et al., 2001). The targeting of p53 by both E6-AP and Mdm2 demonstrates how substrates are targeted by variety of E3 ligases dependent on the context. The final class of E3 ligases are known as RING-between-RING (RBR) E3s (Morreale and Walden, 2016). These enzymes contain two RING domains separated by an in-between-RING domain (IBR) (Morreale and Walden, 2016). The first RING domain, RING1, recruits the E2-ubiquitin complex while the second RING domain, RING2, contains a catalytic cysteine for the ubiquitin transfer (Morreale and Walden, 2016). A prototypical RBR E3 ligase is Parkin which targets Mfn1 and Mfn2, GTPases that play a role in oxidative phosphorylation (Youle and van der Bliek, 2012). While RING E3s allow the direct transfer of ubiquitin onto the substrate from the E2 enzyme, HECT domain E3s

and RBR E3s transfer ubiquitin in a two-step process where ubiquitin is transferred from the E2 onto the catalytic cysteine on the E3 before being conjugated to the substrate (Morreale and Walden, 2016) (**Figure 1-1**).

While the identity of the E1 enzyme does not impact which specific target protein will be eventually ubiquitinated, E2s and E3s have been observed to possess substrate specificity. It has been shown that E2 enzymes are capable of directing ubiquitin onto specific lysines of the target substrates (David et al., 2010) and are believed to interact with only specific E3 enzymes (Hegde, 2004). E3 enzymes are considered to have the highest level of specificity for target substrates (David et al., 2011; Hegde, 2004), typically through highly-conserved binding domains (Zheng and Shabek, 2017). Thus, the different combinations of E2 and E3 enzymes confer a high degree of specificity on the substrate to be ubiquitinated.

It is important to note that ubiquitination is a reversible post-translational modification. Ubiquitin can be cleaved off a substrate protein by a class of enzymes known as Deubiquitinating enzymes (DUBs)(de Poot et al., 2017). The dynamics of substrate ubiquitination by E1, E2s, and E3s and de-ubiquitination by DUBs provides opportunity for further spatiotemporal control over the downstream fate of a protein substrate and its role in downstream molecular pathways, such as molecular forms of learning and memory.

1.2.2. Ubiquitination is Dysregulated in Neurodevelopmental Disorders

Mutations have been found in 13% of known E3 ubiquitin ligase genes that lead to neurological disorders (George et al., 2018). Neurodevelopment is highly susceptible to disruptions in the UPS, as it is a delicate time period that requires tight regulation of protein synthesis and degradation for the appropriate establishment and connectivity of synapses to form

functioning neural networks. Severe dysregulation of synaptic connectivity may result from improper regulation of protein synthesis and degradation during development. A number of neurodevelopmental diseases, such as autism spectrum disorder (ASD) (Tastet et al., 2015; Tsai et al., 2012; Yi et al., 2015), Angelman syndrome (Greer et al., 2010; Kishino et al., 1997; Lee et al., 2014), and Juberg-Marsidi Syndrome (Friez et al., 2016) are associated with disrupted ubiquitination pathways (George et al., 2018).

Current research is focused on discovering E3 ligases disrupted in neurodevelopmental disorders and elucidating their roles in neurodevelopment. For example, loss-of-function mutations for the HACE1 E3 ubiquitin ligase were discovered to underlie an autosomal recessive neurodevelopmental syndrome (Hollstein et al., 2015). More than fifty years after the discovery of Angelman Syndrome (Angelman, 1965), it is now known that Ube3A, the E3 ligase mutated in Angelman syndrome patients, regulates LTP and dendritic spine morphology (Silva-Santos et al., 2015). Aside from those implicated in known disorders, multiple E3 ligases have been shown to play critical roles in neurodevelopment such as neurite growth, dendritic morphogenesis, axonal growth, differentiation, neural tube formation, and synaptogenesis (Upadhyay et al., 2017). Ubiquitination can regulate Hedgehog signaling, a highly-studied molecular pathway shown to regulate cell fate and neural tube patterning (Di Marcotullio et al., 2006). The ITCH E3 ubiquitin ligase ubiquitinates the transcription factor Gli1, thereby targeting Gli1 for degradation and suppressing Hedgehog signaling (Di Marcotullio et al., 2006). E3 ubiquitin ligase functions are crucial for neurodevelopmental and disrupted functioning may then lead to neurodevelopmental disorders (Upadhyay et al., 2017).

The identification of dysregulated ubiquitination as a shared pathologic mechanism in ASD, Angelman syndrome, and other forms of intellectual disability hints at a proposed shared

neurobiology amongst neurodevelopmental disorders. While neurodevelopmental disorders such as ASD, Angelman syndrome, and schizophrenia have distinct signs and symptoms, dysregulation of protein homeostasis has been suggested as a shared etiology amongst them (Chen et al., 2018; English et al., 2015; Gkogkas et al., 2013). Though inadequate or excessive protein synthesis may lead to the observed pathology, alteration in in the UPS may also directly lead to observed phenotypes (George et al., 2018). Understanding mechanisms of disrupted protein homeostasis, either through protein synthesis or degradation, in a neurodevelopmental disorder will assist in the elucidation of pathologic mechanisms in related neurodevelopmental disorders.

1.3. Fragile X Syndrome

One neurodevelopmental disease that currently has no FDA-approved treatments is fragile X syndrome (FXS), the most common heritable form of intellectual disability. Patients with FXS suffer from a wide variety of symptoms such as severe intellectual disability, sensory disorders, hyperactivity, reproductive issues, and seizures (Penagarikano et al., 2007). Unlike other neurodevelopmental diseases with complex or unknown genetics, FXS is caused by the loss of only one protein, the Fragile X Mental Retardation Protein (FMRP) (Penagarikano et al., 2007). FMRP is an RNA-binding protein that is encoded by the *FMRI* gene. In typical fragile X syndrome patients, there is an expansion of a (CGG)_n trinucleotide repeat in the 5' promotor region of the *FMRI* gene (Penagarikano et al., 2007). Once the number of repeats goes above 200, the *FMRI* gene is methylated and subsequently silenced (Penagarikano et al., 2007). As discussed below, some cases of FXS are due to a missense mutation and not full gene silencing.

Despite lacking only FMRP, symptoms of FXS are complex and multifaceted. This suggests that FMRP must play a vital role in multiple cellular processes. The fragile X field has

focused on elucidating the function of FMRP through the use of postmortem tissue from human patients as well as the *Fmr1* knockout (*Fmr1* KO) rodent models (Banerjee et al., 2018).

1.3.1. Dysregulation of Dendritic Spines in Fragile X Syndrome

As in other neurodevelopmental diseases (Penzes et al., 2011; Wang et al., 2017), patients with FXS have been observed to have a distinct dendritic spine phenotype (Hinton et al., 1991; Irwin et al., 2001). Dendritic spines are the protrusions from the postsynaptic neuron's dendrite that receive stimulation from the presynaptic axon and allow for the transmission of the signal to the postsynaptic cell body (Colgan and Yasuda, 2014). Dendritic spine morphology is typically correlated with the maturity of the spine (Yuste and Bonhoeffer, 2001). During early development, immature dendritic spines can be observed as having a long, thin, filapodial shape (Lei et al., 2016). As development progresses, synaptic pruning occurs and mature spines can be identified as having a stubby/mushroom morphology (Lei et al., 2016). Improper spine formation or pruning can be an underlying pathology for neurodevelopmental disorders, as they suggest improper network formations.

An increased distribution of thin, elongated, immature-appearing dendritic spines have been documented in postmortem brain samples from FXS patients, suggesting regulation of spine morphology is downstream of FMRP (De Rubeis et al., 2013; Hinton et al., 1991; Irwin et al., 2001). It is hypothesized that absence of FMRP causes deficits in synaptic pruning, leading to the increased distribution of immature-appearing spines and synapses (Bagni and Greenough, 2005; Pfeiffer and Huber, 2007, 2009; Weiler and Greenough, 1999). When FMRP is expressed acutely and postsynaptically in *Fmr1* KO neurons, there is a decrease in the number of synapses, further offering evidence that FMRP regulates synaptic pruning (Pfeiffer and Huber, 2007).

Studies on MEF2-induced synapse elimination have provided support for the hypothesis that FMRP is involved in synaptic pruning (Pfeiffer et al., 2010). Myocyte-enhancing factor (MEF2) is an activity-dependent transcription factor that has been described to control gene expression and play a critical role in development (Potthoff and Olson, 2007). Activation of MEF2 in neurons leads to the elimination of synapses, as observed through reduced mini-excitatory postsynaptic currents and reduced spine numbers (Barbosa et al., 2008; Pfeiffer et al., 2010). When MEF2 is expressed in *Fmr1* KO neurons, there is no reduction in synapses (Pfeiffer et al., 2010). MEF2-induced synapse elimination can be rescued by transfecting wildtype FMRP into the *Fmr1* KO neurons, providing evidence that FMRP plays a vital role in MEF2-induced synapse elimination (Pfeiffer et al., 2010). The work of multiple groups in FXS models of disease ranging from human postmortem samples to *Fmr1* KO mice have demonstrated FMRP's regulatory role in dendritic spine development, pruning, and synapse formation/elimination (He and Portera-Cailliau, 2013). Disruptions in these processes may be the pathology underlying the learning and memory phenotypes in FXS patients.

1.3.2. Aberrant mGluR-LTD in Fragile X Syndrome

In addition to the impact that FMRP has on the establishment and elimination of synapses and dendritic spines, FMRP has been well studied to regulate LTD following mGluR signaling (Bear et al., 2004; Huber et al., 2002; Tian et al., 2017). mGluR-LTD is a molecular form of learning and memory in which the connection between two neurons is weakened (Bear and Malenka, 1994). When wildtype neurons are treated with dihydroxyphenylglycine (DHPG), a mGluR5 agonist, there is a significant decrease in the excitatory postsynaptic (EPSC) amplitude. With the observations of altered dendritic spine formation and pruning, it was initially

hypothesized that *Fmr1* KO neurons would have disruptions in mGluR-LTD (Bear et al., 2004). However, when *Fmr1* KO neurons are treated with DHPG, mGluR-LTD is enhanced compared to the response of wildtype neurons (Huber et al., 2002). In wild type brain slices, DHPG stimulation in vivo leads to the elongation of dendritic protrusion in layer 2/3 neurons (Cruz-Martin et al., 2012). However, dendrites in brain slices from *Fmr1* KO mice do not elongate following DHPG stimulation (Cruz-Martin et al., 2012), further demonstrating aberrant responses to mGluR stimulation in the absence of FMRP. The discovery of the regulation of mGluR-LTD by FMRP demonstrates not only does FMRP play a role in the establishment of connections between neurons, but it regulates activity-dependent synaptic plasticity. Stimulation of mGluRs was previously observed to lead to rapid protein synthesis in synaptoneuroosomes (Weiler and Greenough, 1993), leading the field to turn to investigate whether or not FMRP regulates protein synthesis downstream of this mGluR signaling as well.

1.3.3. Dysregulated Protein Synthesis in Fragile X Syndrome

Increased basal rates of protein synthesis and loss of stimulus-induced protein synthesis have been observed in both the mouse model of FXS (Gross et al., 2010; Liu et al., 2012; Sharma et al., 2010) and cells from FXS patients (Gross and Bassell, 2012), providing evidence that FMRP has a direct influence on protein synthesis.

As a follow-up on the observation that FXS leads to aberrant mGluR-LTD responses, FXS models have demonstrated dysregulated mGluR5 activation of protein synthesis and signal transduction (Bear et al., 2004; Gross et al., 2010; Osterweil et al., 2010; Sharma et al., 2010). This dysregulation specifically impacts mammalian target of rapamycin (mTOR) signaling pathways (Gross et al., 2015a; Sharma et al., 2010). There are several downstream molecules contributing

to altered mGluR5-mediated signal transduction that are dysregulated in FXS, including PI3K, ERK and S6K (Richter et al., 2015). Taken together with observations of dysregulated mGluR-LTD, these studies suggest a connection between dysregulated protein synthesis and intellectual disability phenotypes in fragile X syndrome patients (Banerjee et al., 2018). A molecular understanding of the underlying mechanisms by which FMRP can regulate mRNA translation and related signaling pathways is necessary to better understand the pathology in human patients.

1.4. FMRP Functions as a Translational Repressor

With the well-characterized phenotype of exaggerated protein synthesis in FXS model cells, it is understood that FMRP acts as a molecular break on protein synthesis and represses the translation of specific mRNAs (Banerjee et al., 2018). Many of the mRNAs targeted by FMRP are critical for synaptic structure and function, such as *PSD-95*, *Arc*, and *Shank1* (Ascano et al., 2012; Darnell et al., 2011; Pasciuto and Bagni, 2014b). The impact that FMRP has on synaptic functioning is also emphasized by over 30% of the presynaptic proteome and 26% of the postsynaptic proteome being targeted by FMRP (Darnell et al., 2011). While it has been of much interest to determine which mRNAs are dysregulated in FXS, it has been identified that there are multiple mechanisms by which FMRP can repress translation. In order to provide any mechanistic insight into dysregulated protein synthesis in FXS models, it is critical to have an understanding how FMRP can physiologically regulate translation. As will be discussed below, FMRP can regulate the translation of these target mRNAs through multiple mechanisms such as polyribosome stalling, association with the RNA-induced silencing complex (RISC), and other less well-characterized mechanisms.

1.4.1. FMRP Directly Binds RNA

It is well known that FMRP can interact directly with multiple mRNAs to regulate their translation (Banerjee et al., 2018). Therefore, many studies have focused on identifying common sequence motifs amongst confirmed FMRP target RNAs (Ascano et al., 2012; Darnell et al., 2001; Darnell et al., 2011; Suhl et al., 2014). Initial studies identified the G-quartet structure as a reoccurring feature of FMRP targets through both FMRP-RNA co-immunoprecipitation (RIP-CHIP) (Brown et al., 2001) and oligonucleotide-based systematic evolution of ligands by exponential enrichment (SELEX) (Darnell et al., 2001). 14 of the RNAs identified to bind FMRP were also altered in polysome distribution in lymphoblastoid cell lines derived from fragile X patients (Darnell et al., 2001), demonstrating that translation of these mRNAs was dysregulated. After the identification of the G-quadruplex as a recognition motif for FMRP, others identified a group of mRNAs targeted by FMRP that contain sequences rich in uracil residues (Chen et al., 2003) through the use of a modified SELEX protocol. Interestingly, in *Fmr1* KO mice, the mRNA levels of identified uracil-rich targets remain unchanged, suggesting a different fate for uracil-rich targets of FMRP compared to G-quadruplex-rich targets of FMRP (Chen et al., 2003). RIP-CHIP was also utilized to identify ACUK and WGGA as two key RNA-recognition elements for FMRP (Ascano et al., 2012). Together, these studies demonstrate an enrichment of cis-element-specific binding sites in the 5' and 3' untranslated regions (UTRs) of FMRP targets (Ascano et al., 2012; Stefanovic et al., 2015; Suhl et al., 2014; Zhang et al., 2014b). Crosslinking-immunoprecipitation has been combined with high-throughput sequencing (HIT-CLIP) to generate an extensive list of FMRP targets *in vivo* (Darnell et al., 2011). HIT-CLIP revealed that FMRP binds most frequently to the coding regions of mRNA as opposed to motifs within the 5' and 3' UTRs (Darnell et al., 2011). Comparison of targets generated by each of these methods demonstrates overlap for

multiple mRNAs, strengthening the hypothesis that dysregulation of the translation of these mRNAs may be central to the pathology underlying FXS.

Aside from elucidating which motifs on RNA are targets for FMRP, it is critical to understand what structural properties of FMRP are critical for binding RNA. FMRP contains multiple structural motifs that allow it to bind directly to its RNA targets, such as KH domains and an RGG box (Ashley et al., 1993; Siomi et al., 1993). A single point mutation in *FMR1* reveals the importance of FMRP's KH2 domain for RNA binding (De Boulle et al., 1993; Siomi et al., 1994). The missense mutation of an isoleucine 304 to asparagine (I304N) in the KH2 domain of *FMR1* was discovered in a patient diagnosed with fragile X syndrome despite lack of *FMR1* silencing and a sufficient production of FMRP (Siomi et al., 1994). The severe phenotype due to one missense mutation indicates that an essential function of FMRP relies on an intact KH2 domain. Indeed, while wildtype FMRP is able to bind RNA, binding of FMRP I304N to RNA is impaired (Siomi et al., 1994). This suggests that loss of mRNA binding by FMRP is causative of FXS.

FMRP also contains an RGG box, a motif rich in arginines and glycines (Siomi et al., 1993). The RGG box facilitates the recognition and binding of G-quadruplexes to FMRP (Blackwell et al., 2010; Ramos et al., 2003). The function of RGG box binding to FMRP targets may therefore be important for mRNA localization (Stefanovic et al 2015; Subramanian et al 2011). Together with the KH2 domain, the RGG box plays a critical role in promoting the binding of FMRP directly onto mRNA. However, it is unclear if binding to mRNA alone is sufficient to repress its translation; FMRP may need to recruit other cellular machinery to accomplish this task.

1.4.2. FMRP Interacts with the RNA-Induced Silencing Complex

One of the ways that FMRP can regulate the translation of specific mRNAs is through its interaction with microRNAs (miRNAs) and components of the RNA-Induced Silencing Complex (RISC), such as Argonaute1 and Argonaute2 (Jin et al., 2004; Li et al., 2014; Muddashetty et al., 2011). Specific miRNAs guide RISC to target mRNAs and repress their translation via mRNA degradation or prevention of translation initiation (Meister et al., 2004). FMRP binding to target mRNA contributes to the ability of the miRNA-RISC complex to recognize the target mRNA (Li et al., 2014; Muddashetty et al., 2011). For example, FMRP promotes the binding of a miR-125a-RISC complex onto *PSD-95* mRNA and prevent its translation (Muddashetty et al., 2011). Additionally, FMRP promotes the miR-196a mediated translational repression of *HoxB8*, a mRNA that FMRP can directly bind (Li et al., 2014). As another example, FMRP cooperates with miR-125b to suppress translation of *NR2A* mRNA (Edbauer et al., 2010). miRNAs and RISC have been implicated in other neurodevelopmental disorders; miR-137 is a risk factor for schizophrenia (Schizophrenia Psychiatric Genome-Wide Association Study, 2011) and its dysregulation impacts neurodevelopmental pathways, such as BDNF signaling (Thomas et al., 2017). Thus, the effect of FMRP on neurodevelopment via the miRNA-RISC complex demonstrates another aspect to the shared neurobiology underlying neurodevelopmental disorders as a whole.

1.4.3. FMRP Binds Polyribosomes

FMRP has been well characterized to directly associate with polyribosomes (Corbin et al., 1997; Darnell et al., 2011; Stefani et al., 2004), suggesting another mode by which FMRP can directly regulate translation. It is currently thought that FMRP association reversibly stalls ribosomes (Darnell et al., 2011). FMRP-lacking mouse brains have an increased ribosome transit

rate (Udagawa et al., 2013), suggesting that FMRP directly stalls ribosomes. Specific regions of FMRP interact with polyribosomes to affect translation. Exploitation of the I304N FMRP mutation (as described above) has demonstrated the essential role of the KH2 domain in FMRP-polyribosome association (Darnell et al., 2005; Feng et al., 1997). Additionally, arginines within the RGG box promote FMRP-polyribosome association (Blackwell et al., 2010). However, it is unclear whether the KH2 domain and RGG box utilize cooperative or separate mechanisms to associate to polyribosomes.

FMRP's stalling of polyribosomes can be exploited to better understand pathology resulting from impaired translation in FXS models. Recent studies have utilized Translating Ribosome Affinity Purification (TRAP) to identify novel mechanisms by which FMRP mediates translation (Ouwenga et al., 2017; Thomson et al., 2017). Since FMRP-lacking neurons have an increased translation rate (Udagawa et al., 2013), TRAP followed by RNA-sequencing can identify excessively translated transcripts due to FMRP loss. This method has explored understudied targets of FMRP, such as *muscarinic acetylcholine receptor 4* mRNA (Thomson et al., 2017). Combination of the TRAP method with synaptoneurosomal fractionation demonstrates an enrichment of FMRP binding in mRNA that are translated in dendrites (Ouwenga et al., 2017; Thomson et al., 2017). This method provides a novel tool to observe how FMRP may play distinct roles in different regions of the neuron and thus help to elucidate how FMRP regulates local translation.

Despite the advances in FMRP research, it is unclear if the translational phenotypes in FXS cells are primarily due to the loss of FMRP binding to polyribosomes or if other mechanisms, such as direct binding to RNA or the RNA-induced silencing complex, are primary contributors to the underlying pathology.

1.4.4. Regulation of FMRP and *FMR1* mRNA by Association with other RNA-binding Proteins

Elucidation of RNA binding proteins that interact with FMRP and *FMR1* mRNA have given insight into potential mechanisms of FMRP-mediated translational regulation, as well as impairments in neurodevelopmental disorders other than FXS. Aside from interacting with protein components of RISC, FMRP interacts with other RNA-binding proteins to regulate translation. FMRP's direct association to MOV10, an RNA helicase, modulates the ability of RISC to bind to target mRNA (Kenny et al., 2014). FMRP can recruit MOV10 to unwind mRNA for association with RISC to lead to translational suppression (Kenny et al., 2014). On other mRNAs, the FMRP-MOV10 interaction may prevent RISC association, which promotes translation (Kenny et al., 2014). Thus, FMRP's association with MOV10 is both cooperative and dynamic, leading to different consequences on translation for specific mRNAs. It is unknown if posttranslational modifications may impact FMRP's ability to associate with MOV10 and promote/inhibit RISC association on mRNAs.

New evidence in a *Drosophila* model demonstrates an interaction between FMRP and the RNA-binding protein dNab2, the ortholog of human ZC3H14 (Bienkowski et al., 2017). ZC3H14 is a poly(A)-binding protein whose loss leads to an inherited form of intellectual disability (Pak et al., 2011). dNab2 and dFMRP interact in neurons in both the cytoplasm and nucleus (Bienkowski et al., 2017). Additionally, dNab2 directly binds to *CAMKII α* mRNA, a well-characterized FMRP target (Darnell et al., 2011), and suppresses its translation (Bienkowski et al., 2017). These observations suggest that dNab2 may facilitate the ability of dFMRP to repress translation of *CAMKII α* mRNA in neurons. Elucidation of whether or not dNab2/ZC3H14 is integral to the repression of mRNA by FMRP will help to contribute to the growing literature on mechanisms of

FMRP-mediated repression. With both dFMRP and dNab2 being linked to intellectual disability, the discovery of this interaction between dFMRP and dNab2 supports the hypothesis of a shared underlying neurobiology in intellectual disability.

Investigation of a variant in the 3'UTR of the *FMRI* gene found in developmentally delayed patients without FXS revealed a novel interaction with the RNA-binding protein HuR (also known as ELAVL1) (Suhl et al., 2015). HuR typically binds adenine/guanine rich elements in mRNAs and promotes mRNA stabilization (Brennan and Steitz, 2001). The inability of HuR to bind *FMRI* mRNA in this patient leads to a loss of RNA stability, as demonstrated by a faster mRNA decay rate of mutated *FMRI* mRNA compared to wildtype *FMRI* (Suhl et al., 2015). Aside from the direct influence HuR binding has on *FMRI* mRNA stability, the interaction is necessary for mGluR5-dependent protein synthesis in primary neurons (Suhl et al., 2015). mGluR-dependent protein synthesis was impaired in cells expressing mutated *FMRI* 3'UTR (Suhl et al., 2015). Thus, the interaction between HuR and *FMRI* mRNA has downstream consequences on translation and expression of FMRP.

1.5. Reversal of FMRP-mediated Repression

As described in section 1.1, translational repression of mRNAs by an RNA-binding protein may be reversible. This reversibility is essential for the neuron to exert spatiotemporal control over the translation of specific mRNAs. As many of FMRP's RNA targets play critical roles synaptic structure and function (Darnell et al., 2011), there needs to be a mechanism for the reversal of FMRP-mediated translational repression of these targets. While several mechanisms have been proposed to explain how FMRP represses protein synthesis, the mechanism of reversing the

repression is not well understood. Chapter 3 will focus on a proposed mechanism for the reversal of protein synthesis downstream of FMRP.

The mGluR signaling pathway, as described above, serves as a primary example as to the physiologic reversal of FMRP's repression of translation. The translation of FMRP-target RNAs is observed following mGluR stimulation with DHPG (Muddashetty et al., 2007; Muddashetty et al., 2011), suggesting that mGluR signaling leads to a post-translational modification of FMRP and prevents its ability to repress translation.

1.5.1. FMRP Modification as a Molecular Switch

Recent evidence indicates that post-translational modifications of FMRP are necessary to guide the miRNA-RISC complex to the target mRNA (Li et al., 2014; Muddashetty et al., 2011). Phosphorylated FMRP at serine 499 promotes the formation of a miR-125a-RISC complex on *PSD-95* mRNA to repress translation (Muddashetty et al., 2011). Downstream of mGluR5 signaling, FMRP is dephosphorylated by PP2A; this posttranslational event acts as a switch to de-repress translation (Muddashetty et al., 2011; Narayanan et al., 2007). The dephosphorylation of FMRP disrupts the interaction of FMRP to Argonaute2 as well promotes the release of miR-125a-RISC from *PSD-95* mRNA; release from RISC results in the translation of *PSD-95* (Muddashetty et al., 2011). Phosphorylation of FMRP as a translational repressive switch has also been observed for other miRNA-mRNA interactions. Phosphorylated FMRP promotes miR-196a-induced translational repression of *HoxB8* (Li et al., 2014). The phosphorylation/dephosphorylation of FMRP did not impact the ability of FMRP to bind directly to the target mRNA (Li et al., 2014). Thus, it is the association of other repressive complexes, such as RISC, to target mRNA that is

dependent on the phosphorylation state of FMRP. In both of the mentioned studies, mGluR5 stimulation was utilized to modulate the phosphorylated state of FMRP.

Evidence suggests that multiple kinases may regulate FMRP phosphorylation. Ribosomal protein S6 kinase, S6K1, plays a role in activity regulated phosphorylation of FMRP at serine 499 (Narayanan et al., 2008). However, phosphorylation of FMRP at serine 499 is also modulated by Casein Kinase II (Bartley et al., 2016; Bartley et al., 2014). Secondary phosphorylation of FMRP at other serines is may also be a regulatory step (Bartley et al., 2016). Despite the various models of FMRP phosphorylation, it has been well established that the phosphorylated state of FMRP is a mechanism for FMRP to recruit miRNA-dependent pathways to inhibit the translation of target mRNAs.

Similar to how phosphorylation affects the association of FMRP to RISC (Li et al., 2014; Muddashetty et al., 2011), phosphorylation can also regulate the downstream effects of FMRP-polyribosome interactions (Ceman et al., 2003). Both phosphorylated and unphosphorylated FMRP can bind polyribosomes, but it has been observed that primarily the phosphorylated form of FMRP is associated with stalled polyribosomes (Ceman et al., 2003). Thus, dephosphorylation may play a key role in regulating the reversibility of FMRP-mediated translational suppression. A major unanswered question is how FMRP mediated ribosome stalling is directly regulated by physiological signals. With how FMRP phosphorylation affects the ability of FMRP to interact with RISC and polyribosomes, it is a possibility that these two pathways of translational regulation are tightly coordinated with one another.

1.5.2. Ubiquitination of FMRP

The ubiquitination and subsequent degradation of FMRP has also been observed to occur downstream of mGluR signaling (**Figure 1-2**) (Hou et al., 2006). However, it was unclear if the dephosphorylation of FMRP occurs sequentially with the ubiquitination event or if these are two distinct pathways. Through the inhibition of the proteasome with MG-132, it was observed that dephosphorylation of FMRP is not dependent on the ubiquitin-proteasome system (Nalavadi et al., 2012). However, by utilizing okadaic acid to inhibit PP2A, it was determined that the ubiquitination and degradation of FMRP is dependent on its dephosphorylation by PP2A (Nalavadi et al., 2012). This work by Nalavadi et al. proposed a model by which mGluR5 stimulation leads to a sequence of dephosphorylation and then ubiquitination of FMRP. However, it is still unclear whether the ubiquitination of FMRP is necessary for the RISC-release and translation of *PSD-95* mRNA described previously.

As described earlier, there is a high level of specificity for the substrates an E3 ubiquitin ligase will ubiquitinate. Thus, there must be a specific E3 ubiquitin ligase that is responsible for ubiquitinating FMRP downstream of mGluR5-mediated dephosphorylation. The regulatory subunit Cdh1 (encoded by the Fizzy and Cell Division Cycle Related 1, *FZR1*, gene) of the E3 ubiquitin ligase Anaphase Promoting Complex (APC) was observed to associate *in vivo* (Huang et al., 2015) and *in vitro* (**Figure 1-3**) with FMRP (Huang et al., 2015). Knockdown of Cdh1 prevented DHPG-induced degradation of FMRP (Huang et al., 2015), suggesting that the Cdh1-APC E3 ubiquitin ligase complex may be responsible for ubiquitinating FMRP following mGluR stimulation. Thus, the Cdh1-APC complex may be a critical E3 ubiquitin ligase for the reversal of FMRP-mediated translational repression. In Chapter 3, we investigate if Cdh1-APC expression is sufficient to reverse FMRP-mediated repression of translation.

1.6. The Anaphase Promoting Complex (APC)

The Anaphase Promoting Complex (APC) is a largely studied E3 ubiquitin ligase composed of 11-13 subunit proteins (Barford, 2011). As a multi-subunit RING E3 ubiquitin ligase (refer to section 1.2.1 for more detail on this class of E3 ubiquitin ligases), APC contains two essential binding sites: one for binding to an E2 ubiquitin conjugating enzyme actively coupled to ubiquitin, and one for binding the targeted protein substrate (Barford, 2011). The catalytic core of APC consists of the Apc2 Cullin protein and APC11 RING protein (Tang et al., 2001). APC catalyzes the ubiquitination of substrates when the C-terminal domain of Apc2 forms a tight complex with APC11 (Tang et al., 2001). As discussed further in-depth below, APC has been primarily characterized for its role in promoting the transition from metaphase to anaphase during mitosis through the tagging of specific substrates with ubiquitin for ultimate degradation by the 26S proteasome (Sudakin et al., 1995). While the APC core subunits contain the catalytic activity for ubiquitination of substrates, the specificity of APC for its substrates may be determined by adaptor regulatory subunits (Barford, 2011).

The two primary regulatory subunits for APC are Cdc20 (together forming Cdc20-APC) and Cdh1 (forming Cdh1-APC) (Barford, 2011). Cdc20 association with APC is required for proper APC activity during early mitosis whereas Cdh1 association with APC is required for APC activity during late mitosis and G1 (Visintin et al., 1997). Cdc20 and Cdh1 regulate each other's activation and association with APC. In early mitosis, Cdk phosphorylates Cdh1 on nine conserved residues, inhibiting its activity (Zachariae et al., 1998). Cdc20-APC ubiquitinates Cdk to be targeted for proteasomal degradation (Barford, 2011). The reduction of Cdk levels leads to the de-repression of Cdh1 and formation of Cdh1-APC complexes (Barford, 2011). Cdh1-APC can then

ubiquitinate Cdc20 and lead to reduction of Cdc20-APC levels (Barford, 2011). The opposing activity of Cdc20-APC and Cdh1-APC allows for specific substrates to be degraded in either the Cdc20-APC or Cdh1-APC phase of the cell cycle (Barford, 2011). Both Cdc20 and Cdh1 contain WD40 domains that are required for substrate interactions (Kraft et al., 2005). Without binding to Cdc20 or Cdh1, APC is unable to target and ubiquitinate substrates (Barford, 2011).

The APC has been observed to target substrates containing one of two conserved motifs. The first APC-targeting motif to be discovered was the “Destruction box” (D-box), originally discovered in sea urchin cyclin B, which is a nine-residue sequence consisting of RxALGxIxN (Glotzer et al., 1991; Zachariae, 2004). Mutating the Arginine, Leucine or Asparagine prevents recognition and ubiquitination of substrates by APC (Glotzer et al., 1991). Cryo-electron microscopy of Cdh1-APC followed by biochemistry revealed that only lysines within ten or more residues C-terminal to the D-box are effective substrates for Cdh1-APC (Chang et al., 2015). More recently, another motif known as the KEN box (KENxxxN) was also identified as a targeting motif for APC (Pfleger and Kirschner, 2000). Some APC substrates have only the D-box, only the KEN box, or both motifs (Pfleger and Kirschner, 2000). Only Cdh1-APC is capable of targeting KEN box-only containing substrates (Barford, 2011). Cryo-electron microscopy has revealed that Apc2 Cullin domain in the catalytic core of APC works with Cdh1 as a co-receptor for the D-box on target substrates (da Fonseca et al., 2011), which suggests that Cdc20 and Cdh1 alone are not sufficient for substrate recognition; APC catalytic core subunits are required.

While much research has been focused on the characterization of the D-box and KEN box, some targets of APC do not contain either of these motifs (Barford, 2011). Additionally, while some substrates such as Cyclin A and Nek2A contain modified D-boxes, mutation of their D-boxes did not prevent their degradation (den Elzen and Pines, 2001; Hayes et al., 2006). Thus, some

targets of APC contain noncanonical motifs that have yet to be fully elucidated. The mechanisms underlying APC's targeting and ubiquitination of substrates are vital for the regulation of cell cycle progression in mitotic cells.

1.6.1. Role of APC in Mitotic Cells

In mitotic cells, APC plays a regulatory role in the progression of the cell cycle through mitosis and into S phase (Sudakin et al., 1995). APC's ability to progress the cell cycle is dependent on precise temporal ubiquitination and subsequent degradation of key mitotic proteins, such as cyclins (Sudakin et al., 1995).

APC is activated in metaphase following kinetochore attachment (Barford, 2011). Cdc20-APC is active during early mitosis and targets two well described substrates: securin and M cyclins (Sudakin et al., 1995). Upon ubiquitination and degradation of securin, a protease known as separase is released (Morgan, 2007). Separase goes on to cleave the protein complex cohesion, which holds sister chromatids together during metaphase (Morgan, 2007). The sister chromatids are then freed and able to move to opposite mitotic poles for the start of anaphase. M cyclins (cyclin A and cyclin B), partner with and activate M-Cdk (Morgan, 2007). Ubiquitination by Cdc20-APC and subsequent degradation of M cyclins results in the inactivation of M-Cdk and progression of the cell cycle (Morgan, 2007). It is important to note that activation of Cdc20-APC is dependent on M-Cdk activity, so by leading to the inactivation of M-Cdk, Cdc20-APC causes its own inactivation (Rahal and Amon, 2008).

As discussed above, Cdk inactivation also allows for the activation of Cdh1. So, as Cdc20-APC is inactivated during metaphase, Cdh1 is activated and able to bind APC. During late mitosis, Cdh1-APC targets and promotes the degradation of other cell cycle proteins vital for DNA

replication, such as Cdc6 and geminin (Qiao et al., 2010). Cdc6 plays a regulatory role in DNA synthesis through the formation of pre-replicative complex and loading of minichromosome maintenance complex onto DNA (Leatherwood, 1998). Geminin inhibits Cdt1, which ultimately prevents the assembly of the pre-replicative complex (McGarry and Kirschner, 1998). Once geminin is ubiquitinated by Cdh1-APC and then degraded in late mitosis, Cdt1 can be active and start the assembly of the pre-replicative complex (McGarry and Kirschner, 1998). By targeting the destruction of Cdc6 and geminin, Cdh1-APC helps to ensure that DNA is only replicated once during the cell cycle.

As APC plays such a vital role in the progression of the cell cycle and replication of DNA, it is unsurprising that dysregulation of APC can lead to the pathogenesis of cancer via tumorigenesis (Qiao et al., 2010; Zhang et al., 2014a). Mutations in APC core subunits have been uncovered in multiple forms of cancer (Zhou et al., 2016). Cdh1 has been characterized as a tumor suppressor, especially with its targeting of Skp2 (Fujita et al., 2008a; Fujita et al., 2008b). Skp2 is an E3 ubiquitin ligase that regulates the transition from G₁ to S phase of the cell cycle. If Skp2 is not properly regulated, the cell cycle may be dysregulated and tumorigenesis may occur. Cdh1's upstream regulation of Skp2 has been correlated to several forms of malignancy including: non-Hodgkin lymphoma (Lwin et al., 2007), prostate cancer (Gao et al., 2009), breast cancer (Fujita et al., 2008a), and colorectal cancer (Fujita et al., 2008b). Cdc20 has been characterized to act as an oncogene, where high expression of Cdc20 is correlated to poor prognosis in patients with non-small cell lung cancer (Kato et al., 2012) and colorectal cancer (Wu et al., 2013). With Cdc20's role as an oncogene, there has been an interest in using pharmacology to target it and suppress neoplastic cell death (Zhou et al., 2016).

1.6.2. Role of APC in Postmitotic Neurons

Despite the breadth of knowledge on APC's functioning in mitotic cells, it has been less clear as to what the role of this E3 ubiquitin ligase complex is in postmitotic cells, such as neurons. Interestingly, the ability of Cdh1-APC to maintain the G1 phase in mitotic cells is necessary for the differentiation of neuroblastoma cells (Cuende et al., 2008) and the ability of neural progenitor cells to exit cell cycle and differentiate into cortical neurons (Delgado-Esteban et al., 2013). Thus, the role of APC in mitotic cells are not completely independent of its roles in postmitotic cells.

There is some discussion as to whether or not Cdc20 regulates processes in postmitotic cells. While one group has found that Cdc20 is not expressed in cortical neurons older than day *in vitro* 4 (DIV 4) (Almeida et al., 2005), another group asserts that Cdc20 is expressed in postmitotic neurons and regulates postsynaptic dendritic development and complexity (Kim et al., 2009). A potential source of this discrepancy is may be due to the age of the rodent pups that were used for primary neuron dissection. While Almeida et al. used embryonic day 16 rats, Kim et al. used postnatal day 6 rats for primary neuron culturing (Almeida et al., 2005; Kim et al., 2009). The contrasting results based upon age at dissection perhaps suggests that Cdc20-APC may have a role at very specific timepoints in neurodevelopment.

In the studies observing Cdc20 presence in postmitotic neurons, knockdown of Cdc20 in rat cerebellar, cerebral cortical, and hippocampal neurons led to a decrease in dendritic length and simplified the dendritic arbor (Kim et al., 2009). Furthermore, it was determined that the centrosomal localization of Cdc20 is critical for its regulation of dendritic morphogenesis (Kim et al., 2009). The same research group also observed that Cdc20-APC drives presynaptic differentiation via clustering of synaptic vesicle and active zone proteins (Yang et al., 2009). Thus, research in the last 10 years has uncovered a novel role of Cdc20-APC in neurodevelopment. These

findings beg the question: does the role of Cdc20 in neurons suggest that APC's other activating subunit, Cdh1, also have a regulatory role outside of cell cycle?

Cdh1-APC is observed to be highly enriched in neurons (Gieffers et al., 1999). Cdh1-APC helps to maintain the antioxidant status of neurons through its targeting of Pfkfb3, an enzyme critical for glycolysis (Herrero-Mendez et al., 2009). Whereas the expression of Cdh1-APC is high in cortical neurons to reduce Pfkfb3, astrocytes have lower Cdh1-APC activity (Herrero-Mendez et al., 2009). The stark difference in Cdh1-APC activity in neurons compared to astrocytes demonstrates that there are neuron-specific mechanisms that APC regulates outside of its canonical role in cell cycle progression.

Evidence from invertebrate models has demonstrated Cdh1-APC is a regulator of synaptic connections (Teng and Tang, 2005). In *Drosophila*, genetic deletion of the maternal *Drosophila* ortholog of Apc2 (a critical Cdh1-APC subunit as discussed above), *morula*, lead to an increase in neuromuscular synapses compared to controls (van Roessel et al., 2004). Targeted expression of *morula* in all postmitotic neurons, but not in muscles, rescued the synapse number, which demonstrates Cdh1-APC regulates synaptic formation via effects on neurons (van Roessel et al., 2004). Additionally, a study in *C. elegans* observed that Cdh1-APC regulates the abundance of Glutamate receptor 1 (GluR1) in the ventral nerve cord (Juo and Kaplan, 2004). Blockade of clathrin-mediated endocytosis prevented the increase of GluR1, suggesting that Cdh1-APC regulates GluR1 via its trafficking from the plasma membrane to the endosome (Juo and Kaplan, 2004). While these two studies in invertebrate model systems helped to demonstrate a distinct regulatory role of Cdh1-APC in postmitotic neurons, studies in mammalian systems are critical to fully elucidate Cdh1-APC's role in neurodevelopment.

In mammalian systems, whereas Cdc20-APC regulates dendritic development, Cdh1-APC has been observed to regulate axonal growth (Huynh et al., 2009; Konishi et al., 2004). Knockdown of Cdh1 in cerebellar granule neurons leads to a dramatic increase in axonal lengths; the ubiquitin ligase activity of Cdh1-APC was required to suppress axonal growth (Konishi et al., 2004). Axons from neurons with reduced Cdh1 expression extended across distinct layers of the cerebellar cortex, demonstrating that Cdh1-APC plays a regulatory role in limiting the growth of axons in a layer-specific manner during cerebellar development (Konishi et al., 2004).

Recently, there has been much interest in elucidating the potential role of Cdh1-APC in learning and memory. Genetic reduction of Cdh1 *in vivo* leads to defects in mGluR-LTD in the hippocampus (Huang et al., 2015) as well as LTP in both the hippocampus and the amygdala (Li et al., 2008; Pick et al., 2012; Pick et al., 2013). However, different behavioral phenotypes were observed dependent on time point and cell type of Cdh1 knock down. When Cdh1 is knocked out in excitatory neurons in the hippocampus and forebrain late in brain development, mice demonstrate normal spatial learning and memory with enhanced reversal learning (Pick et al., 2012). Additionally, the Cdh1-conditional knockout mice have impaired fear memory compared to wildtype controls (Pick et al., 2012). Conversely, mice lacking Cdh1 in all neurons from the onset of differentiation exhibit an impairment in reversal learning and do not exhibit impaired fear memory (Pick et al., 2013). The authors of these studies have suggested that the difference phenotypes in these two knockout models may be due to differential targets of Cdh1-APC during development versus post-development. Despite the varying phenotypes in behavioral studies with Cdh1 knockouts, it can be asserted that Cdh1-APC regulates learning and memory via neuronal mechanisms.

In order to better understand Cdh1-APC's role in postmitotic neurons, it is necessary to identify interacting proteins as well as its substrates for ubiquitination. The aforementioned study on Cdh1-APC function in *Drosophila* (van Roessel et al., 2004) observed that knockdown of *morula* (*Drosophila* ortholog of APC2) lead to an increase in Liprin- α , a multidomain scaffolding protein that regulates AMPA receptor trafficking (Wyszynski et al., 2002), which was reversed upon expression of *morula*. Reducing expression of Liprin- α prevented the increase in synapses following *morula*-knockdown (van Roessel et al., 2004). It has been speculated that Liprin- α underlies Cdh1-APC's effects on synapse number as well as axonal growth (Teng and Tang, 2005). Inhibitor of DNA binding 2 (Id2) and Ski-related novel gene (SnoN) have also been identified as ubiquitination substrates of Cdh1-APC that regulate axonal growth and morphology (Lasorella et al., 2006; Stegmuller et al., 2008; Stegmuller et al., 2006). Id2 mutations in the D-box, the Cdh1-interacting motif, lead to increased axonal growth similar to the phenotypes observed in Cdh1 knockdown studies (Konishi et al., 2004; Lasorella et al., 2006).

While the identified neuronal substrates of Cdh1-APC are helpful to understand the regulation of axonal growth, it is still unclear how Cdh1-APC may regulate molecular forms of learning and memory. The recent novel finding of FMRP as a substrate of Cdh1-APC (as discussed above) (Huang et al., 2015) helps to elucidate another mechanism by which Cdh1-APC regulates learning and memory in postmitotic neurons. The regulation of FMRP, a protein implicated in a neurodevelopmental disorder, links Cdh1-APC to neurodevelopmental disorders, outside of its known connection to cancer. As neurodevelopmental disorders have a shared underlying neurobiology, Cdh1-APC may target additional RNA binding proteins to further exert its regulation over neurodevelopment. In Chapter 3, we further characterize the regulation of FMRP by Cdh1-APC. In Chapter 4, we identify novel interactions between Cdh1 and other RNA binding

proteins to discover a novel role of Cdh1-APC as a regulator of translation in postmitotic neurons. The findings in this dissertation further elucidate the role of Cdh1-APC in postmitotic cells independent of its known regulation of cell cycle.

1.7. Critical Questions in the Field

As discussed in this chapter, previous research has established that Cdh1-APC is an E3 ubiquitin ligase that promotes the ubiquitination of FMRP, an RNA-binding protein that is well-characterized to repress translation and form RNA granules. While this pathway appears to have implications for neurodevelopment, it is unclear what are the downstream consequences of FMRP-ubiquitination by Cdh1-APC. These critical questions remain based upon previous findings **(Figure 6-4)**:

1. Does modification of FMRP by Cdh1-APC act as a molecular switch to allow for protein synthesis?
2. Does Cdh1-APC interact with other regulators of protein synthesis aside from FMRP?
3. Does Cdh1-APC regulate the formation of the formation of RNA granules, such as stress granules via modification of FMRP?

1.8. Dissertation Hypothesis and Objectives

Due to the importance of protein homeostasis for molecular forms of learning and memory, the overall objective of this presented thesis research was to further investigate and provide new insight into the mechanism and regulation of neuronal protein synthesis and protein degradation dynamics involved in homeostasis. Previous studies from our lab and others have shown that translational repression by FMRP is reversed upon mGluR stimulation (Muddashetty et al., 2011),

FMRP is ubiquitinated downstream of mGluR stimulation (Hou et al., 2006; Nalavadi et al., 2012), and that Cdh1-APC interacts with FMRP (Huang et al., 2015). These past studies provide the scientific premise for this thesis to test the hypothesis that Cdh1-APC ubiquitinates FMRP and associated translational machinery to act as a molecular switch to remove translational repression and allow for downstream protein synthesis. In Chapter 3, we characterize Cdh1-mediated regulation of FMRP and protein synthesis downstream of FMRP to address “Question 1” above. Chapter 4 is focused on addressing “Question 2” by identifying a novel role of Cdh1-APC as a regulator of protein synthesis in postmitotic neurons through its interactions with translational machinery. Chapter 5 explores stress granule dynamics as a potential novel mechanism of this regulation to answer “Question 3”. Finally, Chapter 6 summarizes our findings in the context of current literature and expands upon future directions of this research to better elucidate mechanisms of protein homeostasis in brain development and possible alterations in fragile X syndrome related neurodevelopmental brain disorders.

1.9. Figures

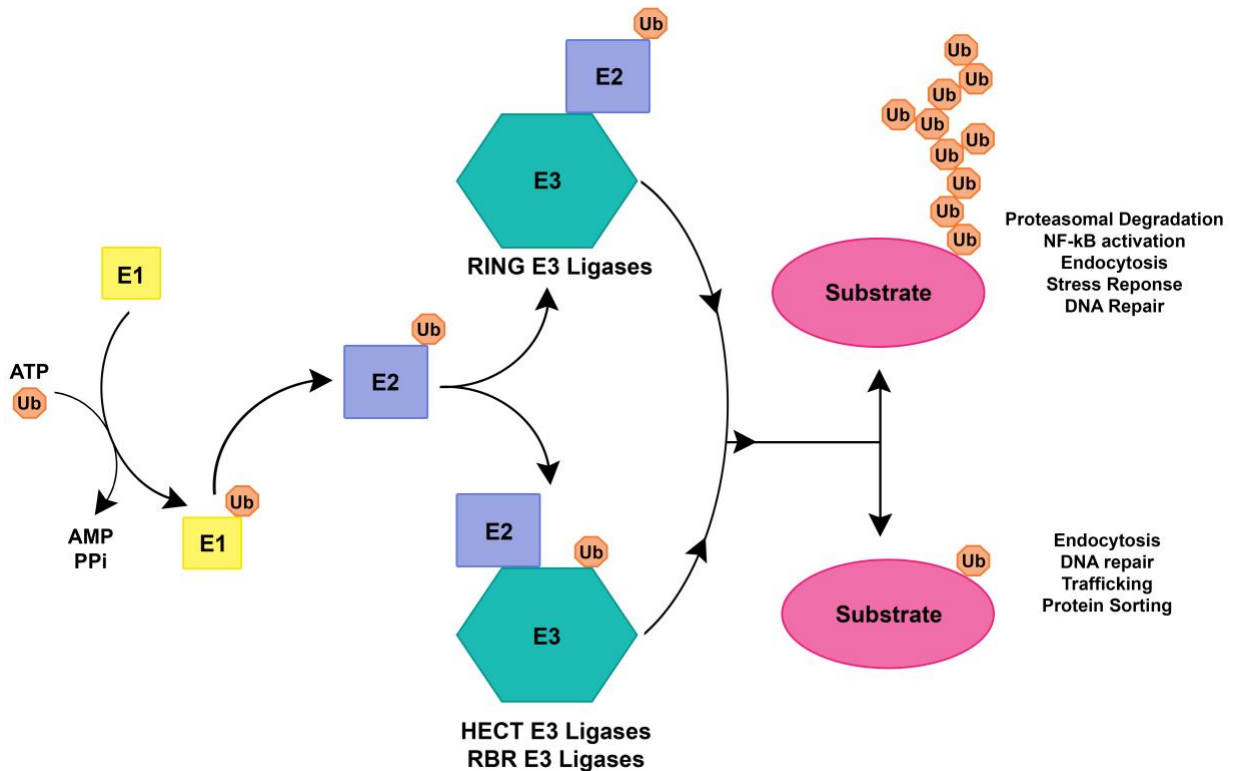


Figure 1-1: The Ubiquitination Pathway

Figure adapted from Mabb & Ehlers 2010. Prior to the ubiquitination of a substrate, a ubiquitin-activating enzyme, known as an E1 enzyme, will activate a ubiquitin protein in an ATP-dependent process, which results in the attachment of ubiquitin onto a catalytic cysteine on the E1. The ubiquitin will then be transferred onto a cysteine on a ubiquitin conjugating enzyme (E2 enzyme). The E2-ubiquitin complex will then be recognized and bound to a ubiquitin-ligase enzyme (E3 enzyme). Dependent on the class of E3 enzyme, the E2 may then directly transfer the ubiquitin onto a lysine residue on the target substrate (such as with RING E3 ligases). Other classes of E3s, such as HECT and RBR E3 enzymes, will utilize a two-step process where the ubiquitin will be transferred from the E2 onto a catalytic cysteine on the E3. Then, the ubiquitin can be bound to a lysine on the target substrate. The attachment of a single ubiquitin onto a substrate is known as monoubiquitination. Monoubiquitination can lead to downstream signaling of endocytosis, DNA

repair, trafficking, or protein sorting. Ubiquitin has lysine residues that may be ubiquitinated, which allows for intricate branches of ubiquitin chains to be added to a substrate, known as polyubiquitination. Polyubiquitination commonly leads to proteasomal degradation of the target substrate. NF- κ B signaling, endocytosis, stress response, and DNA repair may also happen downstream of polyubiquitination.

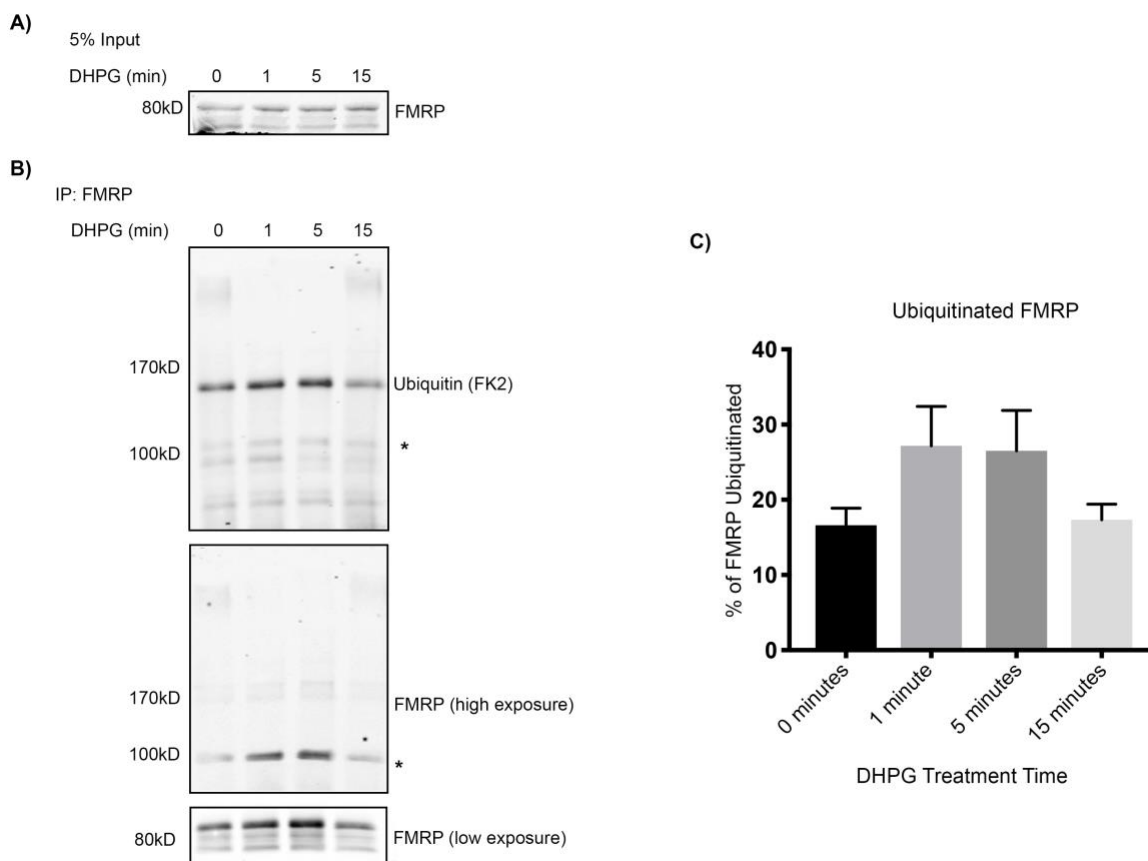


Figure 1-2: mGluR stimulation promotes the ubiquitination of FMRP

A) High-density DIV 14-16 neurons were treated with 10 μ M MG-132 overnight and then stimulated with 50 μ M (S)-3,5-Dihydroxyphenylglycine (DHPG) for the times indicated and then subsequently lysed. **B)** Lysate underwent FMRP immunoprecipitation. Immunoblotting was performed for FMRP and conjugated ubiquitin (FK2 clone). Asterisk indicates high-molecular weight form of FMRP that is immunoreactive to both FMRP and ubiquitin (thereby interpreted as ubiquitinated FMRP). N=3. **C)** Quantification of the higher molecular weight FMRP normalized to the total FMRP immunoprecipitated. All samples were then normalized to the PBS only condition (no DHPG) for each trial.

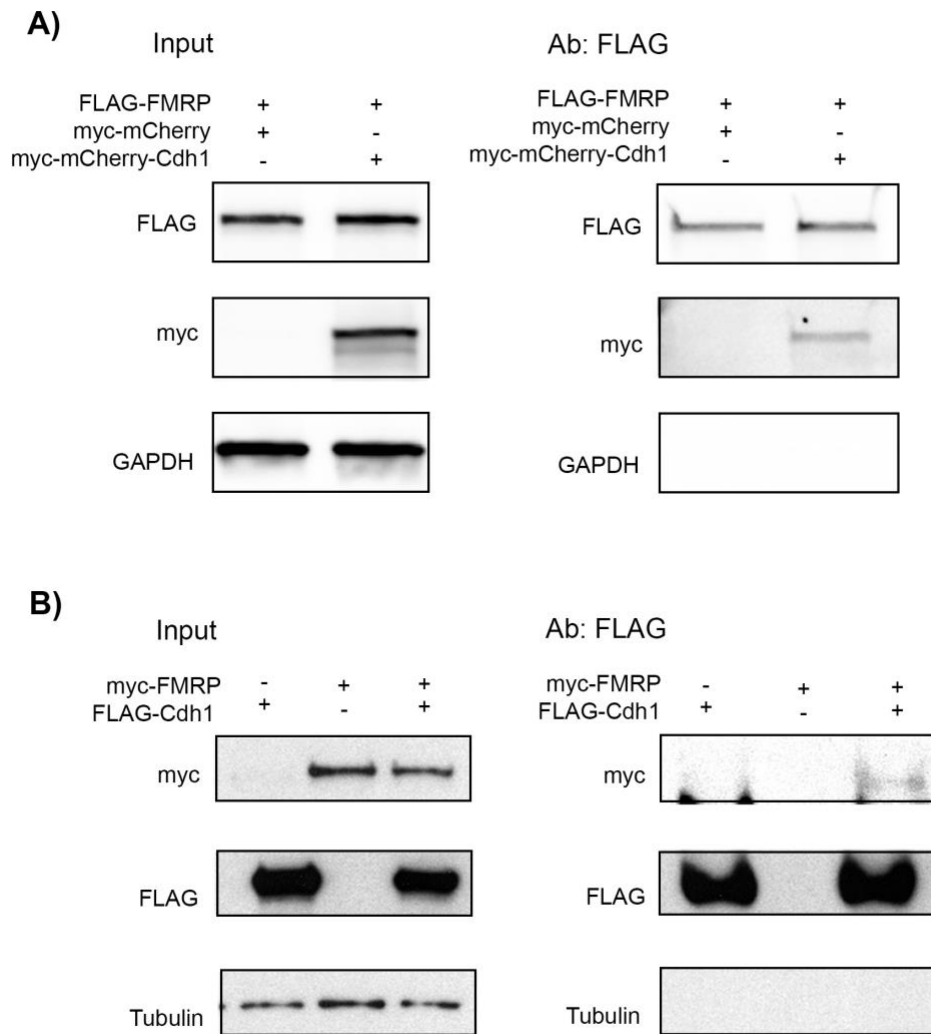


Figure 1-3: FMRP and Cdh1-APC interact in *vitro*

A) N2A cells were co-transfected with FLAG-FMRP and myc-mCherry or myc-mCherry-Cdh1.

B) Lysates were immunoprecipitated with FLAG antibody-coupled beads. Immunoprecipitated proteins were eluted with 3x FLAG peptide. Lysates underwent electrophoresis and immunoblotting for FLAG, myc, and GAPDH.

C) N2A cells were transfected with myc-FMRP or FLAG-Cdh1 alone or co-transfected with both plasmids.

D) Lysates then underwent FLAG immunoprecipitation as in A) followed by electrophoresis and immunoblotting for myc, FLAG, and tubulin.

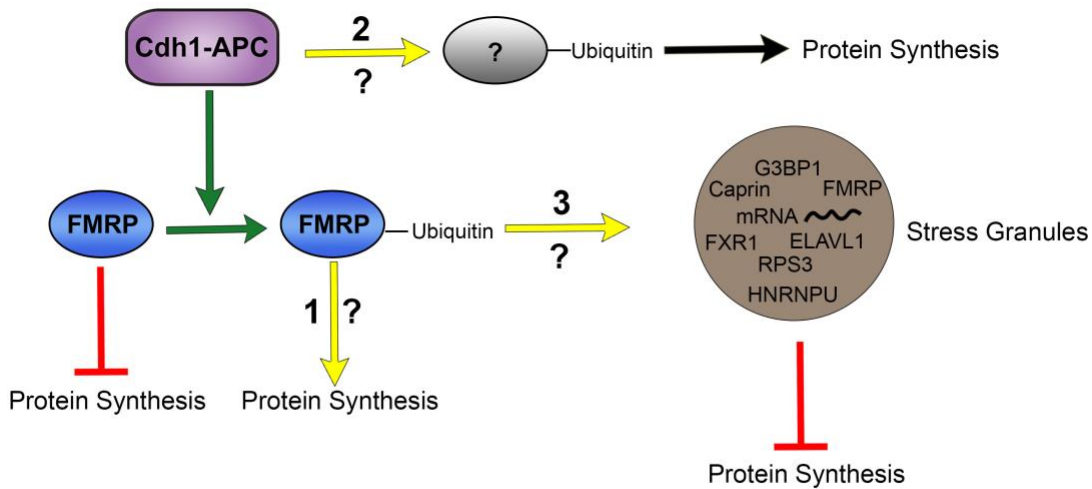


Figure 1-4: Critical questions explored by dissertation

It has been previously observed that Cdh1-APC ubiquitinates FMRP (Huang et al., 2015), and that FMRP represses downstream protein synthesis (Banerjee et al., 2018). It is unclear if ubiquitination of FMRP is a necessary step for the reversal of FMRP-mediated translational repression (1). Additionally, it is unknown if Cdh1-APC interacts with other proteins that regulate protein synthesis (2). As FMRP is characterized to form translationally-repressive RNA granules (Christie et al., 2009), we sought to determine if Cdh1-APC mediates the ability for stress granules to form in a FMRP-dependent mechanism (3).

Chapter 2 :

Materials & Methods

Cell Culture

Primary cortical neurons were prepared from C57BL/6J mouse embryos of either sex on embryonic day 17 from timed pregnant mice delivered from Charles River. Cortices were dissected from embryos, trypsinized (0.25% EDTA-free, Life Technologies) at 37°C for 10 minutes and then rinsed with warm HBSS containing 10mM HEPES (HBSS/HEPES, Fisher Scientific). Cells were then dissociated in MEM (Cellgro/Corning) containing FBS (MEM/FBS, Hyclone). Neurons were plated in MEM/FBS on cell culture dishes previously coated with 1mg/mL poly-L-lysine (Sigma-Aldrich) in borate buffer (40mM boric acid, 15mM sodium tetraborate, pH 8.5) overnight at 37°C hours followed by three 1-hour washes with sterile water. Two hours after plating, neuronal media was changed to glial conditioned media (GCM). GCM was obtained by plating secondary glial cells in Neurobasal medium (Gibco) with 1x Glutamax (Gibco), and 1x B-27 (Gibco) and then sterile filtering the media 24 hours later. Animal protocols were approved by the institutional Animal Care and Use Committee at Emory University.

For experiments in **Figure 5-5**, *Fmr1*-KO and littermate wildtype control mice were obtained as previously described (Bulow et al., 2019). *Fmr1*^{HET} females (backcrossed on C57BL/6J background) were crossed with WT C57BL/6J males (Jackson Laboratory) to generate litters of pups with mixed genotypes (*Fmr1*-KO, *Fmr1*^{HET}, or wild-type). Cerebral cortices were dissected and cultured from genotyped WT and *Fmr1*-KO pups on P0-P3.

Neuro2A (N2A) cells, a mouse neuroblastoma cell line, were cultured as previously described (Williams et al., 2016). N2A cells were cultured in DMEM media supplemented with 10% fetal bovine serum (FBS, Hyclone) and 10mM Hepes (Invitrogen) at 37° C in 10% CO₂.

Pharmacology

To inhibit Cdh1-APC activity, cells were treated with 1-2 μ M Apcin (Sigma-Aldrich) for 16-18 hours or treated with 12 μ M proTAME (Cayman Chemicals) for 4 hours. To induce stress granules, cells were treated with 0.5mM Sodium Arsenite (Millipore-Sigma) for 45 minutes.

Plasmids

The following plasmids were utilized for this work: mCMV-TurboRFP shRNA control (Dharmacon VSC11715), mCMV-TurboRFP shRNA Cdh1 (Dharmacon V3SVMM08_13411185) (both Dharmacon plasmids were packaged into lentivirus by the Emory University Viral Vector Core), mCherry-myc and mCherry-Cdh1-myc (both designed and generated by the Emory Integrated Genomics Core; packaged into lentivirus by the Emory University Viral Vector Core), Myc-DDK (Origene PS10001), Myc-DDK-Cdh1 (Origene MR207910), pMyc-FMRP (generated by Bassell lab), GFP-FLAG (generated by Bassell lab), and GFP-FLAG-FMRP-WT (generated by Bassell lab), and GFP-FLAG-FMRP-DBM (generated by Bassell lab).

Primers were designed for the FMRP-DBM construct based upon the point mutations described previously (Huang et al., 2015) by the QuikChange Primer Design tool (Agilent). The primers and GFP-FLAG-FMRP-WT plasmid were utilized with the QuikChangeII Site-Directed Mutagenesis Kit (Agilent) per manufacturer's instructions to generate the GFP-FLAG-FMRP-DBM construct.

Antibodies

Antibody	Company	Catalog #
Mouse anti-β-Actin	Thermo Fisher	AM4302
Rabbit anti-Caprin	Proteintech	15112-1-AP
Mouse anti-FLAG	Sigma	F1804
Rabbit anti-FLAG	Bethyl	A190-102A
Rabbit anti-FMR1 C terminal	Sigma	F4055
Rabbit anti-FMRP 7G-1	DSHB	7G1-1-S
Mouse anti-FMRP	BioLegend	834701
Rabbit anti-FXR1	Proteintech	13194-1-AP
Rabbit anti-GAPDH	Cell Signaling	2118S
Rabbit anti-G3BP1	Proteintech	13057-2-AP
Rabbit anti-hnRNP-U	Proteintech	14599-1-AP
Rabbit anti-HuR	Proteintech	11910-1-AP
Guinea Pig anti-MAP2	Synaptic Systems	188 004
Rabbit anti-myc	Bethyl	A190
Mouse anti-puromycin	Millipore	MABE343
Mouse anti-puromycin	Kerafast	EQ0001
Mouse anti-RPS3	Proteintech	66046-1-IG
Mouse anti-tubulin	Sigma-Aldrich	T6199
Mouse anti-Ubiquitin (FK2)	Millipore	04-263
Alexa Fluor 488 Donkey anti-Rabbit IgG (H+L)	Life Technologies	A21206

Donkey Anti-Mouse IgG Cy3	Jackson ImmunoResearch	715-165-150
Donkey Anti-Rabbit IgG Cy3	Jackson ImmunoResearch	711-165-152
Alexa Fluor 647 Goat anti-Guinea Pig IgG (H+L)	Thermo Fisher Scientific	A21450
Donkey anti-Rabbit IgG IR 800CW	LiCor	926-32213
Donkey anti-Mouse IgG IR 680LT	LiCor	926-68022

FMRP Immunoprecipitation

Day *in vitro* (DIV) 14-16 high-density cortical neurons were treated with MG-132 (Sigma) (10 μ M, 16-18 hours) and then stimulated with PBS or DHPG for five minutes (50 μ M). Cells were then washed twice with 1x PBS and lysed in buffer containing 50mM Tris pH 7.5, 300mM NaCl, 30mM EDTA, 0.5% Triton X-100, 10 μ M idoacetamide, 10mM N-ethylmaleimide, cOmplete protease inhibitor (Roche), and phosSTOP (Sigma-Aldrich). Cells were sonicated followed by incubation on ice for 30 minutes. Cell lysates were centrifuged at 20,817 x g for 20 minutes. Lysate was then incubated with Agarose G (Sigma) conjugated to mouse anti-FMRP 7G-1 (DSHB) for 2-4 hours. After incubation, agarose was washed 3 times with lysis buffer. Proteins were then eluted using 4x Sample Buffer (Bio-Rad) and were run on an SDS-PAGE gel (Sigma) for electrophoresis.

FLAG Immunoprecipitation

FLAG immunoprecipitation was performed as described by Gokhale et al. (Gokhale et al., 2012). N2A cells were transfected using PoyMag Neo (OZ Biosciences) for 24 hours, as per manufacturer instructions. Cells were rinsed twice with 1x PBS and lysed in buffer A (150mM NaCl, 10mM HEPES, 1mM EGTA, and 0.1mM MgCl₂, pH 7.4) with 0.5% Triton-X100 and cOmplete protease inhibitor (Roche). Cells were sonicated followed by incubation on ice for 30 minutes. Cell lysates were centrifuged at 20,817 x g for 15 minutes. Clarified supernatant was collected and protein concentration was measured by Bradford Assay (Bio-Rad). 500ug of protein extract was added to 30uL of Sheep anti-Mouse IgG Dynabeads (Invitrogen 11031) conjugated to mouse monoclonal anti-FLAG (Sigma F315) and incubated for 2-4 hours at 4° C. As a control, immunoprecipitation was performed in the presence of antigenic 3x-FLAG peptide (340uM, Sigma F4799). After incubation, beads were washed 6 times with buffer A with 0.1% Triton X-100. Proteins were eluted from the beads with 2-hour incubation on ice with buffer A and 340uM 3x-FLAG-antigenic peptide. For proteomic analysis, proteins eluted from the beads were combined and concentrated by TCA precipitation.

For FLAG immunoprecipitation experiments, samples were run on a 4-20% Criterion TGX gel (Bio-Rad) and transferred onto PVDF membrane. Blots were blocked with 5% milk in 1x TBS-0.5% TritonX-100 for 30 minutes at room temperature. Blots were incubated overnight at 4°C in primary antibody diluted in 3% BSA, 0.5% Sodium Azide, and 1x PBS. Blots were incubated in HRP secondary antibodies (Sigma) diluted in 5% milk in 1x TBS-0.5% TritonX-100 for 40 minutes at room temperature. Three 5-minute washes with TBS-0.5% TritonX-100 were performed before and after addition of secondary antibodies. Blots were developed using Western Lightning ECL Pro (Perkin Elmer) and Amersham Hyperfilm (GE Lifesciences).

Puromycylation

N2A cells were transfected with Lipofectamine 2000 (Invitrogen) per manufacturer's protocol for 24 hours prior to assay. Cells were washed with warm DMEM and incubated with or without 10µg/mL puromycin (Sigma-Aldrich) for 45 minutes (N2A cells) or 75 minutes (cortical neurons) at 37°C. The protein synthesis inhibitor anisomycin (Sigma-Aldrich) was used as a control at 40µM. Cells were then washed ice cold 1x PBS and lysed in buffer A with 0.5% Triton-X100. Lysates were sonicated and incubated on ice for 30 minutes. Lysate protein concentration was then measured by BCA assay (ThermoFisher Scientific) and then used for western blotting.

FMRP Expression

FMRP expression was assessed following transfection of N2A cells with using Lipofectamine 2000 (Invitrogen) according to manufacturer instructions. Cells were lysed in buffer A (150mM NaCl, 10mM HEPES, 1mM EGTA, and 0.1mM MgCl₂, pH 7.4) with 0.5% Triton-X100 and Complete anti-protease (Roche). Cells were sonicated followed by incubation on ice for 30 minutes. Cell lysates were centrifuged at 16,100 x g for 15 minutes. Protein concentration was then measured by BCA assay (ThermoFisher Scientific) and lysates were used for western blotting.

Western Blotting

Western blotting was performed as previously described (Thomas et al., 2017). Samples were resolved by SDS-PAGE on a 4-20% Mini-Protean TGX protein gel (Bio-Rad) and transferred to a nitrocellulose membrane. Blots were blocked in Odyssey Blocking Buffer (LI-COR), and incubated overnight at 4°C in primary antibodies diluted in a 1:1 mix of blocking buffer and PBS-

Tween-0.1%. Blots were incubated in secondary antibodies (LI-COR) diluted in PBS-Tween-0.1% for 1 hour at room temperature. Three 10-minute washes with PBS-Tween-0.1% were performed before and after addition of secondary antibodies. Blots were viewed on a Bio-Rad ChemiDoc MP. Protein levels were assessed by quantitative densitometry using ImageJ.

Silver Staining

SDS-PAGE gels were fixed overnight in 50% methanol, 12% acetic acid, and 0.5% Formaldehyde. Gels were then washed in 50% ethanol three times, 20 minutes each. Gels were then soaked for one minute in 0.3% sodium thiosulfate and then incubated in silver solution (2% silver nitrate, 0.75% formaldehyde). Silver stains were developed to desired intensity in solution consisting of 1.2% sodium carbonate, 0.1% formaldehyde, and 12×10^{-5} % sodium thiosulfate.

Proteomics Analysis

Samples were analyzed for interactome analysis by MS Bioworks. Proteomics samples were separated on a 10% Bis-Tris Novex mini-gel (Invitrogen) using the MES buffer system. The gel was stained with Coomassie and excised into ten equally sized segments. Gel segments were processed using a robot (Progest, DigiLab). First, gel segments were washed with 25mM ammonium bicarbonate followed by acetonitrile. They were then reduced with 10mM dithiothreitol at 60°C followed by alkylation with 50mM iodoacetamide at RT. Then, segments were digested with trypsin (Promega) at 37°C for 4 hours. They were then quenched with formic acid and the supernatant was analyzed directly without further processing. The gel digests were analyzed by nano LC/MS/MS with a Waters NanoAcquity HPLC system interfaced to a ThermoFisher Q Exactive. Peptides were loaded on a trapping column and eluted over a 75µm

analytical column at 350nL/min; both columns were packed with Luna C18 resin (Phenomenex). The mass spectrometer was operated in data-dependent mode, with MS and MS/MS performed in the Orbitrap at 70,000 FWHM resolution and 17,500 FWHM resolution, respectively. The fifteen most abundant ions were selected for MS/MS. Data were searched using a local copy of Mascot.

Bioinformatic Analysis

Gene ontology analysis was performed with Database Annotation, Visualization and Integrated Discovery (DAVID, <https://david.ncifcrf.gov>). Cytoscape with Enrichment Map plugin for visualizing DAVID outputs was used to represent the Biological Processes enriched within the Cdh1 interactome.

Ubiquitin Immunoprecipitation

Prior FLAG immunoprecipitation samples were eluted with 3xFLAG peptide. Immunoprecipitate was precleared with protein A agarose beads and wash buffer (25mM Tris-HCl, 150mM NaCl, 1mM EDTA, 1% NP-40, 5% Glycerol, 10uM idoacetamide, 10mM N-ethylmaleimide, cOmplete protease inhibitor (Roche), and phosSTOP (Sigma-Aldrich)) at room temperature for one hour. FLAG immunoprecipitate was then co-incubated with either mouse IgG or Biotin-TUBEs (Tandem Ubiquitin Binding Entities) (UM301, LifeSensors) overnight at 4°C. Samples were then co-incubated with Streptavidin Dynabeads (Invitrogen) at room temperature for one hour. Beads were then washed three times with wash buffer and eluted with 4x sample buffer (Bio-RAD). Eluted samples were then used for western blotting or silver staining.

Immunofluorescence

Cells were fixed in 4% paraformaldehyde for 15 minutes, washed three times for 10 minutes in PBS. Cells were blocked for 1 hour in blocking solution consisting of 5% normal donkey serum, 0.1% bovine serum albumin, and 0.1% Triton-X 100 in PBS. Cells were incubated overnight in primary antibodies diluted in blocking solution. The next day, cells were washed 3 times for 10 minutes in PBS. They were incubated in secondary antibodies in blocking solution for one hour at room temperature. Cells were washed 3 times for 10 minutes. Coverslips with the cells were dipped in ultrapure water and then mounted using Prolong Gold Antifade mounting media (Invitrogen). Cells were imaged using a Keyence BZ-X810 or a Nikon Eclipse TE300 widefield fluorescence microscope with a 60X objective.

Quantification of Stress Granules

Coverslips for immunocytochemistry were blinded during imaging and quantification. Imaged neurons were classified as being stress granule positive or negative based on G3BP1 staining. Diffuse G3BP1 staining was classified as stress granule negative whereas cells with punctate G3BP1 staining were classified as stress granule positive. The total number of stress granule positive or negative neurons for each condition were then input into GraphPad Prism and a z-test was ran on the data.

Number of stress granules in the soma of each cell were quantified using Image J plugin TrackMate (Tinevez et al., 2017) with the Laplacian of Gaussian detector (threshold set from 5-15). Total area of the cell body was quantified using Image J plugin Mitomorphology macro (Dagda et al., 2009) with threshold set as 130-180. The number of granules were normalized to the cell body area.

Statistical analysis

Statistical analyses and graphs were prepared in GraphPad Prism (v.8). All data are expressed as mean +/- SEM. Replicates are reported in the figure legends or directly on the figures. For all experiments, α was set as 0.05. See figure legends for specific statistical analyses.

Chapter 3 :

Cdh1-APC Regulates FMRP-Mediated Protein Synthesis

Portions of this chapter were adapted from the following publication:

Valdez-Sinon AN, Lai A, Shi L, Lancaster CL, Gokhale A, Faundez V, Bassell GJ. Cdh1-APC interactions with FMRP and ribosomal components regulate protein synthesis and stress granule dynamics in neural cells. *Cell Reports, In Revision*.

3.1. Introduction

The Fragile X Mental Retardation Protein (FMRP) is well known to repress translation through several proposed mechanisms that include recruiting the RNA-induced silencing complex (RISC) and stalling polyribosomes (see section 1.4) (Banerjee et al., 2018). FMRP represses the translation of many mRNAs that are critical for synaptic structure and function; 32% of FMRP targets overlap with the postsynaptic proteome (Darnell et al., 2011). With the targeting of many synaptic proteins, it is critical for there to be a mechanism to reverse the ability of FMRP to repress translation. For example, glutamate receptor (mGluR) stimulation induces the translation of *PSD-95*, an mRNA target of FMRP that is well established to contribute to alterations in synaptic strength (Muddashetty et al., 2011). It is still unclear what specific molecular mechanisms regulate the ability of FMRP to repress translation.

Dephosphorylation and subsequent ubiquitination of FMRP downstream of mGluR stimulation were identified to allow for the translation of *PSD-95* mRNA (Muddashetty et al., 2011; Nalavadi et al., 2012). As discussed in section 1.2, the ubiquitination of substrates is tightly regulated by the activity of three classes of ubiquitination enzymes: E1s, E2s, and E3s. E3 ubiquitin ligases have the most specificity for the protein substrate to be ubiquitinated. Thus, it became of interest to identify the E3 ubiquitin ligase that is responsible for the ubiquitination of FMRP.

Recently, the Anaphase Promoting Complex, an E3 ubiquitin ligase, and its Cdh1 regulatory subunit (Cdh1-APC) were identified to mediate mGluR induced LTD (mGluR-LTD) upstream of FMRP and modulate FMRP ubiquitination (Huang et al., 2015). However, it is unclear whether Cdh1-APC has an effect on other processes downstream of FMRP, for example the ability of FMRP to repress protein synthesis. Here we sought to further characterize the ability of Cdh1-

APC to ubiquitinate FMRP by determining if Cdh1-APC may serve as a molecular switch to reverse the ability of FMRP to repress protein synthesis.

3.2. Results

3.2.1. Cdh1-APC Ubiquitinates FMRP Downstream of mGluR5 Signaling in Cortical Neurons

Our lab, along with others, have observed that FMRP is ubiquitinated following mGluR stimulation (**Figure 1-2**) (Hou et al., 2006; Nalavadi et al., 2012). Since Cdh1-APC interacts with FMRP (**Figure 1-3**) (Huang et al., 2015), we hypothesized that manipulation of its E3 ligase activity would alter FMRP modification following mGluR stimulation.

To observe endogenous ubiquitination of FMRP, an FMRP immunoprecipitation approach was utilized in which day *in vitro* 14 (DIV 14) cortical neurons are enriched for ubiquitinated proteins via the inhibition of the proteasome with the drug MG-132. Perturbing the activity of the proteasome allows for the detection of polyubiquitinated proteins that would otherwise be degraded. Following MG-132 treatment, neurons were then stimulated with mGluR5 agonist (S)-3,5-Dihydroxyphenylglycine (DHPG), lysed, and underwent FMRP immunoprecipitation. Bands that are immunoreactive on western blotting for both FMRP and ubiquitin can be interpreted to be a ubiquitinated form of FMRP.

Initially, a pharmacologic approach was used to manipulate the activity of Cdh1-APC. The ability of Cdh1-APC to ubiquitinate target proteins has been previously shown to be inhibited via the drug Apcin (Sackton et al., 2014). We utilized Apcin to inhibit Cdh1-APC activity in DIV 14 cortical neurons in addition to MG-132 treatment. Neurons were then stimulated with DHPG and underwent FMRP immunoprecipitation. In untreated neurons, DHPG stimulation leads to the increase in a ubiquitinated form of FMRP as previously demonstrated (**Figure 1-2, Figure 3-1**). Neurons treated with Apcin were unable to elicit an increase in ubiquitination of FMRP following

mGluR5 stimulation (**Figure 3-1**). Thus, blockade of Cdh1-APC activity prevents FMRP-ubiquitination, suggesting that Cdh1-APC is responsible for ubiquitinating FMRP. These results support the hypothesis that Cdh1-APC regulates FMRP ubiquitination.

To further confirm the regulatory role of Cdh1-APC in FMRP ubiquitination, cortical neurons were transduced with a lentivirus expressing a Cdh1 shRNA for 7 days. On DIV 14, neurons underwent DHPG stimulation and subsequent FMRP immunoprecipitation. Similar to neurons with inhibited Cdh1-APC activity, FMRP was not ubiquitinated following mGluR stimulation in Cdh1-knockdown neurons. Thus, both inhibition of Cdh1-APC activity and knock down of Cdh1 expression are sufficient to disrupt mGluR-induced ubiquitination of FMRP. Both sets of immunoprecipitation experiments demonstrate that FMRP ubiquitination downstream of mGluR signaling is regulated by Cdh1-APC.

3.2.2. Cdh1-APC Reverses FMRP-mediated Repression of Protein Synthesis

Based on the observations that Cdh1-APC ubiquitinates FMRP and previous evidence that Cdh1-APC regulates mGluR-LTD (Huang et al., 2015), we hypothesized that Cdh1-APC may have a role in other molecular processes downstream of FMRP. We decided to focus on potential effects of protein synthesis since FMRP has been well characterized to repress protein synthesis (Banerjee et al., 2018; Richter et al., 2015) (see section 1.4). Currently, the mechanisms involved in regulating the repressive activity of FMRP are largely unknown. Since protein synthesis of PSD-95, a FMRP target, is dependent on the ubiquitin-proteasome-system (UPS) (Nalavadi et al., 2012) and Cdh1-APC is part of the UPS, it was hypothesized that Cdh1-APC acts as a molecular switch to halt the translational-repressive activity of FMRP.

To assess protein synthesis, puromycylation was utilized wherein cells are treated with puromycin, a tRNA analog, and then lysed and immunoblotted for puromycin (**Figure 3-2**). Neuro2A (N2A) cells, a mouse neuroblastoma cell line, were co-transfected with mCherry and either GFP or GFP-FMRP. Based on previous evidence that FMRP leads to an increased rate of protein synthesis in both mouse (Liu et al., 2012) and human (Gross and Bassell, 2012) patient cells, FMRP is considered to be a translational repressors. Thus, it was expected that overexpression of FMRP would cause a decrease in protein synthesis. Immunoblotting the puromycin-labeled lysate demonstrated that that GFP-FMRP significantly represses steady state protein (**Figure 3-2**). If Cdh1-APC regulates protein synthesis downstream of FMRP as hypothesized, then co-expression of Cdh1 with FMRP was expected to lead to similar protein synthesis levels as co-expression of Cdh1 with GFP, thereby rescuing protein synthesis. When N2A cells were co-transfected with mCherry-Cdh1 and either GFP or GFP-FMRP, FMRP expression no longer repressed protein synthesis as compared to control levels (**Figure 3-2**). These data reveal a novel finding that Cdh1 acts as a molecular switch to reverse FMRP's repression of protein synthesis. Previous to this work, there was no evidence of a protein that could reverse the translational repression mediated by FMRP. Our results help to elucidate the currently unclear mechanisms underlying de-repression of protein synthesis downstream of FMRP.

3.2.3. Cdh1-APC Interaction with FMRP Affects FMRP Expression

Following our observations that Cdh1-APC regulates FMRP modification and subsequently leads to a de-repression of protein synthesis, we investigated how the interaction between Cdh1-APC and FMRP may regulate these effects. It is well described in Cdh1-APC literature that Cdh1 targets substrates containing a “Destruction box” motif (Glutzer et al., 1991;

Zachariae, 2004). Not only does FMRP contain this Destruction box motif, but it is well conserved across species (**Figure 3-3**). It has been shown that mutating the arginine, leucine, or asparagine in the motif prevents recognition and ubiquitination of substrates by Cdh1-APC (Glotzer et al., 1991). Others have previously utilized a “Destruction box mutant” of FMRP in which the critical arginine and leucine in the Destruction box are mutated into alanines, rendering it unable to bind to Cdh1 (Huang et al., 2015). We generated a “Destruction box mutant” of FMRP (FMRP DBM) from a GFP-FLAG-FMRP wildtype vector (FMRP WT) in order to better characterize the downstream consequences of Cdh1-APC’s interaction with FMRP (**Figure 3-3**).

FMRP WT or FMRP DBM was transfected into N2A cells for 24 hours. Following lysis of the cells, steady state expression of FMRP was assessed via western blotting. FMRP DBM had a significantly higher steady state expression compared to FMRP WT, suggesting that FMRP DBM is more stable and resistant to degradation (**Figure 3-3**). Since Cdh1-APC is characterized to facilitate K-11 linked polyubiquitination of a target substrate (Budhavarapu et al., 2012), which in turn leads to recognition and degradation by the proteasome, prevention of ubiquitination by Cdh1-APC would lead to an increase in protein expression of the target substrate. The increase in FMRP DBM expression supports previous reports that preventing Cdh1-FMRP interaction decreases FMRP ubiquitination (Huang et al., 2015). Thus, the direct interaction between Cdh1-APC and FMRP is necessary for Cdh1-mediated degradation of FMRP.

3.2.4. Cdh1-APC Interaction with FMRP Regulates Protein Synthesis

After demonstrating that Cdh1-APC reverses the repression of protein synthesis and Cdh1-FMRP interaction regulates FMRP expression, we hypothesized that that the interaction of Cdh1 and FMRP may have consequences on protein synthesis downstream of FMRP. It has been

previously observed that single point mutations in the *FMR1* gene can alter FMRP's ability to regulate translation (Banerjee et al., 2018; Feng et al., 1997; Richter et al., 2015). Here we investigate whether two missense mutations in the FMRP DBM construct, which lacks ability to associate with Cdh1-APC, could be sufficient to cause a perturbation in protein synthesis.

N2A were cells transfected with FMRP WT or FMRP DBM for 24 hours, then underwent puromycylation and subsequent cellular lysis. Cells transfected with FMRP DBM had decreased protein synthesis compared to FMRP WT- transfected cells (**Figure 3-4**, compare lanes 3 and 4); suggesting that there is more repression of protein synthesis in cells that overexpress FMRP DBM. Thus, an FMRP mutant that is unable to interact with Cdh1-APC more strongly represses protein synthesis than wildtype FMRP. These data suggest that the physical interaction between Cdh1-APC and FMRP is necessary for Cdh1-APC to regulate FMRP-mediated protein synthesis.

3.3. Discussion

While it has been known that there needs to be a physiologic switch to allow for protein synthesis downstream of FMRP, regulators of this process have been unknown. For the first time, we demonstrate that FMRP-mediated repression of protein synthesis can be reversed upon expression of Cdh1. We also observe that the direct interaction between FMRP and Cdh1-APC via the D-box motif on FMRP is necessary for Cdh1-APC-mediated degradation of FMRP as well as the reversal of translational repression downstream of FMRP. Taken together, our data support previous observations that Cdh1-APC regulates FMRP and shed light on the current unknown details of how repression of translation by FMRP is reversed.

For our assays on FMRP ubiquitination in primary neurons (**Figure 3-1**), we specifically chose to work with neurons that were DIV 14-16 due to their cytoskeletal complexity at that stage.

By DIV 12, mouse neurons reach the threshold of being polarized, meaning that at least 60% of neurons have an apical dendrite (Baj et al., 2014). At DIV 13-15, there is then a stabilization of the dendritic arbor (Baj et al., 2014). Thus, by selecting to use neurons at DIV 14 we are assured there are mature dendritic spines present. We did not use neurons older than DIV 16 due to the decrease in transduction efficiency of the shRNA lentiviruses as the neurons age. It is possible that neurons that are older than DIV 16 may have more robust changes in FMRP ubiquitination following mGluR stimulation due to their maturity.

Previous research has already shown that Cdh1-APC regulates ubiquitination of FMRP in the mouse hippocampus (Huang et al., 2015). As a lot of research in the FMRP field shows variability in phenotypes dependent on brain region and age (He and Portera-Cailliau, 2013), it was critical to assess how Cdh1-APC regulates FMRP in the cortex. Additionally, the previous study on Cdh1-APC ubiquitinating FMRP assessed ubiquitination using a slightly different method. While both our work and the work of Huang et al. utilize FMRP immunoprecipitation, Huang et al., only visualized conjugated ubiquitin on immunoblot to determine whether or not FMRP is ubiquitinated. This approach may be overgeneralized to truly observe the ubiquitination of FMRP. Since FMRP binds to a large number of proteins (Pasciuto and Bagni, 2014a), it is possible that the ubiquitin being visualized in the immunoblot are conjugated to FMRP-interacting proteins. Blotting for ubiquitin alone provides no distinction for ubiquitin that is conjugated to FMRP compared to ubiquitin that is conjugated to interacting proteins. To address this issue, we chose to immunoblot for both FMRP and conjugated ubiquitin. With our approach, we can confidently interpret that any bands showing immunoreactivity for both FMRP and ubiquitin as FMRP that has ubiquitin conjugated to it. However, with this much stricter criteria we may be missing other ubiquitinated forms of FMRP that are harder to see with dual antibodies.

The dominant band that we saw immunoreactivity for both FMRP and conjugated ubiquitin in both sets of our FMRP-ubiquitination experiments appeared at around 120kDa. When considering the molecular weight of both FMRP and ubiquitin, we can deduce approximately how many ubiquitins are attached onto this enriched form of FMRP. FMRP has a molecular weight of approximately 80 kDa and ubiquitin has a molecular weight of 8.5kDa. This suggests that our observed form of ubiquitinated FMRP has approximately five ubiquitin molecules attached to it. However, we cannot determine from our experiment whether FMRP is multi-monoubiquitinated whereby all five ubiquitin molecules are individually attached to FMRP on five separate lysine residues or if the ubiquitin molecules are arranged as a polyubiquitin chain with only one lysine directly attached to FMRP. If FMRP is being polyubiquitinated following mGluR5 stimulation, it is of high importance to elucidate which lysine residues on ubiquitin are being polyubiquitinated (i.e. K11, K27, K29, K33, K48, or K63). As discussed in Chapter 1, the consequences of polyubiquitination are difficult to predict without knowing the linkages for the polyubiquitin chains. Further investigation of the ubiquitin linkages on FMRP will help to better characterize the roles of less-understood ubiquitin linkages, such as K27, K28, and K33.

Our data demonstrate that two single point mutations in FMRP at positions 276 and 279 are sufficient to alter protein synthesis and lead to more repression of protein synthesis compared to wildtype FMRP. As mentioned above, another point mutation in FMRP, I304N, has been demonstrated to be sufficient to lead to altered protein synthesis (Feng et al., 1997); however, this point mutation caused an increase in protein synthesis. The I304N point mutation appears to mimic FMRP loss of function, as evidenced by intellectual disability phenotypes despite production of FMRP protein (De Boulle et al., 1993). Conversely, the FMRP DBM mutation appears to have a dominant negative molecular phenotype by further repressing protein synthesis. Contrasting the

effects of these two mutants of FMRP may help to better understand the functions of specific domains in the FMRP sequence. While the I304N mutation occurs in the KH2 domain of FMRP, the specific point mutations in the FMRP DBM mutant reside in the KH1 domain. Thus, both the KH1 and KH2 domains of FMRP may regulate protein synthesis. While the KH2 domain has been observed to mediate the effect of FMRP on polyribosomes (Feng et al., 1997), it is unclear if the KH1 domain may regulate protein synthesis through other mechanisms (i.e. recruitment of RISC). Thus, our work may help to elucidate the currently unclear functions of the KH1 domain within FMRP. Interestingly, the full Destruction-box motif in FMRP spans parts of the KH1 domain and the KH2 domain. It may be of future interest to produce other Destruction-box mutants that include mutations in the KH2 domain section as well as the KH1 domain of the motif to help distinguish how each of the KH domains may contribute to translational regulation.

Our work in this chapter suggests that a novel role of Cdh1-APC, beyond its already characterized ability to ubiquitinate FMRP (Huang et al., 2015), is to regulate FMRP-mediated repression of translation. Prior to this work, it has been unclear what molecular interactions may act as a molecular switch to allow for protein synthesis downstream of FMRP. As FMRP is necessary for neurodevelopment, its regulation by Cdh1-APC further suggests a cooperative role for Cdh1-APC in neurodevelopment as well. Thus, the findings from this chapter motivated us to better characterize the broader role of Cdh1-APC to regulate protein synthesis in neural cells, which has important implications to better understand the function of Cdh1-APC function neurodevelopment.

3.4. Figures

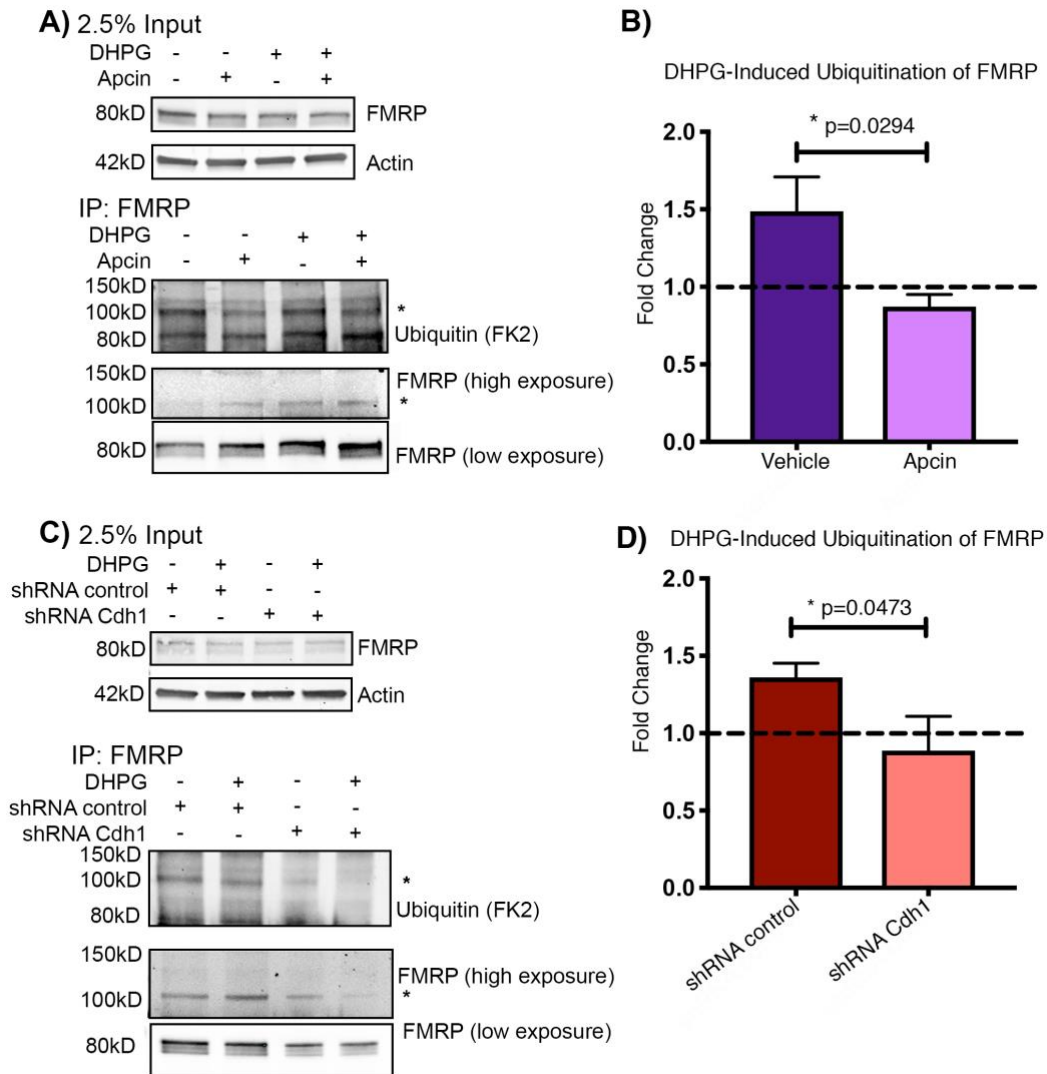


Figure 3-1: Cdh1-APC regulates FMRP ubiquitination in neurons downstream of mGluR signaling

A) DIV 13 cortical neurons were treated with MG-132 (10 μ M) and Apcin (1 μ M) for 16-18 hours. Neurons were then stimulated with DHPG (50 μ M, 5 minutes) on DIV 14. Lysates underwent FMRP immunoprecipitation and subsequent immunoblotting for conjugated ubiquitin and FMRP. Asterisk indicates high-molecular weight form of FMRP that is immunoreactive to both FMRP and ubiquitin. **B)** Quantification of difference in ubiquitinated FMRP following DHPG stimulation; n=3. **C)** DIV 7 neurons were transduced with shRNA-expressing lentivirus, and on

DIV 13 neurons were treated with MG-132 (10 μ M) for 16-18 hours and were stimulated with DHPG (50 μ M, 5 minutes) on DIV 14. Lysates underwent FMRP immunoprecipitation as described in A). **D)** Quantification of difference in ubiquitinated FMRP following DHPG stimulation; n=4.

*p<0.05 Statistical significance calculated by Student's t test.

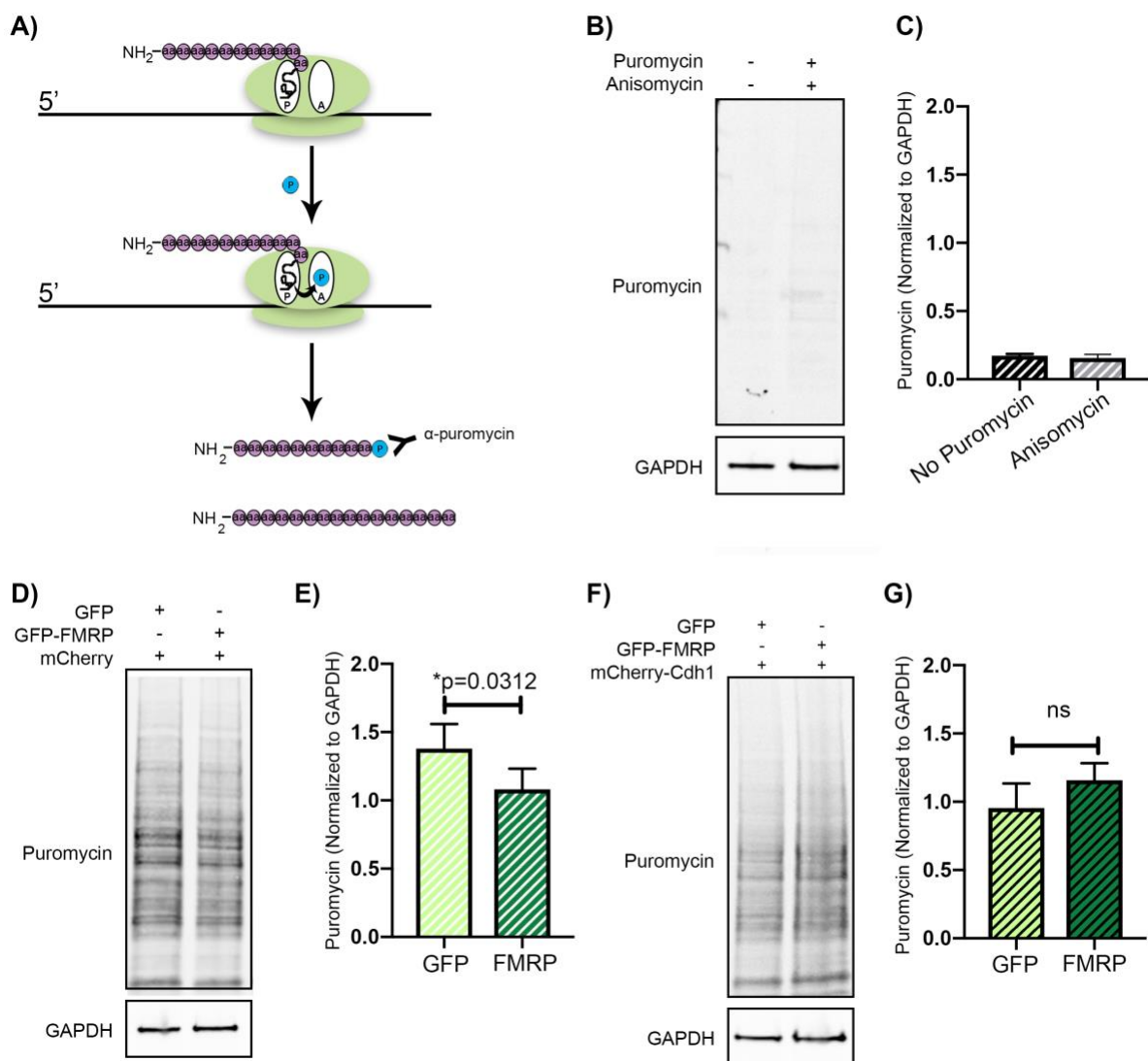


Figure 3-2: Cdh1 reverses FMRP-mediated repression of translation

A) Schematic of puromylation. Puromycin is a tRNA analog, that when added to cell culture media, can be incorporated into elongating polypeptide chains. Newly synthesized proteins can then be identified by probing puromycin with antibodies. **B)** To confirm the specificity of the puromylation, N2A cells were either treated with no puromycin or with anisomycin to terminate protein synthesis. **C)** Quantification of puromycin normalized to GAPDH. **D)** N2A cells were transfected with GFP or GFP-FMRP and mCherry. Cells underwent puromylation (10μg/mL)

for 45 minutes were then lysed and immunoblotted for puromycin and GAPDH. **E)** Quantification of puromycin normalized to GAPDH in **E**); n=4. **F)** N2A cells were transfected with GFP or GFP-FMRP and mCherry-Cdh1. Cells underwent puromycylation (10 μ g/mL) for 45 minutes were then lysed. **G)** Quantification of puromycin normalized to GAPDH in **F**); n=4.

*p<0.05 Statistical significance calculated by Student's t test.

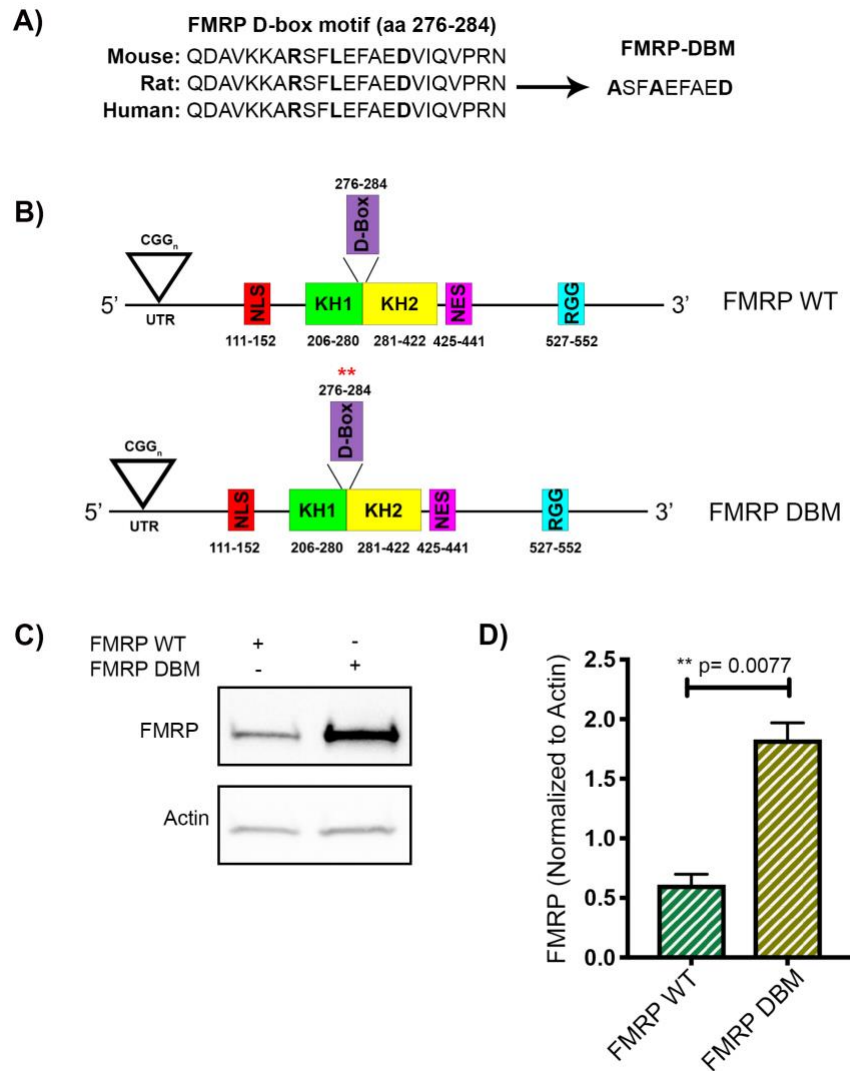


Figure 3-3: Cdh1-APC interaction affects FMRP expression

A) FMRP contains a “Destruction box” motif that is well conserved across species. FMRP-Destruction box mutant (FMRP DBM) was generated by mutating two amino acids as described previously (Huang et al., 2015). **B)** Schematic comparing wildtype FMRP (FMRP WT) to FMRP DBM constructs. Note that the Destruction box motif spans the KH1 and KH2 domains of FMRP, which are two domains that have been studied to regulate FMRP’s ability to bind mRNA and regulate protein synthesis (see section 1.4.1.). **C)** FMRP WT or FMRP DBM constructs were

transfected into N2A cells; cells were then lysed, underwent electrophoresis and immunoblotted for FMRP and actin. **D)** Quantification steady state FMRP normalized to actin. N=4

Statistical significance calculated by Student's t test. **p<0.01

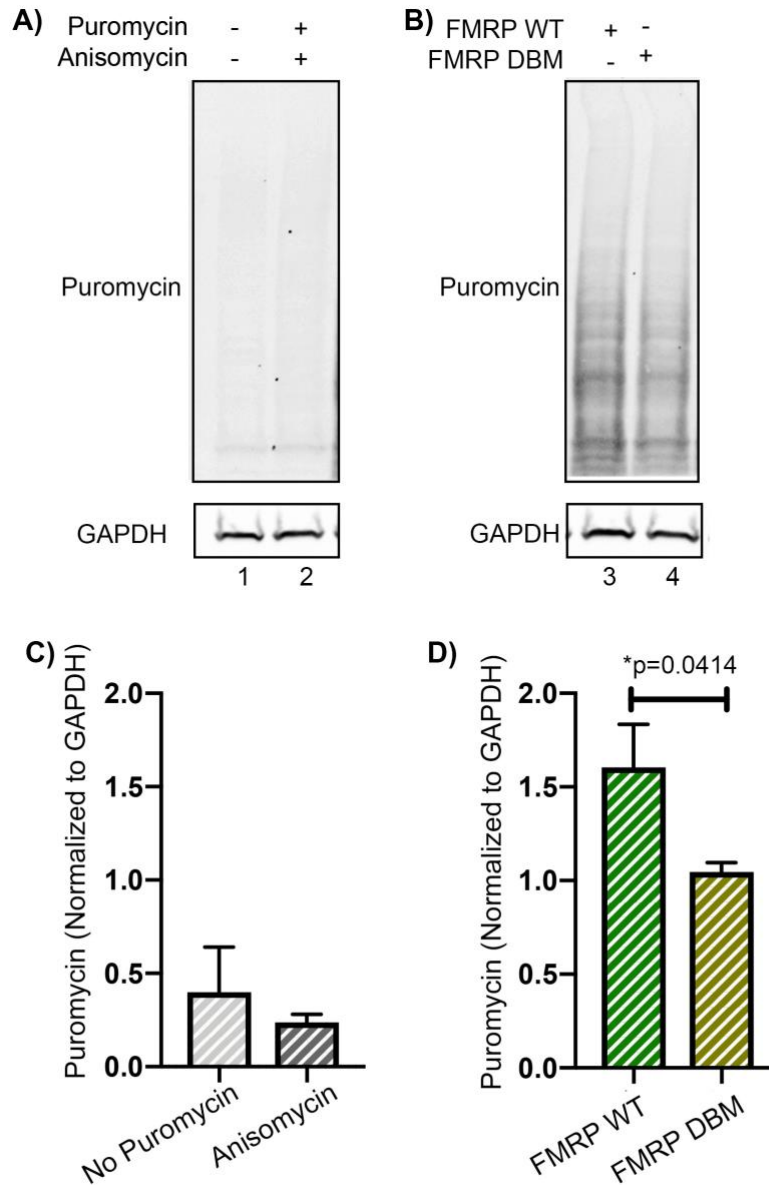
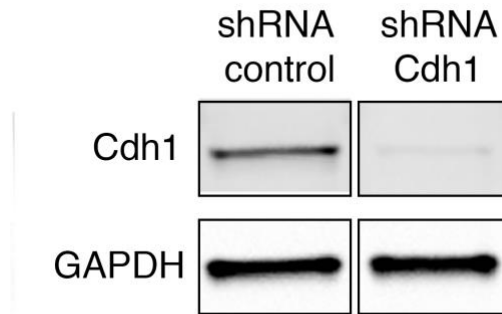


Figure 3-4: Cdh1-APC interaction with FMRP regulates protein synthesis

A) and **B)** N2A cells were transfected with FMRP WT or FMRP DBM for 24 hours and underwent 45 minutes of puromycylation (10 μ g/mL). **C)** Quantification of puromycin normalized to GAPDH for the control conditions of no puromycin and anisomycin. **D)** Quantification of puromycin normalized to GAPDH. n=5

Statistical significance calculated by Student's t test.

3.5. Supplemental Figures



Supplemental Figure 3-1: Validation of Cdh1 Knockdown

N2A cells were transfected with shRNA targeting Cdh1 or a control shRNA from Dharmacon utilizing Lipofectamine 2000 (Invitrogen). 72 hours after transfection, cells were lysed and immunoblotted to assess knockdown efficiency. Upon confirmation of knockdown, the Dharmacon plasmids were sent to the Emory Viral Vector core for lentiviral production.

Chapter 4 :

Cdh1-APC Associates with Translational Machinery and is a Novel Regulator of Protein Synthesis

Portions of this chapter were adapted from the following publication:

Valdez-Sinon AN, Lai A, Shi L, Lancaster CL, Gokhale A, Faundez V, Bassell GJ. Cdh1-APC interactions with FMRP and ribosomal components regulate protein synthesis and stress granule dynamics in neural cells. *Cell Reports, In Revision*.

4.1. Introduction

Cdh1-APC has been observed to interact with and ubiquitinate FMRP (**Figure 3-1**) (Huang et al., 2015), an RNA-binding protein known to repress the translation of mRNAs critical for synaptic structure and function (Darnell et al., 2011). Ubiquitination of FMRP has been proposed as a molecular switch to reverse the repression of protein synthesis by FMRP (Nalavadi et al., 2012), and thus, regulation of a FMRP by Cdh1-APC as observed in Chapter 3 suggests a link between Cdh1-APC and protein synthesis. Control over protein synthesis is critical for neurodevelopment, as evidenced by a hallmark pathology of exaggerated protein synthesis in neurodevelopmental disorders such as fragile X syndrome (Gross and Bassell, 2012; Gross et al., 2010; Sharma et al., 2010). Thus, regulation of protein synthesis in neurons by Cdh1-APC may be critical for neurodevelopment.

A previous study demonstrated that genetic reduction of Cdh1 leads to reduced expression of mGluR-LTD (Huang et al., 2015). Since mGluR-LTD requires new protein synthesis (Kauderer and Kandel, 2000), it is possible that Cdh1-mediated alterations of LTD are due to changes in protein synthesis. Based on these findings, it was hypothesized that perturbation of Cdh1-APC activity regulates protein synthesis. As it is currently not known whether Cdh1-APC regulates protein synthesis, our findings reveal a new function for Cdh1-APC. Furthermore, we undertake a proteomics approach to characterize for the first time the proteins that interact with Cdh1-APC and provide new insight into the underlying molecular mechanisms involved in protein synthesis regulation by Cdh1-APC.

4.2. Results

4.2.1. Cdh1-APC Regulates Protein Synthesis Independent of Cell Cycle

To assess whether Cdh1-APC affects protein synthesis, Cdh1 was genetically knocked down in DIV 7 cortical neurons using lentivirus expressing shRNA against Cdh1. To label newly synthesized proteins, DIV 14-16 cells underwent puromycylation as described in Chapter 3. Neurons with Cdh1 knocked down demonstrated a reduced signal of puromycin as compared to control cells, suggesting that inhibition of Cdh1-APC indeed leads to a decrease in protein synthesis (**Figure 4-1**). This result supports the hypothesis that Cdh1-APC has a novel function as regulator of protein synthesis. In another approach, Cdh1 was pharmacologically inhibited in DIV 14-16 cortical neurons with Apcin (2 μ M) for 16-18 hours (Sackton et al., 2014). Similar to knockdown Cdh1, pharmacologic inhibition of Cdh1-APC lead to a significant reduction in protein synthesis (**Figure 4-1**). The observation of decreased protein synthesis in postmitotic cortical neurons suggests that the inhibitory effects of Cdh1-APC on protein synthesis are independent of its role in mitotic cells. The role of Cdh1-APC in regulation of protein synthesis has not been investigated previously, and our work demonstrating that Cdh1-APC can regulate protein synthesis sheds light on a potential novel function of the Cdh1-APC complex in postmitotic neurons.

4.2.2. Cdh1-APC interactome is enriched with regulators of protein synthesis

Following observations of a novel role of Cdh1-APC in protein synthesis, we sought to elucidate the mechanism by which Cdh1-APC may be affecting protein synthesis. As FMRP has already been identified as an interactor and substrate of Cdh1-APC E3 ligase activity (**Figures 1-3, 3-1**) (Huang et al., 2015), we aimed to determine whether Cdh1-APC interacts with other RNA binding proteins known to regulate translation. To take an unbiased approach in identifying other

Cdh1-interactors, N2A cells were transfected with FLAG-Cdh1 and lysates underwent FLAG-immunoaffinity chromatography with FLAG-peptide elution (**Figure 4-2**) (Comstra et al., 2017; Gokhale et al., 2012). A portion of the lysate was co-incubated with FLAG peptide to outcompete FLAG-Cdh1 and allow for identification of nonspecific binding proteins to bead-antibody complexes. Following confirmation of sufficient protein pulldown with silver staining (**Figure 4-2**), the immunoprecipitate was analyzed by mass spectrometry. 185 unique proteins were identified as the Cdh1 interactome (**Table 4-1**). The interactome included known components of the Cdh1-APC complex, such as APC1, APC2, APC7, CDC16, CDC23, and CDC27. Enrichment of APC subunits validated the specificity of the technical approach. A DAVID analysis was then conducted to identify common biological processes amongst the interactome (**Table 4-2**). Aside from expected enrichment in categories related to the ubiquitin-proteasome system such as protein K11-linked ubiquitination (GO: 00709791, $p=7.57 \times 10^{-6}$), the interactome was highly enriched in categories related to protein synthesis (**Figure 4-2, Table 4-2**). Of interest, 36.7% of the Cdh1 interactome was categorized into translation (GO: 0006412, $p=4.09 \times 10^{-73}$). Other translation-related biological processes that were enriched in the Cdh1 interactome include: formation of translation preinitiation complex (GO: 0001731, $p=8.07 \times 10^{-13}$), regulation of translational initiation (GO:0006446, $p=2.22 \times 10^{-12}$), positive regulation of translation (GO:0045727, $p=2.16 \times 10^{-4}$), negative regulation of translation (GO:0017148, $p=1.39 \times 10^{-7}$), and ribosomal subunit assembly (GO:0000027, $p=7.76 \times 10^{-12}$; GO:0000028, $p=2.05 \times 10^{-11}$). The significant enrichment of proteins involved in translational processes supports a novel role of Cdh1-APC in translation regulation outside of its canonical roles in ubiquitination and cell cycle.

With its known function as an E3 ligase complex, we hypothesized that the proteins enriched in the mass spectrometry results were ubiquitination targets of Cdh1-APC. As a first step

to investigate this hypothesis, we performed another FLAG immunoprecipitation of FLAG-Cdh1 lysate and used the eluted proteins for a secondary ubiquitin immunoprecipitation experiment. This experimental approach aimed to identify which proteins in the Cdh1 interactome are ubiquitinated. Upon immunoblotting for conjugated ubiquitin, we saw no enrichment of ubiquitinated proteins within the Cdh1-interactome (**Figure 4-3**). Upon silver staining, the ubiquitin immunoprecipitation did not contain any unique proteins compared to a mouse IgG control condition, further suggesting that the proteins identified as interacting with Cdh1-APC might not necessarily be substrates of its ubiquitin catalytic activity. However, as will be discussed below, there are caveats to this method and how the data is to be interpreted. Thus, it is not at all conclusive whether or not Cdh1 ubiquitinates the proteins identified in the interactome and much more work is needed.

With these sets of immunoprecipitation experiments, we have uncovered the novel interactome of Cdh1. Taken together with the puromycylation data in neural cells, our findings suggest a noncanonical role of Cdh1-APC as a regulator of protein synthesis, in contrast to its well-characterized regulation of protein degradation.

4.3. Discussion

Data from this chapter identify a novel function of Cdh1-APC as a regulator of protein synthesis in neural cells. Cdh1-APC has been classically studied as a regulator of cell cycle in mitotic cells (Sudakin et al., 1995) and recent studies have explored its role in postmitotic neurons (Huang et al., 2015; Konishi et al., 2004; Li et al., 2008; Pick et al., 2012; Pick et al., 2013). Not only do we demonstrate a novel role for Cdh1-APC in translation, but the regulation of protein synthesis by Cdh1-APC occurs in postmitotic neurons. Thus, the role of Cdh1-APC in regulation protein synthesis does not rely on its ability to regulate the promotion of anaphase in mitotic cells.

However, it is unclear if the cell-division independent role of Cdh1-APC in protein synthesis only occurs in neural-lineage cells. As there are functions of Cdh1-APC that are neuronal specific, such as maintenance of antioxidant status (Herrero-Mendez et al., 2009), it is possible that its function as a translational regulator is also neuronal specific. Interestingly, additional experiments in human fibroblasts did not show any changes in protein synthesis following Cdh1-APC manipulation (**Supplemental Figure 4-1**). It is possible that Cdh1's novel role in regulating protein synthesis may only occur in neural lineage cells types.

Additionally, it is unclear whether any related changes in protein synthesis are due to Cdh1-APC's ubiquitination of other proteins in its interactome. While it is most likely that Cdh1-APC ubiquitinates the interactome we identified, it is possible that it has non-canonical functions through binding to these proteins. For example, as eIF4E (an identified interactor of Cdh1) can be physically bound by eIF4-BP to prevent translation, perhaps Cdh1 is binding to initiation factors to synergize and promote the initiation of translation. In **Figure 4-3**, it is possible that we were unable to determine if components of the Cdh1 interactome were ubiquitination substrates due to the transient nature of contact between Cdh1, as the regulatory subunit of the APC E3 ligase, and its target substrate (Pierce et al., 2009). Thus, substrates of Cdh1 that have already been ubiquitinated may not necessarily be enriched for during the FLAG immunoaffinity chromatography experiments. Cross-linking methods, such as the use of dithiobis-(succinimidyl propionate) (Zlatic et al., 2010) or ultraviolet irradiation (Darnell et al., 2011) may help in future studies to stabilize the interaction between Cdh1 and its substrates. Alternatively, the use of a technique known as BioID may help to identify transient Cdh1 substrates. BioID consists of fusing biotin ligase to a protein of interest; nearby proteins that interact with the protein of interest will then be biotinylated and downstream processes such as mass spectrometry can then identify the

biotinylated proteins (Roux et al., 2018). While this approach would identify proteins that had been ubiquitinated by Cdh1, proteins that are solely interactors of Cdh1 and not target substrates would also be biotinylated. Thus, it would be unlikely that one could distinguish which of the biotinylated proteins are true target substrates of Cdh1-mediated ubiquitination.

Alternatively, an experimental approach similar to the one utilized in Chapter 3 to observe ubiquitination of FMRP (**Figure 3-1**) can be applied to determine whether or not specific interactors of Cdh1 as identified by mass spectrometry are indeed ubiquitinated by Cdh1-APC. Cdh1-APC activity in cortical neurons would first be manipulated either through pharmacologic inhibition with Apcin or genetic knockdown with lentivirus. Then, cells would be treated with a proteasome inhibitor, such as MG-132, to allow for the accumulation of ubiquitinated proteins. Lysate from these neurons would undergo immunoprecipitation for selected candidates based on the mass spectrometry data, such as ribosomal subunits, initiation factors, G3BP1, and Caprin1. Immunoblotting would be performed for both conjugated ubiquitin and the immunoprecipitated protein; high weight molecular bands that are immunoreactive for both ubiquitin and the protein of interest would be interpreted as ubiquitinated forms of that protein. Alterations in the amount of ubiquitinated protein following manipulations of Cdh1-APC activity would indicate that Cdh1-APC specifically ubiquitinates that specific interacting protein. For example, if eiF3B is immunoprecipitated and its ubiquitination is decreased upon Apcin treatment or Cdh1-knockdown, it can be concluded that Cdh1-APC ubiquitinates eiF3B. Additionally, lysate from the immunoprecipitation could be analyzed with mass spectrometry to identify specific lysines on the candidate ubiquitin substrates that may be ubiquitinated based on Cdh1-APC activity. While these experimental approaches allow for more specificity in determining whether or not Cdh1-APC ubiquitinates specific proteins, it is not high-throughput; such an undertaking would require

optimization of immunoprecipitations for multiple proteins. Since there were 185 proteins identified within the Cdh1 interactome, it would be necessary to select a limited number of candidate proteins to proceed with this immunoprecipitation-based approach. Further elucidation of downstream processes dependent upon Cdh1-APC activity may help to inform which of our candidate proteins may be the most high-yield to perform these sets of experiments on to determine whether or not Cdh1-APC ubiquitinates that protein.

Puromycylation data from two types of neural cells: mitotic Neuro2A cells and postmitotic cortical neurons demonstrate a novel role of Cdh1 in regulating protein synthesis. This finding was strengthened upon identification of translational regulators, such as initiation factors, ribosomal proteins, and RNA binding proteins in an unbiased mass spectrometry analysis of the Cdh1 interactome. Identification of the Cdh1 interactome provides potential mechanisms of action by which Cdh1-APC may be regulating protein synthesis. In the subsequent chapter, we investigate one of the potential mechanisms by which Cdh1-APC is able to regulate protein synthesis in neural cells.

4.4. Figures

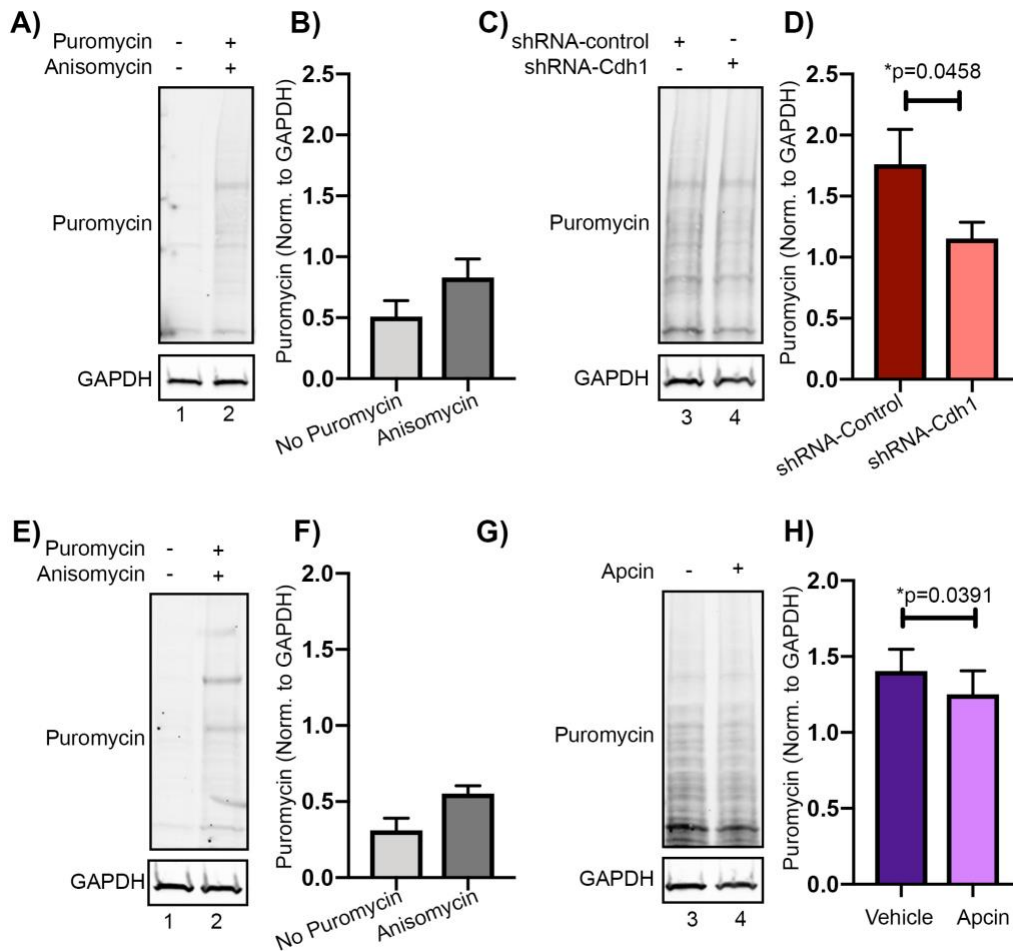


Figure 4-1: Cdh1-APC regulates protein synthesis independent of cell cycle

A) and **C)** DIV 7 cortical neurons were transduced with lentivirus expressing either shRNA against Cdh1 or a control sequence. On DIV14, transduced neurons underwent 75 minutes of puromylation (10 μ g/mL). **B)** & **D)** Quantification of puromycin normalized to GAPDH for J); n=4. **E)** and **G)** DIV 14 cortical neurons were treated with Apcin (2 μ M) for 16-18 hours and underwent 75 minutes of puromylation (10 μ g/mL). **F)** & **H)** Quantification of puromycin normalized to GAPDH for D); n=4.

Statistical significance calculated by Student's t test. *p<0.05

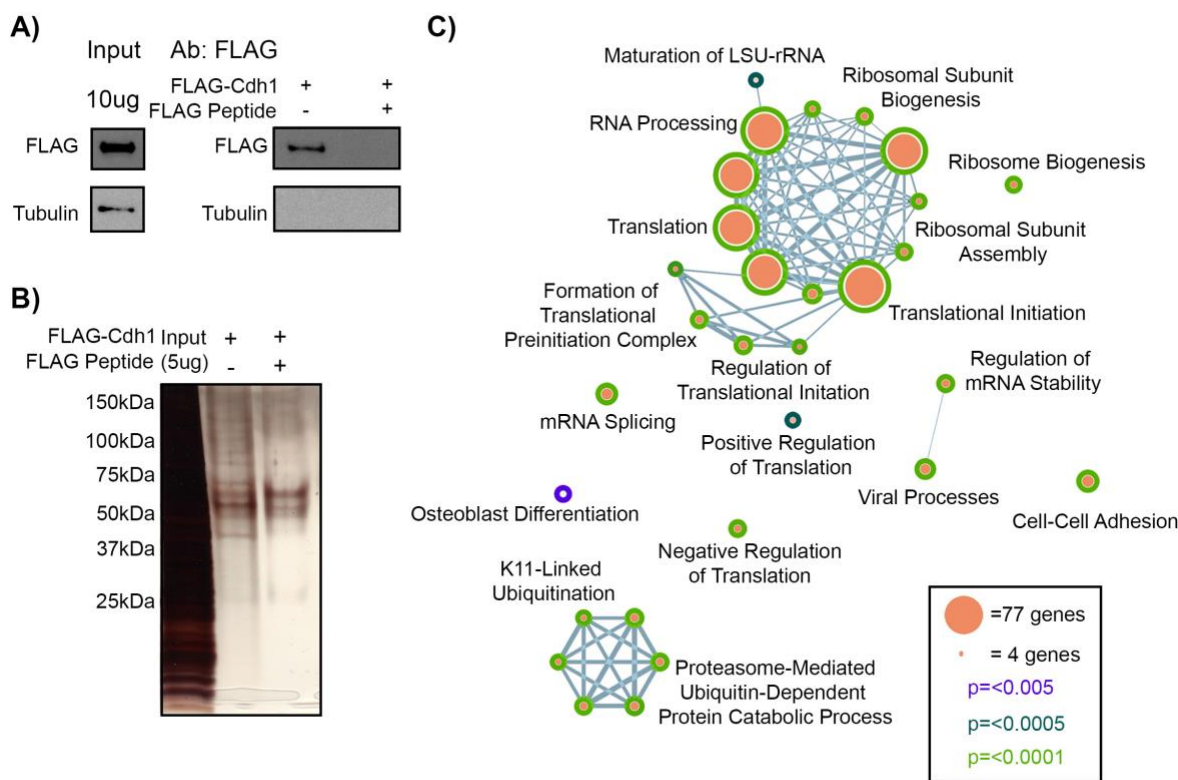


Figure 4-2: Cdh1 interactome is enriched with translational regulators

A) N2A cells were transfected with FLAG-Cdh1. Lysate was incubated with immunomagnetic beads coupled to FLAG antibody either in the absence or presence of antigenic 3x FLAG peptide. Chemiluminescent western blotting demonstrates an enrichment of FLAG-Cdh1. **B)** Silver stain shows an enrichment of putative Cdh1 interacting proteins from sample without FLAG peptide co-incubation. **C)** DAVID Biological Processes GO-term analysis on peptides enriched 4-fold compared to controls from mass spectrometry results. Size of the nodes indicate number of genes in the Cdh1 interactome within a specific biological process category. The color of the border of each of the nodes represents the p-value as generated by the DAVID analysis.

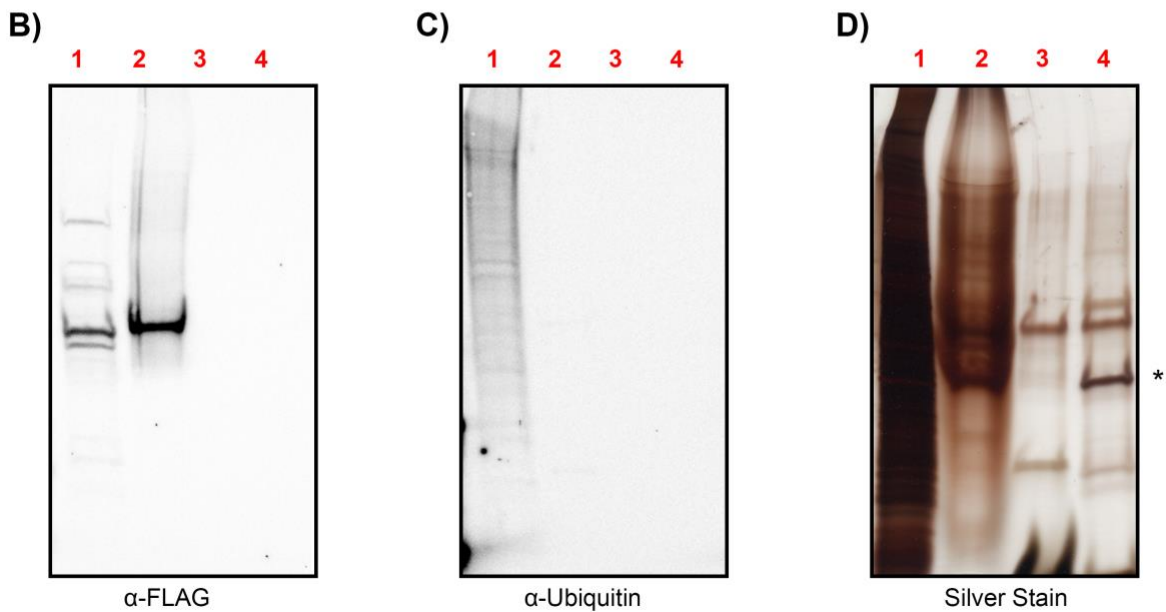
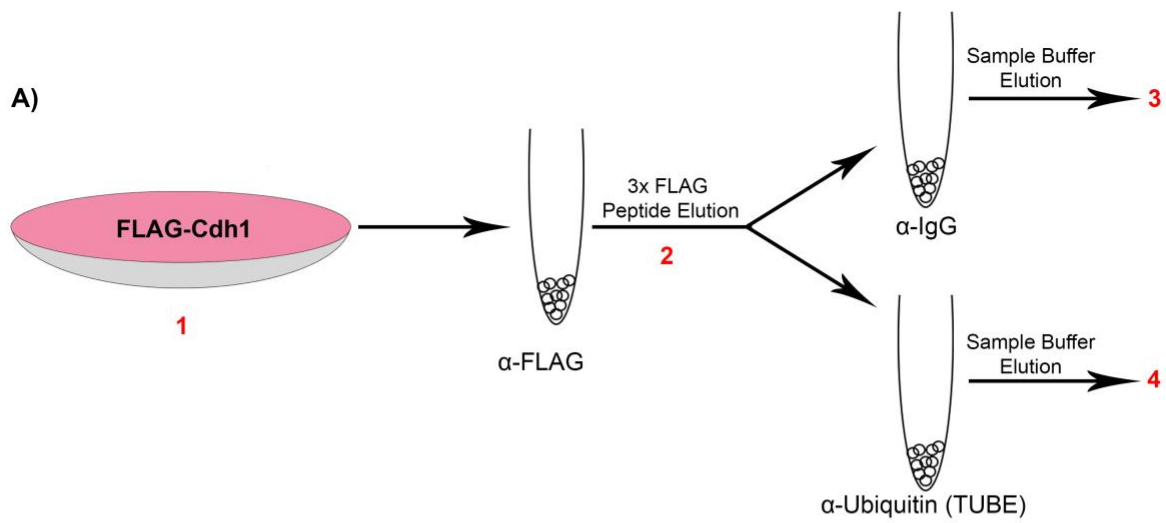


Figure 4-3: Cdh1-APC's interactome is enriched with noncanonical binding partners linked to translation

A) Experimental approach to FLAG-Ubiquitin immunoprecipitation experiment. N2A cells were transfected with FLAG-Cdh1 and lysed. Lysate was used for a FLAG immunoprecipitation followed by 3x FLAG peptide elution. Immunoprecipitate was then split between a secondary immunoprecipitation for Ubiquitin (utilizing TUBEs) or mouse IgG as a control. Numbers indicate

sample type for lanes in images below. **B)** FLAG immunoblot, demonstrating an enrichment of FLAG-Cdh1 in the initial lysate (lane 1) as well as the FLAG immunoprecipitate (lane 2). **C)** Conjugated ubiquitin immunoblot, demonstrating an enrichment of ubiquitin only in the initial lysate (lane 1). **D)** Silver stain showing total protein for all samples. Asterisk indicates band with eluted TUBE reagent.

4.5. Tables

Identified Proteins (185)	Molecular Weight	Spectral Count			
		N	N+	C	C+
Polyadenylate-binding protein 1 OS=Mus musculus GN=Pabpc1 PE=1 SV=2	71 kDa	0	0	81	0
Heat shock cognate 71 kDa protein OS=Mus musculus GN=Hspa8 PE=1 SV=1	71 kDa	18	10	79	4
Ribonucleoside-diphosphate reductase subunit M2 OS=Mus musculus GN=Rrm2 PE=1 SV=1	45 kDa	0	0	45	0
Receptor of activated protein C kinase 1 OS=Mus musculus GN=Rack1 PE=1 SV=3	35 kDa	0	0	39	0
Y-box-binding protein 3 OS=Mus musculus GN=Ybx3 PE=1 SV=2	39 kDa	0	0	35	0
La-related protein 1 OS=Mus musculus GN=Larp1 PE=1 SV=3	121 kDa	0	0	33	0
40S ribosomal protein S10 OS=Mus musculus GN=Rps10 PE=1 SV=1	19 kDa	0	0	33	0
40S ribosomal protein S3a OS=Mus musculus GN=Rps3a PE=1 SV=3	30 kDa	0	0	33	0
Eukaryotic translation initiation factor 3 subunit B OS=Mus musculus GN=Eif3b PE=1 SV=1	91 kDa	0	0	31	0
40S ribosomal protein S3 OS=Mus musculus GN=Rps3 PE=1 SV=1	27 kDa	0	3	30	0
40S ribosomal protein SA OS=Mus musculus GN=Rpsa PE=1 SV=4	33 kDa	0	0	30	0
60S ribosomal protein L10a OS=Mus musculus GN=Rpl10a PE=1 SV=3	25 kDa	0	3	29	0
40S ribosomal protein S4, X isoform OS=Mus musculus GN=Rps4x PE=1 SV=2	30 kDa	0	0	29	0
Pre-mRNA-processing factor 19 OS=Mus musculus GN=Prpf19 PE=1 SV=1	55 kDa	5	0	28	0
60S ribosomal protein L12 OS=Mus musculus GN=Rpl12 PE=1 SV=2	18 kDa	0	0	28	0
60S ribosomal protein L11 OS=Mus musculus GN=Rpl11 PE=1 SV=4	20 kDa	0	0	28	0
Signal recognition particle subunit SRP68 OS=Mus musculus GN=Srp68 PE=1 SV=2	71 kDa	0	0	27	0

Identified Proteins (185)	Molecular Weight	Spectral Count			
		N	N+	C	C+
60S acidic ribosomal protein P0 OS=Mus musculus GN=Rplp0 PE=1 SV=3	34 kDa	0	2	26	0
40S ribosomal protein S18 OS=Mus musculus GN=Rps18 PE=1 SV=3	18 kDa	0	2	26	0
Probable ATP-dependent RNA helicase DDX5 OS=Mus musculus GN=Ddx5 PE=1 SV=2	69 kDa	6	0	25	0
Cell division cycle 5-like protein OS=Mus musculus GN=Cdc5l PE=1 SV=2	92 kDa	2	0	24	0
60S ribosomal protein L10-like OS=Mus musculus GN=Rpl10l PE=2 SV=1	25 kDa	0	0	24	0
60S ribosomal protein L26 OS=Mus musculus GN=Rpl26 PE=1 SV=1	17 kDa	0	0	22	0
Heat shock protein HSP 90-beta OS=Mus musculus GN=Hsp90ab1 PE=1 SV=3	83 kDa	4	0	21	0
60S ribosomal protein L18a OS=Mus musculus GN=Rpl18a PE=1 SV=1	21 kDa	0	0	21	0
40S ribosomal protein S11 OS=Mus musculus GN=Rps11 PE=1 SV=3	18 kDa	0	0	20	0
60S ribosomal protein L5 OS=Mus musculus GN=Rpl5 PE=1 SV=3	34 kDa	0	0	20	0
40S ribosomal protein S20 OS=Mus musculus GN=Rps20 PE=1 SV=1	13 kDa	0	0	20	0
Eukaryotic translation initiation factor 3 subunit A OS=Mus musculus GN=Eif3a PE=1 SV=5	162 kDa	0	0	20	0
Nucleolin OS=Mus musculus GN=Ncl PE=1 SV=2	77 kDa	0	0	19	0
40S ribosomal protein S13 OS=Mus musculus GN=Rps13 PE=1 SV=2	17 kDa	0	0	19	0
Importin subunit beta-1 OS=Mus musculus GN=Kpnb1 PE=1 SV=2	97 kDa	0	0	19	0
Plasminogen activator inhibitor 1 RNA-binding protein OS=Mus musculus GN=Serbp1 PE=1 SV=2	45 kDa	0	0	19	0
La-related protein 4 OS=Mus musculus GN=Larp4 PE=1 SV=2	80 kDa	0	0	19	0
Caprin-1 OS=Mus musculus GN=Caprin1 PE=1 SV=2	78 kDa	0	0	18	0
40S ribosomal protein S7 OS=Mus musculus GN=Rps7 PE=2 SV=1	22 kDa	0	2	18	0

Identified Proteins (185)	Molecular Weight	Spectral Count			
		N	N+	C	C+
Pleiotropic regulator 1 OS=Mus musculus GN=Plrg1 PE=1 SV=1	57 kDa	0	0	18	0
60S acidic ribosomal protein P2 OS=Mus musculus GN=Rplp2 PE=1 SV=3	12 kDa	0	0	18	0
Regulator of nonsense transcripts 1 OS=Mus musculus GN=Upf1 PE=1 SV=2	124 kDa	0	0	18	0
60S ribosomal protein L13a OS=Mus musculus GN=Rpl13a PE=1 SV=4	23 kDa	0	0	18	0
Tubulin beta-5 chain OS=Mus musculus GN=Tubb5 PE=1 SV=1	50 kDa	5	3	17	0
Heterogeneous nuclear ribonucleoprotein U OS=Mus musculus GN=Hnrnpu PE=1 SV=1	88 kDa	5	0	17	0
40S ribosomal protein S5 OS=Mus musculus GN=Rps5 PE=1 SV=3	23 kDa	0	0	17	0
Myb-binding protein 1A OS=Mus musculus GN=Mybbp1a PE=1 SV=2	152 kDa	0	0	17	0
40S ribosomal protein S15a OS=Mus musculus GN=Rps15a PE=1 SV=2	15 kDa	0	0	16	0
60S ribosomal protein L17 OS=Mus musculus GN=Rpl17 PE=1 SV=3	21 kDa	0	0	15	0
Heterogeneous nuclear ribonucleoprotein M OS=Mus musculus GN=Hnrnpm PE=1 SV=3	78 kDa	0	0	15	0
40S ribosomal protein S16 OS=Mus musculus GN=Rps16 PE=1 SV=4	16 kDa	0	0	15	0
IgE-binding protein OS=Mus musculus GN=Iap PE=2 SV=1	63 kDa	0	0	15	0
Nuclease-sensitive element-binding protein 1 OS=Mus musculus GN=Ybx1 PE=1 SV=3	36 kDa	0	0	15	0
Eukaryotic translation initiation factor 3 subunit C OS=Mus musculus GN=Eif3c PE=1 SV=1	106 kDa	0	0	14	0
Transcriptional activator protein Pur-alpha OS=Mus musculus GN=Pura PE=1 SV=1	35 kDa	0	0	14	0
40S ribosomal protein S15 OS=Mus musculus GN=Rps15 PE=1 SV=2	17 kDa	0	0	13	0
Matrin-3 OS=Mus musculus GN=Matr3 PE=1 SV=1	95 kDa	2	0	13	0
Fragile X mental retardation syndrome-related protein 1 OS=Mus musculus GN=Fxr1 PE=1 SV=2	76 kDa	0	0	13	0

Identified Proteins (185)	Molecular Weight	Spectral Count			
		N	N+	C	C+
40S ribosomal protein S9 OS=Mus musculus GN=Rps9 PE=1 SV=3	23 kDa	0	0	12	0
Nucleophosmin OS=Mus musculus GN=Npm1 PE=1 SV=1	33 kDa	0	0	12	0
40S ribosomal protein S12 OS=Mus musculus GN=Rps12 PE=1 SV=2	15 kDa	0	0	12	0
60S ribosomal protein L30 OS=Mus musculus GN=Rpl30 PE=1 SV=2	13 kDa	0	0	12	0
Eukaryotic translation initiation factor 3 subunit I OS=Mus musculus GN=Eif3i PE=1 SV=1	36 kDa	0	0	12	0
60S ribosomal protein L9 OS=Mus musculus GN=Rpl9 PE=2 SV=2	22 kDa	0	0	11	0
60S ribosomal protein L37a OS=Mus musculus GN=Rpl37a PE=1 SV=2	10 kDa	0	0	11	0
60S ribosomal protein L23 OS=Mus musculus GN=Rpl23 PE=1 SV=1	15 kDa	2	0	11	0
60S ribosomal protein L22 OS=Mus musculus GN=Rpl22 PE=1 SV=2	15 kDa	0	0	11	0
60S ribosomal protein L13 OS=Mus musculus GN=Rpl13 PE=1 SV=3	24 kDa	0	0	11	0
60S ribosomal protein L8 OS=Mus musculus GN=Rpl8 PE=1 SV=2	28 kDa	0	0	11	0
40S ribosomal protein S19 OS=Mus musculus GN=Rps19 PE=1 SV=3	16 kDa	0	0	10	0
60S ribosomal protein L14 OS=Mus musculus GN=Rpl14 PE=1 SV=3	24 kDa	0	0	10	0
60S ribosomal protein L7a OS=Mus musculus GN=Rpl7a PE=1 SV=2	30 kDa	0	0	10	0
ATP synthase subunit gamma, mitochondrial OS=Mus musculus GN=Atp5c1 PE=1 SV=1	33 kDa	0	0	10	0
Protein regulator of cytokinesis 1 OS=Mus musculus GN=Prc1 PE=1 SV=2	70 kDa	0	0	9	0
40S ribosomal protein S2 OS=Mus musculus GN=Rps2 PE=1 SV=3	31 kDa	0	2	9	0
40S ribosomal protein S17 OS=Mus musculus GN=Rps17 PE=1 SV=2	16 kDa	0	0	9	0
60S ribosomal protein L23a OS=Mus musculus GN=Rpl23a PE=1 SV=1	18 kDa	0	0	9	0

Identified Proteins (185)	Molecular Weight	Spectral Count			
		N	N+	C	C+
60S ribosomal protein L31 OS=Mus musculus GN=Rpl31 PE=1 SV=1	14 kDa	0	0	9	0
Eukaryotic translation initiation factor 3 subunit F OS=Mus musculus GN=Eif3f PE=1 SV=2	38 kDa	0	0	9	0
Eukaryotic translation initiation factor 3 subunit D OS=Mus musculus GN=Eif3d PE=1 SV=2	64 kDa	0	0	9	0
Proline-, glutamic acid- and leucine-rich protein 1 OS=Mus musculus GN=Pelp1 PE=1 SV=2	118 kDa	0	0	9	0
Heterogeneous nuclear ribonucleoprotein F OS=Mus musculus GN=Hnrnpf PE=1 SV=3	46 kDa	3	0	9	0
La-related protein 4B OS=Mus musculus GN=Larp4b PE=1 SV=2	82 kDa	0	0	9	0
Putative ATP-dependent RNA helicase Pl10 OS=Mus musculus GN=D1Pas1 PE=1 SV=1	73 kDa	2	0	8	0
60S ribosomal protein L6 OS=Mus musculus GN=Rpl6 PE=1 SV=3	34 kDa	0	0	8	0
40S ribosomal protein S23 OS=Mus musculus GN=Rps23 PE=1 SV=3	16 kDa	0	0	8	0
60S ribosomal protein L15 OS=Mus musculus GN=Rpl15 PE=2 SV=4	24 kDa	0	0	8	0
Pre-mRNA-splicing factor SPF27 OS=Mus musculus GN=Bcas2 PE=1 SV=1	26 kDa	0	0	8	0
60S ribosomal protein L24 OS=Mus musculus GN=Rpl24 PE=1 SV=2	18 kDa	0	0	8	0
Eukaryotic translation initiation factor 3 subunit L OS=Mus musculus GN=Eif3l PE=1 SV=1	67 kDa	0	0	8	0
Cell division cycle protein 27 homolog OS=Mus musculus GN=Cdc27 PE=1 SV=1	92 kDa	0	0	8	0
60S ribosomal protein L28 OS=Mus musculus GN=Rpl28 PE=1 SV=2	16 kDa	0	0	8	0
Heterogeneous nuclear ribonucleoprotein Q OS=Mus musculus GN=Syncrip PE=1 SV=2	70 kDa	0	0	7	0
Calcium/calmodulin-dependent protein kinase type II subunit alpha OS=Mus musculus GN=Camk2a PE=1 SV=2	54 kDa	0	0	7	0
Nuclear valosin-containing protein-like OS=Mus musculus GN=Nvl PE=1 SV=1	94 kDa	0	0	7	0

Identified Proteins (185)	Molecular Weight	Spectral Count			
		N	N+	C	C+
Putative ATP-dependent RNA helicase DHX30 OS=Mus musculus GN=Dhx30 PE=1 SV=1	137 kDa	0	0	7	0
Ras GTPase-activating protein-binding protein 2 OS=Mus musculus GN=G3bp2 PE=1 SV=2	54 kDa	0	0	7	0
Cell division cycle protein 16 homolog OS=Mus musculus GN=Cdc16 PE=1 SV=1	71 kDa	0	0	7	0
40S ribosomal protein S21 OS=Mus musculus GN=Rps21 PE=1 SV=1	9 kDa	0	0	7	0
Beta-enolase OS=Mus musculus GN=Eno3 PE=1 SV=3	47 kDa	0	0	7	0
Heterogeneous nuclear ribonucleoprotein L OS=Mus musculus GN=Hnrnpl PE=1 SV=2	64 kDa	2	0	6	0
60S ribosomal protein L3 OS=Mus musculus GN=Rpl3 PE=1 SV=3	46 kDa	0	0	6	0
60S ribosomal protein L35a OS=Mus musculus GN=Rpl35a PE=1 SV=2	13 kDa	0	0	6	0
40S ribosomal protein S25 OS=Mus musculus GN=Rps25 PE=1 SV=1	14 kDa	0	3	6	0
60S ribosomal protein L18 OS=Mus musculus GN=Rpl18 PE=1 SV=3	22 kDa	0	0	6	0
Heterogeneous nuclear ribonucleoprotein K OS=Mus musculus GN=Hnrnpk PE=1 SV=1	51 kDa	2	0	6	0
60S ribosomal protein L21 OS=Mus musculus GN=Rpl21 PE=1 SV=3	19 kDa	0	0	6	0
78 kDa glucose-regulated protein OS=Mus musculus GN=Hspa5 PE=1 SV=3	72 kDa	0	0	6	0
Spermatogenesis-associated serine-rich protein 2 OS=Mus musculus GN=Spats2 PE=1 SV=1	59 kDa	0	0	6	0
60S ribosomal protein L34 OS=Mus musculus GN=Rpl34 PE=1 SV=2	13 kDa	0	0	6	0
40S ribosomal protein S8 OS=Mus musculus GN=Rps8 PE=1 SV=2	24 kDa	0	0	6	0
Histidine ammonia-lyase OS=Mus musculus GN=Hal PE=1 SV=1	72 kDa	0	0	6	0
Eukaryotic translation initiation factor 3 subunit H OS=Mus musculus GN=EIF3H PE=1 SV=1	40 kDa	0	0	6	0
Cytoskeleton-associated protein 4 OS=Mus musculus GN=Ckap4 PE=1 SV=2	64 kDa	0	0	6	0

Identified Proteins (185)	Molecular Weight	Spectral Count			
		N	N+	C	C+
Periodic tryptophan protein 1 homolog OS=Mus musculus GN=Pwp1 PE=1 SV=1	56 kDa	0	0	6	0
ATP-dependent RNA helicase DHX36 OS=Mus musculus GN=Dhx36 PE=1 SV=2	114 kDa	0	0	6	0
Stress-70 protein, mitochondrial OS=Mus musculus GN=Hspa9 PE=1 SV=3	73 kDa	0	0	6	0
Calcium/calmodulin-dependent protein kinase type II subunit beta OS=Mus musculus GN=Camk2b PE=1 SV=2	60 kDa	0	0	6	0
60S ribosomal protein L36 OS=Mus musculus GN=Rpl36 PE=3 SV=2	12 kDa	0	2	5	0
40S ribosomal protein S14 OS=Mus musculus GN=Rps14 PE=1 SV=3	16 kDa	0	0	5	0
60S ribosomal protein L4 OS=Mus musculus GN=Rpl4 PE=1 SV=3	47 kDa	0	0	5	0
Uncharacterized protein C7orf50 homolog OS=Mus musculus PE=1 SV=3	22 kDa	0	0	5	0
60S ribosomal protein L7 OS=Mus musculus GN=Rpl7 PE=1 SV=2	31 kDa	0	0	5	0
60S ribosomal protein L27a OS=Mus musculus GN=Rpl27a PE=1 SV=5	17 kDa	0	0	5	0
YTH domain-containing family protein 2 OS=Mus musculus GN=Ythdf2 PE=1 SV=1	62 kDa	0	0	5	0
60S ribosomal protein L19 OS=Mus musculus GN=Rpl19 PE=1 SV=1	23 kDa	0	0	5	0
Myosin-binding protein C, fast-type OS=Mus musculus GN=Mybpc2 PE=1 SV=1	127 kDa	0	0	5	0
Ras GTPase-activating protein-binding protein 1 OS=Mus musculus GN=G3bp1 PE=1 SV=1	52 kDa	0	0	5	0
Protein-glutamine gamma-glutamyltransferase E OS=Mus musculus GN=Tgm3 PE=1 SV=2	77 kDa	0	0	4	0
Small proline-rich protein 2D OS=Mus musculus GN=Sprr2d PE=2 SV=1	9 kDa	0	0	4	0
Cold shock domain-containing protein E1 OS=Mus musculus GN=Csde1 PE=1 SV=1	89 kDa	0	0	4	0
60S ribosomal protein L27 OS=Mus musculus GN=Rpl27 PE=1 SV=2	16 kDa	0	0	4	0

Identified Proteins (185)	Molecular Weight	Spectral Count			
		N	N+	C	C+
RNA-binding protein Raly OS=Mus musculus GN=Raly PE=1 SV=3	33 kDa	0	0	4	0
Eukaryotic translation initiation factor 3 subunit K OS=Mus musculus GN=Eif3k PE=1 SV=1	25 kDa	0	0	4	0
ELAV-like protein 1 OS=Mus musculus GN=Elav1 PE=1 SV=2	36 kDa	0	0	4	0
Ribosomal biogenesis protein LAS1L OS=Mus musculus GN=Las1l PE=1 SV=1	89 kDa	0	0	4	0
Anaphase-promoting complex subunit 2 OS=Mus musculus GN=Anapc2 PE=1 SV=2	95 kDa	0	0	4	0
Nucleolar and spindle-associated protein 1 OS=Mus musculus GN=Nusap1 PE=1 SV=1	49 kDa	0	0	4	0
Nucleolar RNA helicase 2 OS=Mus musculus GN=Ddx21 PE=1 SV=3	94 kDa	0	0	4	0
Eukaryotic translation initiation factor 3 subunit M OS=Mus musculus GN=Eif3m PE=1 SV=1	43 kDa	0	0	4	0
S-phase kinase-associated protein 1 OS=Mus musculus GN=Skp1 PE=1 SV=3	19 kDa	0	0	4	0
Ubiquitin carboxyl-terminal hydrolase 10 OS=Mus musculus GN=Usp10 PE=1 SV=3	87 kDa	0	0	4	0
Nuclear RNA export factor 1 OS=Mus musculus GN=Nxf1 PE=1 SV=3	70 kDa	0	0	4	0
Transcriptional activator protein Pur-beta OS=Mus musculus GN=Purb PE=1 SV=3	34 kDa	0	0	4	0
40S ribosomal protein S28 OS=Mus musculus GN=Rps28 PE=1 SV=1	8 kDa	0	0	3	0
RNA binding motif protein, X-linked-like-1 OS=Mus musculus GN=Rbmx1l PE=1 SV=1	42 kDa	0	0	3	0
Cyclin-A2 OS=Mus musculus GN=Ccna2 PE=1 SV=2	47 kDa	0	0	3	0
Heterogeneous nuclear ribonucleoprotein U-like protein 2 OS=Mus musculus GN=Hnrnpul2 PE=1 SV=2	85 kDa	0	0	3	0
Disks large homolog 4 OS=Mus musculus GN=Dlg4 PE=1 SV=1	80 kDa	0	0	3	0
Anaphase-promoting complex subunit 7 OS=Mus musculus GN=Anapc7 PE=1 SV=3	63 kDa	0	0	3	0
Proteasome subunit alpha type-7 OS=Mus musculus GN=Psma7 PE=1 SV=1	28 kDa	0	0	3	0

Identified Proteins (185)	Molecular Weight	Spectral Count			
		N	N+	C	C+
Heterogeneous nuclear ribonucleoprotein A1 OS=Mus musculus GN=Hnrnpa1 PE=1 SV=2	34 kDa	0	0	3	0
Interleukin enhancer-binding factor 3 OS=Mus musculus GN=Ilf3 PE=1 SV=2	96 kDa	0	0	3	0
Testis-expressed sequence 10 protein OS=Mus musculus GN=Tex10 PE=1 SV=1	105 kDa	0	0	3	0
Cell division cycle protein 23 homolog OS=Mus musculus GN=Cdc23 PE=1 SV=2	69 kDa	0	0	3	0
Putative helicase MOV-10 OS=Mus musculus GN=Mov10 PE=1 SV=2	114 kDa	0	0	3	0
Chromodomain-helicase-DNA-binding protein 8 OS=Mus musculus GN=Chd8 PE=1 SV=1	291 kDa	0	0	2	0
Testis-expressed sequence 15 protein OS=Mus musculus GN=Tex15 PE=2 SV=1	311 kDa	0	0	2	0
Proteasome subunit beta type-5 OS=Mus musculus GN=Psmb5 PE=1 SV=3	29 kDa	0	0	2	0
Microtubule-associated protein 1B OS=Mus musculus GN=Map1b PE=1 SV=2	270 kDa	0	0	2	0
40S ribosomal protein S27 OS=Mus musculus GN=Rps27 PE=1 SV=3	9 kDa	0	0	2	0
Proteasome subunit alpha type-4 OS=Mus musculus GN=Pma4 PE=1 SV=1	29 kDa	0	0	2	0
Adenosylhomocysteinase OS=Mus musculus GN=Ahcy PE=1 SV=3	48 kDa	0	0	2	0
Eukaryotic translation initiation factor 4 gamma 1 OS=Mus musculus GN=Eif4g1 PE=1 SV=1	176 kDa	0	0	2	0
Proteasome subunit beta type-6 OS=Mus musculus GN=Psmb6 PE=1 SV=3	25 kDa	0	0	2	0
THO complex subunit 4 OS=Mus musculus GN=Alyref PE=1 SV=3	27 kDa	0	0	2	0
Myosin-8 OS=Mus musculus GN=Myh8 PE=2 SV=2	223 kDa	0	0	2	0
mRNA turnover protein 4 homolog OS=Mus musculus GN=Mrto4 PE=1 SV=1	28 kDa	0	0	2	0
Eukaryotic translation initiation factor 4E OS=Mus musculus GN=Eif4e PE=1 SV=1	25 kDa	0	0	2	0
Non-POU domain-containing octamer-binding protein OS=Mus musculus GN=Nono PE=1 SV=3	55 kDa	0	0	2	0

Identified Proteins (185)	Molecular Weight	Spectral Count			
		N	N+	C	C+
Guanine nucleotide-binding protein-like 3 OS=Mus musculus GN=Gnl3 PE=1 SV=2	61 kDa	0	0	2	0
Interleukin enhancer-binding factor 2 OS=Mus musculus GN=Ilf2 PE=1 SV=1	43 kDa	0	0	2	0
DNA damage-binding protein 1 OS=Mus musculus GN=Ddb1 PE=1 SV=2	127 kDa	0	0	2	0
G-protein coupled receptor-associated sorting protein 1 OS=Mus musculus GN=Gprasp1 PE=1 SV=1	152 kDa	0	0	2	0
T-complex protein 1 subunit theta OS=Mus musculus GN=Cct8 PE=1 SV=3	60 kDa	0	0	2	0
RNA-binding protein 14 OS=Mus musculus GN=Rbm14 PE=1 SV=1	69 kDa	0	0	2	0
Calpain-1 catalytic subunit OS=Mus musculus GN=Capn1 PE=1 SV=1	82 kDa	0	0	2	0
Transcription factor 25 OS=Mus musculus GN=Tcf25 PE=1 SV=2	77 kDa	0	0	2	0
AP-2 complex subunit alpha-2 OS=Mus musculus GN=Ap2a2 PE=1 SV=2	104 kDa	0	0	2	0
CLIP-associating protein 1 OS=Mus musculus GN=Clasp1 PE=1 SV=2	169 kDa	0	0	2	0
T-complex protein 1 subunit delta OS=Mus musculus GN=Cct4 PE=1 SV=3	58 kDa	0	0	2	0
Guanine nucleotide-binding protein-like 3-like protein OS=Mus musculus GN=Gnl3l PE=1 SV=1	65 kDa	0	0	2	0
Vinculin OS=Mus musculus GN=Vcl PE=1 SV=4	117 kDa	0	0	2	0
Importin subunit alpha-1 OS=Mus musculus GN=Kpna2 PE=1 SV=2	58 kDa	0	0	2	0
40S ribosomal protein S29 OS=Mus musculus GN=Rps29 PE=3 SV=2	7 kDa	0	0	2	0
Anaphase-promoting complex subunit 1 OS=Mus musculus GN=Anapc1 PE=1 SV=2	216 kDa	0	0	2	0
Calpain small subunit 2 OS=Mus musculus GN=Capns2 PE=2 SV=1	27 kDa	0	0	2	0

Table 4-1: Cdh1 interactome

Table of proteins identified in the Cdh1 interactome following immunoaffinity chromatography and mass spectrometry analysis of FLAG-Cdh1 transfected cells. Proteins are listed from highest

enrichment in the samples to lowest enrichment. N indicates nontransfected cells and C indicates FLAG-Cdh1 transfected cells. + indicates lysates co-incubated with FLAG peptide to control for nonspecific binding.

Term	Count	%	PValue	Genes	Fold Enrichment
Phosphoprotein	146	82.49	5.53E-31	RPL18, RALY, RPL19, PRC1, RPL14, RPL13, SRP68, RPL15, SYNCRIP, RPLP2, CDC16, VCL, NONO, RPLP0, DHX36, DDX21, RPL11, RPL12, DHX30, CCNA2, GNL3, ANAPC1, ANAPC2, HAL, YTHDF2, SKP1, HNRNPU, MRT04, NVL, RPS17, RPS14, SERBP1, PSMA4, ATP5C1, RPS13, RPS10, RPS11, MYBBP1A, AHCY, PSMA7, EIF3C, EIF3D, RPS27, MOV10, EIF3A, RPS28, PSMB6, EIF3B, HNRNPK, RPS29, RPL7, PELP1, SPATS2, EIF3H, RPL6, HNRNPF, NPM1, EIF3F, RPL3, EIF3K, EIF3L, RPL5, CLASP1, EIF3I, RPS20, RPL4, PABPC1, RPL10A, TCF25, EIF3M, RPSA, CKAP4, RPS9, CDC23, RPL23A, NXF1, DDX5, CDC27, HNRNPA1, RPS5, LARP4B, RPS8, FXR1, EIF4E, CCT4, RPL18A, CCT8, RBMXL1, HSP90AB1, YBX3, RPS2, YBX1, LARP1, RPS3, PLRG1, RPS3A, DLG4, USP10, KPNB1, DDB1, GPRASP1, G3BP1, G3BP2, LAS1L, CDC5L, NCL, PURB, PURA, EIF4G1, LARP4, RRM2, KPNA2, MATR3, RPL27A, RACK1, RPL30, CHD8, RPL31, RPL34, CSDE1, TGM3, ENO3, CAMK2B, HSPA5, CAMK2A, HSPA8, HSPA9, BCAS2, UPF1, ALYREF, MAPIB, RPL26, ELAVL1, ILF3, RPL24, RPL28, CAPRIN1, PWP1, CAPN1, ILF2, HNRNPUL2, RPL23, RPL13A, RPL22, RBM14, TEX10	2.06

Term	Count	%	PValue	Genes	Fold Enrichment
Acetylation	122	68.93	1.11E-53	RALY, RPL14, RPL13, SRP68, SYNCRIP, RPLP2, VCL, NONO, DDX21, RPL11, DHX36, RPL12, CCNA2, GNL3, RPL35A, CAPNS2, YTHDF2, HNRNPU, NVL, RPS18, RPS19, PSMA4, SERBP1, RPS15, ATP5C1, RPS12, RPS13, ANAPC7, RPS11, MYBBP1A, AHCY, PSMA7, RPS25, EIF3C, EIF3D, MOV10, EIF3A, EIF3B, PSMB6, HNRNPK, RPS29, RPL7, PELP1, RPL6, RPL9, HNRNPF, EIF3F, NPM1, EIF3K, RPL3, EIF3L, EIF3I, RPL5, RPS20, PABPC1, RPL10A, RPL7A, RPL4, RPS21, RPS23, EIF3M, RPSA, CKAP4, RPS9, CDC23, NXF1, DDX5, LARP4B, RPS5, HNRNPA1, RPS8, RPS7, FXR1, EIF4E, CCT4, CCT8, RBMXL1, HSP90AB1, YBX3, RPS2, YBX1, LARP1, RPS3, PLRG1, RPS3A, USP10, KPNB1, DDB1, G3BP1, RPS4X, NCL, PURB, PURA, EIF4G1, LARP4, KPNA2, MATR3, RPL27A, RPL36, RACK1, PRPF19, RPL30, RPL31, RPL34, CSDE1, TGM3, ENO3, HSPA5, HSPA8, HSPA9, BCAS2, ALYREF, MAP1B, ELAVL1, RPL27, ILF3, RPL24, CAPRIN1, RPL28, CAPN1, RPL13A, RBM14	4.14
Cytoplasm	96	54.24	1.12E-18	HSP90AB1, RPL18, PRC1, SRP68, YBX3, SYNCRIP, CDC16, YBX1, LARP1, VCL, RPS3, RPS3A, RPLP0, USP10, DHX36, DHX30, CCNA2, KPNB1, CAPNS2, DDB1, G3BP1, GPRASP1, G3BP2, YTHDF2, LAS1L, CDC5L, RPS4X, NCL, MYH8, HNRNPU, MRTO4, RPS18, PSMA4, RRM2, SERBP1, RPS12, RPS10, MYBBP1A, KPNA2, AHCY, PSMA7, PSMB5, RACK1, PRPF19, EIF3C, EIF3D, MOV10, EIF3A, PSMB6, EIF3B, HNRNPK, PELP1, SPATS2, SPRR2D, EIF3H, EIF3F, NPM1, RPL8, CSDE1, RPL3, EIF3K, ENO3, EIF3L, RPL5, EIF3I, CAMK2B, CLASP1, RPS20, HSPA5, PABPC1, EIF3M, HSPA8, RPSA, UPF1, CKAP4, ALYREF, MAP1B, ELAVL1, RPS9, ILF3, NXF1, HNRNPA1, LARP4B, CAPRIN1, RPS8, FXR1, RPS7, CAPN1, TEX15, EIF4E, CCT4, ILF2, RPL13A, CCT8, RBM14, TEX10	2.32

Term	Count	%	PValue	Genes	Fold Enrichment
Translational Initiation	77	43.50	2.31E-120	RPL18, RPL17, RPL19, RPL14, RPL13, RPL15, RPLP2, RPS2, LARP1, RPS3, RPS3A, RPLP0, RPL11, RPL12, RPL35A, RPS4X, EIF4G1, RPS18, RPS19, RPS16, RPS17, RPS14, RPS15, RPS12, RPS13, RPS10, RPS11, RPL27A, RPS15A, RPL36, RPS25, EIF3C, EIF3D, RPS27, RPL30, EIF3A, RPS28, EIF3B, RPS29, RPL7, RPL31, EIF3H, RPL6, RPL34, RPL9, EIF3F, RPL8, RPL3, EIF3K, EIF3L, RPL5, EIF3I, RPS20, RPL4, RPL10A, RPL7A, PABPC1, RPS21, RPS23, EIF3M, RPSA, RPL26, RPL27, RPS9, RPL24, RPL23A, RPS5, RPL28, RPS8, RPS7, EIF4E, RPL23, RPL18A, RPL13A, RPL22, RPL21, RPL37A	53.93
Ribonucleoprotein	72	40.68	1.29E-85	RPL18, RALY, RPL17, RPL19, RPL14, RPL13, SRP68, RPL15, SYNCRIP, RPLP2, RPS2, RPS3, RPS3A, RPLP0, RPL11, RPL12, RPL35A, RPS4X, HNRNPU, RPS18, RPS19, RPS16, RPS17, RPS14, RPS15, RPS12, RPS13, RPS10, RPS11, RPL27A, RPS15A, RPL36, RPS25, RPL10L, RPS27, RPL30, RPS28, HNRNPK, RPS29, RPL7, RPL6, RPL31, RPL34, RPL9, HNRNPF, RPL8, RPL3, RPL5, RPS20, RPL4, RPL7A, RPL10A, RPS21, RPS23, RPSA, RPL26, RPS9, RPL27, RPL23A, RPL24, RPS5, HNRNPA1, RPL28, RPS8, RPS7, RPL23, RPL18A, RPL13A, RPL22, RPL21, RBMXL1, RPL37A	28.28
Nucleus	71	40.11	2.08E-05	RALY, PRC1, SRP68, YBX3, SYNCRIP, GNL3L, YBX1, RPS3, NONO, PLRG1, RPS3A, RPLP0, USP10, RPL11, DDX21, DHX36, KPNB1, CCNA2, GNL3, DDB1, G3BP1, YTHDF2, LAS1L, CDC5L, NCL, PURB, HNRNPU, PURA, MRTO4, NVL, RPS19, PSMA4, SERBP1, RPS10, KPNA2, MYBBP1A, MATR3, PSMA7, PSMB5, PRPF19, RACK1, CHD8, PSMB6, HNRNPK, PELP1, HNRNPF, NPM1, EIF3K, RPL3, RPL5, PABPC1, TCF25, HSPA8, HSPA9, BCAS2, RPSA, UPF1, ALYREF, ELAVL1, ILF3, NXF1, DDX5, CDC27, HNRNPA1, PWP1, TEX15, ILF2, HNRNPUL2, RBMXL1, RBM14, TEX10	1.57

Term	Count	%	PValue	Genes	Fold Enrichment
rRNA Processing	68	38.42	6.57E-84	RPL18, RPL17, RPL19, RPL14, RPL13, RPL15, RPLP2, RPS2, RPS3, RPS3A, RPLP0, DDX21, RPL11, RPL12, RPL35A, LAS1L, RPS4X, MRTO4, RPS18, RPS19, RPS16, RPS17, RPS14, RPS15, RPS12, RPS13, RPS10, RPS11, RPL27A, RPS15A, RPL36, RPS25, RPS27, RPL30, RPS28, RPS29, RPL7, PELP1, RPL6, RPL31, RPL9, RPL34, RPL8, RPL3, RPL5, RPS20, RPL7A, RPL10A, RPL4, RPS21, RPS23, RPSA, RPL26, RPS9, RPL27, RPL23A, RPL24, RPS5, RPL28, RPS8, RPS7, RPL23, RPL18A, RPL13A, RPL22, RPL21, RPL37A, TEX10	30.49
Nuclear-transcribed mRNA catabolic process, nonsense-mediated decay	66	37.29	2.42E-101	RPL18, RPL17, RPL19, RPL14, RPL13, RPL15, RPLP2, RPS2, RPS3, RPS3A, RPLP0, RPL11, RPL12, RPL35A, RPS4X, EIF4G1, RPS18, RPS19, RPS16, RPS17, RPS14, RPS15, RPS12, RPS13, RPS10, RPS11, RPL27A, RPS15A, RPL36, RPS25, RPS27, RPL30, RPS28, RPS29, RPL7, RPL6, RPL31, RPL9, RPL34, RPL8, RPL3, RPL5, RPS20, RPL7A, RPL10A, PABPC1, RPL4, RPS21, RPS23, RPSA, UPF1, RPL26, RPS9, RPL27, RPL23A, RPL24, RPS5, RPL28, RPS8, RPS7, RPL23, RPL18A, RPL13A, RPL22, RPL21, RPL37A	53.22
Translation	65	36.72	4.09E-73	RPL18, RPL17, RPL19, RPL14, RPL13, RPL15, RPLP2, RPS2, RPS3, RPS3A, RPLP0, RPL11, RPL12, RPL35A, RPS4X, EIF4G1, RPS18, RPS19, RPS16, RPS17, RPS14, RPS15, RPS12, RPS13, RPS10, RPS11, RPL27A, RPS15A, RPL36, RPS25, RPL10L, RPS27, RPL30, RPS28, RPS29, RPL7, RPL6, RPL31, RPL34, RPL9, RPL8, RPL3, RPL5, RPS20, RPL7A, RPL10A, RPL4, RPS21, RPS23, RPSA, RPL26, RPS9, RPL27, RPL23A, RPL24, RPS5, RPL28, RPS8, RPS7, RPL23, RPL18A, RPL13A, RPL22, RPL21, RPL37A	24.65

Term	Count	%	PValue	Genes	Fold Enrichment
SRP-dependent Cotranslational Protein Targeting to Membrane	64	36.16	1.46E-106	RPL18, RPL17, RPL19, RPL14, RPL13, SRP68, RPL15, RPLP2, RPS2, RPS3, RPS3A, RPLP0, RPL11, RPL12, RPL35A, RPS4X, RPS18, RPS19, RPS16, RPS17, RPS14, RPS15, RPS12, RPS13, RPS10, RPS11, RPL27A, RPS15A, RPL36, RPS25, RPS27, RPL30, RPS28, RPS29, RPL7, RPL6, RPL31, RPL34, RPL9, RPL8, RPL3, RPL5, RPS20, RPL7A, RPL10A, RPL4, RPS21, RPS23, RPSA, RPL26, RPS9, RPL27, RPL23A, RPL24, RPS5, RPS8, RPL28, RPS7, RPL23, RPL18A, RPL13A, RPL22, RPL21, RPL37A	65.33
Ribosomal protein	64	36.16	1.87E-86	RPL18, RPL17, RPL19, RPL14, RPL13, RPL15, RPLP2, RPS2, RPS3, RPS3A, RPLP0, RPL11, RPL12, RPL35A, RPS4X, RPS18, RPS19, RPS16, RPS17, RPS14, RPS15, RPS12, RPS13, RPS10, RPS11, RPL27A, RPS15A, RPL36, RPS25, RPL10L, RPS27, RPL30, RPS28, RPS29, RPL7, RPL6, RPL31, RPL34, RPL9, RPL8, RPL3, RPL5, RPS20, RPL7A, RPL10A, RPL4, RPS21, RPS23, RPSA, RPL26, RPS9, RPL27, RPL23A, RPL24, RPS5, RPL28, RPS8, RPS7, RPL23, RPL18A, RPL13A, RPL22, RPL21, RPL37A	40.23
Ribosome	64	36.16	1.65E-78	RPL18, RPL17, RPL19, RPL14, RPL13, RPL15, RPLP2, RPS2, RPS3, RPS3A, RPLP0, RPL11, RPL12, RPL35A, RPS4X, RPS18, RPS19, RPS16, RPS17, RPS14, RPS15, RPS12, RPS13, RPS10, RPS11, RPL27A, RPS15A, RPL36, RPS25, RPL10L, RPS27, RPL30, RPS28, RPS29, RPL7, RPL6, RPL31, RPL34, RPL9, RPL8, RPL3, RPL5, RPS20, RPL7A, RPL10A, RPL4, RPS21, RPS23, RPSA, RPL26, RPS9, RPL27, RPL23A, RPL24, RPS5, RPL28, RPS8, RPS7, RPL23, RPL18A, RPL13A, RPL22, RPL21, RPL37A	25.21
Viral Transcription	63	35.59	5.94E-97	RPL18, RPL17, RPL19, RPL14, RPL13, RPL15, RPLP2, RPS2, RPS3, RPS3A, RPLP0, RPL11, RPL12, RPL35A, RPS4X, RPS18, RPS19, RPS16, RPS17, RPS14, RPS15, RPS12, RPS13, RPS10, RPS11, RPL27A, RPS15A, RPL36, RPS25, RPS27, RPL30, RPS28, RPS29, RPL7, RPL6, RPL31, RPL34, RPL9, RPL8, RPL3, RPL5, RPS20, RPL7A, RPL10A, RPL4, RPS21, RPS23, RPSA, RPL26, RPS9, RPL27, RPL23A, RPL24, RPS5,	53.97

Term	Count	%	PValue	Genes	Fold Enrichment
				RPS8, RPL28, RPS7, RPL23, RPL18A, RPL13A, RPL22, RPL21, RPL37A	
RNA-binding	54	30.51	1.15E-36	RALY, SRP68, SYNCRIP, YBX1, RPS3, LARP1, NONO, RPL11, DDX21, DHX36, RPL12, DHX30, RPL35A, G3BP1, G3BP2, YTHDF2, CDC5L, RPS4X, NCL, HNRNPU, EIF4G1, RPS18, LARP4, SERBP1, RPS11, MATR3, EIF3D, EIF3A, MOV10, EIF3B, HNRNPK, RPL7, HNRNPF, RPL8, NPM1, CSDE1, RPL5, PABPC1, UPF1, ALYREF, RPS9, ELAVL1, ILF3, RPL23A, NXF1, DDX5, LARP4B, HNRNPA1, CAPRIN1, FXR1, EIF4E, RPL22, RBMXL1, RBM14	9.44
Ubl Conjugation	49	27.68	7.03E-14	RALY, HSP90AB1, RPL19, RPL14, RPL13, GNL3L, RPS2, YBX1, LARP1, RPS3, NONO, CHD8, HNRNPK, RPS3A, RPLP0, HNRNPF, NPM1, RPL3, CSDE1, RPL5, USP10, EIF3I, DDX21, RPL4, HSPA5, RPL10A, RPS20, RPS21, CCNA2, HSPA8, GNL3, DDB1, RPL26, G3BP2, CDC23, ILF3, CDC5L, SKP1, DDX5, HNRNPA1, NCL, HNRNPU, RPL18A, RPS17, SERBP1, CCT8, RBMXL1, RBM14, MATR3	3.34
Isopeptide bond	47	26.55	2.21E-19	RALY, RPL19, RPL14, RPL13, SYNCRIP, GNL3L, RPS2, YBX1, LARP1, RPS3, NONO, CHD8, HNRNPK, RPS3A, RPLP0, HNRNPF, NPM1, RPL3, CSDE1, RPL5, EIF3I, DDX21, RPL4, HSPA5, RPL10A, RPS20, RPS21, KPNB1, HSPA8, GNL3, RPL26, G3BP2, CDC23, ILF3, CDC5L, SKP1, DDX5, HNRNPA1, NCL, HNRNPU, RPL18A, RPS17, SERBP1, CCT8, RBMXL1, RBM14, MATR3	4.83
Methylation	37	20.90	1.65E-13	YBX3, SYNCRIP, LARP1, RPS3, NONO, HNRNPK, RPS29, RPL4, HSPA5, PABPC1, HSPA8, HSPA9, UPF1, ALYREF, G3BP1, G3BP2, ELAVL1, RPL23A, ILF3, NXF1, HNRNPA1, NCL, LARP4B, MYH8, PURB, CAPRIN1, HNRNPU, EIF4G1, RPS19, LARP4,	4.30

Term	Count	%	PValue	Genes	Fold Enrichment
				CCT4, HNRNPUL2, ILF2, SERBP1, RBMXL1, RPS10, RPS11	
Nucleotide-binding, Alpha-Beta Plait	20	11.30	7.24E-12	RALY, ALYREF, G3BP1, G3BP2, ELAVL1, SYNCRIP, RPL23A, NXF1, HNRNPA1, NCL, LARP4B, NONO, EIF3B, LARP4, HNRNPF, RBMXL1, DDX21, PABPC1, RBM14, MATR3	7.99
Host-virus Interaction	20	11.30	9.01E-10	RPSA, DDB1, ALYREF, SYNCRIP, NXF1, PSMA7, HNRNPA1, PSMB5, RACK1, EIF4G1, PSMB6, HNRNPK, EIF4E, PSMA4, RPLP0, NPM1, CCNA2, KPNA2, KPNB1, HSPA8	6.04
Cell-cell Adhesion	18	10.17	3.31E-09	HSP90AB1, RPL14, RPL15, RPL24, RPL23A, RPS2, LARPI, RACK1, EIF4G1, PSMB6, HNRNPK, RPL6, SERBP1, RPL34, CCT8, HSPA5, RPL7A, HSPA8	6.37
mRNA Splicing	17	9.60	8.79E-10	BCAS2, RALY, ALYREF, SYNCRIP, CDC5L, DDX5, HNRNPA1, YBX1, HNRNPU, PRPF19, NONO, HNRNPK, PLRG1, HNRNPF, RBMXL1, PABPC1, HSPA8	7.60
mRNA Splicing, via Spliceosome	17	9.60	1.33E-09	BCAS2, RALY, ALYREF, ELAVL1, SYNCRIP, CDC5L, DDX5, HNRNPA1, YBX1, HNRNPU, NONO, PRPF19, HNRNPK, PLRG1, HNRNPF, PABPC1, HSPA8	7.35
mRNA Processing	17	9.60	2.86E-08	BCAS2, RALY, ALYREF, SYNCRIP, CDC5L, DDX5, HNRNPA1, YBX1, HNRNPU, PRPF19, NONO, HNRNPK, PLRG1, HNRNPF, RBMXL1, PABPC1, HSPA8	5.95
RNA Recognition-Motif (RRM)	15	8.47	2.26E-09	RALY, ALYREF, G3BP1, G3BP2, SYNCRIP, ELAVL1, NCL, HNRNPA1, NONO, EIF3B, HNRNPF, RBMXL1, PABPC1, RBM14, MATR3	8.27
RNA Recognition Motif Domain	15	8.47	3.17E-08	RALY, ALYREF, G3BP1, G3BP2, SYNCRIP, ELAVL1, NCL, HNRNPA1, NONO, EIF3B, HNRNPF, RBMXL1, PABPC1, RBM14, MATR3	7.00
Viral Process	15	8.47	2.90E-06	DDB1, SYNCRIP, NXF1, PSMA7, HNRNPA1, RACK1, EIF4G1, PSMB5, HNRNPK, EIF4E, PSMB6, PSMA4, NPM1, CCNA2, HSPA8	4.81
RNA transport	15	8.47	3.04E-06	UPF1, ALYREF, NXF1, FXR1, EIF4G1, EIF3C, EIF3D, EIF3A, EIF3B, EIF4E, EIF3H, EIF3F, EIF3I, PABPC1, KPNB1	4.67

Term	Count	%	PValue	Genes	Fold Enrichment
Spliceosome	14	7.91	6.83E-11	BCAS2, RALY, ALYREF, SYNCRIP, CDC5L, DDX5, HNRNPA1, HNRNPU, PRPF19, HNRNPK, PLRG1, HNRNPF, PABPC1, HSPA8	12.82
Cytoplasmic Translation	13	7.34	4.78E-18	RPL35A, RPL7, RPL22, RPL6, RPL31, RPLP0, RPL9, RPL15, RPL8, RPL26, RPLP2, RPL36, MRTO4	49.90
Protein Biosynthesis	13	7.34	7.54E-09	LARP1, EIF4G1, EIF3C, EIF3D, EIF3A, EIF4E, EIF3B, EIF3H, EIF3F, EIF3K, EIF3L, EIF3I, EIF3M	9.94
Initiation Factor	12	6.78	2.10E-12	EIF3C, EIF4G1, EIF3D, EIF3A, EIF4E, EIF3B, EIF3H, EIF3F, EIF3K, EIF3L, EIF3I, EIF3M	24.06
Proteasome-Mediated Ubiquitin-Dependent Protein Catabolic Process	12	6.78	8.87E-06	ANAPC1, PSMB5, ANAPC2, PSMB6, PSMA4, DDB1, CDC23, CDC16, ANAPC7, SKP1, PSMA7, CDC27	5.67
Diamond-Blackfan anemia	11	6.21	4.66E-18	RPL35A, RPS28, RPS19, RPS29, RPS17, RPL15, RPL26, RPS10, RPL5, RPL11, RPS7	85.27
Regulation of Translational Initiation	11	6.21	2.22E-12	EIF3C, EIF4G1, EIF3D, EIF3A, EIF3B, EIF3H, EIF3F, EIF3K, EIF3L, EIF3I, EIF3M	29.32
Positive Regulation of Ubiquitin-Protein Ligase Activity Involved in Regulation of Mitotic Cell Cycle Transition	11	6.21	5.83E-09	ANAPC1, PSMB5, ANAPC2, PSMB6, PSMA4, CDC23, CDC16, ANAPC7, SKP1, PSMA7, CDC27	13.89
Spliceosome	11	6.21	1.64E-04	BCAS2, PRPF19, HNRNPK, PLRG1, ALYREF, RBMXL1, CDC5L, DDX5, HNRNPA1, HNRNPU, HSPA8	4.43
Formation of Translation Preinitiation Complex	10	5.65	8.07E-13	EIF3C, EIF3D, EIF3A, EIF3B, EIF3H, EIF3F, EIF3K, EIF3L, EIF3I, EIF3M	41.72
Negative Regulation of Ubiquitin-Protein Ligase Activity Involved in Mitotic Cell Cycle	10	5.65	4.80E-08	ANAPC1, PSMB5, ANAPC2, PSMB6, PSMA4, CDC23, CDC16, ANAPC7, PSMA7, CDC27	13.51
Anaphase-Promoting Complex-Dependent Catabolic Process	10	5.65	1.24E-07	ANAPC1, PSMB5, ANAPC2, PSMB6, PSMA4, CDC23, CDC16, ANAPC7, PSMA7, CDC27	12.15
Regulation of mRNA Stability	10	5.65	1.22E-06	EIF4G1, PSMB5, PSMB6, SERBP1, PSMA4, ELAVL1, YTHDF2, PABPC1, PSMA7, HSPA8	9.32

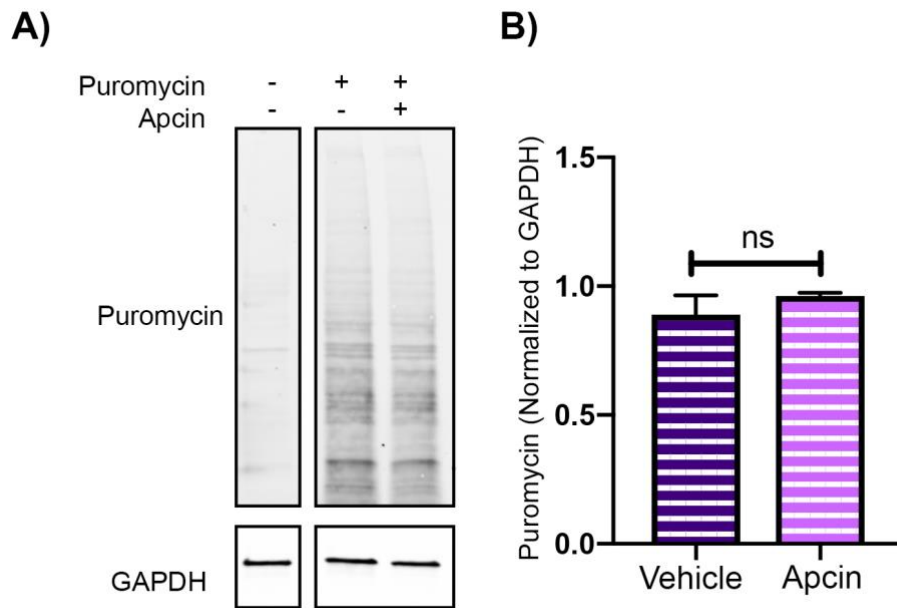
Term	Count	%	PValue	Genes	Fold Enrichment
Ribosomal Small Subunit Assembly	9	5.08	7.76E-12	RPSA, RPS27, RPS28, RPS19, RPS17, RPS14, RPS15, RPS10, RPS5	45.45
Ribosomal Large Subunit Assembly	9	5.08	2.05E-11	RPL10L, RPL6, RPL3, RPL5, RPL24, RPL11, RPL23A, RPL12, MRTO4	41.12
Negative Regulation of Translation	9	5.08	1.39E-07	RACK1, EIF4E, RPL13A, SYNCRIP, ILF3, CAPRN1, RPS3, PURA, FXR1	14.89
Citrullination	9	5.08	1.84E-06	RPL19, RPL13A, ALYREF, RPL23A, RPS11, RPL4, RPS2, MYBBP1A, HNRNPU	10.79
domain:RRM 2	9	5.08	1.41E-05	NONO, HNRNPF, ELAVL1, SYNCRIP, PABPC1, RBM14, HNRNPA1, NCL, MATR3	8.21
domain:RRM 1	9	5.08	1.41E-05	NONO, HNRNPF, ELAVL1, SYNCRIP, PABPC1, RBM14, HNRNPA1, NCL, MATR3	8.21
Oocyte Meiosis	9	5.08	8.84E-04	ANAPC1, ANAPC2, CDC23, CAMK2B, CDC16, ANAPC7, SKP1, CDC27, CAMK2A	4.42
rRNA-binding	8	4.52	9.08E-10	RPS18, RPL8, RPS9, RPL5, RPL11, RPL23A, RPS11, RPS4X	38.76
Ribosome Biogenesis	8	4.52	7.36E-08	NVL, RPS18, RPS28, RPLP0, RPL34, GNL3L, RPL7A, GNL3	21.32
domain:RRM	8	4.52	1.85E-04	RALY, LARP4, EIF3B, ALYREF, G3BP1, G3BP2, NXF1, LARP4B	6.76
Helicase	8	4.52	2.33E-04	CHD8, MOV10, UPF1, G3BP1, DDX21, DHX36, DDX5, DHX30	6.50
Nucleic Acid-Binding, OB-fold	7	3.95	8.79E-05	RPS28, RPL8, YBX3, CSDE1, RPS11, YBX1, RPS23	9.59
Translation Regulation	7	3.95	2.87E-04	EIF4G1, RACK1, EIF4E, RPL13A, SYNCRIP, LARP4B, RPS3	7.75
Osteoblast Differentiation	7	3.95	7.45E-04	ALYREF, RPS15, SYNCRIP, DDX21, RPS11, MYBBP1A, HNRNPU	6.46
Translation Protein SH3-like Domain	6	3.39	1.32E-07	RPL14, RPL6, RPL21, RPL8, RPL26, RPL27	45.19
Ribosomal Small Subunit Biogenesis	6	3.39	4.49E-07	RPS28, RPS19, RPS16, RPS17, RPS15, RPS7	35.98
site:Not acetylated	6	3.39	1.77E-06	RPS19, RPS16, RPL9, G3BP1, G3BP2, RPL24	28.50
Regulation of Ubiquitin-Protein Ligase Activity Involved in Mitotic Cell Cycle	6	3.39	3.26E-06	ANAPC1, ANAPC2, CDC23, CDC16, ANAPC7, CDC27	25.03
Ribosomal Large Subunit Biogenesis	6	3.39	5.07E-06	RPL35A, RPL14, RPL7, RPL26, RPL5, RPL11	23.03
Protein K11-linked Ubiquitination	6	3.39	7.57E-06	ANAPC1, ANAPC2, CDC23, CDC16, ANAPC7, CDC27	21.32

Term	Count	%	PValue	Genes	Fold Enrichment
Positive Regulation of Translation	6	3.39	2.16E-04	NPM1, ELAVL1, PABPC1, RPS4X, LARP4B, LARP1	10.86
Ribosomal Protein L2 Domain 2	5	2.82	1.65E-05	RPL14, RPL6, RPL8, RPL26, RPL27	31.01
Viral Translational Termination-Reinitiation	4	2.26	1.08E-05	EIF3D, EIF3A, EIF3B, EIF3L	76.76
IRES-dependent Viral Translational Initiation	4	2.26	3.71E-05	EIF3D, EIF3A, EIF3B, EIF3F	54.83
region of interest:RNA-binding RGG-box	4	2.26	2.21E-04	HNRNPK, HNRNPA1, HNRNPU, FXR1	32.57
Maturation of LSU-rRNA	4	2.26	4.54E-04	LAS1L, RPL10A, RPL7A, TEX10	25.59
Threonine Protease	4	2.26	6.30E-04	PSMB5, PSMB6, PSMA4, PSMA7	23.26
Proteasome, Subunit Alpha/Beta	4	2.26	7.15E-04	PSMB5, PSMB6, PSMA4, PSMA7	22.20

Table 4-2: Biological Processes Gene Ontology analysis

Proteins with at least a four-fold difference in Cdh1-transfected cells compared to control cells were entered into the DAVID Functional Annotation Bioinformatics Microarray Analysis tool (<https://david.ncifcrf.gov>) to classify proteins based on biological processes.

4.6. Supplemental Figures



Supplemental Figure 4-1: Cdh1-APC does not affect protein synthesis in fibroblasts

A) Human fibroblasts were treated with Apcin (1 μ M) for 16-18 hours and underwent 75 minutes of puromycylation (10 μ g/mL). **B)** Quantification of puromycin normalized to GAPDH for D); n=4.

Statistical significance calculated by Student's t test. *p<0.05

Chapter 5 :

Cdh1-APC Regulates Stress Granule Dynamics

Portions of this chapter were adapted from the following publication:

Valdez-Sinon AN, Lai A, Shi L, Lancaster CL, Gokhale A, Faundez V, Bassell GJ. Cdh1-APC interactions with FMRP and ribosomal components regulate protein synthesis and stress granule dynamics in neural cells. *Cell Reports, In Revision*.

5.1. Introduction

Following our observation of enrichment of the Cdh1 interactome with translational regulatory proteins, we sought to first validate these Cdh1-interacting proteins and then elucidate a potential mechanism by which Cdh1-APC may be regulating protein synthesis. Interestingly, mass spectrometry in Chapter 4 identified that Cdh1 interacts with one of the FMRP autosomal homologs, FXR1. FMRP and FXR1 have been shown to interact and form cytoplasmic granules that have the ability to repress the translation of mRNA (Gareau et al., 2013; Mazroui et al., 2002). These granules are referred to as Fragile X granules (FXG), are found in neurons (Christie et al., 2009), and have similar properties to stress granules. Stress granules are membrane-less organelles that sequester pools of mRNA and prevent their translation (Protter and Parker, 2016). As discussed in Chapter 1, the formation of stress granules is a well-studied mechanism by which cells can regulate spatiotemporal control over protein synthesis.

The role of the ubiquitination proteasome system (UPS) in the formation of stress granules has been the topic of recent research although underlying mechanisms are not well understood (Markmiller et al., 2019; Mazroui et al., 2007; Xie et al., 2018). It has been observed that the deubiquitination enzyme USP10 (and its ortholog Ubp3) is required for the assembly of stress granules in both yeast and mammalian cells (Nostramo and Herman, 2016). Since USP10 is responsible for removing ubiquitin chains off substrate proteins, it could be hypothesized that attachment of ubiquitin chains onto a substrate protein (such as by an E3 ligase) may also regulate stress granule assembly, presumably inhibiting their formation. However, to date, there has not been an E3 ligase identified to regulate stress granule formation. Based on our observed interactions of Cdh1 with FMRP and FXR1 (**Figures 1-2; 5-1**) as well literature asserting a role

of the UPS in stress granule dynamics, we aimed to elucidate if Cdh1-APC could regulate stress granule dynamics.

5.2. Results

5.2.1. Cdh1-APC Interacts with Stress Granule Proteins

To determine if Cdh1-APC may regulate stress granule dynamics, it was necessary to first elucidate if Cdh1-APC interacts with any stress granule proteins. The Cdh1 interactome (**Table 4-1**) was compared to previously published lists of stress granule proteins (Jain et al., 2016; Markmiller et al., 2018). The Cdh1-interactome was highly enriched for stress granule proteins (28% of the interactome) (**Table 5-1**). Using co-immunoprecipitation and immunoblotting, we confirmed that the established stress granule proteins HNRNPU, Caprin1, GB3P1, ELAVL1, and RPS3 interact with Cdh1 (**Figure 5-1**). As it has been well described that stress granules can prevent the translation of mRNA (Protter and Parker, 2016), it was hypothesized that Cdh1-APC can regulate protein synthesis through the control of stress granule dynamics.

5.2.2. Cdh1-APC Antagonizes Stress Granule Assembly

Following observations that inhibition of Cdh1-APC leads to a decrease in protein synthesis, it was hypothesized that this translational repressive state may be due to favored formation of RNA granules. As a model system to investigate the interplay between protein synthesis and RNA granules, the sodium arsenite paradigm (NaAsO₂) (Markmiller et al., 2019) was used to stimulate stress granule formation. DIV 15 mouse cortical neurons were treated with Apcin (2μM) for 16-18 hours followed by treatment with NaAsO₂ (0.5mM, 45 minutes) and immunostained for G3BP1, an interactor of Cdh1 and known stress granule protein. Control and

Apcin-treated neurons form stress granules upon sodium arsenite treatment with no global differences in morphology (**Figure 5-2, Supplemental Figure 5-1**). When comparing stress granules in both sets of neurons, the percentage of stress granule positive neurons was significantly greater in the Apcin-treated neurons compared to the control neurons (**Figure 5-2**). While only 26% of control neurons formed stress granules, 56% of Apcin-treated neurons were stress-granule positive. Additionally, Apcin-treated neurons contained significantly more stress granules than vehicle-treated neurons. As an additional approach to assess the effects of pharmacologic inhibition of Cdh1-APC on stress granule formation, cortical neurons were treated with proTAME (12 μ M), another known pharmacologic inhibitor of Cdh1-APC (Fuchsberger et al., 2016). Vehicle and proTAME-treated neurons underwent NaAsO₂ treatment (0.5mM, 45 minutes) followed by fixation and immunostaining. Similar to Apcin treatment, inhibition of Cdh1-APC with proTAME lead to an increase in stress granule formation (**Supplemental Figure 5-2**). Thus, inhibition of Cdh1-APC activity is sufficient to increase the formation of stress granules.

To further confirm the role of Cdh1-APC on stress granule formation, DIV 7 cortical neurons were transduced with a virus expressing RFP-tagged shRNA against Cdh1 or an RFP-tagged non-targeting control. On DIV 14, neurons were treated with NaAsO₂ (0.5mM, 45 minutes) and immunostained for G3BP1. Similar to the results with pharmacologic inhibition of Cdh1-APC, knockdown of Cdh1 resulted in an increase in stress granule formation (**Figure 5-3**). Whereas 44% of the control neurons formed stress granules, 69% of neurons expressing the RFP-shRNA against Cdh1 formed stress granules. There was also a significant increase in number of stress granules in shRNA-Cdh1 neurons compared to control neurons.

These results provide a novel link between Cdh1-APC activity and stress granule formation. The findings suggest a novel physiologic function of Cdh1-APC to antagonize stress granules, perhaps acting through its regulation of factors involved in protein synthesis.

5.2.3. Stress granule formation reduces protein synthesis

To approach the hypothesis that Cdh1-APC may regulate protein synthesis through stress granule dynamics, it was necessary to confirm that stress granule formation leads to a decrease in protein synthesis. N2A cells and DIV 14 cortical neurons were treated with NaAsO₂ (0.5mM) or water as a control for 45 minutes and concurrently underwent puromycin labeling. Upon immunoblotting for puromycin, there was a substantial decrease in protein synthesis with NaAsO₂ treatment in both cell types (**Supplemental Figure 5-3**). The decrease in protein synthesis with stress granule formation confirms that stress granule dynamics are a potential mechanism by which Cdh1-APC may be regulating protein synthesis

5.2.4. Cdh1-APC regulates stress granules in a FMRP-dependent mechanism

With previous literature identifying that FMRP is a ubiquitination target of Cdh1-APC (**Figure 3-1**) (Huang et al., 2015), we hypothesized that the regulation of stress granules by Cdh1-APC may be FMRP-dependent. Mass spectrometry was performed following FLAG immunoprecipitation of FLAG-FMRP transfected N2As (**Table 5-2**). All but one of the stress granule proteins previously identified in our Cdh1 interactome also interacted with FMRP (**Tables 4-1, 5-1, Supplemental Figure 5-5**). This extensive overlap in interactome suggests that the interaction between Cdh1-APC and FMRP is critical for the consequences on stress granule dynamics, and that FMRP may be the primary link between Cdh1 and stress granules. Furthermore, the enrichment of stress granule proteins within the FMRP interactome and well-described

inhibition of translation initiation within stress granules provides validation for FMRP-mediated regulation of translation at the level of translation initiation (Napoli et al., 2008), in addition to its role in the regulation of ribosome elongation in polysomes (Richter et al., 2015).

To explore how interaction with FMRP may affect Cdh1-mediated regulation of stress granule formation, the FMRP D-box Mutant (FMRP DBM, see Chapter 3), a form of FMRP unable to bind Cdh1 was utilized. N2A cells were transfected with wildtype FMRP (FMRP WT) or FMRP DBM and then treated with NaAsO₂ to promote stress granule formation. Areas of FMRP co-localization with G3BP1-positive stress granules were observed, supporting previous evidence that FMRP is a stress granule protein. Cells transfected with FMRP DBM had more stress granules in response to arsenite treatment compared to those transfected with FMRP WT (59% versus 35%) (**Figure 5-4**). FMRP-DBM expressing N2A cells also contained significantly more granules than FMRP-WT cells. These results demonstrate that if Cdh1-APC is unable to bind FMRP, then Cdh1-APC cannot antagonize stress granule dynamics. Thus, Cdh1-APC modulates stress granule dynamics via its interaction with FMRP.

To further clarify if FMRP is necessary for Cdh1-APC to regulate stress granule formation, cortical neurons from *Fmr1*-KO mice and wildtype littermates underwent treatment with Apcin and sodium arsenite to induce stress granule formation. Similar to previous experiments, Apcin treatment increased the formation of stress granules in wildtype cortical neurons (**Figure 5-5**). However, Apcin treatment did not elicit any changes in the formation of stress granules in *Fmr1*-KO neurons (**Figure 5-5**). Inability to increase the formation of stress granules in *Fmr1*-KO neurons supports our hypothesis that FMRP is necessary for Cdh1-APC to regulate stress granule formation.

Taken together, these findings demonstrate a novel and convergent role of Cdh1-APC to regulate stress granule formation and protein synthesis in neurons. Furthermore, we link the novel function of Cdh1-APC as a translational regulator to its interaction with FMRP, a protein linked to protein synthesis, synapse development, and function.

5.3. Discussion

Recent studies have provided conflicting reports on the role of ubiquitination in stress granule dynamics. In two studies, manipulation of the ubiquitin proteasome system (UPS) did affect stress granule formation (Mazroui et al., 2007; Xie et al., 2018). However, in a recent study, pharmacologic inhibition of the E1 ubiquitin activating enzyme did not affect stress granule assembly or disassembly, suggesting that active conjugation of ubiquitin does not regulate stress granule formation (Markmiller et al., 2019). It is important to note that these prior studies used methods that would broadly impact UPS, unlike our studies that target only one specific E3 ligase (as opposed to the E1 activating enzyme). Our data show that Cdh1-APC, a well-known E3 ubiquitin ligase, indeed regulates stress granule formation. To our knowledge, this is the first E3 ligase shown to play a role in stress granule dynamics through regulation of protein synthesis. Another possible reason for the differences in our observation of UPS function in stress granule formation is cell-type specificity. While our study used neurons, Markmiller et al. utilized HeLa and 293T HEK cells, which are both non-neuronal cell lines. It is possible that our observed phenotypes of stress granule and protein synthesis regulation by Cdh1-APC may only occur in neural-lineage cell types. Furthermore, a previous study by Markmiller et al. demonstrated that there are cell-specific changes in the stress granule interactome, with neurons having the most diverse stress granule interactome (Markmiller et al., 2018). Interestingly, the neuron stress granule interactome is enriched with quality control factors (Markmiller et al., 2018). As the UPS

is involved in cell quality control, this previous evidence supports our findings that an E3 ubiquitin ligase regulates neuronal stress granule dynamics. Thus, our data taken together with that of Markmiller et al. suggest that Cdh1-APC and the UPS may play a cell-type specific role that contributes to additional spatiotemporal control of protein homeostasis that is critical in neural cells.

While Cdh1-APC activity impacts stress granule formation, we did not observe that Cdh1 co-localizes with stress granules (**Supplemental Figure 5-4**); Cdh1 has also not been identified as a stress granule protein (Jain et al., 2016; Markmiller et al., 2018). This suggests that while Cdh1-APC interacts with stress granule proteins perhaps dynamically, it is not an integral component of stress granule. The study by Markmiller et al. (2018) concluded that stress granule proteins interact in a pre-existing network in unstressed conditions, and that the stress stimulus causes the formation of the stress granules. The dynamic ability of the stress granule protein network to quickly respond to stress suggests modifying events that include posttranslational modifications. It is likely that there are antagonistic modifications that regulate the dynamics between assembly and disassembly. Our data suggest that ubiquitination is a molecular switch to antagonize stress granule formation. Thus, our working model is that Cdh1-APC modifies (presumably by ubiquitinating) stress granule proteins, making them less efficiently incorporated into stress granules. Further work is needed to know whether Cdh1-APC acts locally and directly upon stress granules or if it acts remotely to antagonize the recruitment of factors into stress granules.

It is still unclear how ubiquitination of FMRP by Cdh1-APC impacts the ability to form stress granules. One possibility is that ubiquitination of FMRP leads to its degradation by the proteasome, and its absence prevents the formation of stress granules. A previous study demonstrated that loss of FMRP disrupts stress granule formation, potentially due to its

aggregation properties (Didiot et al., 2009). Thus, it is most likely that the degradation of FMRP following ubiquitination by Cdh1-APC mediates the changes in stress granule dynamics. However, another possibility is that the ubiquitination of FMRP elicits downstream signaling that causes a dynamic change in the stress granule proteome that is independent of FMRP degradation. Further investigation of how FMRP shuttling between diverse granules and polyribosomes is altered following ubiquitination will be necessary to better understand how Cdh1-APC can carry out changes in protein synthesis. Elucidation of this mechanism can be utilized to identify points of pathophysiology in forms of neurodevelopmental disorders that are characterized by dysregulated protein synthesis and/or disrupted ubiquitination pathways.

5.4. Figures

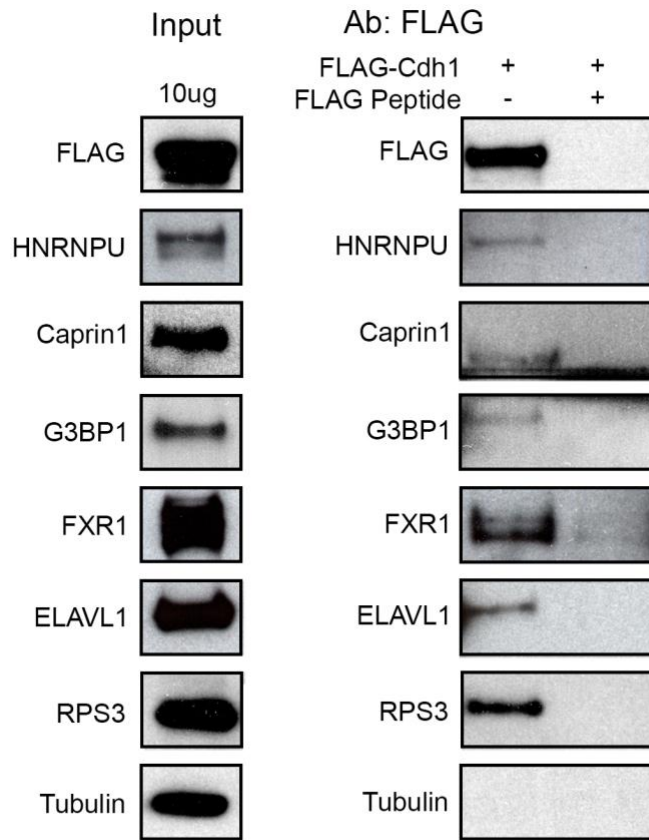


Figure 5-1: Confirmed stress granule interactors of Cdh1

N2A cells transfected with FLAG-Cdh1 underwent FLAG immunoprecipitation and subsequent immunoblotting for proteins identified with mass spectrometry. Lysate co-incubated with 3x FLAG peptide was used as a control to determine if any of the interactions were nonspecific.

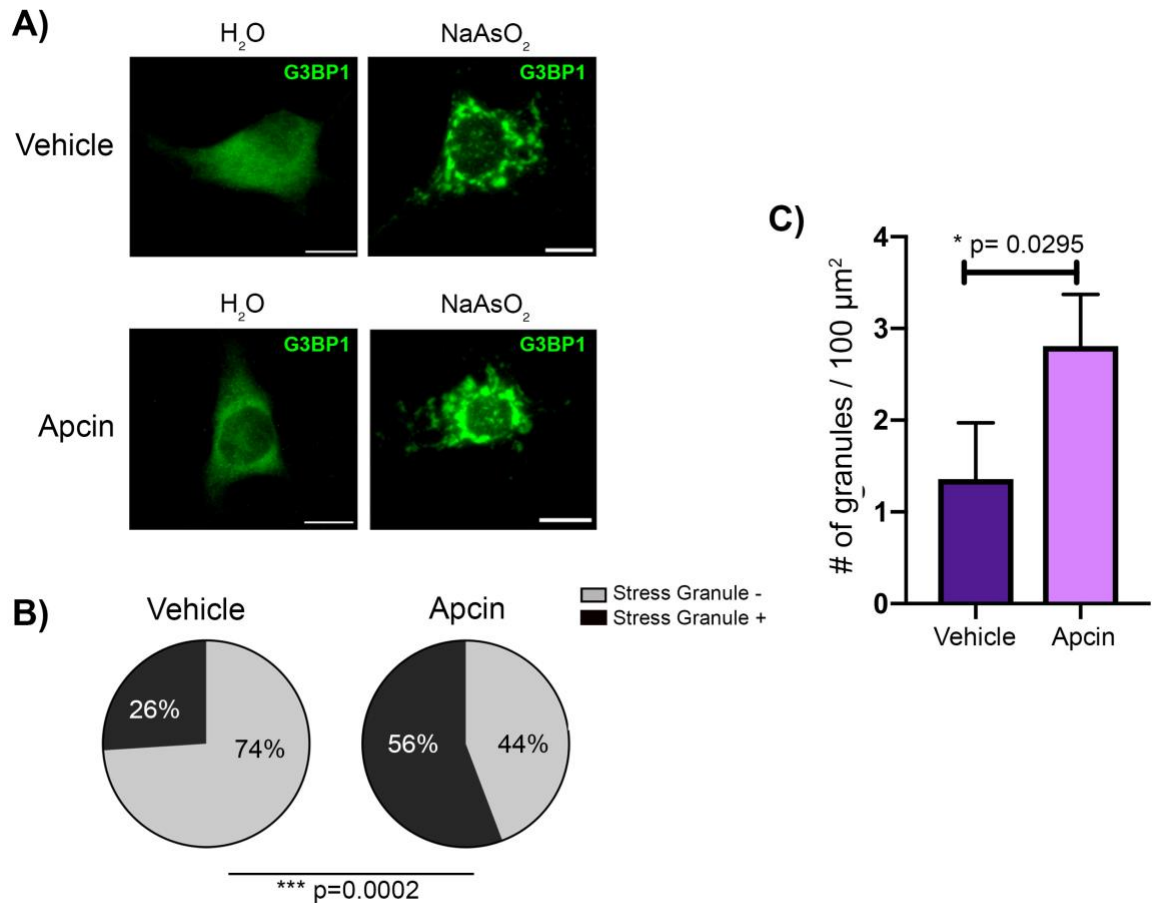


Figure 5-2: Cdh1-APC regulates stress granule formation in neurons

A) DIV 14 cortical neurons were treated with vehicle (DMSO) or Apcin for 16-18 hours. Neurons were then treated with sodium arsenite (NaAsO₂) (0.5mM) or water for 45 minutes hour prior to fixation. Immunofluorescence was done with antibodies against G3BP. Scale bar indicates 10μm.

B) User-blind scoring of neurons that were stress granule positive or stress granule negative following arsenite treatment. N=73 neurons for vehicle, 78 neurons for Apcin. **C)** Number of stress granules in within the soma.

B) Statistical significance was calculated by Z test. ***p<0.005. **C)** Statistical significance calculated by Student's t-test. *p<0.05.

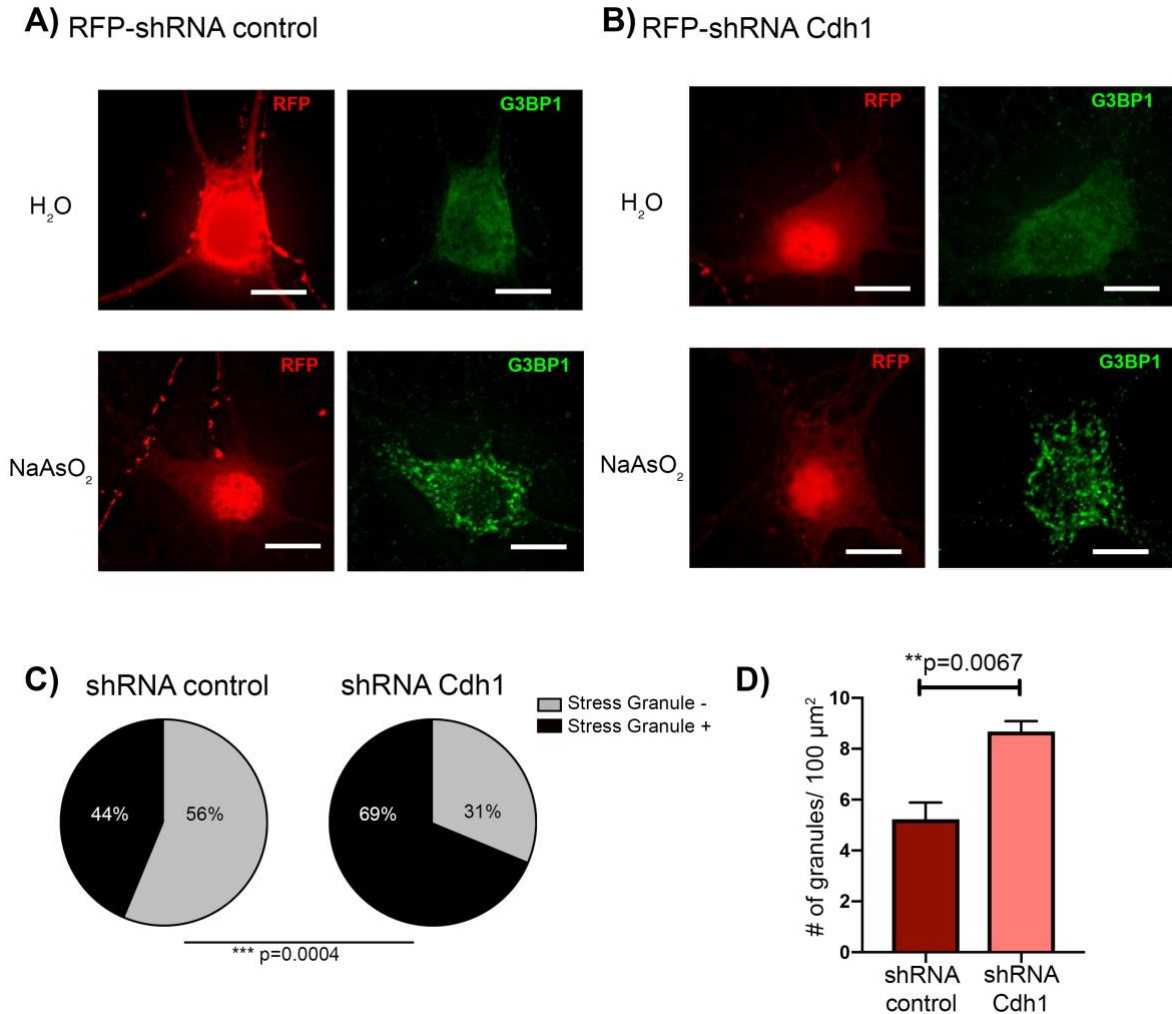


Figure 5-3: Knockdown of Cdh1 increases stress granule formation

A) & B) DIV 7 neurons were transduced with lentivirus expressing RFP-tagged non-targeting construct (**A**) or RFP-tagged shRNA against Cdh1 (**B**). At DIV 14, neurons were then treated with sodium arsenite (NaAsO₂) (0.5mM) or water for 45 minutes hour prior to fixation. Immunofluorescence was done with antibodies against G3BP. Scale bar indicates 10μm **C)** User-blind scoring of neurons that were stress granule positive or stress granule negative following arsenite treatment. N=80 neurons for both groups. **D)** Number of stress granules within the soma. **C)** Statistical significance was calculated by Z test. ***p<0.005. **D)** Statistical significance calculated by Student's t-test. **p<0.01.

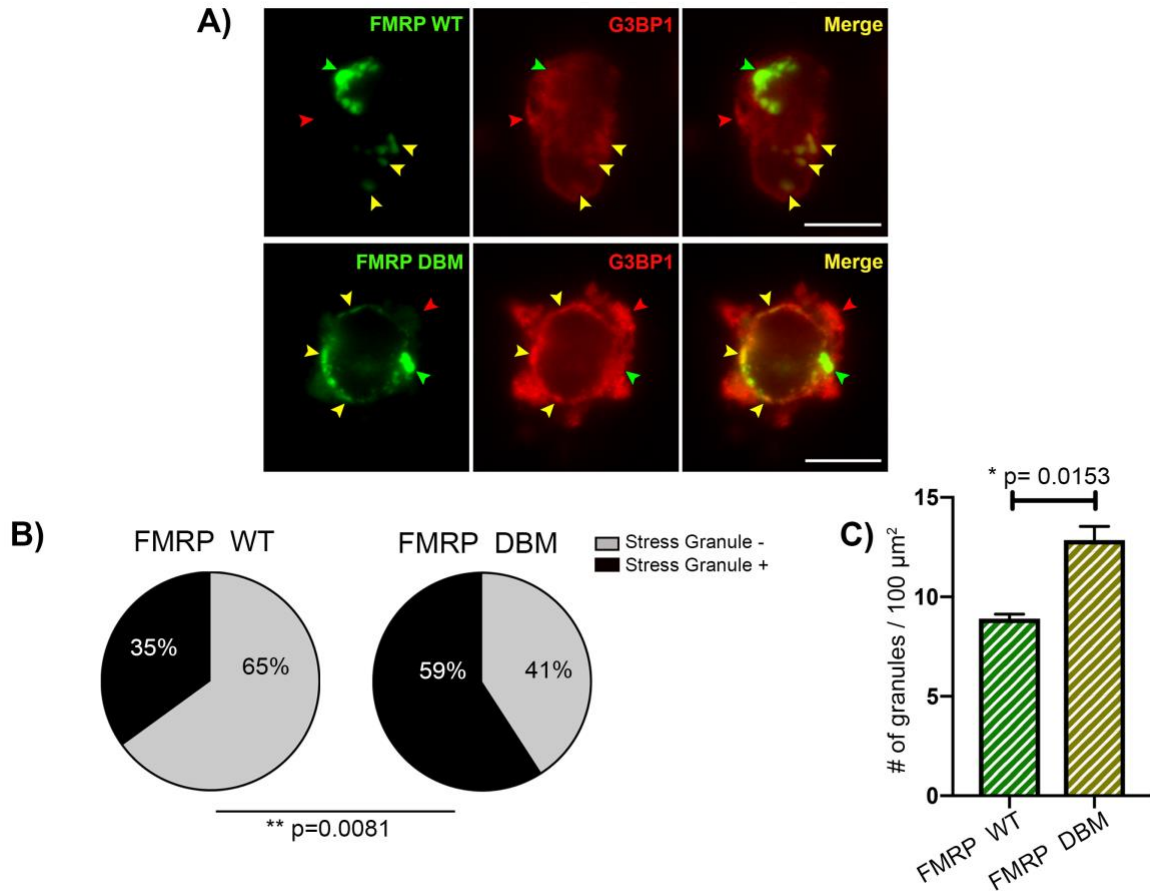


Figure 5-4: Cdh1-APC interaction with FMRP regulates stress granule formation

A) N2A cells were transfected with GFP-FMRP WT or GFP-FMRP DBM and treated with sodium arsenite for 45 minutes. Cells were then fixed and immunostained for G3BP1. Green arrowheads indicate FMRP expression. Red arrowheads indicate stress granules based upon G3BP1 staining. Yellow arrowheads indicate co-localization of FMRP with G3BP1-positive stress granules. Scale bar indicates 10μm. **B)** Quantification of stress granule negative or positive cells. N=60 cells for both conditions. **C)** Number of granules in within the soma.

B) Statistical significance calculated by Z test. **p<0.01. **C)** Statistical significance calculated by Student's t-test. *p<0.05.

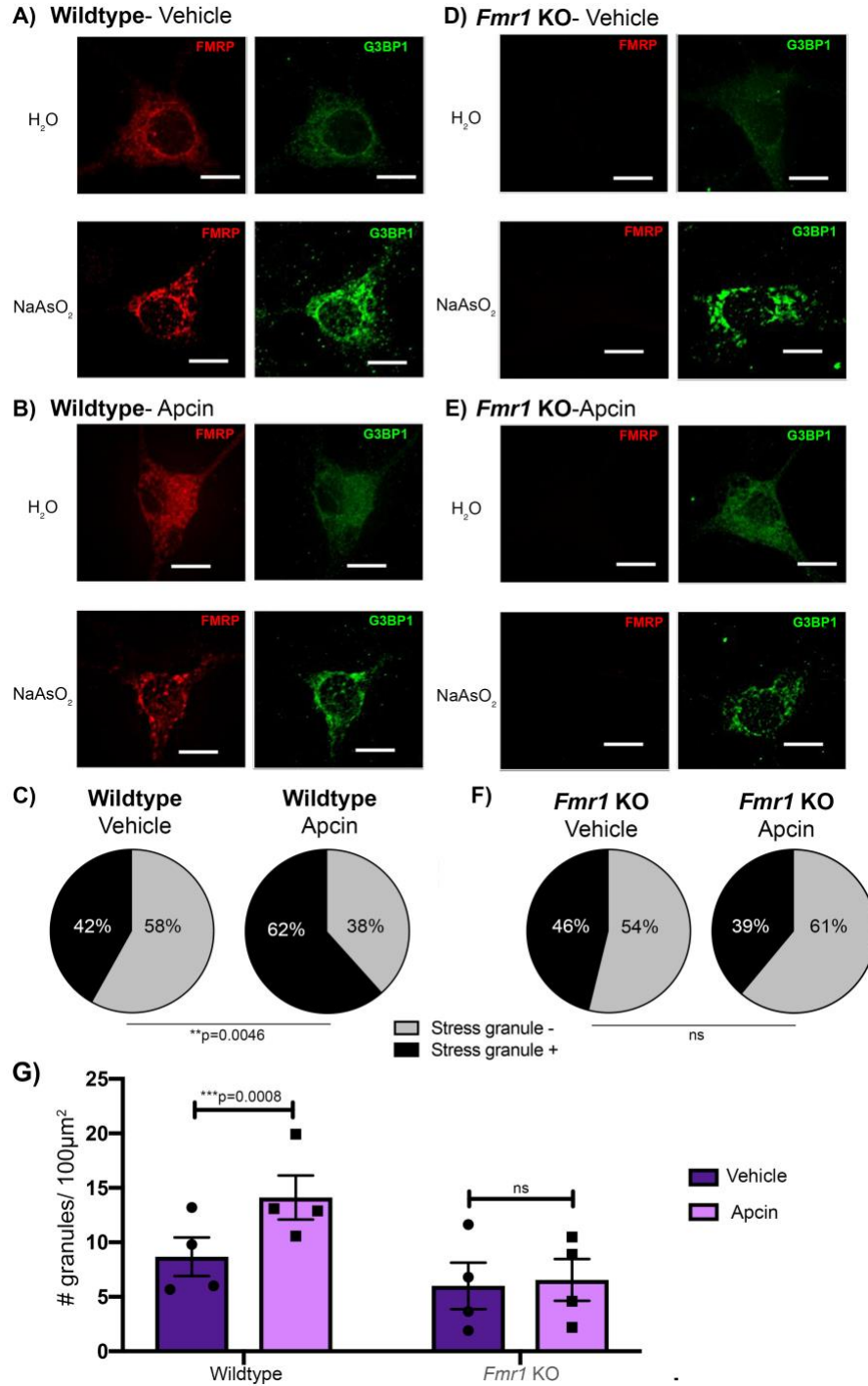


Figure 5-5: Cdh1-APC regulates stress granule dynamics via a FMRP-dependent mechanism

A, B) Postnatal wildtype DIV 14-16 cortical neurons were treated with vehicle (DMSO) (**A**) or Apcin (**B**) for 16-18 hours. Neurons were then treated with sodium arsenite and immunostained.

Scale bar indicates 10 μ m. **C)** Quantification of stress granule negative or positive cells. n=74 cells for Vehicle-treated and 73 cells for Apcin-treated. **D, E)** Postnatal *Fmr1*- knockout (KO) DIV 14-16 cortical neurons were treated with vehicle (DMSO) (**D**) or Apcin (**E**) for 16-18 hours and treated with sodium arsenite and fixed as described above. **F)** Quantification of stress granule negative or positive cells. N=78 cells for Vehicle-treated and 77 cells for Apcin-treated. **G)** Quantification of number of stress granules in the soma per 100 μ m² for all four conditions, n=4. Statistical significance was calculated by Z test (**C,F**) and two-way ANOVA (**G**).

5.5. Tables

Gene	Protein
CAPRN1	Caprin-1
CDC5L	Cell Division Cycle 5-Like Protein
CSDE1	Cold shock domain-containing protein E1
DDX21	Nucleolar RNA helicase 2
DDX5	Probable ATP-dependent RNA helicase DDX5
DHX30	Putative ATP-dependent RNA helicase DHX30
DHX36	ATP-dependent RNA helicase DHX36
EIF3A	Eukaryotic Translation Initiation Factor 3 Subunit A
EIF3B	Eukaryotic Translation Initiation Factor 3 Subunit B
EIF3C	Eukaryotic Translation Initiation Factor 3 Subunit C
EIF3D	Eukaryotic Translation Initiation Factor 3 Subunit D
EIF3F	Eukaryotic Translation Initiation Factor 3 Subunit F
EIF3H	Eukaryotic Translation Initiation Factor 3 Subunit H
EIF3I	Eukaryotic Translation Initiation Factor 3 Subunit I
EIF3K	Eukaryotic Translation Initiation Factor 3 Subunit K
EIF3L	Eukaryotic Translation Initiation Factor 3 Subunit L
EIF3M	Eukaryotic Translation Initiation Factor 3 Subunit M
EIF4E	Eukaryotic Translation Initiation Factor 4E
EIF4G1	Eukaryotic Translation Initiation Factor 4G1
ELAVL1	ELAV-like Protein 1
FXR1	Fragile X mental retardation syndrome-related protein 1
G3BP1	Ras GTPase-activating protein-binding protein 1
G3BP2	Ras GTPase-activating protein-binding protein 2
HNRNPA1	Heterogenous Nuclear Ribonucleoprotein A1
HNRNPK	Heterogenous Nuclear Ribonucleoprotein K
HNRNPL	Heterogenous Nuclear Ribonucleoprotein L
HNRNPM	Heterogenous Nuclear Ribonucleoprotein M
HNRNPU	Heterogenous Nuclear Ribonucleoprotein U
HSPA8	Heat shock cognate 71 kDA protein
HSPA9	Stress-70 protein, mitochondrial
ILF3	Interleukin enhancer-binding factor 3
KPNA2	Importin subunit alpha-1
LARP1	La-related protein 1
LARP4	La-related protein 4
LARP4B	La-related protein 4B

Gene	Protein
MOV10	Putative helicase MOV-10
NONO	Non-POU domain-containing octamer-binding protein
PABPC1	Polyadenylate-binding protein 1
PURA	Transcriptional activator protein Pur-alpha
PURB	Transcriptional activator protein Pur-beta
RACK1	Receptor of activated protein C kinase 1
RPS18	40S ribosomal protein S18
RPS19	40S ribosomal protein S19
RPS3	40S ribosomal protein S3
RPL3	60S ribosomal protein L3
SERBP1	Plasminogen activator inhibitor 1 RNA-binding protein
SYNCRIP	Heterogeneous nuclear ribonucleoprotein Q
UPF1	Regulator of nonsense transcripts 1
USP10	Ubiquitin carboxyl-terminal hydrolase 10
YBX1	Y-Box Binding Protein 1
YBX3	Y-Box Binding Protein 3
YTHDF2	YTH domain-containing family protein 2

Table 5-1: Table of stress granule proteins in Cdh1 interactome

The list of Cdh1-interacting proteins (Table 3-1) was compared to tables in previous literature (Jain et al., 2016; Markmiller et al., 2018) to identify which proteins in the Cdh1-interactome are implicated in stress granule formation and function. Out of the 185 proteins in the Cdh1 interactome, we identified 52 as being known stress granule proteins.

Identified Proteins (397)	Molecular Weight	Spectral Count		Stress Granule ?
		W T	W T+	
Actin, cytoplasmic 2 OS=Mus musculus GN=Actg1 PE=1 SV=1	42 kDa	333	89	
Synaptic functional regulator FMR1 OS=Mus musculus GN=Fmr1 PE=1 SV=1	69 kDa	319	0	
Desmoplakin OS=Mus musculus GN=Dsp PE=1 SV=1	333 kDa	294	282	
Fragile X mental retardation syndrome-related protein 1 OS=Mus musculus GN=Fxr1 PE=1 SV=2	76 kDa	180	0	Yes
Junction plakoglobin OS=Mus musculus GN=Jup PE=1 SV=3	82 kDa	131	124	
Actin, alpha cardiac muscle 1 OS=Mus musculus GN=Actc1 PE=1 SV=1	42 kDa	106	0	
Polyadenylate-binding protein 1 OS=Mus musculus GN=Pabpc1 PE=1 SV=2	71 kDa	99	0	Yes
Heat shock cognate 71 kDa protein OS=Mus musculus GN=Hspa8 PE=1 SV=1	71 kDa	95	10	Yes
Fragile X mental retardation syndrome-related protein 2 OS=Mus musculus GN=Fxr2 PE=1 SV=1	74 kDa	79	0	Yes
Eukaryotic translation initiation factor 3 subunit C OS=Mus musculus GN=Eif3c PE=1 SV=1	106 kDa	78	0	Yes
Eukaryotic translation initiation factor 3 subunit B OS=Mus musculus GN=Eif3b PE=1 SV=1	91 kDa	69	0	Yes
Probable ATP-dependent RNA helicase DDX5 OS=Mus musculus GN=Ddx5 PE=1 SV=2	69 kDa	63	0	Yes
60S ribosomal protein L3 OS=Mus musculus GN=Rpl3 PE=1 SV=3	46 kDa	63	0	Yes
60S ribosomal protein L5 OS=Mus musculus GN=Rpl5 PE=1 SV=3	34 kDa	62	0	
Coronin-1C OS=Mus musculus GN=Coro1c PE=1 SV=2	53 kDa	61	0	
Heterogeneous nuclear ribonucleoprotein U OS=Mus musculus GN=Hnrnpu PE=1 SV=1	88 kDa	59	0	Yes
Protein flightless-1 homolog OS=Mus musculus GN=Flil PE=1 SV=1	145 kDa	59	0	
LIM domain and actin-binding protein 1 OS=Mus musculus GN=Lima1 PE=1 SV=3	84 kDa	55	0	
40S ribosomal protein S3a OS=Mus musculus GN=Rps3a PE=1 SV=3	30 kDa	54	0	
Eukaryotic translation initiation factor 3 subunit A OS=Mus musculus GN=Eif3a PE=1 SV=5	162 kDa	54	0	Yes
Spectrin alpha chain, non-erythrocytic 1 OS=Mus musculus GN=Sptan1 PE=1 SV=4	285 kDa	54	0	
Protein PRRC2C OS=Mus musculus GN=Prrc2c PE=1 SV=3	311 kDa	52	0	
Spectrin beta chain, non-erythrocytic 1 OS=Mus musculus GN=Sptbn1 PE=1 SV=2	274 kDa	51	0	
60S ribosomal protein L4 OS=Mus musculus GN=Rpl4 PE=1 SV=3	47 kDa	50	0	

Identified Proteins (397)	Molecular Weight	Spectral Count		Stress Granule ?
		W T	W T+	
Keratin, type II cytoskeletal 2 oral OS=Mus musculus GN=Krt76 PE=1 SV=1	63 kDa	48	66	
Drebrin OS=Mus musculus GN=Dbn1 PE=1 SV=4	77 kDa	47	0	
IgE-binding protein OS=Mus musculus GN=Iap PE=2 SV=1	63 kDa	45	0	
ATP-dependent RNA helicase A OS=Mus musculus GN=Dhx9 PE=1 SV=2	149 kDa	43	0	
40S ribosomal protein S4, X isoform OS=Mus musculus GN=Rps4x PE=1 SV=2	30 kDa	43	0	
60S ribosomal protein L7 OS=Mus musculus GN=Rpl7 PE=1 SV=2	31 kDa	43	0	
Caprin-1 OS=Mus musculus GN=Caprin1 PE=1 SV=2	78 kDa	42	0	Yes
Receptor of activated protein C kinase 1 OS=Mus musculus GN=Rack1 PE=1 SV=3	35 kDa	42	0	Yes
60S acidic ribosomal protein P0 OS=Mus musculus GN=Rplp0 PE=1 SV=3	34 kDa	39	0	
Eukaryotic translation initiation factor 3 subunit D OS=Mus musculus GN=Eif3d PE=1 SV=2	64 kDa	38	0	Yes
Nucleolin OS=Mus musculus GN=Ncl PE=1 SV=2	77 kDa	37	0	
60S ribosomal protein L11 OS=Mus musculus GN=Rpl11 PE=1 SV=4	20 kDa	37	0	
40S ribosomal protein S3 OS=Mus musculus GN=Rps3 PE=1 SV=1	27 kDa	37	0	Yes
Serine/arginine-rich splicing factor 1 OS=Mus musculus GN=Srsf1 PE=1 SV=3	28 kDa	36	0	
Vimentin OS=Mus musculus GN=Vim PE=1 SV=3	54 kDa	35	0	
Heterogeneous nuclear ribonucleoprotein M OS=Mus musculus GN=Hnrnpm PE=1 SV=3	78 kDa	34	0	Yes
RNA binding motif protein, X-linked-like-1 OS=Mus musculus GN=Rbmx11 PE=1 SV=1	42 kDa	34	0	
Protein PRRC2A OS=Mus musculus GN=Prrc2a PE=1 SV=1	229 kDa	34	0	
Ig gamma-1 chain C region secreted form OS=Mus musculus GN=Ighg1 PE=1 SV=1	36 kDa	33	12	
Leucine-rich repeat flightless-interacting protein 2 OS=Mus musculus GN=Lrrfip2 PE=1 SV=1	47 kDa	33	0	
Desmoglein-1-beta OS=Mus musculus GN=Dsg1b PE=1 SV=1	114 kDa	31	45	
Glyceraldehyde-3-phosphate dehydrogenase OS=Mus musculus GN=Gapdh PE=1 SV=2	36 kDa	30	40	
Ubiquitin-40S ribosomal protein S27a OS=Mus musculus GN=Rps27a PE=1 SV=2	18 kDa	30	5	
40S ribosomal protein SA OS=Mus musculus GN=Rpsa PE=1 SV=4	33 kDa	30	0	
ATP-dependent RNA helicase DDX3X OS=Mus musculus GN=Ddx3x PE=1 SV=3	73 kDa	29	0	

Identified Proteins (397)	Molecular Weight	Spectral Count		Stress Granule ?
		W T	W T+	
Probable helicase senataxin OS=Mus musculus GN=Setx PE=1 SV=1	298 kDa	29	0	
60S ribosomal protein L6 OS=Mus musculus GN=Rpl6 PE=1 SV=3	34 kDa	29	0	
DNA topoisomerase 3-beta-1 OS=Mus musculus GN=Top3b PE=1 SV=1	97 kDa	29	0	
60S ribosomal protein L18a OS=Mus musculus GN=Rpl18a PE=1 SV=1	21 kDa	28	0	
Splicing factor 3B subunit 3 OS=Mus musculus GN=Sf3b3 PE=1 SV=1	136 kDa	28	0	
Annexin A2 OS=Mus musculus GN=Anxa2 PE=1 SV=2	39 kDa	27	26	
Spermatogenesis-associated serine-rich protein 2 OS=Mus musculus GN=Spats2 PE=1 SV=1	59 kDa	27	0	
60S ribosomal protein L8 OS=Mus musculus GN=Rpl8 PE=1 SV=2	28 kDa	27	0	
Serine/arginine repetitive matrix protein 2 OS=Mus musculus GN=Srrm2 PE=1 SV=3	295 kDa	26	0	
Tropomodulin-3 OS=Mus musculus GN=Tmod3 PE=1 SV=1	40 kDa	26	0	
Protein-glutamine gamma-glutamyltransferase K OS=Mus musculus GN=Tgm1 PE=1 SV=2	90 kDa	25	20	
Microtubule-associated protein 1B OS=Mus musculus GN=Map1b PE=1 SV=2	270 kDa	24	0	
Regulator of nonsense transcripts 1 OS=Mus musculus GN=Upf1 PE=1 SV=2	124 kDa	24	0	Yes
Heterogeneous nuclear ribonucleoprotein H OS=Mus musculus GN=Hnrnp1 PE=1 SV=3	49 kDa	24	0	
Eukaryotic translation initiation factor 3 subunit H OS=Mus musculus GN=Eif3h PE=1 SV=1	40 kDa	24	0	Yes
Peripherin OS=Mus musculus GN=Prph PE=1 SV=2	54 kDa	24	0	
Tudor domain-containing protein 3 OS=Mus musculus GN=Tdrd3 PE=1 SV=4	82 kDa	23	0	
ELAV-like protein 2 OS=Mus musculus GN=Elavl2 PE=2 SV=1	40 kDa	23	0	
Ras GTPase-activating protein-binding protein 2 OS=Mus musculus GN=G3bp2 PE=1 SV=2	54 kDa	23	0	Yes
Pre-mRNA-processing-splicing factor 8 OS=Mus musculus GN=Prpf8 PE=1 SV=2	274 kDa	23	0	
Eukaryotic translation initiation factor 3 subunit L OS=Mus musculus GN=Eif3l PE=1 SV=1	67 kDa	23	0	Yes
Ig kappa chain C region OS=Mus musculus PE=1 SV=1	12 kDa	22	6	
Lysozyme C-1 OS=Mus musculus GN=Lyz1 PE=1 SV=1	17 kDa	22	25	
40S ribosomal protein S2 OS=Mus musculus GN=Rps2 PE=1 SV=3	31 kDa	22	0	
Elongation factor 1-alpha 1 OS=Mus musculus GN=Eef1a1 PE=1 SV=3	50 kDa	21	3	

Identified Proteins (397)	Molecular Weight	Spectral Count		Stress Granule ?
		W T	W T+	
40S ribosomal protein S11 OS=Mus musculus GN=Rps11 PE=1 SV=3	18 kDa	21	0	
Unconventional myosin-Ib OS=Mus musculus GN=Myo1b PE=1 SV=3	129 kDa	20	0	
Myb-binding protein 1A OS=Mus musculus GN=Mybbp1a PE=1 SV=2	152 kDa	20	0	
Nuclease-sensitive element-binding protein 1 OS=Mus musculus GN=Ybx1 PE=1 SV=3	36 kDa	20	0	Yes
60S ribosomal protein L10 OS=Mus musculus GN=Rpl10 PE=1 SV=3	25 kDa	20	0	
Eukaryotic translation initiation factor 3 subunit G OS=Mus musculus GN=Eif3g PE=1 SV=2	36 kDa	20	0	Yes
Eukaryotic translation initiation factor 3 subunit I OS=Mus musculus GN=Eif3i PE=1 SV=1	36 kDa	20	0	Yes
Alpha-actinin-4 OS=Mus musculus GN=Actn4 PE=1 SV=1	105 kDa	20	0	
Golgin subfamily A member 3 OS=Mus musculus GN=Golga3 PE=1 SV=3	167 kDa	20	0	
Splicing factor, proline- and glutamine-rich OS=Mus musculus GN=Sfpq PE=1 SV=1	75 kDa	19	0	
Heterogeneous nuclear ribonucleoprotein K OS=Mus musculus GN=Hnrnpk PE=1 SV=1	51 kDa	19	0	Yes
AP-2 complex subunit alpha-1 OS=Mus musculus GN=Ap2a1 PE=1 SV=1	108 kDa	19	0	
Pre-mRNA-splicing factor ATP-dependent RNA helicase DHX15 OS=Mus musculus GN=Dhx15 PE=1 SV=2	91 kDa	18	0	
U5 small nuclear ribonucleoprotein 200 kDa helicase OS=Mus musculus GN=Snrnp200 PE=1 SV=1	245 kDa	18	0	
60S ribosomal protein L14 OS=Mus musculus GN=Rpl14 PE=1 SV=3	24 kDa	18	0	
Ubiquitin-associated protein 2-like OS=Mus musculus GN=Ubp2l1 PE=1 SV=1	117 kDa	18	0	Yes
Serine/arginine-rich splicing factor 3 OS=Mus musculus GN=Srsf3 PE=1 SV=1	19 kDa	17	0	
60S ribosomal protein L15 OS=Mus musculus GN=Rpl15 PE=2 SV=4	24 kDa	17	0	
ATP-dependent RNA helicase DDX1 OS=Mus musculus GN=Ddx1 PE=1 SV=1	83 kDa	17	0	
Unconventional myosin-Va OS=Mus musculus GN=Myo5a PE=1 SV=2	216 kDa	17	0	
AP-2 complex subunit alpha-2 OS=Mus musculus GN=Ap2a2 PE=1 SV=2	104 kDa	17	0	
60S ribosomal protein L12 OS=Mus musculus GN=Rpl12 PE=1 SV=2	18 kDa	16	0	
Zinc finger CCCH-type antiviral protein 1 OS=Mus musculus GN=Zc3hav1 PE=1 SV=1	107 kDa	16	0	

Identified Proteins (397)	Molecular Weight	Spectral Count		Stress Granule ?
		W T	W T+	
Ras GTPase-activating protein-binding protein 1 OS=Mus musculus GN=G3bp1 PE=1 SV=1	52 kDa	16	0	Yes
Heterogeneous nuclear ribonucleoprotein F OS=Mus musculus GN=Hnrnpf PE=1 SV=3	46 kDa	16	0	
ADP/ATP translocase 2 OS=Mus musculus GN=Slc25a5 PE=1 SV=3	33 kDa	16	0	
La-related protein 1 OS=Mus musculus GN=Larp1 PE=1 SV=3	121 kDa	16	0	Yes
Heterogeneous nuclear ribonucleoproteins C1/C2 OS=Mus musculus GN=Hnrnpc PE=1 SV=1	34 kDa	16	0	
AP-2 complex subunit beta OS=Mus musculus GN=Ap2b1 PE=1 SV=1	105 kDa	15	0	
Ubiquitin-associated protein 2 OS=Mus musculus GN=Ubp2 PE=1 SV=1	118 kDa	15	0	
Signal-induced proliferation-associated 1-like protein 1 OS=Mus musculus GN=Sipa1l1 PE=1 SV=2	197 kDa	15	0	
Plakophilin-1 OS=Mus musculus GN=Pkp1 PE=1 SV=1	81 kDa	14	18	
Heat shock protein HSP 90-beta OS=Mus musculus GN=Hsp90ab1 PE=1 SV=3	83 kDa	14	0	
60S ribosomal protein L23 OS=Mus musculus GN=Rpl23 PE=1 SV=1	15 kDa	14	0	
Arginase-1 OS=Mus musculus GN=Arg1 PE=1 SV=1	35 kDa	14	4	
78 kDa glucose-regulated protein OS=Mus musculus GN=Hspa5 PE=1 SV=3	72 kDa	14	0	
116 kDa U5 small nuclear ribonucleoprotein component OS=Mus musculus GN=Eftud2 PE=1 SV=1	109 kDa	14	0	
ATP synthase subunit gamma, mitochondrial OS=Mus musculus GN=Atp5c1 PE=1 SV=1	33 kDa	14	0	
Nuclear fragile X mental retardation-interacting protein 2 OS=Mus musculus GN=Nufip2 PE=1 SV=1	76 kDa	14	0	Yes
F-actin-capping protein subunit beta OS=Mus musculus GN=Capzb PE=1 SV=3	31 kDa	14	0	
Eukaryotic translation initiation factor 3 subunit F OS=Mus musculus GN=Eif3f PE=1 SV=2	38 kDa	14	0	Yes
Nucleolar RNA helicase 2 OS=Mus musculus GN=Ddx21 PE=1 SV=3	94 kDa	13	0	Yes
Serine/arginine-rich splicing factor 7 OS=Mus musculus GN=Srsf7 PE=1 SV=1	31 kDa	13	0	
Heterogeneous nuclear ribonucleoprotein A3 OS=Mus musculus GN=Hnrnpa3 PE=1 SV=1	40 kDa	13	0	Yes
40S ribosomal protein S20 OS=Mus musculus GN=Rps20 PE=1 SV=1	13 kDa	13	0	
Putative ATP-dependent RNA helicase DHX30 OS=Mus musculus GN=Dhx30 PE=1 SV=1	137 kDa	13	0	Yes

Identified Proteins (397)	Molecular Weight	Spectral Count		Stress Granule ?
		W T	W T+	
60S ribosomal protein L13 OS=Mus musculus GN=Rpl13 PE=1 SV=3	24 kDa	13	0	
Splicing factor 3B subunit 1 OS=Mus musculus GN=Sf3b1 PE=1 SV=1	146 kDa	13	0	
Transcriptional activator protein Pur-alpha OS=Mus musculus GN=Pura PE=1 SV=1	35 kDa	13	0	Yes
Eukaryotic initiation factor 4A-III OS=Mus musculus GN=Eif4a3 PE=1 SV=3	47 kDa	13	0	Yes
Coronin-2B OS=Mus musculus GN=Coro2b PE=1 SV=2	55 kDa	13	0	
Probable ATP-dependent RNA helicase DDX17 OS=Mus musculus GN=Ddx17 PE=1 SV=1	72 kDa	13	0	
Plasminogen activator inhibitor 1 RNA-binding protein OS=Mus musculus GN=Serbp1 PE=1 SV=2	45 kDa	12	0	Yes
Matrin-3 OS=Mus musculus GN=Matr3 PE=1 SV=1	95 kDa	12	0	
Nucleophosmin OS=Mus musculus GN=Npm1 PE=1 SV=1	33 kDa	12	0	
Pre-mRNA-processing factor 6 OS=Mus musculus GN=Prpf6 PE=1 SV=1	107 kDa	12	0	
Heterogeneous nuclear ribonucleoprotein L OS=Mus musculus GN=Hnrnpl PE=1 SV=2	64 kDa	12	0	Yes
Cytoskeleton-associated protein 4 OS=Mus musculus GN=Ckap4 PE=1 SV=2	64 kDa	12	0	
F-actin-capping protein subunit alpha-1 OS=Mus musculus GN=Capza1 PE=1 SV=4	33 kDa	12	0	
Alpha-actinin-1 OS=Mus musculus GN=Actn1 PE=1 SV=1	103 kDa	12	0	
Gasdermin-A OS=Mus musculus GN=Gsdma PE=2 SV=1	50 kDa	11	13	
La-related protein 4 OS=Mus musculus GN=Larp4 PE=1 SV=2	80 kDa	11	0	Yes
Transformer-2 protein homolog beta OS=Mus musculus GN=Tra2b PE=1 SV=1	34 kDa	11	0	
60S ribosomal protein L7a OS=Mus musculus GN=Rpl7a PE=1 SV=2	30 kDa	11	0	
RNA-binding protein Raly OS=Mus musculus GN=Raly PE=1 SV=3	33 kDa	11	0	
ATPase family AAA domain-containing protein 3 OS=Mus musculus GN=Atad3 PE=1 SV=1	67 kDa	11	0	
Leucine zipper protein 1 OS=Mus musculus GN=Luzp1 PE=1 SV=2	119 kDa	11	0	
Serine/threonine-protein kinase 38 OS=Mus musculus GN=Stk38 PE=1 SV=1	54 kDa	11	0	
Heterogeneous nuclear ribonucleoprotein Q OS=Mus musculus GN=Syncr1 PE=1 SV=2	70 kDa	11	0	Yes
Thyroid hormone receptor-associated protein 3 OS=Mus musculus GN=Thrap3 PE=1 SV=1	108 kDa	11	0	
Y-box-binding protein 3 OS=Mus musculus GN=Ybx3 PE=1 SV=2	39 kDa	11	0	Yes

Identified Proteins (397)	Molecular Weight	Spectral Count		Stress Granule ?
		W T	W T+	
ADP/ATP translocase 1 OS=Mus musculus GN=Slc25a4 PE=1 SV=4	33 kDa	11	0	
Peroxiredoxin-2 OS=Mus musculus GN=Prdx2 PE=1 SV=3	22 kDa	10	10	
Non-POU domain-containing octamer-binding protein OS=Mus musculus GN=Nono PE=1 SV=3	55 kDa	10	0	Yes
Nuclear valosin-containing protein-like OS=Mus musculus GN=Nvl PE=1 SV=1	94 kDa	10	0	
Alpha-enolase OS=Mus musculus GN=Eno1 PE=1 SV=3	47 kDa	10	0	
Myelin expression factor 2 OS=Mus musculus GN=Myef2 PE=1 SV=1	63 kDa	10	0	
Serine/arginine-rich splicing factor 6 OS=Mus musculus GN=Srsf6 PE=1 SV=1	39 kDa	10	0	
Bleomycin hydrolase OS=Mus musculus GN=Blmh PE=1 SV=1	53 kDa	10	5	
60S acidic ribosomal protein P2 OS=Mus musculus GN=Rplp2 PE=1 SV=3	12 kDa	10	0	
Pre-mRNA-processing factor 19 OS=Mus musculus GN=Prpf19 PE=1 SV=1	55 kDa	10	0	
Transcription intermediary factor 1-beta OS=Mus musculus GN=Trim28 PE=1 SV=3	89 kDa	10	0	
Constitutive coactivator of PPAR-gamma-like protein 1 OS=Mus musculus GN=FAM120A PE=1 SV=2	122 kDa	10	0	
tRNA-splicing ligase RtcB homolog OS=Mus musculus GN=Rtcb PE=1 SV=1	55 kDa	10	0	
Eukaryotic translation initiation factor 3 subunit E OS=Mus musculus GN=Eif3e PE=1 SV=1	52 kDa	10	0	Yes
Ubiquitin carboxyl-terminal hydrolase 10 OS=Mus musculus GN=Usp10 PE=1 SV=3	87 kDa	10	0	Yes
Transformer-2 protein homolog alpha OS=Mus musculus GN=Tra2a PE=1 SV=1	32 kDa	10	0	
Unconventional myosin-Ic OS=Mus musculus GN=Myo1c PE=1 SV=2	122 kDa	10	0	
ELAV-like protein 3 OS=Mus musculus GN=Elavl3 PE=1 SV=1	40 kDa	10	0	Yes
60S ribosomal protein L17 OS=Mus musculus GN=Rpl17 PE=1 SV=3	21 kDa	9	0	
Tubulin alpha-1B chain OS=Mus musculus GN=Tuba1b PE=1 SV=2	50 kDa	9	0	
AP-2 complex subunit mu OS=Mus musculus GN=Ap2m1 PE=1 SV=1	50 kDa	9	0	
Serine/arginine-rich splicing factor 2 OS=Mus musculus GN=Srsf2 PE=1 SV=4	25 kDa	9	0	
Centromere-associated protein E OS=Mus musculus GN=Cenpe PE=1 SV=1	287 kDa	9	2	
Interleukin enhancer-binding factor 3 OS=Mus musculus GN=Ilf3 PE=1 SV=2	96 kDa	9	0	Yes
60S ribosomal protein L13a OS=Mus musculus GN=Rpl13a PE=1 SV=4	23 kDa	9	0	

Identified Proteins (397)	Molecular Weight	Spectral Count		Stress Granule ?
		W T	W T+	
Transcriptional activator protein Pur-beta OS=Mus musculus GN=Purb PE=1 SV=3	34 kDa	9	0	Yes
Bcl-2-associated transcription factor 1 OS=Mus musculus GN=Bclaf1 PE=1 SV=2	106 kDa	9	0	
WD repeat-containing protein 1 OS=Mus musculus GN=Wdr1 PE=1 SV=3	66 kDa	9	0	
40S ribosomal protein S6 OS=Mus musculus GN=Rps6 PE=1 SV=1	29 kDa	9	0	Yes
Centrosomal protein of 170 kDa OS=Mus musculus GN=Cep170 PE=1 SV=2	175 kDa	9	0	
60S ribosomal protein L35a OS=Mus musculus GN=Rpl35a PE=1 SV=2	13 kDa	9	0	
40S ribosomal protein S16 OS=Mus musculus GN=Rps16 PE=1 SV=4	16 kDa	9	0	
Poly(rC)-binding protein 2 OS=Mus musculus GN=Pcbp2 PE=1 SV=1	38 kDa	9	0	
Cold shock domain-containing protein E1 OS=Mus musculus GN=Csde1 PE=1 SV=1	89 kDa	9	0	Yes
Eukaryotic translation initiation factor 2 subunit 3, X-linked OS=Mus musculus GN=Eif2s3x PE=1 SV=2	51 kDa	9	0	
F-actin-capping protein subunit alpha-2 OS=Mus musculus GN=Capza2 PE=1 SV=3	33 kDa	9	0	
Tubulin beta-4B chain OS=Mus musculus GN=Tubb4b PE=1 SV=1	50 kDa	9	0	
RNA-binding protein 14 OS=Mus musculus GN=Rbm14 PE=1 SV=1	69 kDa	8	0	
Tubulin beta-5 chain OS=Mus musculus GN=Tubb5 PE=1 SV=1	50 kDa	8	0	
60S ribosomal protein L27a OS=Mus musculus GN=Rpl27a PE=1 SV=5	17 kDa	8	0	
Double-stranded RNA-binding protein Staufen homolog 1 OS=Mus musculus GN=Stau1 PE=1 SV=1	54 kDa	8	0	Yes
60S ribosomal protein L27 OS=Mus musculus GN=Rpl27 PE=1 SV=2	16 kDa	8	0	
Polymerase delta-interacting protein 3 OS=Mus musculus GN=Poldip3 PE=1 SV=1	46 kDa	8	0	
60S ribosomal protein L28 OS=Mus musculus GN=Rpl28 PE=1 SV=2	16 kDa	8	0	
Polypyrimidine tract-binding protein 1 OS=Mus musculus GN=Ptbp1 PE=1 SV=2	56 kDa	8	0	
Periodic tryptophan protein 1 homolog OS=Mus musculus GN=Pwp1 PE=1 SV=1	56 kDa	8	0	
La-related protein 4B OS=Mus musculus GN=Larp4b PE=1 SV=2	82 kDa	8	0	Yes
40S ribosomal protein S8 OS=Mus musculus GN=Rps8 PE=1 SV=2	24 kDa	8	0	

Identified Proteins (397)	Molecular Weight	Spectral Count		Stress Granule ?
		W T	W T+	
Heterogeneous nuclear ribonucleoprotein U-like protein 2 OS=Mus musculus GN=Hnrnpul2 PE=1 SV=2	85 kDa	8	0	
ATP-dependent RNA helicase DHX29 OS=Mus musculus GN=Dhx29 PE=1 SV=1	154 kDa	8	0	
Poly(U)-binding-splicing factor PUF60 OS=Mus musculus GN=Puf60 PE=1 SV=2	60 kDa	8	0	
Coronin-2A OS=Mus musculus GN=Coro2a PE=2 SV=1	60 kDa	8	0	
Ig kappa chain V-II region 26-10 OS=Mus musculus PE=1 SV=1	12 kDa	7	4	
60S ribosomal protein L26 OS=Mus musculus GN=Rpl26 PE=1 SV=1	17 kDa	7	0	
Kinesin-like protein KIF2A OS=Mus musculus GN=Kif2a PE=1 SV=2	80 kDa	7	0	
60S ribosomal protein L10a OS=Mus musculus GN=Rpl10a PE=1 SV=3	25 kDa	7	0	
40S ribosomal protein S10 OS=Mus musculus GN=Rps10 PE=1 SV=1	19 kDa	7	0	
Nucleolar GTP-binding protein 1 OS=Mus musculus GN=Gtbp4 PE=1 SV=3	74 kDa	7	0	
CCR4-NOT transcription complex subunit 1 OS=Mus musculus GN=Cnot1 PE=1 SV=2	267 kDa	7	0	
40S ribosomal protein S15a OS=Mus musculus GN=Rps15a PE=1 SV=2	15 kDa	7	0	
40S ribosomal protein S19 OS=Mus musculus GN=Rps19 PE=1 SV=3	16 kDa	7	0	Yes
ELAV-like protein 1 OS=Mus musculus GN=Elavl1 PE=1 SV=2	36 kDa	7	0	Yes
40S ribosomal protein S27 OS=Mus musculus GN=Rps27 PE=1 SV=3	9 kDa	7	0	
E3 ubiquitin-protein ligase TRIM21 OS=Mus musculus GN=Trim21 PE=1 SV=1	54 kDa	7	0	
Eukaryotic translation initiation factor 4B OS=Mus musculus GN=Eif4b PE=1 SV=1	69 kDa	7	0	
E3 SUMO-protein ligase RanBP2 OS=Mus musculus GN=Ranbp2 PE=1 SV=2	341 kDa	7	0	
Protein FRG1 OS=Mus musculus GN=Frg1 PE=1 SV=2	29 kDa	7	0	
40S ribosomal protein S23 OS=Mus musculus GN=Rps23 PE=1 SV=3	16 kDa	7	0	
DnaJ homolog subfamily A member 1 OS=Mus musculus GN=Dnaja1 PE=1 SV=1	45 kDa	7	0	
E3 ubiquitin/ISG15 ligase TRIM25 OS=Mus musculus GN=Trim25 PE=1 SV=2	72 kDa	7	0	
Poly(rC)-binding protein 1 OS=Mus musculus GN=Pcbp1 PE=1 SV=1	37 kDa	7	0	
Protein RCC2 OS=Mus musculus GN=Rcc2 PE=1 SV=1	56 kDa	6	0	
Rho guanine nucleotide exchange factor 2 OS=Mus musculus GN=Arhgef2 PE=1 SV=4	112 kDa	6	0	

Identified Proteins (397)	Molecular Weight	Spectral Count		Stress Granule ?
		W T	W T+	
Cell growth-regulating nucleolar protein OS=Mus musculus GN=Lyar PE=1 SV=2	44 kDa	6	0	
40S ribosomal protein S14 OS=Mus musculus GN=Rps14 PE=1 SV=3	16 kDa	6	0	
Elongation factor 2 OS=Mus musculus GN=Eef2 PE=1 SV=2	95 kDa	6	0	
60S ribosomal protein L34 OS=Mus musculus GN=Rpl34 PE=1 SV=2	13 kDa	6	0	
60S ribosomal protein L30 OS=Mus musculus GN=Rpl30 PE=1 SV=2	13 kDa	6	0	
Histidine ammonia-lyase OS=Mus musculus GN=Hal PE=1 SV=1	72 kDa	6	0	
RRP15-like protein OS=Mus musculus GN=Rrp15 PE=1 SV=2	31 kDa	6	0	
ATP-dependent RNA helicase DHX36 OS=Mus musculus GN=Dhx36 PE=1 SV=2	114 kDa	6	0	Yes
60S ribosomal protein L37a OS=Mus musculus GN=Rpl37a PE=1 SV=2	10 kDa	6	0	
YTH domain-containing family protein 2 OS=Mus musculus GN=Ythdf2 PE=1 SV=1	62 kDa	6	0	Yes
U4/U6 small nuclear ribonucleoprotein Prp31 OS=Mus musculus GN=Prpf31 PE=1 SV=3	55 kDa	6	0	
Homeobox protein Rhox5 OS=Mus musculus GN=Rhox5 PE=2 SV=1	23 kDa	6	0	
RNA cytidine acetyltransferase OS=Mus musculus GN=Nat10 PE=1 SV=1	115 kDa	6	0	
Splicing factor U2AF 35 kDa subunit OS=Mus musculus GN=U2af1 PE=1 SV=4	28 kDa	6	0	
Eukaryotic translation initiation factor 2 subunit 1 OS=Mus musculus GN=Eif2s1 PE=1 SV=3	36 kDa	6	0	Yes
Glutamate-rich WD repeat-containing protein 1 OS=Mus musculus GN=Grwd1 PE=1 SV=2	49 kDa	6	0	
14-3-3 protein sigma OS=Mus musculus GN=Sfn PE=1 SV=2	28 kDa	6	0	
RNA-binding protein 39 OS=Mus musculus GN=Rbm39 PE=1 SV=2	59 kDa	6	0	
Protein arginine N-methyltransferase 5 OS=Mus musculus GN=Prmt5 PE=1 SV=3	73 kDa	6	0	
Small proline-rich protein 2D OS=Mus musculus GN=Sprr2d PE=2 SV=1	9 kDa	5	6	
SRSF protein kinase 1 OS=Mus musculus GN=Srpk1 PE=1 SV=2	73 kDa	5	0	
rRNA 2'-O-methyltransferase fibrillarin OS=Mus musculus GN=Fbl PE=1 SV=2	34 kDa	5	0	
CLIP-associating protein 1 OS=Mus musculus GN=Clasp1 PE=1 SV=2	169 kDa	5	0	
Serine/threonine-protein kinase MARK2 OS=Mus musculus GN=Mark2 PE=1 SV=3	86 kDa	5	0	

Identified Proteins (397)	Molecular Weight	Spectral Count		Stress Granule ?
		W T	W T+	
Guanine nucleotide-binding protein-like 3 OS=Mus musculus GN=Gnl3 PE=1 SV=2	61 kDa	5	0	
Stress-70 protein, mitochondrial OS=Mus musculus GN=Hspa9 PE=1 SV=3	73 kDa	5	0	Yes
40S ribosomal protein S18 OS=Mus musculus GN=Rps18 PE=1 SV=3	18 kDa	5	0	Yes
Cell division cycle 5-like protein OS=Mus musculus GN=Cdc5l PE=1 SV=2	92 kDa	5	0	Yes
Sphingosine-1-phosphate lyase 1 OS=Mus musculus GN=Sgpl1 PE=1 SV=1	64 kDa	5	0	
Zinc finger RNA-binding protein OS=Mus musculus GN=Zfr PE=1 SV=2	117 kDa	5	0	
60S ribosomal protein L18 OS=Mus musculus GN=Rpl18 PE=1 SV=3	22 kDa	5	0	
14-3-3 protein zeta/delta OS=Mus musculus GN=Ywhaz PE=1 SV=1	28 kDa	5	0	
RNA-binding protein 27 OS=Mus musculus GN=Rbm27 PE=1 SV=3	119 kDa	5	0	
Protein FAM98A OS=Mus musculus GN=Fam98a PE=1 SV=1	55 kDa	5	0	
60S ribosomal protein L38 OS=Mus musculus GN=Rpl38 PE=1 SV=3	8 kDa	5	0	
40S ribosomal protein S12 OS=Mus musculus GN=Rps12 PE=1 SV=2	15 kDa	5	0	
Calmodulin OS=Mus musculus GN=Calm1 PE=1 SV=2	17 kDa	5	0	
60S acidic ribosomal protein P1 OS=Mus musculus GN=Rplp1 PE=1 SV=1	11 kDa	5	0	
Pre-mRNA 3'-end-processing factor FIP1 OS=Mus musculus GN=Fip1l1 PE=1 SV=1	65 kDa	5	0	
Pinin OS=Mus musculus GN=Pnn PE=1 SV=4	82 kDa	5	0	
Ribosomal RNA processing protein 1 homolog B OS=Mus musculus GN=Rrp1b PE=1 SV=2	81 kDa	5	0	
Protein argonaute-2 OS=Mus musculus GN=Ago2 PE=1 SV=3	97 kDa	5	0	Yes
Kinesin-like protein KIF20B OS=Mus musculus GN=Kif20b PE=1 SV=3	204 kDa	5	0	
Coronin-1B OS=Mus musculus GN=Coro1b PE=1 SV=1	54 kDa	5	0	
Heterogeneous nuclear ribonucleoprotein A0 OS=Mus musculus GN=Hnrnpa0 PE=1 SV=1	31 kDa	5	0	Yes
RNA-binding protein with serine-rich domain 1 OS=Mus musculus GN=Rnps1 PE=1 SV=1	34 kDa	5	0	
Hemoglobin subunit alpha OS=Mus musculus GN=Hba PE=1 SV=2	15 kDa	4	4	
DNA topoisomerase 2-alpha OS=Mus musculus GN=Top2a PE=1 SV=2	173 kDa	4	0	
Pyruvate kinase PKM OS=Mus musculus GN=Pkm PE=1 SV=4	58 kDa	4	2	
60S ribosomal protein L36a OS=Mus musculus GN=Rpl36a PE=1 SV=2	12 kDa	4	0	

Identified Proteins (397)	Molecular Weight	Spectral Count		Stress Granule ?
		W T	W T+	
U4/U6.U5 tri-snRNP-associated protein 1 OS=Mus musculus GN=Sart1 PE=1 SV=1	91 kDa	4	0	
ATP-dependent RNA helicase DDX50 OS=Mus musculus GN=Ddx50 PE=2 SV=1	82 kDa	4	0	
Myosin-10 OS=Mus musculus GN=Myh10 PE=1 SV=2	229 kDa	4	0	
60S ribosomal protein L22 OS=Mus musculus GN=Rpl22 PE=1 SV=2	15 kDa	4	0	
NF-kappa-B-repressing factor OS=Mus musculus GN=Nkrf PE=2 SV=3	78 kDa	4	0	
Serine/arginine-rich splicing factor 5 OS=Mus musculus GN=Srsf5 PE=1 SV=2	31 kDa	4	0	
Vasohibin-1 OS=Mus musculus GN=Vash1 PE=2 SV=4	42 kDa	4	0	
Pumilio homolog 2 OS=Mus musculus GN=Pum2 PE=1 SV=2	114 kDa	4	0	
Tropomyosin alpha-3 chain OS=Mus musculus GN=Tpm3 PE=1 SV=3	33 kDa	4	0	
Protein Red OS=Mus musculus GN=Ik PE=1 SV=2	66 kDa	4	0	
Pre-mRNA-splicing factor SYF1 OS=Mus musculus GN=Xab2 PE=1 SV=1	100 kDa	4	0	
Proteasome subunit alpha type-4 OS=Mus musculus GN=Psm4 PE=1 SV=1	29 kDa	4	0	
Splicing factor 3A subunit 1 OS=Mus musculus GN=Sf3a1 PE=1 SV=1	89 kDa	4	0	
RNA-binding protein FUS OS=Mus musculus GN=Fus PE=1 SV=1	53 kDa	4	0	
Serine/threonine-protein phosphatase PGAM5, mitochondrial OS=Mus musculus GN=Pgam5 PE=1 SV=1	32 kDa	4	0	
U5 small nuclear ribonucleoprotein 40 kDa protein OS=Mus musculus GN=Snrnp40 PE=1 SV=1	39 kDa	4	0	
RuvB-like 1 OS=Mus musculus GN=Ruvbl1 PE=1 SV=1	50 kDa	4	0	
40S ribosomal protein S21 OS=Mus musculus GN=Rps21 PE=1 SV=1	9 kDa	4	0	
Putative helicase MOV-10 OS=Mus musculus GN=Mov10 PE=1 SV=2	114 kDa	4	0	Yes
Twinfilin-1 OS=Mus musculus GN=Twf1 PE=1 SV=2	40 kDa	4	0	
OTU domain-containing protein 4 OS=Mus musculus GN=Otud4 PE=1 SV=1	123 kDa	4	0	
SRSF protein kinase 2 OS=Mus musculus GN=Srpk2 PE=1 SV=2	77 kDa	4	0	
Tripartite motif-containing protein 35 OS=Mus musculus GN=Trim35 PE=1 SV=2	57 kDa	4	0	
Eukaryotic translation initiation factor 4 gamma 3 OS=Mus musculus GN=EIF4G3 PE=1 SV=2	175 kDa	4	0	
Pre-mRNA-splicing factor SLU7 OS=Mus musculus GN=Slu7 PE=1 SV=1	68 kDa	4	0	
Neurabin-2 OS=Mus musculus GN=Ppp1r9b PE=1 SV=1	90 kDa	4	0	

Identified Proteins (397)	Molecular Weight	Spectral Count		Stress Granule ?
		W T	W T+	
Rho GTPase-activating protein 21 OS=Mus musculus GN=Arhgap21 PE=1 SV=1	216 kDa	4	0	
Histone H2B type 1-F/J/L OS=Mus musculus GN=Hist1h2bf PE=1 SV=2	14 kDa	3	0	
Nesprin-2 OS=Mus musculus GN=Syne2 PE=1 SV=2	783 kDa	3	0	
Heterogeneous nuclear ribonucleoproteins A2/B1 OS=Mus musculus GN=Hnrnpa2b1 PE=1 SV=2	37 kDa	3	0	
FERM domain-containing protein 4A OS=Mus musculus GN=Frmd4a PE=1 SV=2	114 kDa	3	0	
Heterogeneous nuclear ribonucleoprotein A1 OS=Mus musculus GN=Hnrnpa1 PE=1 SV=2	34 kDa	3	0	Yes
Spermatogenesis-associated protein 5 OS=Mus musculus GN=Spata5 PE=1 SV=2	97 kDa	3	0	
Kinesin-like protein KIF23 OS=Mus musculus GN=Kif23 PE=1 SV=1	109 kDa	3	0	
Triosephosphate isomerase OS=Mus musculus GN=Tpi1 PE=1 SV=4	32 kDa	3	0	
Eukaryotic translation initiation factor 2 subunit 2 OS=Mus musculus GN=Eif2s2 PE=1 SV=1	38 kDa	3	0	
mRNA turnover protein 4 homolog OS=Mus musculus GN=Mrto4 PE=1 SV=1	28 kDa	3	0	
Coatomer subunit alpha OS=Mus musculus GN=Copa PE=1 SV=2	138 kDa	3	0	
3'-5' exoribonuclease 1 OS=Mus musculus GN=Eri1 PE=1 SV=2	39 kDa	3	0	
FACT complex subunit SPT16 OS=Mus musculus GN=Supt16h PE=1 SV=2	120 kDa	3	0	
Nucleolar transcription factor 1 OS=Mus musculus GN=Ubtf PE=1 SV=1	90 kDa	3	0	
Elongation factor 1-gamma OS=Mus musculus GN=Eef1g PE=1 SV=3	50 kDa	3	0	
40S ribosomal protein S5 OS=Mus musculus GN=Rps5 PE=1 SV=3	23 kDa	3	0	
KH domain-containing, RNA-binding, signal transduction-associated protein 1 OS=Mus musculus GN=Khdrbs1 PE=1 SV=2	48 kDa	3	0	
Eukaryotic translation initiation factor 3 subunit J-A OS=Mus musculus GN=Eif3j1 PE=2 SV=1	29 kDa	3	0	
60S ribosomal protein L31 OS=Mus musculus GN=Rpl31 PE=1 SV=1	14 kDa	3	0	
Elongation factor 1-delta OS=Mus musculus GN=Eef1d PE=1 SV=3	31 kDa	3	0	
Double-stranded RNA-binding protein Staufen homolog 2 OS=Mus musculus GN=Stau2 PE=1 SV=1	63 kDa	3	0	
Serine/arginine repetitive matrix protein 1 OS=Mus musculus GN=Srrm1 PE=1 SV=2	107 kDa	3	0	

Identified Proteins (397)	Molecular Weight	Spectral Count		Stress Granule ?
		W T	W T+	
Protein regulator of cytokinesis 1 OS=Mus musculus GN=Prc1 PE=1 SV=2	70 kDa	3	0	
SAFB-like transcription modulator OS=Mus musculus GN=Sltn PE=1 SV=1	117 kDa	3	0	
Catalase OS=Mus musculus GN=Cat PE=1 SV=4	60 kDa	3	2	
40S ribosomal protein S24 OS=Mus musculus GN=Rps24 PE=1 SV=1	15 kDa	3	0	
Serine/threonine-protein kinase RIO1 OS=Mus musculus GN=Riok1 PE=1 SV=2	65 kDa	3	0	
Cleavage and polyadenylation specificity factor subunit 1 OS=Mus musculus GN=Cpsf1 PE=1 SV=1	161 kDa	3	0	
60S ribosomal protein L19 OS=Mus musculus GN=Rpl19 PE=1 SV=1	23 kDa	3	0	
Zinc finger CCHC domain-containing protein 9 OS=Mus musculus GN=Zcchc9 PE=2 SV=2	30 kDa	3	0	
RNA-binding protein 10 OS=Mus musculus GN=Rbm10 PE=1 SV=1	103 kDa	3	0	
Eukaryotic translation initiation factor 3 subunit M OS=Mus musculus GN=Eif3m PE=1 SV=1	43 kDa	3	0	Yes
Heterogeneous nuclear ribonucleoprotein A/B OS=Mus musculus GN=Hnrnpab PE=1 SV=1	31 kDa	3	0	
Polyadenylate-binding protein 2 OS=Mus musculus GN=Pabpn1 PE=1 SV=3	32 kDa	3	0	
pre-mRNA 3' end processing protein WDR33 OS=Mus musculus GN=Wdr33 PE=1 SV=1	145 kDa	3	0	
Eukaryotic translation initiation factor 4E OS=Mus musculus GN=Eif4e PE=1 SV=1	25 kDa	3	0	Yes
Protein phosphatase Slingshot homolog 2 OS=Mus musculus GN=Ssh2 PE=1 SV=2	158 kDa	3	0	
Ribosome-binding protein 1 OS=Mus musculus GN=Rrbp1 PE=1 SV=2	173 kDa	2	0	
Bifunctional glutamate/proline--tRNA ligase OS=Mus musculus GN=Eprs PE=1 SV=4	170 kDa	2	0	
Peroxisome oxidoreductin-1 OS=Mus musculus GN=Prdx1 PE=1 SV=1	22 kDa	2	5	
Prelamin-A/C OS=Mus musculus GN=Lmna PE=1 SV=2	74 kDa	2	0	
Hemicentin-1 OS=Mus musculus GN=Hmcn1 PE=1 SV=1	612 kDa	2	0	
AP-3 complex subunit beta-2 OS=Mus musculus GN=Ap3b2 PE=1 SV=2	119 kDa	2	0	
Probable rRNA-processing protein EBP2 OS=Mus musculus GN=Ebna1bp2 PE=2 SV=1	35 kDa	2	0	
RNA-binding protein 28 OS=Mus musculus GN=Rbm28 PE=1 SV=4	84 kDa	2	0	
RNA-binding protein 34 OS=Mus musculus GN=Rbm34 PE=1 SV=1	41 kDa	2	0	

Identified Proteins (397)	Molecular Weight	Spectral Count		Stress Granule ?
		W T	W T+	
Lupus La protein homolog OS=Mus musculus GN=Ssb PE=1 SV=1	48 kDa	2	0	
Myosin-9 OS=Mus musculus GN=Myh9 PE=1 SV=4	226 kDa	2	0	
Nuclear RNA export factor 1 OS=Mus musculus GN=Nxf1 PE=1 SV=3	70 kDa	2	0	
40S ribosomal protein S7 OS=Mus musculus GN=Rps7 PE=2 SV=1	22 kDa	2	0	
Uncharacterized protein C7orf50 homolog OS=Mus musculus PE=1 SV=3	22 kDa	2	0	
G-protein coupled receptor-associated sorting protein 1 OS=Mus musculus GN=Gprasp1 PE=1 SV=1	152 kDa	2	0	
Calmodulin-regulated spectrin-associated protein 3 OS=Mus musculus GN=Camsap3 PE=1 SV=1	135 kDa	2	0	
Ribosomal L1 domain-containing protein 1 OS=Mus musculus GN=Rsl1d1 PE=1 SV=1	50 kDa	2	0	
TAR DNA-binding protein 43 OS=Mus musculus GN=Tardbp PE=1 SV=1	45 kDa	2	0	
5'-3' exoribonuclease 2 OS=Mus musculus GN=Xrn2 PE=1 SV=1	109 kDa	2	0	
60S ribosomal protein L24 OS=Mus musculus GN=Rpl24 PE=1 SV=2	18 kDa	2	0	
Histone deacetylase complex subunit SAP18 OS=Mus musculus GN=Sap18 PE=1 SV=1	18 kDa	2	0	
Treacle protein OS=Mus musculus GN=Tcof1 PE=1 SV=1	135 kDa	2	0	
Cytochrome c oxidase subunit NDUFA4 OS=Mus musculus GN=Ndufa4 PE=1 SV=2	9 kDa	2	0	
Holliday junction recognition protein OS=Mus musculus GN=Hjrp PE=1 SV=1	74 kDa	2	0	
Elongator complex protein 1 OS=Mus musculus GN=Ikbkap PE=1 SV=2	150 kDa	2	0	
THO complex subunit 4 OS=Mus musculus GN=Alyref PE=1 SV=3	27 kDa	2	0	
Transcription factor 25 OS=Mus musculus GN=Tcf25 PE=1 SV=2	77 kDa	2	0	
Interleukin enhancer-binding factor 2 OS=Mus musculus GN=Ilf2 PE=1 SV=1	43 kDa	2	0	
A-kinase anchor protein 8 OS=Mus musculus GN=Akap8 PE=1 SV=1	76 kDa	2	0	
Proteasome subunit beta type-6 OS=Mus musculus GN=Psm6 PE=1 SV=3	25 kDa	2	0	
Pre-mRNA-splicing factor CWC22 homolog OS=Mus musculus GN=Cwc22 PE=1 SV=1	105 kDa	2	0	
Tyrosine-protein kinase JAK1 OS=Mus musculus GN=Jak1 PE=1 SV=1	133 kDa	2	0	
Protein S100-A14 OS=Mus musculus GN=S100a14 PE=1 SV=1	12 kDa	2	0	
40S ribosomal protein S15 OS=Mus musculus GN=Rps15 PE=1 SV=2	17 kDa	2	0	

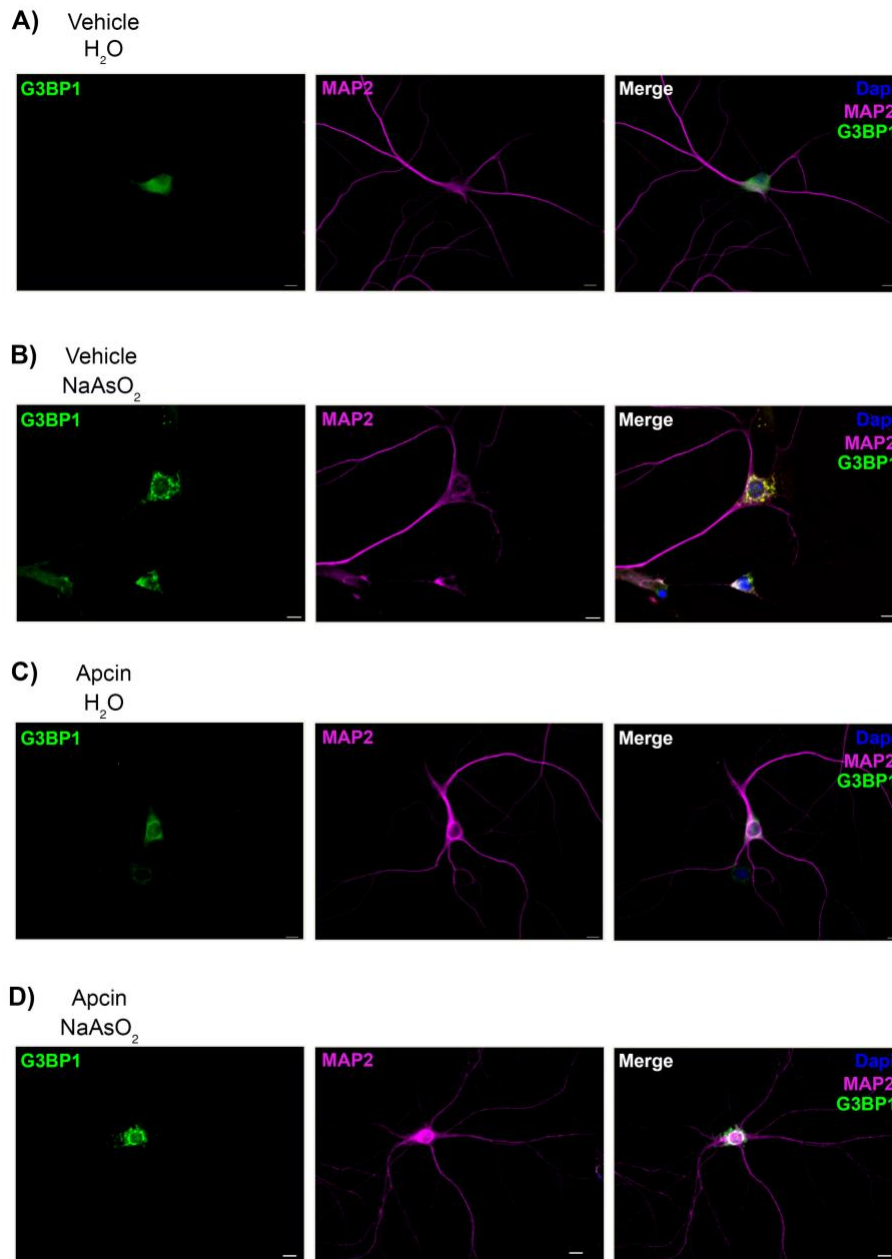
Identified Proteins (397)	Molecular Weight	Spectral Count		Stress Granule ?
		W T	W T+	
DnaJ homolog subfamily A member 3, mitochondrial OS=Mus musculus GN=Dnaja3 PE=1 SV=1	52 kDa	2	0	
Cyclin-dependent kinase 11B OS=Mus musculus GN=Cdk11b PE=1 SV=2	92 kDa	2	0	
RNA-binding protein 25 OS=Mus musculus GN=Rbm25 PE=1 SV=2	100 kDa	2	0	
Putative RNA-binding protein Luc7-like 1 OS=Mus musculus GN=Luc7l PE=1 SV=2	44 kDa	2	0	
FACT complex subunit SSRP1 OS=Mus musculus GN=Ssrp1 PE=1 SV=2	81 kDa	2	0	
Aspartate--tRNA ligase, cytoplasmic OS=Mus musculus GN=Dars PE=1 SV=2	57 kDa	2	0	
Arachidonate 12-lipoxygenase, 12R-type OS=Mus musculus GN=Alox12b PE=1 SV=1	81 kDa	2	2	
Histone deacetylase 1 OS=Mus musculus GN=Hdac1 PE=1 SV=1	55 kDa	2	0	
Ataxin-2-like protein OS=Mus musculus GN=Atxn2l PE=1 SV=1	111 kDa	2	0	
Multiple myeloma tumor-associated protein 2 homolog OS=Mus musculus GN=Mmtag2 PE=2 SV=1	29 kDa	2	0	
Protein LSM14 homolog A OS=Mus musculus GN=Lsm14a PE=1 SV=1	51 kDa	2	0	
Splicing factor U2AF 65 kDa subunit OS=Mus musculus GN=U2af2 PE=1 SV=3	54 kDa	2	0	
Hyaluronan mediated motility receptor OS=Mus musculus GN=Hmnr PE=1 SV=4	92 kDa	2	0	
DNA-directed RNA polymerase, mitochondrial OS=Mus musculus GN=Polrmt PE=1 SV=1	137 kDa	2	0	
Ataxin-2 OS=Mus musculus GN=Atxn2 PE=1 SV=1	136 kDa	2	0	
Cleavage and polyadenylation specificity factor subunit 2 OS=Mus musculus GN=Cpsf2 PE=1 SV=1	88 kDa	2	0	
Eukaryotic translation initiation factor 3 subunit K OS=Mus musculus GN=Eif3k PE=1 SV=1	25 kDa	2	0	Yes
Prohibitin-2 OS=Mus musculus GN=Phb2 PE=1 SV=1	33 kDa	2	0	
Nuclear cap-binding protein subunit 3 OS=Mus musculus GN=Ncbp3 PE=1 SV=1	70 kDa	2	0	
WD repeat-containing protein 5 OS=Mus musculus GN=Wdr5 PE=1 SV=1	37 kDa	2	0	
Importin subunit alpha-1 OS=Mus musculus GN=Kpna2 PE=1 SV=2	58 kDa	2	0	Yes
Apoptotic chromatin condensation inducer in the nucleus OS=Mus musculus GN=Acin1 PE=1 SV=3	151 kDa	2	0	
Ran GTPase-activating protein 1 OS=Mus musculus GN=Rangap1 PE=1 SV=2	64 kDa	2	0	

Identified Proteins (397)	Molecular Weight	Spectral Count		Stress Granule ?
		W T	W T+	
Luc7-like protein 3 OS=Mus musculus GN=Luc713 PE=1 SV=1	51 kDa	2	0	
40S ribosomal protein S28 OS=Mus musculus GN=Rps28 PE=1 SV=1	8 kDa	2	0	
DnaJ homolog subfamily B member 11 OS=Mus musculus GN=Dnajb11 PE=1 SV=1	41 kDa	2	0	
Cleavage and polyadenylation specificity factor subunit 7 OS=Mus musculus GN=Cpsf7 PE=1 SV=2	52 kDa	2	0	
Ribosome biogenesis protein NSA2 homolog OS=Mus musculus GN=Nsa2 PE=2 SV=1	30 kDa	2	0	
Splicing factor 3A subunit 3 OS=Mus musculus GN=Sf3a3 PE=1 SV=2	59 kDa	2	0	
Protein mago nashi homolog OS=Mus musculus GN=Magoh PE=2 SV=1	17 kDa	2	0	
Gamma-adducin OS=Mus musculus GN=Add3 PE=1 SV=2	79 kDa	2	0	

Table 5-2: FMRP interactome

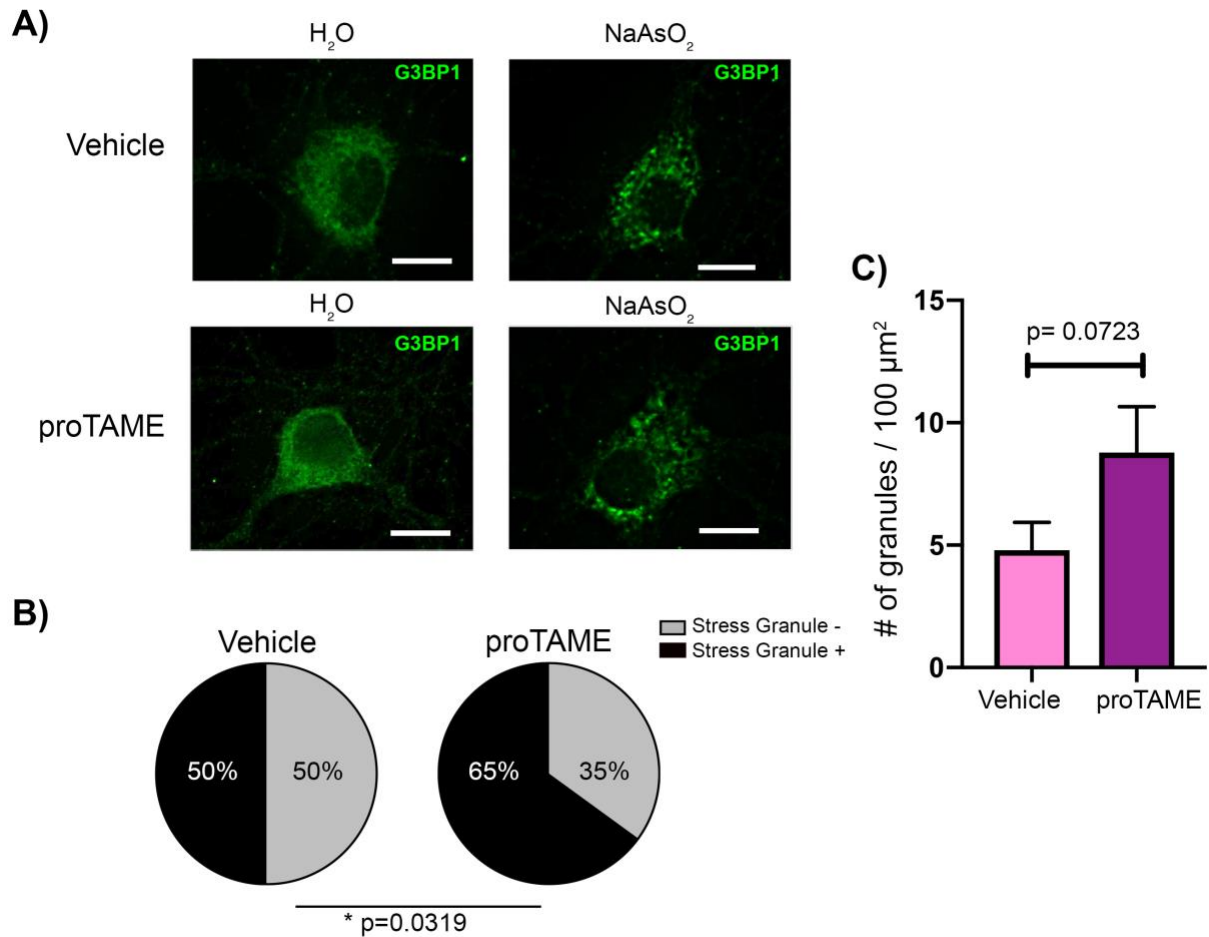
Table of proteins identified in the FMRP interactome following immunoaffinity chromatography and mass spectrometry analysis of FLAG-FMRP transfected cells. Proteins are listed from highest enrichment in the samples to lowest enrichment. + indicates lysates that were co-incubated with FLAG peptide to control for nonspecific binding. Proteins that are known stress granule proteins based on Jain et al. (2016) and Markmiller et al. (2018) are indicated.

5.6. Supplemental Figures



Supplemental Figure 5-1: Neuronal morphology during Sodium Arsenite treatment

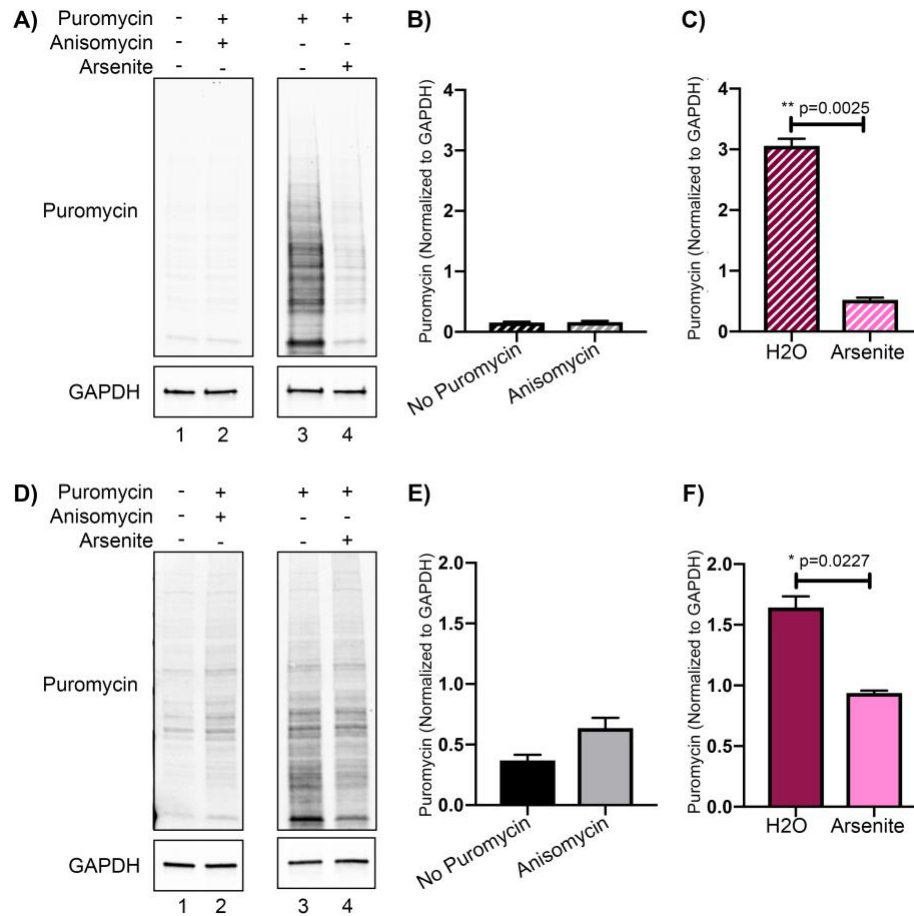
Additional images representing neurons in Figure 5-2. DIV 15 cortical neurons were treated overnight with DMSO (A & B) or 2 μ M Apcin (C & D). Neurons were then treated with water (A & C) or sodium arsenite (B & D) for 45 minutes. Cells were fixed in 4% paraformaldehyde and then immunostained for G3BP, MAP2, and DAPI. Scale bar = 10 μ m



Supplemental Figure 5-2: proTAME treatment increases stress granule formation

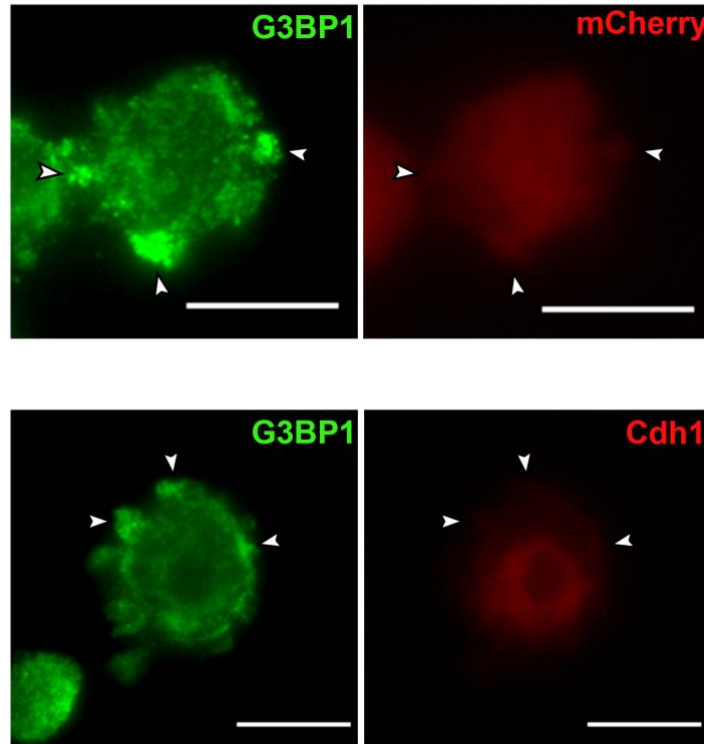
A) DIV 14 cortical neurons were treated with vehicle (DMSO) or proTAME for 3 hours 15 minutes. Neurons were then treated with sodium arsenite (NaAsO₂) (0.5mM) or water for 45 minutes hour prior to fixation. Immunofluorescence was done with antibodies against G3BP. Scale bar indicates 10μM. **B)** User-blind scoring of neurons that were stress granule positive or stress granule negative following arsenite treatment. N=60 neurons for both conditions **C)** Number of granules within the soma.

B) Statistical significance was calculated by Z test. *p<0.05. **C)** Statistical significance calculated by Student's t-test.



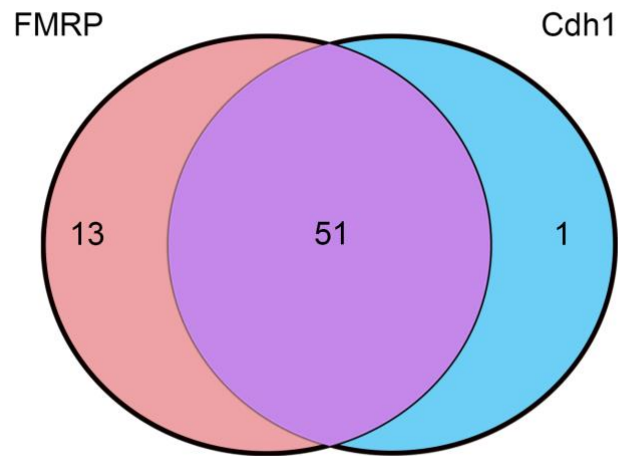
Supplemental Figure 5-3: Stress granule formation decreases protein synthesis

A) N2A cells underwent puromycylation following 45 minutes of treatment with sodium arsenite or water. Anisomycin (40 μ M) and no puromycin were utilized as negative controls. Lysates were immunoblotted for puromycin and GAPDH. **B) & C)** Quantification of puromycin normalized to GAPDH from A). n=3. **D)** DIV 14 cortical neurons cells underwent puromycylation following 45 minutes of treatment with sodium arsenite or water. Anisomycin (40 μ M) and no puromycin were utilized as negative controls. Lysates were immunoblotted for puromycin and GAPDH. **E) & F)** Quantification of puromycin normalized to GAPDH from A). n=3. Statistical significance calculated by Student's t test. *p<0.05



Supplemental Figure 5-4: Cdh1 does not colocalize with stress granules

Neuro2A cells were transfected with mCherry or mCherry-Cdh1. Cells were treated with sodium arsenite for 45 minutes to induce stress granules and then fixed in 4% paraformaldehyde and then immunostained for G3BP. Arrows indicate stress granule accumulation. Scale bar = 10 μ m.



Supplemental Figure 5-5: Overlap between Cdh1 and FMRP interactome

N2A cells were transfected with FLAG-FMRP and underwent FLAG immunoprecipitation followed by mass spectrometry to generate an FMRP interactome (**Table 5-2**). The FMRP interactome was compared to previously published lists of stress granule proteins (Jain et al., 2016; Markmiller et al., 2018) and then to stress granule proteins in the Cdh1 interactome (**Table 5-1**).

Chapter 6 :

General Discussion

6.1. Summary

The overall objective of this thesis research was to further investigate and provide new insight into the mechanism and regulation of neuronal protein synthesis. We tested the hypothesis that Cdh1-APC associates with translational machinery and regulates protein synthesis and stress granule dynamics through FMRP-dependent interactions. We have demonstrated that Cdh1-APC is responsible for FMRP ubiquitination downstream of mGluR5 signaling as well as reversing FMRP-mediated repression of protein synthesis. We uncover a novel function of Cdh1-APC to regulate protein synthesis. Perturbation of Cdh1-APC alone was sufficient to affect basal protein synthesis in postmitotic neurons. We then utilized qualitative proteomics to uncover that the Cdh1-interactome is highly enriched in translational regulatory proteins and identified a new function for Cdh1-APC to regulate stress granule assembly via its interaction with FMRP, further emphasizing Cdh1-APC's novel role as a translational regulator. Taken together, our data reveal a new dual role of Cdh1-APC (**Figure 6-3**) as a regulator of both protein degradation and protein synthesis.

6.2. Cdh1-APC activity across the lifespan

The use of varying time points in different rodent models of Cdh1-knockdown highlight that Cdh1 is critical at different stages in the lifespan. Interestingly, changes in cortical weight and size following Cdh1 knockout are dependent upon when in the lifespan Cdh1 is knocked down. When Cdh1 is depleted in all cells of the embryo except the placenta, a significant decrease in the brain cortex weight and size can be detected as early as embryonic day 14.5 (Delgado-Esteban et al., 2013). However, when Cdh1 is depleted in glutamatergic cells starting at the third postnatal week (~postnatal day 25), differences in cortical weight and size are not apparent until postnatal

day 120 (Bobo-Jimenez et al., 2017). The dependence of cortical weight/size phenotypes on age of Cdh1 knockdown indicates that Cdh1 may have differing roles in the developing brain versus the adult brain. It is critical to put our findings in the context of neurodevelopment and neurodegeneration to better understand the implications of our work on neuronal function and across the lifespan.

6.2.1. Cdh1-APC and neurodevelopment

Cdh1-APC has been previously shown to regulate processes critical for neurodevelopment, such as the differentiation of neural progenitor cells (Cuende et al., 2008; Delgado-Esteban et al., 2013) and learning and memory (Huang et al., 2015; Pick et al., 2012; Pick et al., 2013). Furthermore, the ubiquitination and regulation of FMRP, a protein critical for neurodevelopment (Penagarikano et al., 2007), by Cdh1-APC (Chapter 3)(Huang et al., 2015) further implicates a role for Cdh1-APC in proper neurodevelopment.

A new study identified a novel missense mutation in *Fzr1*, the gene encoding Cdh1, that was associated with microcephaly, psychomotor retardation, and epilepsy in a 4-year old patient (Rodriguez et al., 2019). Discovery of this mutation in Cdh1 as causative of neurodevelopmental pathology further supports a role of Cdh1-APC in neurodevelopment. While investigating the molecular phenotypes of this mutation, it was found that the mutated form of Cdh1 was unable to regulate the exit of cell cycle in neural progenitor cells and was sequestered to the nucleus. While this evidence is helpful to directly link Cdh1-APC to proper neurodevelopment, it is unclear whether or not mutated form of Cdh1 was impaired in the regulation of processes in mature neurons that were investigated by previous work, such as LTP and LTD, or processes investigated in this dissertation, such as protein synthesis. The work presented in this dissertation further offers

protein synthesis as another potential mechanism by which Cdh1-APC regulates neurodevelopment.

Aberrant protein synthesis has been implied as a pathogenic mechanism in several neurodevelopmental disorders, including fragile X syndrome (Richter et al., 2015), autism spectrum disorder (Huber et al., 2015), and schizophrenia (English et al., 2015; Gururajan and van den Buuse, 2014). Thus, the ability of Cdh1-APC to regulate protein synthesis in neural cells as observed in this dissertation is relevant to the study of multiple neurodevelopmental disorders. With the underlying shared neurobiology amongst these neurodevelopmental disorders, Cdh1-APC may be a critical protein whose function is dysregulated in these disorders.

6.2.2. Cdh1-APC and neurodegeneration

In contrast to previous work that has implicated Cdh1-APC in proper neurodevelopment, one previous study linked Cdh1-APC to mechanisms underlying Alzheimer's disease, a form of neurodegeneration associated with advanced age (Bobo-Jimenez et al., 2017). The serine-threonine Rho protein kinase 2 (Rock2) disrupts microtubule stability and has been shown to accumulate in brains of patients with Alzheimer's disease and contribute to the accumulation of amyloid- β (Herskowitz et al., 2013). Bobo-Jimenez et al. found that Rock2 is a target substrate of Cdh1-APC; cortical and hippocampal neurons from Cdh1-knockout (Cdh1-KO) mice had increased Rock2 activity. As a result of the increased Rock2 activity, Cdh1-KO mice had decreased dendritic spine density, memory loss, and neurodegeneration. Thus, there is evidence that in addition to the role that Cdh1-APC plays in neurodevelopment, Cdh1-APC is necessary to regulate molecular pathways that underlie pathologic mechanisms of neurodegeneration.

Our discovery of stress granule assembly regulation by Cdh1-APC has implications for pathologic mechanisms in neurodegenerative disorders. Pervasive stress granule formation is an observed phenotype for some neurodegenerative diseases, such as amyotrophic lateral sclerosis (ALS) (Li et al., 2013; Monahan et al., 2016). Cdh1-APC activity may possibly be a mechanism of action that is perturbed in neurodegenerative diseases, thereby leading to an increase in stress granule formation. Alternatively, it is possible that Cdh1-APC activity may not be dysregulated in neurodegenerative disease, but instead could be a target of pharmacologic intervention; increasing the activity of Cdh1-APC may help to prevent the formation of pathologic stress granules. Our findings that Cdh1-APC regulates stress granule assembly help to better understand the complex dynamics governing stress granule homeostasis and may contribute as a novel therapeutic target for neurodegenerative research.

6.2.3. Relationship between neurodevelopment and neurodegeneration

Our observations of regulation of FMRP ubiquitination (Chapter 3) and protein synthesis (Chapter 4) by Cdh1-APC offer evidence of a role for Cdh1-APC in neurodevelopment whereas the regulation of stress granule assembly (Chapter 5) by Cdh1-APC suggests a role in neurodegeneration. Thus, it can be interpreted that proper functioning of Cdh1-APC in neurons is critical across the lifespan. However, based on previous literature it is unclear if the critical pathways regulated by Cdh1-APC in neurodevelopment are the same as those affected in neurodegeneration.

Dendritic and axonal findings in previous studies support a differential role of Cdh1-APC in neurodevelopment versus neurodegeneration. Whereas Cdh1-APC appears to regulate axonal growth that is necessary for development, (Konishi et al., 2004), its effects on dendritic complexity

has greater implications for adult brain size (Bobo-Jimenez et al., 2017). Thus, it is possible that Cdh1-APC regulation of processes in the presynaptic compartment is critical for neurodevelopment whereas its role in the postsynaptic compartment is implicated in neurodegeneration.

Our research suggests the relationship between stress granule dynamics and protein synthesis as a potential mechanism that is applicable to both neurodevelopment and neurodegeneration. Stress granule formation is mechanism by which protein synthesis can be regulated; thus, it is possible that the aberrant protein synthesis in neurodevelopmental disorder may be due to altered stress granule dynamics. Conversely, pervasive stress granule formation in neurodegenerative diseases may result in altered protein synthesis. Evidence of fragile X granules (Christie et al., 2009) and the decrease of stress granule formation in FMRP-null cells (Didiot et al., 2009) further supports a connection between stress granule formation and protein synthesis that may be a shared mechanism between neurodevelopment and neurodegeneration. Our results provide support for a novel role of Cdh1-APC in regulating stress granule dynamics and protein synthesis in neural cells that is critical across the lifespan. One model to further investigate is that neurodevelopmental disorders like FXS may involve hypoassembly of stress granules due in part to loss of FMRP-dependent regulation by Cdh1-APC, whereas certain neurodegenerative diseases such as ALS involve hyperassembly of stress granules due to loss of other related ubiquitin-modifying enzymes (**Figure 6-1**).

6.3. Insight into mRNP granules

Our study utilizes stress granules induced by sodium arsenite treatment as a model mRNP granule. As there are many other forms of mRNP granules such as processing bodies and RNA

transport granules, our work may have implications for these other diverse RNA granules. The Cdh1 interactome includes proteins that are involved in RNA transport granules in addition to stress granules, such as FMRP (Antar et al., 2004; DICTENBERG et al., 2008) and Caprin (Nakayama et al., 2017; Shiina et al., 2010). With an underlying shared biology amongst RNA transport granules and stress granules, Cdh1-APC may also regulate assembly or disassembly of mRNA transport granules and their translational control at synapses.

Axonal G3BP1 has been shown to incorporate into granules that limit axonal mRNA translation and axon growth (Sahoo et al., 2018). Disruption of these G3BP1-positive mRNP granules appears to be critical for nerve generation *in vivo*. As Cdh1-APC has been shown to similarly limit axonal growth (Konishi et al., 2004) and we demonstrate that Cdh1-APC inhibits the formation of G3BP1-positive granules (Chapter 5), Cdh1-APC may be involved in the disruption of axonal mRNPs necessary for proper nerve regeneration.

6.4. Targeting of E3 ligases as potential therapeutic options

Our studies have identified a new function for Cdh1-APC as an E3 ubiquitin ligase that can regulate stress granule dynamics and protein synthesis in neural cells via its interaction with FMRP. Elucidation of the targets of an E3 ubiquitin ligase as well as the downstream effects of these interactions can be critical to developing potential novel therapeutic targets for pathological conditions. Recently, there has been much interest in exploiting the specificity of the ubiquitin proteasome system for protein degradation. Even with recent pharmacological advances, only approximately 13% of disease-causing genes are targetable with current therapies (Neklesa et al., 2017). Thus, there has been a drive to find new ways of targeting the “undruggable” proteome. To approach a new way of targeting pathologic proteins, a group designed a PROteolysis-TArgeting

Chimera (PROTAC) to target the ubiquitination of methionine aminopeptidase-2 (MetAP-2), a cancer associated drug, by the E3 ubiquitin ligase Skip1-Cullin-F box complex containing Hrt1 (SCF) (Sakamoto et al., 2001). PROTACs are made up of a target-binding ligand, and E3 ligase ligand, and a linker; the design of PROTACs brings the target protein into close proximity with the E3 ubiquitin ligase and promotes its ubiquitination. Aside from promoting the degradation of previously un-targetable proteins, PROTACs have high cellular potency, highly selective degradation, applicability to *in vitro* and *in vivo* systems, and extended pharmacodynamic duration of action (Churcher, 2018).

While PROTAC technology has been primarily implemented towards therapies for cancer (Lai and Crews, 2017; Ottis and Crews, 2017), some studies have focused on the degradation of proteins that are implicated in neurological diseases. For example, one group has utilized PROTAC to induce the degradation of Tau, a pathologic protein in Alzheimer's disease (Chu et al., 2016). The synthesized PROTAC was able to decrease protein expression of Tau in both primary neuronal cells and a mouse-model of Alzheimer's disease, demonstrating the bioavailability of PROTACs in the central nervous system as well as the feasibility of PROTACs for neurological disorders. Interestingly, another group designed a PROTAC to ubiquitinate phosphatidylinositol-3-kinase (PI3K) (Hines et al., 2013), a protein implicated in fragile X syndrome. Excess PI3K synthesis and activity are thought to underlie excessive protein synthesis (Gross and Bassell, 2012; Gross et al., 2010) and cognition (Gross et al., 2015a; Gross et al., 2015b) in models of fragile X syndrome. Thus, use of PROTAC may be highly relevant to fragile X syndrome and related neurodevelopmental disorders.

Our evidence of the role of Cdh1-APC in neural cells suggests its relevance as an E3 ligase complex to utilize in the design of PROTACs as novel therapeutics for neurodevelopmental

diseases. Additionally, our work supports evidence that FMRP is a targeted interactor of Cdh1-APC, which makes it a candidate peptide to use in the development of a PROTAC that utilizes the E3 ubiquitin ligase activity of Cdh1-APC. Additional interactors of Cdh1-APC, such as those identified in Chapter 4 by mass spectrometry, may also be utilized as potential E3 ligase ligands in PROTAC design. Combining our work on the regulatory role of Cdh1-APC in neural cells and advancements in drug discovery with PROTACs may help to address the lack of FDA-approved therapies for many neurological disorders.

6.5. Future Directions

Following our discovery of the novel role of Cdh1-APC in regulation of stress granule dynamics and protein synthesis in neural cells, some questions remain as to the consequences of the interaction of Cdh1-APC with proteins as well other downstream effects Cdh1-APC may have following interaction with FMRP. This section will highlight several experiments that are critical to better understand the role of Cdh1-APC in neural cells and the mechanisms necessary for Cdh1-APC-mediated effects.

6.5.1. Consequences of Cdh1-APC interaction with FMRP and other proteins

A future direction for this work will be to better understand the consequences of Cdh1-APC interactions with stress granule proteins, translational initiation factors, and ribosomal subunits that we identified through mass spectrometry. Cdh1-APC has been characterized to lead to the degradation of its ubiquitination targets following polyubiquitination on the K11 residue of ubiquitin (Budhavarapu et al., 2012). Therefore, Cdh1-APC may be targeting these translational regulatory proteins for degradation via K11-linked polyubiquitination. However, ubiquitination

can lead to fates other than degradation. For example, K63-linked polyubiquitination can cause DNA repair (Liu et al., 2018), endocytosis (Lauwers et al., 2009), or NF- κ B activation (Deng et al., 2000). It is possible that ubiquitination by Cdh1-APC of stress granule proteins, ribosomes, and initiation factors can lead to noncanonical pathways aside from degradation.

To begin to approach whether or not ubiquitination mediated by Cdh1-APC leads to the degradation of target substrates, initial studies can be conducted with cortical neurons that are treated with or without Apcin to inhibit Cdh1-APC activity as well as with and without MG-132, the proteasome inhibitor utilized throughout our studies. Lysate from these cells can then be assessed with western blotting for proteins of interest, such as some of the stress granule proteins (Caprin, G3BP1, HuR), ribosomal proteins, and initiation factors identified by mass spectrometry in Chapter 4. Use of MG-132 with vehicle treated neurons will identify whether or not the protein of interest is degraded by the ubiquitin proteasome system. If the protein is a ubiquitination substrate targeted by the proteasome, the protein band will have higher intensity in the MG-132 treated lysate. If Cdh1-APC causes the ubiquitination of any of these proteins, it would be hypothesized that the Apcin treated neurons will have a greater enrichment of the protein compared to neurons without Apcin treatment. It is expected that there would be no difference in the Apcin-only treated neurons compared to the Apcin-MG-132 treated neurons. While these sets of experiments would be greatly useful to identify if ubiquitination by Cdh1-APC promotes the degradation of any of these proteins, it will be very low-throughput to blot for every protein of interest.

A critical goal is to know whether any of the proteins identified in our Cdh1-FLAG tagged interactome are actually ubiquitinated by Cdh1-APC. To characterize 1) which proteins Cdh1-APC ubiquitinates and 2) what linkage of poly-ubiquitination may be formed on targets of Cdh1-

APC, Tandem Ubiquitin Binding Entities (TUBE) specific for different ubiquitin linkages can be utilized. TUBEs have high specificity for binding to ubiquitin and can be tagged with biotin moieties (Hjerpe et al., 2009). Lysates from cells can be incubated with the biotin-conjugated TUBE and then undergo streptavidin pulldown and mass spectrometry. Thus, any proteins identified by mass spectrometry can be interpreted as being ubiquitinated at time of lysis. Currently, there are TUBEs specific for pan-conjugated ubiquitin, K48 linkages, K63 linkages, or linear polyubiquitin linkages. Cells can be treated with MG-132 to inhibit the proteasome and then with or without Apcin to modulate Cdh1-APC activity. Comparing the with and without Apcin conditions for each set of TUBEs followed by mass spectrometry will help to uncover which proteins Cdh1-APC ubiquitinates as well as the pattern of polyubiquitination linkages. A disadvantage of this approach is that currently there are no TUBE constructs for K11 linkages, which is the predominant polyubiquitination linkage that Cdh1-APC has been observed to regulate. Thus, except for the pan-conjugated ubiquitin TUBE condition, it may not be possible to detect the ubiquitination substrates of Cdh1-APC.

From our studies, we can only conclude that the interaction between Cdh1-APC and FMRP leads to reduction in stress granule formation; we cannot determine whether or not this effect is due to the degradation of FMRP following ubiquitination by Cdh1-APC or if the ubiquitinated form of FMRP is unable to bind to other stress granule proteins. To begin to elucidate whether or not the degradation is necessary to elicit changes in stress granule dynamics, MG-132 can be added to cells that are transfected with either FMRP WT or FMRP DBM prior to arsenite treatment. If degradation of FMRP is necessary to elicit changes in stress granule dynamics, it would be predicted that MG-132 treatment would increase the formation of stress granules in cells transfected with FMRP WT but not those transfected with FMRP DBM. If the percentages of

stress-granule positive cells are similar in FMRP WT cells treated with MG-132 compared to FMRP DBM transfected cells, this suggests that the increased stress granule phenotype in FMRP DBM cells is due to prevention of FMRP-degradation. If ubiquitination of FMRP does not lead to its degradation, it is expected that MG-132 treatment will not alter stress granule formation in either FMRP WT or FMRP DBM cells. Such a result would suggest that Cdh1-APC can modulate downstream processes through solely binding to other proteins and not necessarily ubiquitinating them. This would support our findings in **Figure 4-3**, where we were unable to identify ubiquitinated proteins in the Cdh1 interactome. Since it is thought that ubiquitination targets of Cdh1-APC are typically targeted for degradation, it would be very novel if it is observed that FMRP degradation is not responsible for the regulation of stress granule dynamics downstream of interaction with Cdh1-APC.

6.5.2. Determine if Cdh1 localization affects protein synthesis

The localization of Cdh1 is critical for its previously described roles in cell cycle and axonal growth. While neuroblastoma cells are cycling, Cdh1 is predominantly located in the cytosol. When neuroblastoma cells are treated with retinoic acid to induce cell cycle exit and differentiation, Cdh1 is reduced in the cytosol and enriched in the nucleus (Cuende et al., 2008). It is thought that in order for Cdh1 to promote the exit of cell cycle, it must be localized to the nucleus and then ubiquitinate other cell cycle regulators (Jaquenoud et al., 2002). Additionally, only nuclear-localized forms of Cdh1 can regulate axonal growth in granule neurons (Stegmuller et al., 2006). Conversely, it was demonstrated that nuclear-localized Cdh1 failed to rescue effects on mGluR-LTD in Cdh1 knockout animals; only cytoplasmic Cdh1 could reverse the electrophysiologic phenotypes (Huang et al., 2015). Interestingly, the disease-associated point-

mutation form of Cdh1 is confined to the nucleus, suggesting a deficit in cytoplasmic activity of Cdh1 (Rodriguez et al., 2019). Thus, the localization of Cdh1 is critical for its functioning and can affect downstream processes. It is important to note that in postmitotic neurons, nuclear-localized Cdh1 has presynaptic effects (Stegmuller et al., 2006) whereas cytoplasm-localized Cdh1 has postsynaptic effects (Huang et al., 2015).

Based upon the knowledge of localization-specific effects of Cdh1, it would be of interest to identify whether the protein synthesis phenotypes observed in our studies are dependent on where Cdh1 is localized. To determine this, three forms of Cdh1 plasmids would be utilized: a wildtype form expressing both a nuclear export signal and nuclear localization signal (Cdh1 WT), a form of Cdh1 only expressing a nuclear export signal (Cdh1-NES), and a form of Cdh1 only expressing a nuclear localization signal (Cdh1-NLS). These three constructs could be transfected into Neuro2A cells and/or transduced into postmitotic neurons and then undergo puromycylation. Based on previous observations of the effects of Cdh1 localization, I predict that there will be a difference in effects on protein synthesis dependent on Cdh1 localization. While it would be equally informative if either nuclear-localized Cdh1 or cytoplasmic-localized Cdh1 regulated protein synthesis, I hypothesize that protein synthesis can only be modulated by the Cdh1 WT and Cdh1-NES plasmids. The prediction of cytoplasmic Cdh1 being the primary regulator of protein synthesis is based on the previous evidence demonstrating cytoplasmic Cdh1 as necessary for mGluR-LTD (Huang et al., 2015) and lack of cytoplasmic Cdh1 being associated with intellectual disability (Rodriguez et al., 2019). As the focus of our studies on protein synthesis were based upon the regulation of mGluR-LTD by Cdh1, I would expect a similar dependency on the localization of Cdh1 to the cytoplasm. If there is no difference in protein synthesis based upon expression of Cdh1-NES or Cdh1-NLS, then this would be a novel demonstration of downstream

effects not being dependent on Cdh1 localization. Any result from the Cdh1 localization studies on protein synthesis will be informative in better understanding the role of Cdh1 in neural cells.

6.5.3 Identify if Cdh1-APC solely regulates protein synthesis via FMRP

While it is unknown if Cdh1-APC directly ubiquitinates the interacting stress granule proteins identified in this study, it has been demonstrated that Cdh1-APC ubiquitinates FMRP, a known component that regulates stress granules. Preventing Cdh1-APC interaction with FMRP leads to an increase in formation of stress granules, suggesting that FMRP is necessary for downstream effects on protein synthesis. Future experiments utilizing *Fmr1*-knockout (KO) neurons may help to elucidate whether the ability of Cdh1-APC to regulate translation via stress granules is solely FMRP-dependent. *Fmr1*-KO neurons would be treated with either Apclin or vehicle and undergo puromycylation. If FMRP is necessary for Cdh1-mediated changes in protein synthesis, we would expect no changes in protein synthesis in Apclin compared to vehicle treated neurons. If Cdh1-mediated changes in protein synthesis are FMRP-independent, then it would be expected that Apclin treatment would lead to a reduction in protein synthesis compared to vehicle treatment in *Fmr1*-KO neurons.

If the puromycylation experiments suggest that FMRP is not required for changes in protein synthesis downstream of Cdh1-APC, it may be because interactions between Cdh1-APC and other translational regulators identified by mass spectrometry in Chapter 4 may be sufficient to alter protein synthesis but not stress granule dynamics. The Cdh1-interactome contains translation-categorized proteins than are not associated with stress granules, so it is possible that these interactions are primarily responsible for changes in protein synthesis. However, since we demonstrated in **Figure 3-4** that disruption of Cdh1 interaction with FMRP was sufficient to

reduce protein synthesis, it is most likely that FMRP indeed mediates Apcin-induced changes in protein synthesis. These experiments are crucial for elucidation of the exact mechanism by which Cdh1-APC regulates protein synthesis in neural cells.

6.5.4. Elucidate if Cdh1 regulates spine density downstream of FMRP

Alterations in the density of dendritic spines are considered pathologic (Penzes et al., 2011); dysregulation of spine density is associated with several neurodevelopmental disorders, including fragile X syndrome (Hinton et al., 1991; Irwin et al., 2001) and schizophrenia (Glausier and Lewis, 2013). For development of potential therapeutic targets for neurodevelopmental disorders, it is critical to understand the proteins and pathways that regulate dendritic spine density.

As discussed in-depth in Chapter 1, the overabundance of dendritic spines in fragile X syndrome suggests that FMRP regulates spine morphology and synaptic pruning (Bagni and Greenough, 2005; Pfeiffer and Huber, 2007, 2009; Weiler and Greenough, 1999). However, it is still unclear how FMRP may be regulating these dendritic spine processes. It is possible that the interaction with and ubiquitination of FMRP by Cdh1 may be a level of regulation in dendritic spine development. Demonstration of decreased spine density upon knockdown of Cdh1 supports a role of Cdh1 in spine development (Bobo-Jimenez et al., 2017).

Based upon the overabundance of spines in FMRP-null neurons, it can be hypothesized that the degradation of FMRP downstream of ubiquitination by Cdh1-APC would lead to an increase in spine density. If the ability of Cdh1-APC to ubiquitinate FMRP was inhibited, such as in the Cdh1 knockout neurons, a decrease in spine density would then be expected. To elucidate if the interaction of Cdh1 and FMRP is indeed necessary for proper dendritic spine formation, the FMRP-DBM construct that is unable to bind Cdh1 can be utilized. Both the FMRP-WT and

FMRP-DBM constructs could be packaged into a lentivirus for neuronal transduction. Ideally, cortical neurons from *Fmr1* KO mice would be utilized to prevent any effects of endogenous FMRP. Postmitotic cortical neurons would also be transduced with mRFPruby-tagged Lifeact, a small F-actin binding peptide that allows for clear visualization of dendritic spines (Riedl et al., 2008). Spine density can then be quantified across the conditions. If Cdh1 indeed regulates dendritic spines through a FMRP-dependent mechanism, it would be expected that neurons expressing the FMRP-DBM mutant will have less spine density as compared to the FMRP-WT construct.

Another potential approach to assess whether or not the dendritic effects of Cdh1 knockdown are dependent on FMRP is to transduce cortical neurons from both wildtype and *Fmr1*-KO mice with mRFPruby-tagged Lifeact and later treat with Apcin to inhibit Cdh1-APC activity. Based upon the findings of Bobo-Jimenez et al., it would be expected that treatment with Apcin would decrease dendritic spine density in wildtype neurons compared to vehicle treatment. If the changes on dendritic spine density are dependent on a FMRP-Cdh1 interaction, then it is hypothesized that there would be no difference in *Fmr1* KO neurons between vehicle and Apcin treated conditions. Either set of experiments will help to elucidate the mechanism of FMRP-mediated regulation of dendritic spine density. Better elucidation of this pathway and determination of whether or not Cdh1-APC plays a role may help to better understand mechanisms of disease in other disorders associated with altered spine density, such as schizophrenia.

6.6. Concluding Remarks

We have uncovered that Cdh1-APC is a regulator of protein synthesis in mature cortical neurons. Inhibition of Cdh1-APC activity leads to a decrease in protein synthesis in both Neuro2A cells and postmitotic cortical neurons, demonstrating a novel role for Cdh1-APC independent of its characterized roles in mitotic cells. Proteomic profiling revealed that the Cdh1 interactome is

highly enriched in translational regulatory proteins and stress granule proteins. Stress granule formation leads to decreases in protein synthesis and we observe that Cdh1-APC activity regulates stress granule assembly in cortical neurons; these effects are mediated by interaction of Cdh1-APC with FMRP. Thus, we propose a model in which Cdh1-APC interacts with and ubiquitinates FMRP (**Figure 6-2.1**), which antagonizes the formation of stress granules (**Figure 6-2.3**) and allows for increases in protein synthesis (**Figure 6-2.4**). It is currently unclear whether Cdh1-APC ubiquitinates other stress granule proteins to regulate this process (**Figure 6-2.2**). Our data indicates a dual role of Cdh1-APC in protein homeostasis- it is able to reduce the level of proteins through its role in tagging substrates for degradation by the proteasome and also can lead to an increase in protein synthesis through its antagonism of stress granule formation (**Figure 6-3**). Elucidation of the role of Cdh1-APC in protein synthesis and regulation of translational proteins, such as FMRP, in postmitotic neurons will broaden the understanding of protein homeostasis at the synapse that is vital for protein synthesis dependent synaptic plasticity underlying learning and memory. Furthermore, understanding how the UPS can regulate protein synthesis in the nervous system can provide novel therapeutic insights into existing neurodevelopmental disorders with dysregulated protein homeostasis, such as Fragile X syndrome and Angelman syndrome.

6.7. Figures

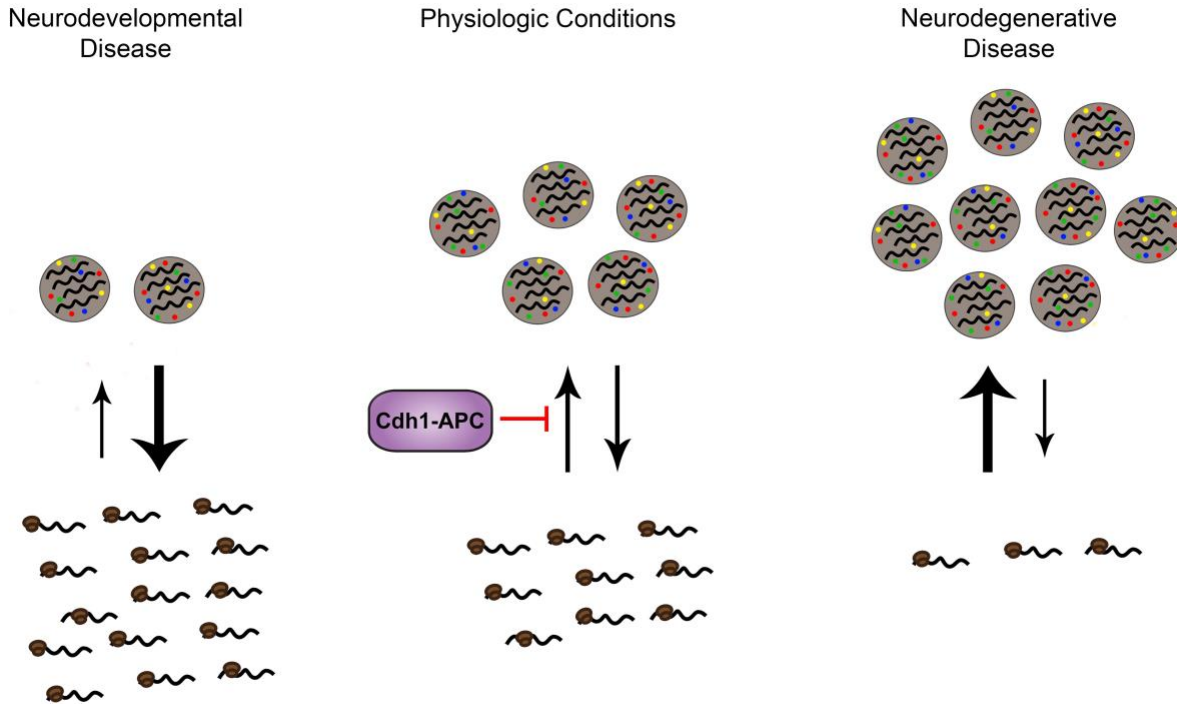


Figure 6-1: Stress granule dynamics across the lifespan

In physiologic conditions (middle), stress granule assembly and disassembly acts a mechanism to regulate protein synthesis. It has been shown in Neurodegenerative diseases (right), such as ALS, that stress granules hyper-assemble and lead to reduced protein synthesis. Neurodevelopmental disorders (left), such as FXS, are characterized by increased levels of protein synthesis, but it is unknown if there is a hypo-assembly of stress granules. We propose that hypo-assembly of stress granules may be a pathologic mechanism in neurodevelopmental diseases. Additionally, the work in this dissertation demonstrates that Cdh1-APC is a complex that regulates the assembly of stress granules, and therefore it may be of interest to investigate manipulation of Cdh1-APC activity as a potential therapeutic opportunity for Neurodegenerative diseases.

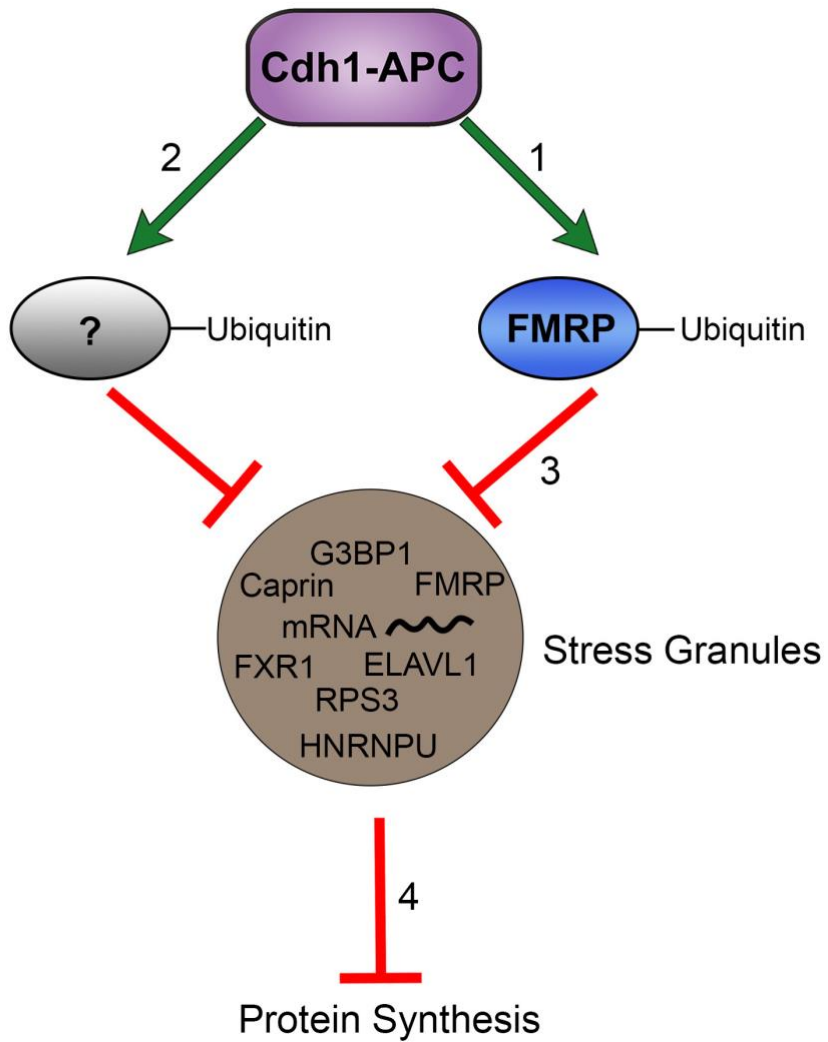


Figure 6-2: Cdh1-APC regulates protein synthesis via stress granules

Model of Cdh1-APC affecting protein synthesis via its interaction and ubiquitination of FMRP (1) and potentially other stress granule proteins (2). Ubiquitination of FMRP prevents stress granule formation (3), ultimately promoting protein synthesis (4).

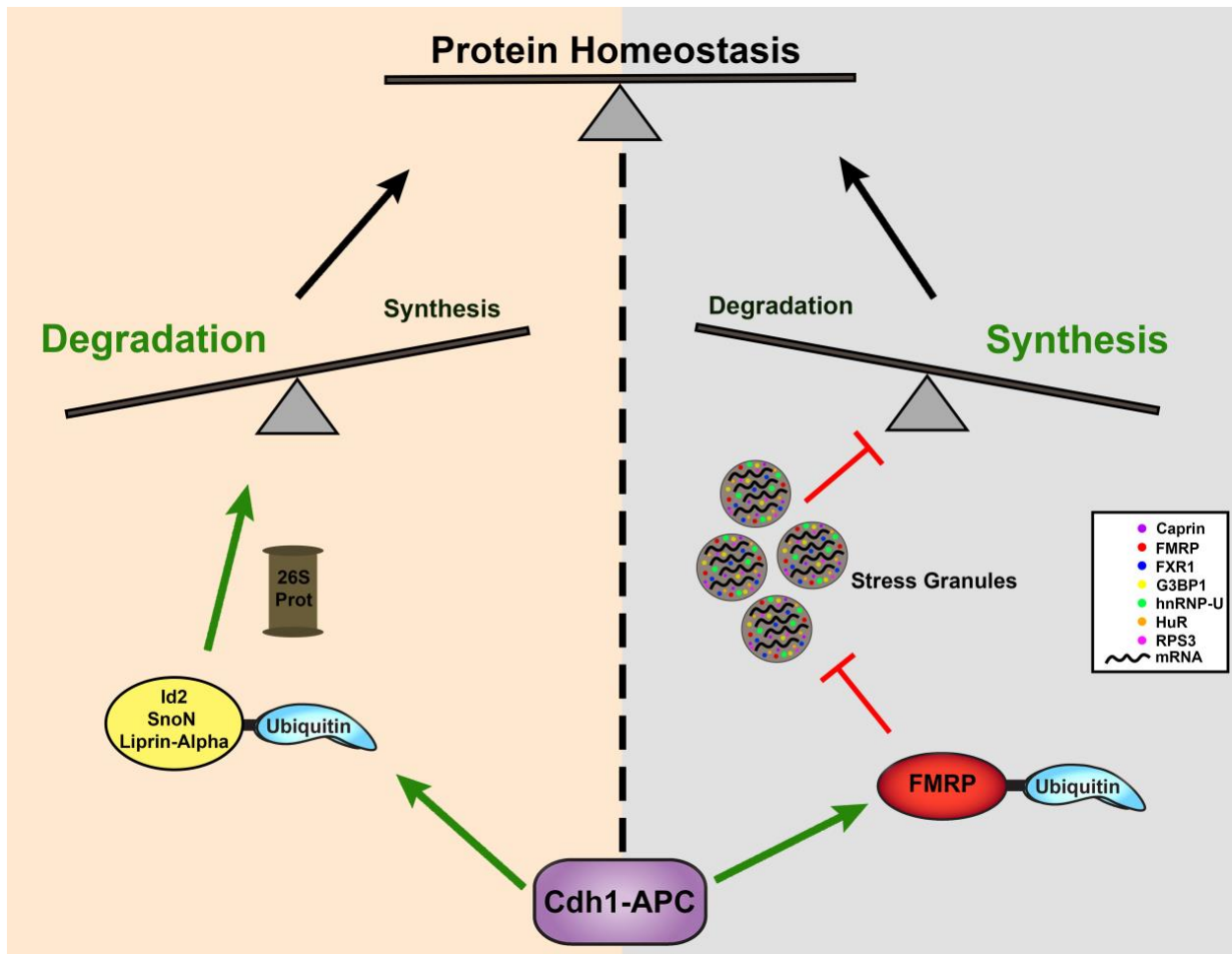


Figure 6-3: Cdh1-APC has a dual role in protein homeostasis

Cdh1-APC contributes to protein homeostasis in neurons via regulation of both protein synthesis and protein degradation. **Left)** Previous literature has reported Id2, SnoN, and Liprin-alpha (see Chapter 1) as ubiquitination targets of Cdh1-APC in neurons. Ubiquitination of these proteins leads to their degradation by the 26S proteasome, thus shifting protein homeostasis towards degradation. Degradation of these substrates in turn leads to downstream effects on axonal growth, axonal morphology, and synapse number. **Right)** Our findings support a role of Cdh1-APC in regulating protein synthesis. We demonstrate that the interaction between Cdh1-APC and FMRP prevents stress granule formation, which acts as molecular switch to prevent the repression of translation. Thus, Cdh1-APC also mediates protein synthesis in neurons. Through the regulation of both

protein synthesis and protein degradation, Cdh1-APC plays a unique role in maintaining protein homeostasis in neurons. Without the regulation of these processes by Cdh1-APC, protein homeostasis can become dysregulated, thereby causing synaptic deficits that contribute to pathologies in learning and memory as evidenced in previous studies (Huang et al., 2015; Pick et al., 2012; Pick et al., 2013).

References

- Abraham, W.C., and Williams, J.M. (2008). LTP maintenance and its protein synthesis-dependence. *Neurobiol Learn Mem* 89, 260-268.
- Alberts, B.M., Hopkin, K., Johnson, A., Morgan, D.O., Raff, M.C., Roberts, K., and Walter, P. (2019). *Essential cell biology*.
- Almeida, A., Bolanos, J.P., and Moreno, S. (2005). Cdh1/Hct1-APC is essential for the survival of postmitotic neurons. *J Neurosci* 25, 8115-8121.
- Angelman, H. (1965). Puppet Children - a Report on 3 Cases. *Dev Med Child Neurol* 7, 681-&.
- Antar, L.N., Afroz, R., Dichtenberg, J.B., Carroll, R.C., and Bassell, G.J. (2004). Metabotropic glutamate receptor activation regulates fragile x mental retardation protein and FMR1 mRNA localization differentially in dendrites and at synapses. *J Neurosci* 24, 2648-2655.
- Ascano, M., Jr., Mukherjee, N., Bandaru, P., Miller, J.B., Nusbaum, J.D., Corcoran, D.L., Langlois, C., Munschauer, M., Dewell, S., Hafner, M., *et al.* (2012). FMRP targets distinct mRNA sequence elements to regulate protein expression. *Nature* 492, 382-386.
- Ashley, C.T., Jr., Wilkinson, K.D., Reines, D., and Warren, S.T. (1993). FMR1 protein: conserved RNP family domains and selective RNA binding. *Science* 262, 563-566.
- Bagni, C., and Greenough, W.T. (2005). From mRNP trafficking to spine dysmorphogenesis: the roots of fragile X syndrome. *Nature Reviews Neuroscience* 6, 376-387.
- Baj, G., Patrizio, A., Montalbano, A., Sciancalepore, M., and Tongiorgi, E. (2014). Developmental and maintenance defects in Rett syndrome neurons identified by a new mouse staging system in vitro. *Front Cell Neurosci* 8, 18.
- Banerjee, A., Ifrim, M.F., Valdez, A.N., Raj, N., and Bassell, G.J. (2018). Aberrant RNA translation in fragile X syndrome: From FMRP mechanisms to emerging therapeutic strategies. *Brain Res* 1693, 24-36.
- Barbosa, A.C., Kim, M.S., Ertunc, M., Adachi, M., Nelson, E.D., McAnally, J., Richardson, J.A., Kavalali, E.T., Monteggia, L.M., Bassel-Duby, R., *et al.* (2008). MEF2C, a transcription factor that facilitates learning and memory by negative regulation of synapse numbers and function. *Proc Natl Acad Sci U S A* 105, 9391-9396.
- Barford, D. (2011). Structure, function and mechanism of the anaphase promoting complex (APC/C). *Q Rev Biophys* 44, 153-190.
- Bartley, C.M., O'Keefe, R.A., Blice-Baum, A., Mihailescu, M.R., Gong, X., Miyares, L., Karaca, E., and Bordey, A. (2016). Mammalian FMRP S499 Is Phosphorylated by CK2 and Promotes Secondary Phosphorylation of FMRP. *eNeuro* 3.

- Bartley, C.M., O'Keefe, R.A., and Bordey, A. (2014). FMRP S499 is phosphorylated independent of mTORC1-S6K1 activity. *PLoS One* 9, e96956.
- Bassell, G.J., Zhang, H., Byrd, A.L., Femino, A.M., Singer, R.H., Taneja, K.L., Lifshitz, L.M., Herman, I.M., and Kosik, K.S. (1998). Sorting of beta-actin mRNA and protein to neurites and growth cones in culture. *J Neurosci* 18, 251-265.
- Bear, M.F., Huber, K.M., and Warren, S.T. (2004). The mGluR theory of fragile X mental retardation. *Trends Neuroscience* 27, 370-377.
- Bear, M.F., and Malenka, R.C. (1994). Synaptic plasticity: LTP and LTD. *Curr Opin Neurobiol* 4, 389-399.
- Bienkowski, R.S., Banerjee, A., Rounds, J.C., Rha, J., Omotade, O.F., Gross, C., Morris, K.J., Leung, S.W., Pak, C., Jones, S.K., *et al.* (2017). The Conserved, Disease-Associated RNA Binding Protein dNab2 Interacts with the Fragile X Protein Ortholog in *Drosophila* Neurons. *Cell Rep* 20, 1372-1384.
- Blackwell, E., Zhang, X., and Ceman, S. (2010). Arginines of the RGG box regulate FMRP association with polyribosomes and mRNA. *Hum Mol Genet* 19, 1314-1323.
- Bobo-Jimenez, V., Delgado-Esteban, M., Angibaud, J., Sanchez-Moran, I., de la Fuente, A., Yajeya, J., Nagerl, U.V., Castillo, J., Bolanos, J.P., and Almeida, A. (2017). APC/C(Cdh1)-Rock2 pathway controls dendritic integrity and memory. *Proc Natl Acad Sci U S A* 114, 4513-4518.
- Bradshaw, K.D., Emptage, N.J., and Bliss, T.V. (2003). A role for dendritic protein synthesis in hippocampal late LTP. *Eur J Neurosci* 18, 3150-3152.
- Brennan, C.M., and Steitz, J.A. (2001). HuR and mRNA stability. *Cell Mol Life Sci* 58, 266-277.
- Brinegar, A.E., and Cooper, T.A. (2016). Roles for RNA-binding proteins in development and disease. *Brain Res* 1647, 1-8.
- Brown, V., Jin, P., Ceman, S., Darnell, J.C., O'Donnell, W.T., Tenenbaum, S.A., Jin, X., Feng, Y., Wilkinson, K.D., Keene, J.D., *et al.* (2001). Microarray identification of FMRP-associated brain mRNAs and altered mRNA translational profiles in fragile X syndrome. *Cell* 107, 477-487.
- Buchan, J.R., and Parker, R. (2009). Eukaryotic stress granules: the ins and outs of translation. *Mol Cell* 36, 932-941.
- Budhavarapu, V.N., White, E.D., Mahanic, C.S., Chen, L., Lin, F.T., and Lin, W.C. (2012). Regulation of E2F1 by APC/C Cdh1 via K11 linkage-specific ubiquitin chain formation. *Cell Cycle* 11, 2030-2038.
- Bulow, P., Murphy, T.J., Bassell, G.J., and Wenner, P. (2019). Homeostatic Intrinsic Plasticity Is Functionally Altered in *Fmr1* KO Cortical Neurons. *Cell Rep* 26, 1378-1388 e1373.

- Ceman, S., O'Donnell, W.T., Reed, M., Patton, S., Pohl, J., and Warren, S.T. (2003). Phosphorylation influences the translation state of FMRP-associated polyribosomes. *Hum Mol Genet* 12, 3295-3305.
- Chang, L., Zhang, Z., Yang, J., McLaughlin, S.H., and Barford, D. (2015). Atomic structure of the APC/C and its mechanism of protein ubiquitination. *Nature* 522, 450-454.
- Chen, L., Yun, S.W., Seto, J., Liu, W., and Toth, M. (2003). The fragile X mental retardation protein binds and regulates a novel class of mRNAs containing U rich target sequences. *Neuroscience* 120, 1005-1017.
- Chen, Y.C., Chang, Y.W., and Huang, Y.S. (2018). Dysregulated Translation in Neurodevelopmental Disorders: An Overview of Autism-Risk Genes Involved in Translation. *Dev Neurobiol*.
- Christie, S.B., Akins, M.R., Schwob, J.E., and Fallon, J.R. (2009). The FXG: a presynaptic fragile X granule expressed in a subset of developing brain circuits. *J Neurosci* 29, 1514-1524.
- Chu, T.T., Gao, N., Li, Q.Q., Chen, P.G., Yang, X.F., Chen, Y.X., Zhao, Y.F., and Li, Y.M. (2016). Specific Knockdown of Endogenous Tau Protein by Peptide-Directed Ubiquitin-Proteasome Degradation. *Cell Chem Biol* 23, 453-461.
- Churcher, I. (2018). PROTAC-Induced Protein Degradation in Drug Discovery: Breaking the Rules or Just Making New Ones? *J Med Chem* 61, 444-452.
- Colgan, L.A., and Yasuda, R. (2014). Plasticity of dendritic spines: subcompartmentalization of signaling. *Annu Rev Physiol* 76, 365-385.
- Comstra, H.S., McCarthy, J., Rudin-Rush, S., Hartwig, C., Gokhale, A., Zlatic, S.A., Blackburn, J.B., Werner, E., Petris, M., D'Souza, P., *et al.* (2017). The interactome of the copper transporter ATP7A belongs to a network of neurodevelopmental and neurodegeneration factors. *Elife* 6.
- Corbin, F., Bouillon, M., Fortin, A., Morin, S., Rousseau, F., and Khandjian, E.W. (1997). The fragile X mental retardation protein is associated with poly(A)⁺ mRNA in actively translating polyribosomes. *Hum Mol Genet* 6, 1465-1472.
- Cruz-Martin, A., Crespo, M., and Portera-Cailliau, C. (2012). Glutamate induces the elongation of early dendritic protrusions via mGluRs in wild type mice, but not in fragile X mice. *PLoS One* 7, e32446.
- Cuende, J., Moreno, S., Bolanos, J.P., and Almeida, A. (2008). Retinoic acid downregulates Rael leading to APC(Cdh1) activation and neuroblastoma SH-SY5Y differentiation. *Oncogene* 27, 3339-3344.
- da Fonseca, P.C., Kong, E.H., Zhang, Z., Schreiber, A., Williams, M.A., Morris, E.P., and Barford, D. (2011). Structures of APC/C(Cdh1) with substrates identify Cdh1 and Apc10 as the D-box co-receptor. *Nature* 470, 274-278.

- Dagda, R.K., Cherra, S.J., 3rd, Kulich, S.M., Tandon, A., Park, D., and Chu, C.T. (2009). Loss of PINK1 function promotes mitophagy through effects on oxidative stress and mitochondrial fission. *J Biol Chem* 284, 13843-13855.
- Darnell, J.C., Fraser, C.E., Mostovetsky, O., Stefani, G., Jones, T.A., Eddy, S.R., and Darnell, R.B. (2005). Kissing complex RNAs mediate interaction between the Fragile-X mental retardation protein KH2 domain and brain polyribosomes. *Genes Dev* 19, 903-918.
- Darnell, J.C., Jensen, K.B., Jin, P., Brown, V., Warren, S.T., and Darnell, R.B. (2001). Fragile X mental retardation protein targets G quartet mRNAs important for neuronal function. *Cell* 107, 489-499.
- Darnell, J.C., Van Driesche, S.J., Zhang, C., Hung, K.Y., Mele, A., Fraser, C.E., Stone, E.F., Chen, C., Fak, J.J., Chi, S.W., *et al.* (2011). FMRP stalls ribosomal translocation on mRNAs linked to synaptic function and autism. *Cell* 146, 247-261.
- David, Y., Ternette, N., Edelmann, M.J., Ziv, T., Gayer, B., Sertchook, R., Dadon, Y., Kessler, B.M., and Navon, A. (2011). E3 ligases determine ubiquitination site and conjugate type by enforcing specificity on E2 enzymes. *J Biol Chem* 286, 44104-44115.
- David, Y., Ziv, T., Admon, A., and Navon, A. (2010). The E2 ubiquitin-conjugating enzymes direct polyubiquitination to preferred lysines. *J Biol Chem* 285, 8595-8604.
- De Boule, K., Verkerk, A.J., Reyniers, E., Vits, L., Hendrickx, J., Van Roy, B., Van den Bos, F., de Graaff, E., Oostra, B.A., and Willems, P.J. (1993). A point mutation in the FMR-1 gene associated with fragile X mental retardation. *Nat Genet* 3, 31-35.
- de Poot, S.A.H., Tian, G., and Finley, D. (2017). Meddling with Fate: The Proteasomal Deubiquitinating Enzymes. *J Mol Biol* 429, 3525-3545.
- De Rubeis, S., Pasciuto, E., Li, K.W., Fernandez, E., Di Marino, D., Buzzi, A., Ostroff, L.E., Klann, E., Zwartkruis, F.J., Komiyama, N.H., *et al.* (2013). CYFIP1 coordinates mRNA translation and cytoskeleton remodeling to ensure proper dendritic spine formation. *Neuron* 79, 1169-1182.
- Delgado-Esteban, M., Garcia-Higuera, I., Maestre, C., Moreno, S., and Almeida, A. (2013). APC/C-Cdh1 coordinates neurogenesis and cortical size during development. *Nat Commun* 4, 2879.
- den Elzen, N., and Pines, J. (2001). Cyclin A is destroyed in prometaphase and can delay chromosome alignment and anaphase. *J Cell Biol* 153, 121-136.
- Deng, L., Wang, C., Spencer, E., Yang, L., Braun, A., You, J., Slaughter, C., Pickart, C., and Chen, Z.J. (2000). Activation of the I κ B kinase complex by TRAF6 requires a dimeric ubiquitin-conjugating enzyme complex and a unique polyubiquitin chain. *Cell* 103, 351-361.

- Di Marcotullio, L., Ferretti, E., Greco, A., De Smaele, E., Po, A., Sico, M.A., Alimandi, M., Giannini, G., Maroder, M., Screpanti, I., *et al.* (2006). Numb is a suppressor of Hedgehog signalling and targets Gli1 for Itch-dependent ubiquitination. *Nat Cell Biol* 8, 1415-1423.
- Dictenberg, J.B., Swanger, S.A., Antar, L.N., Singer, R.H., and Bassell, G.J. (2008). A direct role for FMRP in activity-dependent dendritic mRNA transport links filopodial-spine morphogenesis to fragile X syndrome. *Dev Cell* 14, 926-939.
- Didiot, M.C., Subramanian, M., Flatter, E., Mandel, J.L., and Moine, H. (2009). Cells lacking the fragile X mental retardation protein (FMRP) have normal RISC activity but exhibit altered stress granule assembly. *Mol Biol Cell* 20, 428-437.
- Dupont, S., Mamidi, A., Cordenonsi, M., Montagner, M., Zacchigna, L., Adorno, M., Martello, G., Stinchfield, M.J., Soligo, S., Morsut, L., *et al.* (2009). FAM/USP9x, a deubiquitinating enzyme essential for TGFbeta signaling, controls Smad4 monoubiquitination. *Cell* 136, 123-135.
- Edbauer, D., Neilson, J.R., Foster, K.A., Wang, C.F., Seeburg, D.P., Batterton, M.N., Tada, T., Dolan, B.M., Sharp, P.A., and Sheng, M. (2010). Regulation of synaptic structure and function by FMRP-associated microRNAs miR-125b and miR-132. *Neuron* 65, 373-384.
- English, J.A., Fan, Y., Focking, M., Lopez, L.M., Hryniewiecka, M., Wynne, K., Dicker, P., Matigian, N., Cagney, G., Mackay-Sim, A., *et al.* (2015). Reduced protein synthesis in schizophrenia patient-derived olfactory cells. *Translational Psychiatry* 5, e663.
- Feng, Y., Absher, D., Eberhart, D.E., Brown, V., Malter, H.E., and Warren, S.T. (1997). FMRP associates with polyribosomes as an mRNP, and the I304N mutation of severe fragile X syndrome abolishes this association. *Mol Cell* 1, 109-118.
- Fonseca, R., Vabulas, R.M., Hartl, F.U., Bonhoeffer, T., and Nagerl, U.V. (2006). A balance of protein synthesis and proteasome-dependent degradation determines the maintenance of LTP. *Neuron* 52, 239-245.
- Friez, M.J., Brooks, S.S., Stevenson, R.E., Field, M., Basehore, M.J., Ades, L.C., Sebold, C., McGee, S., Saxon, S., Skinner, C., *et al.* (2016). HUWE1 mutations in Juberg-Marsidi and Brooks syndromes: the results of an X-chromosome exome sequencing study. *BMJ Open* 6, e009537.
- Fuchsberger, T., Martinez-Bellver, S., Giraldo, E., Teruel-Marti, V., Lloret, A., and Vina, J. (2016). Abeta Induces Excitotoxicity Mediated by APC/C-Cdh1 Depletion That Can Be Prevented by Glutaminase Inhibition Promoting Neuronal Survival. *Sci Rep* 6, 31158.
- Fujita, T., Liu, W., Doihara, H., Date, H., and Wan, Y. (2008a). Dissection of the APCCdh1-Skp2 cascade in breast cancer. *Clin Cancer Res* 14, 1966-1975.
- Fujita, T., Liu, W., Doihara, H., and Wan, Y. (2008b). Regulation of Skp2-p27 axis by the Cdh1/anaphase-promoting complex pathway in colorectal tumorigenesis. *Am J Pathol* 173, 217-228.

- Gao, D., Inuzuka, H., Tseng, A., and Wei, W. (2009). Akt finds its new path to regulate cell cycle through modulating Skp2 activity and its destruction by APC/Cdh1. *Cell Div* 4, 11.
- Gareau, C., Martel, D., Coudert, L., Mellaoui, S., and Mazroui, R. (2013). Characterization of Fragile X Mental Retardation Protein granules formation and dynamics in *Drosophila*. *Biol Open* 2, 68-81.
- George, A.J., Hoffiz, Y.C., Charles, A.J., Zhu, Y., and Mabb, A.M. (2018). A Comprehensive Atlas of E3 Ubiquitin Ligase Mutations in Neurological Disorders. *Front Genet* 9, 29.
- Gieffers, C., Peters, B.H., Kramer, E.R., Dotti, C.G., and Peters, J.M. (1999). Expression of the CDH1-associated form of the anaphase-promoting complex in postmitotic neurons. *Proc Natl Acad Sci U S A* 96, 11317-11322.
- Gingras, A.C., Raught, B., Gygi, S.P., Niedzwiecka, A., Miron, M., Burley, S.K., Polakiewicz, R.D., Wyslouch-Cieszynska, A., Aebersold, R., and Sonenberg, N. (2001). Hierarchical phosphorylation of the translation inhibitor 4E-BP1. *Genes Dev* 15, 2852-2864.
- Gkogkas, C.G., Khoutorsky, A., Ran, I., Rampakakis, E., Nevarko, T., Weatherill, D.B., Vasuta, C., Yee, S., Truitt, M., Dallaire, P., *et al.* (2013). Autism-related deficits via dysregulated eIF4E-dependent translational control. *Nature* 493, 371-377.
- Glausier, J.R., and Lewis, D.A. (2013). Dendritic spine pathology in schizophrenia. *Neuroscience* 251, 90-107.
- Glotzer, M., Murray, A.W., and Kirschner, M.W. (1991). Cyclin is degraded by the ubiquitin pathway. *Nature* 349, 132-138.
- Gokhale, A., Larimore, J., Werner, E., So, L., Moreno-De-Luca, A., Lese-Martin, C., Lupashin, V.V., Smith, Y., and Faundez, V. (2012). Quantitative proteomic and genetic analyses of the schizophrenia susceptibility factor dysbindin identify novel roles of the biogenesis of lysosome-related organelles complex 1. *J Neurosci* 32, 3697-3711.
- Greer, P.L., Hanayama, R., Bloodgood, B.L., Mardinly, A.R., Lipton, D.M., Flavell, S.W., Kim, T.K., Griffith, E.C., Waldon, Z., Maehr, R., *et al.* (2010). The Angelman Syndrome protein Ube3A regulates synapse development by ubiquitinating arc. *Cell* 140, 704-716.
- Gross, C., and Bassell, G.J. (2012). Excess protein synthesis in FXS patient lymphoblastoid cells can be rescued with a p110beta-selective inhibitor. *Mol Med* 18, 336-345.
- Gross, C., Chang, C.W., Kelly, S.M., Bhattacharya, A., McBride, S.M., Danielson, S.W., Jiang, M.Q., Chan, C.B., Ye, K., Gibson, J.R., *et al.* (2015a). Increased expression of the PI3K enhancer PIKE mediates deficits in synaptic plasticity and behavior in fragile X syndrome. *Cell Rep* 11, 727-736.
- Gross, C., Nakamoto, M., Yao, X., Chan, C.B., Yim, S.Y., Ye, K., Warren, S.T., and Bassell, G.J. (2010). Excess phosphoinositide 3-kinase subunit synthesis and activity as a novel therapeutic target in fragile X syndrome. *J Neurosci* 30, 10624-10638.

Gross, C., Raj, N., Molinaro, G., Allen, A.G., Whyte, A.J., Gibson, J.R., Huber, K.M., Gourley, S.L., and Bassell, G.J. (2015b). Selective role of the catalytic PI3K subunit p110beta in impaired higher order cognition in fragile X syndrome. *Cell Rep* 11, 681-688.

Guhaniyogi, J., and Brewer, G. (2001). Regulation of mRNA stability in mammalian cells. *Gene* 265, 11-23.

Gururajan, A., and van den Buuse, M. (2014). Is the mTOR-signalling cascade disrupted in Schizophrenia? *J Neurochem* 129, 377-387.

Hayes, M.J., Kimata, Y., Wattam, S.L., Lindon, C., Mao, G., Yamano, H., and Fry, A.M. (2006). Early mitotic degradation of Nek2A depends on Cdc20-independent interaction with the APC/C. *Nat Cell Biol* 8, 607-614.

He, C.X., and Portera-Cailliau, C. (2013). The trouble with spines in fragile X syndrome: density, maturity and plasticity. *Neuroscience* 251, 120-128.

Hegde, A.N. (2004). Ubiquitin-proteasome-mediated local protein degradation and synaptic plasticity. *Prog Neurobiol* 73, 311-357.

Hengstermann, A., Linares, L.K., Ciechanover, A., Whitaker, N.J., and Scheffner, M. (2001). Complete switch from Mdm2 to human papillomavirus E6-mediated degradation of p53 in cervical cancer cells. *Proc Natl Acad Sci U S A* 98, 1218-1223.

Herrero-Mendez, A., Almeida, A., Fernandez, E., Maestre, C., Moncada, S., and Bolanos, J.P. (2009). The bioenergetic and antioxidant status of neurons is controlled by continuous degradation of a key glycolytic enzyme by APC/C-Cdh1. *Nat Cell Biol* 11, 747-752.

Herskowitz, J.H., Feng, Y., Mattheyses, A.L., Hales, C.M., Higginbotham, L.A., Duong, D.M., Montine, T.J., Troncoso, J.C., Thambisetty, M., Seyfried, N.T., *et al.* (2013). Pharmacologic inhibition of ROCK2 suppresses amyloid-beta production in an Alzheimer's disease mouse model. *J Neurosci* 33, 19086-19098.

Hicke, L., Schubert, H.L., and Hill, C.P. (2005). Ubiquitin-binding domains. *Nat Rev Mol Cell Biol* 6, 610-621.

Hines, J., Gough, J.D., Corson, T.W., and Crews, C.M. (2013). Posttranslational protein knockdown coupled to receptor tyrosine kinase activation with phosphoPROTACs. *Proc Natl Acad Sci U S A* 110, 8942-8947.

Hinnebusch, A.G. (2014). The scanning mechanism of eukaryotic translation initiation. *Annu Rev Biochem* 83, 779-812.

Hinton, V.J., Brown, W.T., Wisniewski, K., and Rudelli, R.D. (1991). Analysis of neocortex in three males with the fragile X syndrome. *American Journal of Medical Genetics* 41, 289-294.

- Hjerpe, R., Aillet, F., Lopitz-Otsoa, F., Lang, V., England, P., and Rodriguez, M.S. (2009). Efficient protection and isolation of ubiquitylated proteins using tandem ubiquitin-binding entities. *EMBO Rep* 10, 1250-1258.
- Hollstein, R., Parry, D.A., Nalbach, L., Logan, C.V., Strom, T.M., Hartill, V.L., Carr, I.M., Korenke, G.C., Uppal, S., Ahmed, M., *et al.* (2015). HACE1 deficiency causes an autosomal recessive neurodevelopmental syndrome. *J Med Genet* 52, 797-803.
- Hou, L., Antion, M.D., Hu, D., Spencer, C.M., Paylor, R., and Klann, E. (2006). Dynamic translational and proteasomal regulation of fragile X mental retardation protein controls mGluR-dependent long-term depression. *Neuron* 51, 441-454.
- Huang, J., Ikeuchi, Y., Malumbres, M., and Bonni, A. (2015). A Cdh1-APC/FMRP Ubiquitin Signaling Link Drives mGluR-Dependent Synaptic Plasticity in the Mammalian Brain. *Neuron* 86, 726-739.
- Huber, K.M., Gallagher, S.M., Warren, S.T., and Bear, M.F. (2002). Altered synaptic plasticity in a mouse model of fragile X mental retardation. *Proceedings of the National Academy of Sciences* 99, 7746-7750.
- Huber, K.M., Klann, E., Costa-Mattioli, M., and Zukin, R.S. (2015). Dysregulation of Mammalian Target of Rapamycin Signaling in Mouse Models of Autism. *Journal of Neuroscience* 35, 13836-13842.
- Huibregtse, J.M., Scheffner, M., and Howley, P.M. (1993). Cloning and expression of the cDNA for E6-AP, a protein that mediates the interaction of the human papillomavirus E6 oncoprotein with p53. *Mol Cell Biol* 13, 775-784.
- Huttelmaier, S., Zenklusen, D., Lederer, M., Dichtenberg, J., Lorenz, M., Meng, X., Bassell, G.J., Condeelis, J., and Singer, R.H. (2005). Spatial regulation of beta-actin translation by Src-dependent phosphorylation of ZBP1. *Nature* 438, 512-515.
- Huynh, M.A., Stegmuller, J., Litterman, N., and Bonni, A. (2009). Regulation of Cdh1-APC function in axon growth by Cdh1 phosphorylation. *J Neurosci* 29, 4322-4327.
- Ifrim, M.F., Williams, K.R., and Bassell, G.J. (2015). Single-Molecule Imaging of PSD-95 mRNA Translation in Dendrites and Its Dysregulation in a Mouse Model of Fragile X Syndrome. *J Neurosci* 35, 7116-7130.
- Irwin, S.A., Patel, B., Idupulapati, M., Harris, J.B., Crisostomo, R.A., Larsen, B.P., Kooy, F., Willems, P.J., Cras, P., Kozlowski, P.B., *et al.* (2001). Abnormal dendritic spine characteristics in the temporal and visual cortices of patients with fragile-X syndrome: a quantitative examination. *American Journal of Medical Genetics* 98, 161-167.
- Jackson, R.J., Hellen, C.U., and Pestova, T.V. (2012). Termination and post-termination events in eukaryotic translation. *Adv Protein Chem Struct Biol* 86, 45-93.

- Jain, S., Wheeler, J.R., Walters, R.W., Agrawal, A., Barsic, A., and Parker, R. (2016). ATPase-Modulated Stress Granules Contain a Diverse Proteome and Substructure. *Cell* *164*, 487-498.
- Jaquenoud, M., van Drogen, F., and Peter, M. (2002). Cell cycle-dependent nuclear export of Cdh1p may contribute to the inactivation of APC/C(Cdh1). *EMBO J* *21*, 6515-6526.
- Jin, P., Zarnescu, D.C., Ceman, S., Nakamoto, M., Mowrey, J., Jongens, T.A., Nelson, D.L., Moses, K., and Warren, S.T. (2004). Biochemical and genetic interaction between the fragile X mental retardation protein and the microRNA pathway. *Nat Neurosci* *7*, 113-117.
- Juo, P., and Kaplan, J.M. (2004). The anaphase-promoting complex regulates the abundance of GLR-1 glutamate receptors in the ventral nerve cord of *C. elegans*. *Curr Biol* *14*, 2057-2062.
- Karpova, A., Mikhaylova, M., Thomas, U., Knopfel, T., and Behnisch, T. (2006). Involvement of protein synthesis and degradation in long-term potentiation of Schaffer collateral CA1 synapses. *J Neurosci* *26*, 4949-4955.
- Kato, T., Daigo, Y., Aragaki, M., Ishikawa, K., Sato, M., and Kaji, M. (2012). Overexpression of CDC20 predicts poor prognosis in primary non-small cell lung cancer patients. *J Surg Oncol* *106*, 423-430.
- Kauderer, B.S., and Kandel, E.R. (2000). Capture of a protein synthesis-dependent component of long-term depression. *Proc Natl Acad Sci U S A* *97*, 13342-13347.
- Kedersha, N., Panas, M.D., Achorn, C.A., Lyons, S., Tisdale, S., Hickman, T., Thomas, M., Lieberman, J., McInerney, G.M., Ivanov, P., *et al.* (2016). G3BP-Caprin1-USP10 complexes mediate stress granule condensation and associate with 40S subunits. *J Cell Biol* *212*, 845-860.
- Kenny, P.J., Zhou, H., Kim, M., Skariah, G., Khetani, R.S., Drnevich, J., Arcila, M.L., Kosik, K.S., and Ceman, S. (2014). MOV10 and FMRP regulate AGO2 association with microRNA recognition elements. *Cell Rep* *9*, 1729-1741.
- Kim, A.H., Puram, S.V., Bilimoria, P.M., Ikeuchi, Y., Keough, S., Wong, M., Rowitch, D., and Bonni, A. (2009). A centrosomal Cdc20-APC pathway controls dendrite morphogenesis in postmitotic neurons. *Cell* *136*, 322-336.
- Kishino, T., Lalande, M., and Wagstaff, J. (1997). UBE3A/E6-AP mutations cause Angelman syndrome. *Nature Genetics* *15*, 70-73.
- Kislauskis, E.H., Zhu, X., and Singer, R.H. (1994). Sequences responsible for intracellular localization of beta-actin messenger RNA also affect cell phenotype. *J Cell Biol* *127*, 441-451.
- Kohler, A., and Hurt, E. (2007). Exporting RNA from the nucleus to the cytoplasm. *Nat Rev Mol Cell Biol* *8*, 761-773.
- Konishi, Y., Stegmuller, J., Matsuda, T., Bonni, S., and Bonni, A. (2004). Cdh1-APC controls axonal growth and patterning in the mammalian brain. *Science* *303*, 1026-1030.

- Kraft, C., Vodermaier, H.C., Maurer-Stroh, S., Eisenhaber, F., and Peters, J.M. (2005). The WD40 propeller domain of Cdh1 functions as a destruction box receptor for APC/C substrates. *Mol Cell* *18*, 543-553.
- Lai, A.C., and Crews, C.M. (2017). Induced protein degradation: an emerging drug discovery paradigm. *Nat Rev Drug Discov* *16*, 101-114.
- Lasorella, A., Stegmuller, J., Guardavaccaro, D., Liu, G., Carro, M.S., Rothschild, G., de la Torre-Ubieta, L., Pagano, M., Bonni, A., and Iavarone, A. (2006). Degradation of Id2 by the anaphase-promoting complex couples cell cycle exit and axonal growth. *Nature* *442*, 471-474.
- Lauwers, E., Jacob, C., and Andre, B. (2009). K63-linked ubiquitin chains as a specific signal for protein sorting into the multivesicular body pathway. *J Cell Biol* *185*, 493-502.
- Leatherwood, J. (1998). Emerging mechanisms of eukaryotic DNA replication initiation. *Curr Opin Cell Biol* *10*, 742-748.
- Lee, S.Y., Ramirez, J., Franco, M., Lectez, B., Gonzalez, M., Barrio, R., and Mayor, U. (2014). Ube3a, the E3 ubiquitin ligase causing Angelman syndrome and linked to autism, regulates protein homeostasis through the proteasomal shuttle Rpn10. *Cellular and Molecular Life Sciences* *71*, 2747-2758.
- Lee, Y., and Rio, D.C. (2015). Mechanisms and Regulation of Alternative Pre-mRNA Splicing. *Annu Rev Biochem* *84*, 291-323.
- Lei, W., Omotade, O.F., Myers, K.R., and Zheng, J.Q. (2016). Actin cytoskeleton in dendritic spine development and plasticity. *Curr Opin Neurobiol* *39*, 86-92.
- Li, M., Shin, Y.H., Hou, L., Huang, X., Wei, Z., Klann, E., and Zhang, P. (2008). The adaptor protein of the anaphase promoting complex Cdh1 is essential in maintaining replicative lifespan and in learning and memory. *Nat Cell Biol* *10*, 1083-1089.
- Li, Y., Tang, W., Zhang, L.R., and Zhang, C.Y. (2014). FMRP regulates miR196a-mediated repression of HOXB8 via interaction with the AGO2 MID domain. *Mol Biosyst* *10*, 1757-1764.
- Li, Y.R., King, O.D., Shorter, J., and Gitler, A.D. (2013). Stress granules as crucibles of ALS pathogenesis. *J Cell Biol* *201*, 361-372.
- Liu, P., Gan, W., Su, S., Hauenstein, A.V., Fu, T.M., Brasher, B., Schwerdtfeger, C., Liang, A.C., Xu, M., and Wei, W. (2018). K63-linked polyubiquitin chains bind to DNA to facilitate DNA damage repair. *Sci Signal* *11*.
- Liu, Z.H., Huang, T., and Smith, C.B. (2012). Lithium reverses increased rates of cerebral protein synthesis in a mouse model of fragile X syndrome. *Neurobiol Dis* *45*, 1145-1152.
- Lwin, T., Hazlehurst, L.A., Dessureault, S., Lai, R., Bai, W., Sotomayor, E., Moscinski, L.C., Dalton, W.S., and Tao, J. (2007). Cell adhesion induces p27Kip1-associated cell-cycle arrest

through down-regulation of the SCFSkp2 ubiquitin ligase pathway in mantle-cell and other non-Hodgkin B-cell lymphomas. *Blood* *110*, 1631-1638.

Markmiller, S., Fulzele, A., Higgins, R., Leonard, M., Yeo, G.W., and Bennett, E.J. (2019). Active Protein Neddylation or Ubiquitylation Is Dispensable for Stress Granule Dynamics. *Cell Rep* *27*, 1356-1363 e1353.

Markmiller, S., Soltanieh, S., Server, K.L., Mak, R., Jin, W., Fang, M.Y., Luo, E.C., Krach, F., Yang, D., Sen, A., *et al.* (2018). Context-Dependent and Disease-Specific Diversity in Protein Interactions within Stress Granules. *Cell* *172*, 590-604 e513.

Martin, K.C., and Ephrussi, A. (2009). mRNA localization: gene expression in the spatial dimension. *Cell* *136*, 719-730.

Mazroui, R., Di Marco, S., Kaufman, R.J., and Gallouzi, I.E. (2007). Inhibition of the ubiquitin-proteasome system induces stress granule formation. *Mol Biol Cell* *18*, 2603-2618.

Mazroui, R., Huot, M.E., Tremblay, S., Filion, C., Labelle, Y., and Khandjian, E.W. (2002). Trapping of messenger RNA by Fragile X Mental Retardation protein into cytoplasmic granules induces translation repression. *Hum Mol Genet* *11*, 3007-3017.

McGarry, T.J., and Kirschner, M.W. (1998). Geminin, an inhibitor of DNA replication, is degraded during mitosis. *Cell* *93*, 1043-1053.

Meister, G., Landthaler, M., Patkaniowska, A., Dorsett, Y., Teng, G., and Tuschl, T. (2004). Human Argonaute2 mediates RNA cleavage targeted by miRNAs and siRNAs. *Mol Cell* *15*, 185-197.

Monahan, Z., Shewmaker, F., and Pandey, U.B. (2016). Stress granules at the intersection of autophagy and ALS. *Brain Res* *1649*, 189-200.

Morgan, D.O. (2007). *The cell cycle : principles of control* (London Sunderland, MA: Published by New Science Press in association with Oxford University Press ; Distributed inside North America by Sinauer Associates, Publishers).

Morreale, F.E., and Walden, H. (2016). Types of Ubiquitin Ligases. *Cell* *165*, 248-248 e241.

Muddashetty, R.S., Kelic, S., Gross, C., Xu, M., and Bassell, G.J. (2007). Dysregulated metabotropic glutamate receptor-dependent translation of AMPA receptor and postsynaptic density-95 mRNAs at synapses in a mouse model of fragile X syndrome. *Journal of Neuroscience* *27*, 5338-5348.

Muddashetty, R.S., Nalavadi, V.C., Gross, C., Yao, X., Xing, L., Laur, O., Warren, S.T., and Bassell, G.J. (2011). Reversible inhibition of PSD-95 mRNA translation by miR-125a, FMRP phosphorylation, and mGluR signaling. *Molecular Cell* *42*, 673-688.

Nakayama, K., Ohashi, R., Shinoda, Y., Yamazaki, M., Abe, M., Fujikawa, A., Shigenobu, S., Futatsugi, A., Noda, M., Mikoshiba, K., *et al.* (2017). RNG105/caprin1, an RNA granule protein for dendritic mRNA localization, is essential for long-term memory formation. *Elife* 6.

Nalavadi, V.C., Muddashetty, R.S., Gross, C., and Bassell, G.J. (2012). Dephosphorylation-induced ubiquitination and degradation of FMRP in dendrites: a role in immediate early mGluR-stimulated translation. *Journal of Neuroscience* 32, 2582-2587.

Napoli, I., Mercaldo, V., Boyl, P.P., Eleuteri, B., Zalfa, F., De Rubeis, S., Di Marino, D., Mohr, E., Massimi, M., Falconi, M., *et al.* (2008). The fragile X syndrome protein represses activity-dependent translation through CYFIP1, a new 4E-BP. *Cell* 134, 1042-1054.

Narayanan, U., Nalavadi, V., Nakamoto, M., Pallas, D.C., Ceman, S., Bassell, G.J., and Warren, S.T. (2007). FMRP phosphorylation reveals an immediate-early signaling pathway triggered by group I mGluR and mediated by PP2A. *J Neurosci* 27, 14349-14357.

Neklesa, T.K., Winkler, J.D., and Crews, C.M. (2017). Targeted protein degradation by PROTACs. *Pharmacol Ther* 174, 138-144.

Nostramo, R., and Herman, P.K. (2016). Deubiquitination and the regulation of stress granule assembly. *Curr Genet* 62, 503-506.

Osterweil, E.K., Krueger, D.D., Reinhold, K., and Bear, M.F. (2010). Hypersensitivity to mGluR5 and ERK1/2 leads to excessive protein synthesis in the hippocampus of a mouse model of fragile X syndrome. *J Neurosci* 30, 15616-15627.

Ottis, P., and Crews, C.M. (2017). Proteolysis-Targeting Chimeras: Induced Protein Degradation as a Therapeutic Strategy. *ACS Chem Biol* 12, 892-898.

Ouwenga, R., Lake, A.M., O'Brien, D., Mogha, A., Dani, A., and Dougherty, J.D. (2017). Transcriptomic Analysis of Ribosome-Bound mRNA in Cortical Neurites In Vivo. *J Neurosci* 37, 8688-8705.

Pak, C., Garshasbi, M., Kahrizi, K., Gross, C., Apponi, L.H., Noto, J.J., Kelly, S.M., Leung, S.W., Tzschach, A., Behjati, F., *et al.* (2011). Mutation of the conserved polyadenosine RNA binding protein, ZC3H14/dNab2, impairs neural function in Drosophila and humans. *Proc Natl Acad Sci U S A* 108, 12390-12395.

Pasciuto, E., and Bagni, C. (2014a). SnapShot: FMRP interacting proteins. *Cell* 159, 218-218 e211.

Pasciuto, E., and Bagni, C. (2014b). SnapShot: FMRP mRNA targets and diseases. *Cell* 158, 1446-1446 e1441.

Penagarikano, O., Mulle, J.G., and Warren, S.T. (2007). The pathophysiology of fragile x syndrome. *Annual Review of Genomics and Human Genetics* 8, 109-129.

- Penzes, P., Cahill, M.E., Jones, K.A., VanLeeuwen, J.E., and Woolfrey, K.M. (2011). Dendritic spine pathology in neuropsychiatric disorders. *Nature Neuroscience* *14*, 285-293.
- Pfeiffer, B.E., and Huber, K.M. (2007). Fragile X mental retardation protein induces synapse loss through acute postsynaptic translational regulation. *Journal of Neuroscience* *27*, 3120-3130.
- Pfeiffer, B.E., and Huber, K.M. (2009). The state of synapses in fragile X syndrome. *Neuroscientist* *15*, 549-567.
- Pfeiffer, B.E., Zang, T., Wilkerson, J.R., Taniguchi, M., Maksimova, M.A., Smith, L.N., Cowan, C.W., and Huber, K.M. (2010). Fragile X mental retardation protein is required for synapse elimination by the activity-dependent transcription factor MEF2. *Neuron* *66*, 191-197.
- Pfleger, C.M., and Kirschner, M.W. (2000). The KEN box: an APC recognition signal distinct from the D box targeted by Cdh1. *Genes Dev* *14*, 655-665.
- Pick, J.E., Malumbres, M., and Klann, E. (2012). The E3 ligase APC/C-Cdh1 is required for associative fear memory and long-term potentiation in the amygdala of adult mice. *Learn Mem* *20*, 11-20.
- Pick, J.E., Wang, L., Mayfield, J.E., and Klann, E. (2013). Neuronal expression of the ubiquitin E3 ligase APC/C-Cdh1 during development is required for long-term potentiation, behavioral flexibility, and extinction. *Neurobiol Learn Mem* *100*, 25-31.
- Pierce, N.W., Kleiger, G., Shan, S.O., and Deshaies, R.J. (2009). Detection of sequential polyubiquitylation on a millisecond timescale. *Nature* *462*, 615-619.
- Potthoff, M.J., and Olson, E.N. (2007). MEF2: a central regulator of diverse developmental programs. *Development* *134*, 4131-4140.
- Protter, D.S.W., and Parker, R. (2016). Principles and Properties of Stress Granules. *Trends Cell Biol* *26*, 668-679.
- Qiao, X., Zhang, L., Gamper, A.M., Fujita, T., and Wan, Y. (2010). APC/C-Cdh1: from cell cycle to cellular differentiation and genomic integrity. *Cell Cycle* *9*, 3904-3912.
- Rahal, R., and Amon, A. (2008). Mitotic CDKs control the metaphase-anaphase transition and trigger spindle elongation. *Genes Dev* *22*, 1534-1548.
- Ramos, A., Hollingworth, D., and Pastore, A. (2003). G-quartet-dependent recognition between the FMRP RGG box and RNA. *RNA* *9*, 1198-1207.
- Richter, J.D., Bassell, G.J., and Klann, E. (2015). Dysregulation and restoration of translational homeostasis in fragile X syndrome. *Nature Reviews Neuroscience* *16*, 595-605.
- Riedl, J., Crevenna, A.H., Kessenbrock, K., Yu, J.H., Neukirchen, D., Bista, M., Bradke, F., Jenne, D., Holak, T.A., Werb, Z., *et al.* (2008). Lifeact: a versatile marker to visualize F-actin. *Nature Methods* *5*, 605-607.

- Rodriguez, C., Sanchez-Moran, I., Alvarez, S., Tirado, P., Fernandez-Mayoralas, D.M., Calleja-Perez, B., Almeida, A., and Fernandez-Jaen, A. (2019). A novel human Cdh1 mutation impairs anaphase promoting complex/cyclosome (APC/C) activity resulting in microcephaly, psychomotor retardation and epilepsy. *J Neurochem*.
- Ross, A.F., Oleynikov, Y., Kislauskis, E.H., Taneja, K.L., and Singer, R.H. (1997). Characterization of a beta-actin mRNA zipcode-binding protein. *Mol Cell Biol* *17*, 2158-2165.
- Roux, K.J., Kim, D.I., Burke, B., and May, D.G. (2018). BioID: A Screen for Protein-Protein Interactions. *Curr Protoc Protein Sci* *91*, 19 23 11-19 23 15.
- Sackton, K.L., Dimova, N., Zeng, X., Tian, W., Zhang, M., Sackton, T.B., Meaders, J., Pfaff, K.L., Sigoillot, F., Yu, H., *et al.* (2014). Synergistic blockade of mitotic exit by two chemical inhibitors of the APC/C. *Nature* *514*, 646-649.
- Sahoo, P.K., Lee, S.J., Jaiswal, P.B., Alber, S., Kar, A.N., Miller-Randolph, S., Taylor, E.E., Smith, T., Singh, B., Ho, T.S., *et al.* (2018). Axonal G3BP1 stress granule protein limits axonal mRNA translation and nerve regeneration. *Nat Commun* *9*, 3358.
- Sakamoto, K.M., Kim, K.B., Kumagai, A., Mercurio, F., Crews, C.M., and Deshaies, R.J. (2001). Protacs: chimeric molecules that target proteins to the Skp1-Cullin-F box complex for ubiquitination and degradation. *Proc Natl Acad Sci U S A* *98*, 8554-8559.
- Santini, E., Huynh, T.N., and Klann, E. (2014). Mechanisms of translation control underlying long-lasting synaptic plasticity and the consolidation of long-term memory. *Prog Mol Biol Transl Sci* *122*, 131-167.
- Schizophrenia Psychiatric Genome-Wide Association Study, C. (2011). Genome-wide association study identifies five new schizophrenia loci. *Nat Genet* *43*, 969-976.
- Sharma, A., Hoeffler, C.A., Takayasu, Y., Miyawaki, T., McBride, S.M., Klann, E., and Zukin, R.S. (2010). Dysregulation of mTOR signaling in fragile X syndrome. *J Neurosci* *30*, 694-702.
- Shiina, N., Shinkura, K., and Tokunaga, M. (2005). A novel RNA-binding protein in neuronal RNA granules: regulatory machinery for local translation. *J Neurosci* *25*, 4420-4434.
- Shiina, N., Yamaguchi, K., and Tokunaga, M. (2010). RNG105 deficiency impairs the dendritic localization of mRNAs for Na⁺/K⁺ ATPase subunit isoforms and leads to the degeneration of neuronal networks. *J Neurosci* *30*, 12816-12830.
- Silva-Santos, S., van Woerden, G.M., Bruinsma, C.F., Mientjes, E., Jolfaei, M.A., Distel, B., Kushner, S.A., and Elgersma, Y. (2015). Ube3a reinstatement identifies distinct developmental windows in a murine Angelman syndrome model. *J Clin Invest* *125*, 2069-2076.
- Siomi, H., Choi, M., Siomi, M.C., Nussbaum, R.L., and Dreyfuss, G. (1994). Essential role for KH domains in RNA binding: impaired RNA binding by a mutation in the KH domain of FMR1 that causes fragile X syndrome. *Cell* *77*, 33-39.

- Siomi, H., Siomi, M.C., Nussbaum, R.L., and Dreyfuss, G. (1993). The protein product of the fragile X gene, FMR1, has characteristics of an RNA-binding protein. *Cell* 74, 291-298.
- Solomon, S., Xu, Y., Wang, B., David, M.D., Schubert, P., Kennedy, D., and Schrader, J.W. (2007). Distinct structural features of caprin-1 mediate its interaction with G3BP-1 and its induction of phosphorylation of eukaryotic translation initiation factor 2alpha, entry to cytoplasmic stress granules, and selective interaction with a subset of mRNAs. *Mol Cell Biol* 27, 2324-2342.
- Song, T., Zheng, Y., Wang, Y., Katz, Z., Liu, X., Chen, S., Singer, R.H., and Gu, W. (2015). Specific interaction of KIF11 with ZBP1 regulates the transport of beta-actin mRNA and cell motility. *J Cell Sci* 128, 1001-1010.
- Sossin, W.S., and DesGroseillers, L. (2006). Intracellular trafficking of RNA in neurons. *Traffic* 7, 1581-1589.
- Stefani, G., Fraser, C.E., Darnell, J.C., and Darnell, R.B. (2004). Fragile X mental retardation protein is associated with translating polyribosomes in neuronal cells. *J Neurosci* 24, 7272-7276.
- Stefanovic, S., DeMarco, B.A., Underwood, A., Williams, K.R., Bassell, G.J., and Mihailescu, M.R. (2015). Fragile X mental retardation protein interactions with a G quadruplex structure in the 3'-untranslated region of NR2B mRNA. *Mol Biosyst* 11, 3222-3230.
- Stegmuller, J., Huynh, M.A., Yuan, Z., Konishi, Y., and Bonni, A. (2008). TGFbeta-Smad2 signaling regulates the Cdh1-APC/SnoN pathway of axonal morphogenesis. *J Neurosci* 28, 1961-1969.
- Stegmuller, J., Konishi, Y., Huynh, M.A., Yuan, Z., Dibacco, S., and Bonni, A. (2006). Cell-intrinsic regulation of axonal morphogenesis by the Cdh1-APC target SnoN. *Neuron* 50, 389-400.
- Sudakin, V., Ganoth, D., Dahan, A., Heller, H., Hershko, J., Luca, F.C., Ruderman, J.V., and Hershko, A. (1995). The cyclosome, a large complex containing cyclin-selective ubiquitin ligase activity, targets cyclins for destruction at the end of mitosis. *Mol Biol Cell* 6, 185-197.
- Suhl, J.A., Chopra, P., Anderson, B.R., Bassell, G.J., and Warren, S.T. (2014). Analysis of FMRP mRNA target datasets reveals highly associated mRNAs mediated by G-quadruplex structures formed via clustered WGGA sequences. *Hum Mol Genet* 23, 5479-5491.
- Suhl, J.A., Muddashetty, R.S., Anderson, B.R., Ifrim, M.F., Visootsak, J., Bassell, G.J., and Warren, S.T. (2015). A 3' untranslated region variant in FMR1 eliminates neuronal activity-dependent translation of FMRP by disrupting binding of the RNA-binding protein HuR. *Proc Natl Acad Sci U S A* 112, E6553-6561.
- Swatek, K.N., and Komander, D. (2016). Ubiquitin modifications. *Cell Res* 26, 399-422.

- Tang, Z., Li, B., Bharadwaj, R., Zhu, H., Ozkan, E., Hakala, K., Deisenhofer, J., and Yu, H. (2001). APC2 Cullin protein and APC11 RING protein comprise the minimal ubiquitin ligase module of the anaphase-promoting complex. *Mol Biol Cell* 12, 3839-3851.
- Tastet, J., Decalonne, L., Marouillat, S., Malvy, J., Thepault, R.A., Toutain, A., Paubel, A., Tabagh, R., Benedetti, H., Laumonnier, F., *et al.* (2015). Mutation screening of the ubiquitin ligase gene RNF135 in French patients with autism. *Psychiatric Genetics* 25, 263-267.
- Teng, F.Y., and Tang, B.L. (2005). APC/C regulation of axonal growth and synaptic functions in postmitotic neurons: the Liprin-alpha connection. *Cell Mol Life Sci* 62, 1571-1578.
- Thomas, K.T., Anderson, B.R., Shah, N., Zimmer, S.E., Hawkins, D., Valdez, A.N., Gu, Q., and Bassell, G.J. (2017). Inhibition of the Schizophrenia-Associated MicroRNA miR-137 Disrupts Nrg1alpha Neurodevelopmental Signal Transduction. *Cell Rep* 20, 1-12.
- Thomas, M.G., Martinez Tosar, L.J., Desbats, M.A., Leishman, C.C., and Boccaccio, G.L. (2009). Mammalian Staufen 1 is recruited to stress granules and impairs their assembly. *J Cell Sci* 122, 563-573.
- Thomson, S.R., Seo, S.S., Barnes, S.A., Louros, S.R., Muscas, M., Dando, O., Kirby, C., Wyllie, D.J.A., Hardingham, G.E., Kind, P.C., *et al.* (2017). Cell-Type-Specific Translation Profiling Reveals a Novel Strategy for Treating Fragile X Syndrome. *Neuron* 95, 550-563 e555.
- Tian, Y., Yang, C., Shang, S., Cai, Y., Deng, X., Zhang, J., Shao, F., Zhu, D., Liu, Y., Chen, G., *et al.* (2017). Loss of FMRP Impaired Hippocampal Long-Term Plasticity and Spatial Learning in Rats. *Front Mol Neurosci* 10, 269.
- Tinevez, J.Y., Perry, N., Schindelin, J., Hoopes, G.M., Reynolds, G.D., Laplantine, E., Bednarek, S.Y., Shorte, S.L., and Eliceiri, K.W. (2017). TrackMate: An open and extensible platform for single-particle tracking. *Methods* 115, 80-90.
- Tsai, N.P., Ho, P.C., and Wei, L.N. (2008). Regulation of stress granule dynamics by Grb7 and FAK signalling pathway. *EMBO J* 27, 715-726.
- Tsai, N.P., Wilkerson, J.R., Guo, W., Maksimova, M.A., DeMartino, G.N., Cowan, C.W., and Huber, K.M. (2012). Multiple autism-linked genes mediate synapse elimination via proteasomal degradation of a synaptic scaffold PSD-95. *Cell* 151, 1581-1594.
- Udagawa, T., Farny, N.G., Jakovcevski, M., Kaphzan, H., Alarcon, J.M., Anilkumar, S., Ivshina, M., Hurt, J.A., Nagaoka, K., Nalavadi, V.C., *et al.* (2013). Genetic and acute CPEB1 depletion ameliorate fragile X pathophysiology. *Nat Med* 19, 1473-1477.
- Upadhyay, A., Joshi, V., Amanullah, A., Mishra, R., Arora, N., Prasad, A., and Mishra, A. (2017). E3 Ubiquitin Ligases Neurobiological Mechanisms: Development to Degeneration. *Front Mol Neurosci* 10, 151.
- van Roessel, P., Elliott, D.A., Robinson, I.M., Prokop, A., and Brand, A.H. (2004). Independent regulation of synaptic size and activity by the anaphase-promoting complex. *Cell* 119, 707-718.

- Visintin, R., Prinz, S., and Amon, A. (1997). CDC20 and CDH1: a family of substrate-specific activators of APC-dependent proteolysis. *Science* 278, 460-463.
- Walsh, C. (2006). *Posttranslational modification of proteins : expanding nature's inventory* (Englewood, Colo.: Roberts and Co. Publishers).
- Wang, M., Li, H., Takumi, T., Qiu, Z., Xu, X., Yu, X., and Bian, W.J. (2017). Distinct Defects in Spine Formation or Pruning in Two Gene Duplication Mouse Models of Autism. *Neurosci Bull* 33, 143-152.
- Weiler, I.J., and Greenough, W.T. (1993). Metabotropic glutamate receptors trigger postsynaptic protein synthesis. *Proc Natl Acad Sci U S A* 90, 7168-7171.
- Weiler, I.J., and Greenough, W.T. (1999). Synaptic synthesis of the Fragile X protein: possible involvement in synapse maturation and elimination. *American Journal of Medical Genetics* 83, 248-252.
- Welshhans, K., and Bassell, G.J. (2011). Netrin-1-induced local beta-actin synthesis and growth cone guidance requires zipcode binding protein 1. *J Neurosci* 31, 9800-9813.
- Wheeler, J.R., Matheny, T., Jain, S., Abrisch, R., and Parker, R. (2016). Distinct stages in stress granule assembly and disassembly. *Elife* 5.
- Williams, K.R., McAninch, D.S., Stefanovic, S., Xing, L., Allen, M., Li, W., Feng, Y., Mihailescu, M.R., and Bassell, G.J. (2016). hnRNP-Q1 represses nascent axon growth in cortical neurons by inhibiting Gap-43 mRNA translation. *Molecular Biology of the Cell* 27, 518-534.
- Wolozin, B., and Ivanov, P. (2019). Stress granules and neurodegeneration. *Nat Rev Neurosci* 20, 649-666.
- Wu, W.J., Hu, K.S., Wang, D.S., Zeng, Z.L., Zhang, D.S., Chen, D.L., Bai, L., and Xu, R.H. (2013). CDC20 overexpression predicts a poor prognosis for patients with colorectal cancer. *J Transl Med* 11, 142.
- Wyszynski, M., Kim, E., Dunah, A.W., Passafaro, M., Valtschanoff, J.G., Serra-Pages, C., Streuli, M., Weinberg, R.J., and Sheng, M. (2002). Interaction between GRIP and liprin-alpha/SYD2 is required for AMPA receptor targeting. *Neuron* 34, 39-52.
- Xie, X., Matsumoto, S., Endo, A., Fukushima, T., Kawahara, H., Saeki, Y., and Komada, M. (2018). Deubiquitylases USP5 and USP13 are recruited to and regulate heat-induced stress granules through their deubiquitylating activities. *J Cell Sci* 131.
- Yang, Y., Kim, A.H., Yamada, T., Wu, B., Bilimoria, P.M., Ikeuchi, Y., de la Iglesia, N., Shen, J., and Bonni, A. (2009). A Cdc20-APC ubiquitin signaling pathway regulates presynaptic differentiation. *Science* 326, 575-578.

- Yao, J., Sasaki, Y., Wen, Z., Bassell, G.J., and Zheng, J.Q. (2006). An essential role for beta-actin mRNA localization and translation in Ca²⁺-dependent growth cone guidance. *Nat Neurosci* 9, 1265-1273.
- Yi, J.J., Berrios, J., Newbern, J.M., Snider, W.D., Philpot, B.D., Hahn, K.M., and Zylka, M.J. (2015). An Autism-Linked Mutation Disables Phosphorylation Control of UBE3A. *Cell* 162, 795-807.
- Youle, R.J., and van der Blik, A.M. (2012). Mitochondrial fission, fusion, and stress. *Science* 337, 1062-1065.
- Yuste, R., and Bonhoeffer, T. (2001). Morphological changes in dendritic spines associated with long-term synaptic plasticity. *Annu Rev Neurosci* 24, 1071-1089.
- Zachariae, W. (2004). Destruction with a box: substrate recognition by the anaphase-promoting complex. *Mol Cell* 13, 2-3.
- Zachariae, W., Schwab, M., Nasmyth, K., and Seufert, W. (1998). Control of cyclin ubiquitination by CDK-regulated binding of Hct1 to the anaphase promoting complex. *Science* 282, 1721-1724.
- Zhang, H.L., Singer, R.H., and Bassell, G.J. (1999). Neurotrophin regulation of beta-actin mRNA and protein localization within growth cones. *J Cell Biol* 147, 59-70.
- Zhang, J., Wan, L., Dai, X., Sun, Y., and Wei, W. (2014a). Functional characterization of Anaphase Promoting Complex/Cyclosome (APC/C) E3 ubiquitin ligases in tumorigenesis. *Biochim Biophys Acta* 1845, 277-293.
- Zhang, Y., Gaetano, C.M., Williams, K.R., Bassell, G.J., and Mihailescu, M.R. (2014b). FMRP interacts with G-quadruplex structures in the 3'-UTR of its dendritic target Shank1 mRNA. *RNA Biol* 11, 1364-1374.
- Zheng, N., and Shabek, N. (2017). Ubiquitin Ligases: Structure, Function, and Regulation. *Annu Rev Biochem* 86, 129-157.
- Zhou, Z., He, M., Shah, A.A., and Wan, Y. (2016). Insights into APC/C: from cellular function to diseases and therapeutics. *Cell Div* 11, 9.
- Zlatic, S.A., Ryder, P.V., Salazar, G., and Faundez, V. (2010). Isolation of labile multi-protein complexes by in vivo controlled cellular cross-linking and immuno-magnetic affinity chromatography. *J Vis Exp*.